A NUMERICAL EVALUATION OF THE
METHOD OF EQUIVALENT NONLINEARIZATION

Thesis by

Anne Lin

In Partial Fulfillment of the Requirements

for the Degree of

Doctor of Philosophy

California Institute of Technology

Pasadena, California

1988

(Submitted December 21, 1987)

ACKNOWLEDGEMENTS

ABSTRACT

The Method of Equivalent Nonlinearization, an approach for determining the approximate steady-state probability density function for the random response of nonlinear systems, is evaluated based on numerical simulations.

The approach is a natural extension of the well-known Method of Equivalent Linearization, and is based on approximating the original nonlinear system by an equivalent nonlinear system. As such, the approach relies on the existence of exact solutions for the steady-state probability density function of nonlinear systems.

The approach is applied to a class of systems with nonlinear damping, for which there are no exact solutions. The results show an excellent agreement between simulated and predicted probability density functions for displacement, velocity and energy-based envelope. Several examples were solved, including the case of $(velocity)^m$-damping and the Van der Pol equation.

TABLE OF CONTENTS

CHAPTER I

INTRODUCTION

In the past three decades, a considerable body of knowledge has been accumulated on the modeling of the response statistics of nonlinear oscillators to random excitation. A rather complete formulation can be obtained when the response of second-order systems, to white noise excitation, is modeled as a continuous Markov vector process. In this case, one obtains the Fokker-Planck-Komolgorov equation relating the transition probability density function of the process to the characteristics of the nonlinear system. Unfortunately, this equation has been solved only in a very limited number of cases [7].

Naturally, a number of techniques for obtaining approximate response statistics have arisen in this period. The most widely applied technique has been the Method of Equivalent Linearization, whose application leads to an approximate steady-state probability density function for the joint response of displacement and velocity. This method has been applied in virtually all areas of structural dynamics, ranging from the response of moving structures to a variety of excitation, to the reponse of civil engineering structures, to earthquake, wind and random ocean waves excitation [36].

In spite of this widespread use there are nonlinear systems for which the solutions obtained by the Method of Equivalent Linearization are not adequate or can be improved. This thesis is concerned with such an improvement, through a natural extension of the Method of Equivalent Linearization, the so-called Method of Equivalent Nonlinearization. The latter is applied to a class of nonlinear oscillators with nonlinear damping. This class, among others, comprises oscillators with $(velocity)^m$-damping and self-excited oscillators. To be specific, the accuracy of the Method of Equivalent Nonlinearization is assessed based on extensive numerical simulations for a large number of oscillators belonging to this class.

In Chapter II, the modeling of the response of a nonlinear oscillator as a Markov process is briefly reviewed; the Method of Equivalent Linearization is discussed and applied to a nonlinear oscillator with $(velocity)^2$-damping and linear stiffness. The steady-state probability density functions for displacement, velocity and energy-based envelope are then compared with their counterparts obtained based on numerical simulations of the response of the same oscillator.

The basic requirement of the Method of Equivalent Nonlinearization is that there be exact solutions for nonlinear systems. In Chapter III the exact solution for the steady-state probability density function for a class of nonlinear oscillators is reviewed. With these solutions, the Method of Equivalent Nonlinearization is then applied to the class of oscillators with nonlinear damping discussed above, with both linear and nonlinear stiffness, and approximate solutions are generated for these systems.

The numerical simulation approach is discussed in Chapter IV. Because of the length of the time histories required, the uniform random number generator, the heart of the white noise process generator that served as the excitation for the oscillators, had to satisfy rather stringent conditions. These conditions as well as an efficient time-step integration scheme are also discussed. As a result of this effort, the simulation procedure can be used in a variety of computers ranging from micros to main-frames.

In Chapter V, the approximate solutions generated in Chapter III are compared with solutions based on the simulated results. For each of nine different oscillators belonging to the aforementioned class, response simulations are performed for a range of practical damping levels and excitation levels. Results are presented in terms of histograms for displacement, velocity, energy envelope and expected values for the square of each of these quantities as functions of damping and excitation level.

CHAPTER II

THEORETICAL BACKGROUND

Consider the general class of nonlinear single degree-of-freedom (SDOF) oscillators characterized by the following differential equation,

$$\ddot{x} + g(x, \dot{x}) = w(t), \tag{2.1}$$

with initial conditions given by

$$x(0) = x_0 \quad \text{and} \quad \dot{x}(0) = \dot{x}_0, \tag{2.2}$$

where $g(x, \dot{x})$ is a nonlinear function of the displacement x and the velocity $\dot{x}$, and the forcing function $w(t)$ is the formal derivative of a Wiener process, $W(t)$, having the following characteristics [5,7]:

(a) $w(t_i)$, $i = 1, 2, \ldots, n$ are mutually independent,

(b) $w(t)$ is Gaussian distributed with

$$E[w(t)] = 0,$$

$$E[w(t)w(t + \tau)] = 2D\delta(\tau), \tag{2.3}$$

where $\delta(*)$ is the Dirac delta function and $E[*]$ is the expectation operator.

In searching for the joint probability density function of displacement and velocity, $p(x, \dot{x})$, for all times, the vector of random displacement and random velocity $\{x, \dot{x}\}$ can be modeled as a Markov process [7,27].

A continuous vector process $\mathbf{x}(t)$ is said to be Markovian if and only if for $t_1 < t_2 < \cdots < t_n < \cdots < t_{n+1}$,

$$p(\mathbf{x}_{n+1}, t_{n+1}|\mathbf{x}_1, t_1; \mathbf{x}_2, t_2; \ldots; \mathbf{x}_n, t_n) = p(\mathbf{x}_{n+1}, t_{n+1}|\mathbf{x}_n, t_n). \qquad (2.4)$$

The conditional probability density function $p(\mathbf{x}_{i+1}, t_{i+1}|\mathbf{x}_i, t_i)$ is called the transition probability density function and henceforth in this work will be represented by $p_{tr}(\mathbf{x}_{i+1}, t_{i+1}|\mathbf{x}_i, t_i)$. It gives the density of probability of a transition from one point in phase space at a certain time to another point in phase space at a greater time. The Markov process is completely defined if its transition probability is known and if the state vector at $t = 0$ is known with probability one.

The transition probability density function, $p_{tr}(x, \dot{x}, t|x_0, \dot{x}_0)$, for the vector Markov process for $\{x, \dot{x}\}$ of Eq. (2.1), is the solution of the associated Fokker-Plank-Komolgorov equation given by

$$\frac{\partial p_{tr}}{\partial t} = -\dot{x}\frac{\partial p_{tr}}{\partial x} + \frac{\partial}{\partial \dot{x}}[g(x, \dot{x})p_{tr}] + D\frac{\partial^2 p_{tr}}{\partial \dot{x}^2}, \qquad (2.5)$$

with $p_{tr}(x, \dot{x}, 0|x_0, \dot{x}_0) = \delta(x - x_0)\delta(\dot{x} - \dot{x}_0)$.

Although the problem of obtaining the transition probability, $p_{tr}(x, \dot{x})$, for a general nonlinear second-order system (Eq. (2.1)) can be formulated, to the author's knowledge, up to this date, there are still no known solutions to the complete equation. Even solutions for the steady-state joint probability density function, $p(x, \dot{x})$, given by

$$p(x, \dot{x}) = \lim_{t \to \infty} p_{tr}(x, \dot{x}, t | x_0, \dot{x}_0) \tag{2.6}$$

and obtained as solution of

$$-\dot{x}\frac{\partial p}{\partial x} + \frac{\partial}{\partial \dot{x}}\left[g(x, \dot{x})p\right] + D\frac{\partial^2 p}{\partial \dot{x}^2} = 0 \tag{2.7}$$

are very few, and they are all cases of the solution obtained by Caughey for a particular class of oscillators [7,8,9]. Clearly, the interest in approximate techniques for the solution of Eqs. (2.5) and (2.7) is greatly justified.

The various methods for obtaining approximate solutions for Eq. (2.5) can be loosely classified in two general categories [7,17,33,36]. The first is comprised of methods that deal directly with the Fokker-Planck-Kolmogorov equation (Eq. (2.5)), and the second is comprised of methods that deal directly with the stochastic differential equation (Eq. (2.1)). Examples of the first are the iterative solution of the Fokker-Planck-Kolmogorov equation [7], eigenfunction expansion techniques [22,23,33], perturbation techniques applied to the eigenvalues and asymptotic expansions [6,33]. Examples of the second class are perturbation methods [13,14],

Gausssian and non-Gaussian closure techniques [16,18,32], the method of equivalent linearization [4,35,36], and the method of equivalent nonlinearization [28]. By far the most widely used approximate method in the past 30 years has been the method of equivalent linearization. This is due primarily to the simplicity and relative accuracy of the method. Even though some of the other methods (e.g., eigenfunction expansions) are potentially more accurate, the trade-off to accuracy is an enormous increase in the analytical and numerical work involved. The result is that only first-order solutions are normally obtained † [33]. Because the first-order solutions obtained with the various methods are essentially as accurate as the solutions obtained by the method of equivalent linearization, the simplicity of the method is the overwhelming reason for its widespread use.

2.1 The Method of Equivalent Linearization

The method of equivalent linearization is a statistical extension [4] of the deterministic method of equivalent linearization of Krylov and Bogolibov [30]. As introduced by Caughey [4,7], the basis of the method is to replace an originally *nonlinear* equation by an equivalent *linear* equation whose parameters are determined by minimizing the expected value of the mean- square deficiency, defined as the difference between the linear and nonlinear equations.

---

† Recently, Johnson and Scott [22,23] have extended the work by Payne [33], obtaining higher order solutions with the eigenfunction expansion approach.

To illustrate the application of the method, consider the following nonlinear SDOF system,

$$\ddot{x} + \beta\dot{x} + \omega_n^2 x + \epsilon f(x, \dot{x}) = w(t). \tag{2.8}$$

Following the idea of the method, replace Eq. (2.8) by

$$\ddot{x} + \beta_{eq}\dot{x} + \omega_{eq}^2 x = w(t), \tag{2.9}$$

where β_{eq} and ω_{eq}, the equivalent damping and natural frequency terms, are found by minimizing the expected value of the mean-square deficiency. The deficiency, $\mathcal{D}(x, \dot{x})$, defined as the difference between Eqs. (2.8) and (2.9), is given by

$$\mathcal{D}(x, \dot{x}) = \beta\dot{x} + \omega_n^2 x + \epsilon f(x, \dot{x}) - \beta_{eq}\dot{x} - \omega_{eq}^2 x. \tag{2.10}$$

The minimization of $E\left[\mathcal{D}^2(x, \dot{x})\right]$, which is obtained by setting $\partial E\left[\mathcal{D}^2(x, \dot{x})\right]/\partial\beta_{eq}$ and $\partial E\left[\mathcal{D}^2(x, \dot{x})\right]/\partial\omega_{eq}^2$ to zero, yields

$$\begin{aligned} \beta_{eq} &= \beta + \epsilon\frac{E[\dot{x}f(x, \dot{x})]}{E[\dot{x}^2]}, \\ \omega_{eq}^2 &= \omega_n^2 + \epsilon\frac{E[xf(x, \dot{x})]}{E[x^2]}, \end{aligned} \tag{2.11}$$

where use has been made of the fact that $E[x\dot{x}] = 0$ for a differentiable stationary random process.

The joint probability density function of displacement and velocity, $p(x, \dot{x})$, for Eq. (2.9), which is a linear equation excited by a random Gaussian white noise process, is well known, and now it is an approximate solution for Eq. (2.8). Using this approximate solution, which is a function of β_{eq} and ω_{eq} in Eq. (2.11), yields a set of nonlinear algebraic equations in these parameters. The solutions of this set of algebraic equations will be β_{eq} and ω_{eq}.

As Caughey pointed out [7], if the exact joint probability density function of displacement and velocity, $p(x, \dot{x})$, for Eq. (2.8) is known, then it can be used in Eq. (2.11). Unfortunately, this is rarely the situation, and the approximate solution is what is almost always used.

2.1.1 A Limited Accuracy Assessment

The method of equivalent linearization has been extended to handle the response of a nonlinear system exhibiting hysteretic behavior [3], to multidegree-of-freedom systems [4,40], and has been extensively applied in virtually all fields of structural dynamics [17,35,36]. However, of course, it has its limitations, and results of its application to a certain class of problems, or the use of the resulting joint probability density to obtain certain statistics may not be satisfactory.

To illustrate this point, the method of equivalent linearization is applied to an SDOF system with $(velocity)^2$-damping. The approximate steady-state joint probability function is obtained for two examples and is compared with numerically obtained solutions.

Consider the nonlinear SDOF system with $(velocity)^2$-damping given by

$$\ddot{x} + b\,\dot{x}^2\mathrm{sgn}(\dot{x}) + x = w(t). \tag{2.12}$$

Application of Eq. (2.11), considering that the joint probability density function is given by

$$p(x, \dot{x}) = A\exp\left[-\left(\frac{\beta_{eq}}{2D}\right)\left(\dot{x}^2 + \omega_{eq}^2 x^2\right)\right], \tag{2.13}$$

where A is the normalizing constant, yields $\omega_{eq}^2 = \omega_n^2 = 1$ and $\beta_{eq} = 2D(b/\sqrt{\pi}D)^{2/3}$.

Figs. 2.1 and 2.2 present the comparison, in terms of histograms, between theoretical (solid lines) and simulated (dots) results for the distribution of displacement, velocity and energy-based envelope, for $b = 0.02$ and $b = 0.20$. It is clear from these comparisons that for at least this type of damping, even for small values of the coefficient b, the results obtained from the method of equivalent linearization are not satisfactory. The fact that any moment of the distribution from the theoretical solution may be in good agreement with the exact distribution seems to be merely fortuitous.

It has been known for some time that even for other types of the nonlinear functions $f(x, \dot{x})$, improvements could be achieved by using the method of equivalent nonlinearization. Lutes [28] has applied the method in connection with hysteretic systems, and Caughey [10], in connection with a class of nonlinear systems.

In the next chapters the method of equivalent nonlinearization is formally introduced and its accuracy assessed for a class of oscillators with nonlinear damping.
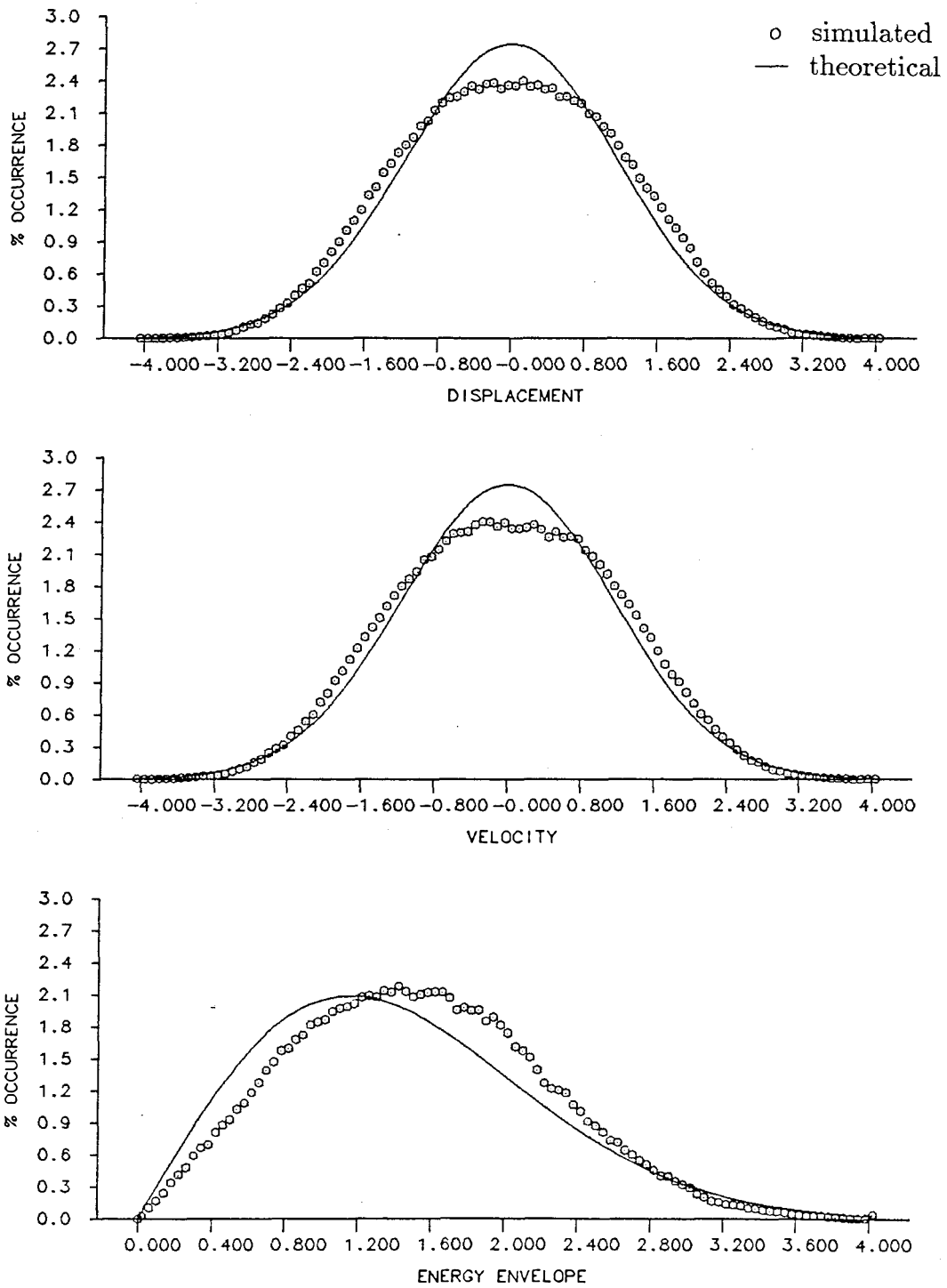
Figure 2.1

$(Velocity)^2$-Damping: $b_{02} \dot{x}^2 \, \mathrm{sgn}(\dot{x})$

$b_{02} = 0.02, \quad D = 0.05$
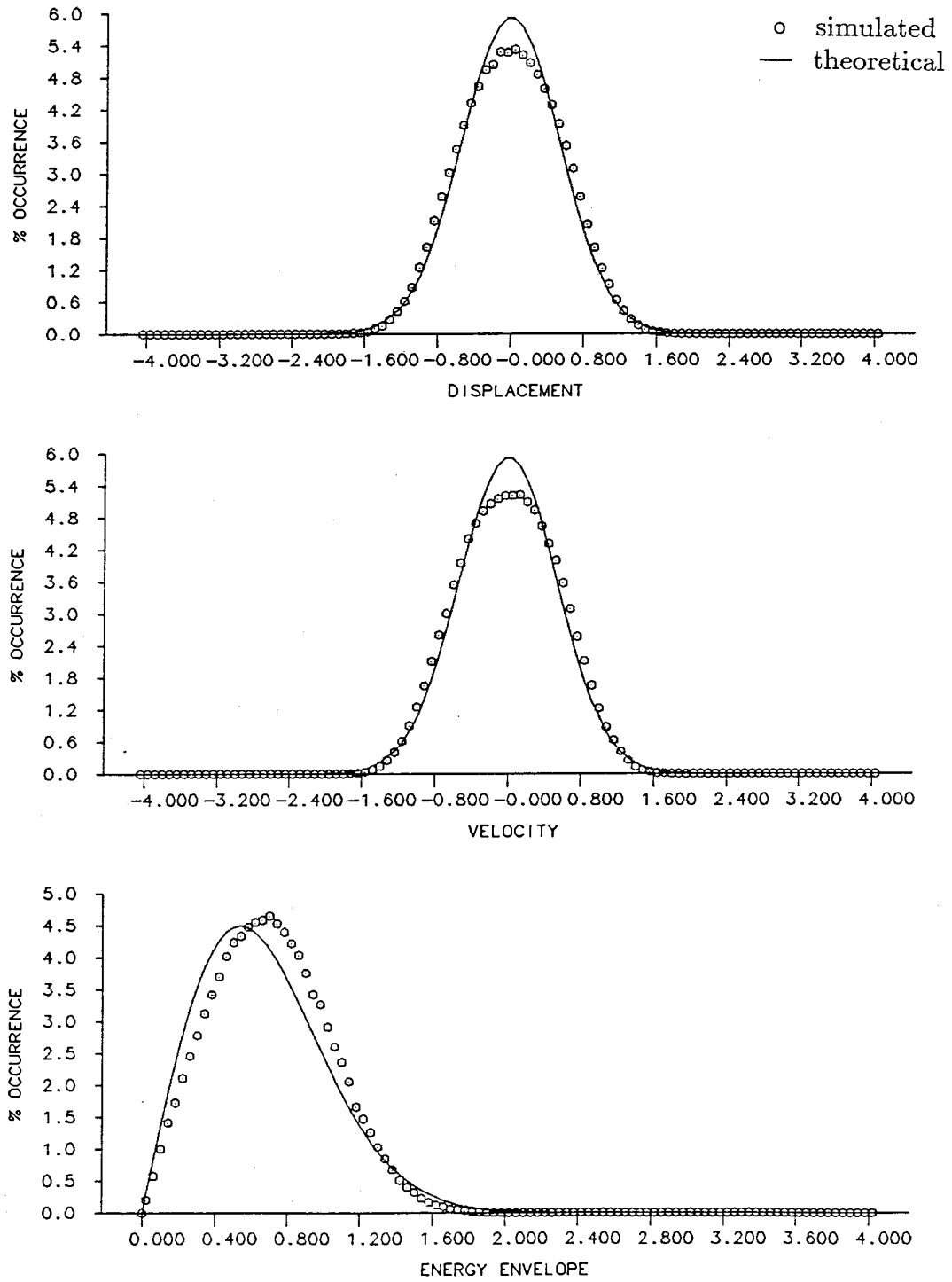
Figure 2.2

$(Velocity)^2$-Damping: $b_{02}\dot{x}^2\ \mathrm{sgn}(\dot{x})$

$b_{02} = 0.20,\ \ D = 0.05$

CHAPTER III

THE METHOD OF EQUIVALENT NONLINEARIZATION

The basic idea behind the Method of Equivalent Nonlinearization, as in the Method of Equivalent Linearization [10], is to replace a nonlinear equation for which the solution is sought by another equation for which the solution is known. In the Method of Equivalent Linearization, the original nonlinear equation is replaced by an equivalent *linear* equation, whereas in the Method of Equivalent Nonlinearization, the original nonlinear equation is replaced by an equivalent *nonlinear* equation. The difference between the two equations is then minimized in mean square, yielding the parameters of the approximate solution for the original nonlinear equation.

3.1 The Exact Solution for a Class of Nonlinear SDOF Systems

Consider the class of nonlinear, single degree-of-freedom (SDOF) systems of the form

$$\ddot{x} + \left(H_y F(H) - \frac{H_{yy}}{H_y} \right) D\dot{x} + \frac{H_x}{H_y} = w(t), \qquad (3.1)$$

with initial conditions given by

$$x(0) = x_0 \quad \text{and} \quad \dot{x}(0) = \dot{x}_0, \tag{3.2}$$

where $\dot{x}$ and $\ddot{x}$ are velocity and acceleration, respectively, $y = \dot{x}^2/2$, and a single and a double subscripted H indicate the first and second partial derivatives, respectively, of $H(y, x)$, the Hamiltonian, with respect to the subscript variable.

Formally, the forcing function $w(t)$ is the derivative of a Wiener process, $W(t)$, and has the following characteristics [7]:

(a) $w(t_i)$, $i = 1, 2, \ldots, n$ are mutually independent,

(b) $w(t)$ is Gaussian distributed with

$$E[w(t)] = 0,$$
$$E[w(t)w(t + \tau)] = 2D\delta(\tau), \tag{3.3}$$

where $\delta(*)$ is the Dirac delta function and $E[*]$ is the expectation operator. The one-sided power spectral density function of $w(t)$ is constant over the entire range of frequencies and is given by

$$G(f) = 4D \quad \text{for} \quad 0 \le f < \infty \quad \text{otherwise zero.} \tag{3.4}$$

In practice, this process, also called random stationary zero-mean Gaussian white-noise process, has a power spectral density function that can be considered constant only over a range of frequencies. This range, however, as will be seen

in Chapter IV, can be chosen wide enough to span all frequencies of interest. Henceforth in this work, this process will be referred to as white noise.

When the vector of displacement and velocity, $\{x, \dot{x}\}$, is treated as a Markov process, the corresponding transition probability density function $p_{tr}(x, \dot{x}, t | x_0, \dot{x}_0)$ is the solution of the Fokker-Planck-Komolgorov equation associated with Eq. (3.1) and given by [7,27],

$$\frac{\partial p_{tr}}{\partial t} = -\dot{x}\frac{\partial p_{tr}}{\partial x} + \frac{\partial}{\partial \dot{x}} \left\{ \left[\left(H_y F(H) - \frac{H_{yy}}{H_y} \right) D\dot{x} + \frac{H_x}{H_y} \right] p_{tr} \right\} + D\frac{\partial^2 p_{tr}}{\partial \dot{x}^2}, \quad (3.5)$$

with $p_{tr}(x, \dot{x}, 0 | x_0, \dot{x}_0) = \delta(x - x_0)\delta(\dot{x} - \dot{x}_0)$.

The steady-state joint probability density function of displacement and velocity, $p(x, \dot{x})$, independent of x_0, $\dot{x}_0$ and the time t, is obtained by finding the limit for $t \rightarrow \infty$ of $p_{tr}(x, \dot{x}, t | x_0, \dot{x}_0)$, yielding

$$-\dot{x}\frac{\partial p}{\partial x} + \frac{\partial}{\partial \dot{x}} \left\{ \left[\left(H_y F(H) - \frac{H_{yy}}{H_y} \right) D\dot{x} + \frac{H_x}{H_y} \right] p \right\} + D\frac{\partial^2 p}{\partial \dot{x}^2} = 0. \quad (3.6)$$

For completeness, an exact solution for Eq. (3.6) is herein derived following the approach developed in [7] and used in [8,9]. In this approach, Eq. (3.6) is separated into the following two partial differential equations

$$-\dot{x}\frac{\partial p}{\partial x} + \frac{\partial}{\partial \dot{x}} \left(\frac{H_x}{H_y}p \right) = 0,$$

$$\frac{\partial}{\partial \dot{x}} \left[\left(H_y F(H) - \frac{H_{yy}}{H_y} \right) \dot{x}p + \frac{\partial p}{\partial \dot{x}} \right] = 0, \quad (3.7)$$

for which a solution can be constructed, noting that this solution is also a solution of Eq. (3.6).

By assuming that $p(\dot{x}, x) = \bar{p}(\dot{x}, x)H_y$, and that $\dot{x} \not\equiv 0$, the first of Eq. (3.7) yields

$$-H_y \frac{\partial \bar{p}}{\partial x} + H_x \frac{\partial \bar{p}}{\partial y} = 0. \tag{3.8}$$

Eq. (3.8) can now be solved by the method of characteristics yielding

$$\bar{p}(x, \dot{x}) = \Psi(H) \qquad \text{and} \qquad p(x, \dot{x}) = \Psi(H)H_y, \tag{3.9}$$

where Ψ is an arbitrary function.

Because the solution $p(x, \dot{x})$, being sought, and its first partial derivatives with respect to x and $\dot{x}$, vanish as $|x| \to \infty$ and $|\dot{x}| \to \infty$, the second of Eq. (3.7) becomes

$$\left(H_y F(H) - \frac{H_{yy}}{H_y} \right) \dot{x} p + \frac{\partial p}{\partial \dot{x}} = 0. \tag{3.10}$$

Substituting Eq. (3.9) into (3.10) and integrating the resulting equation yields

$$p(x, \dot{x}) = AH_y \exp \left(- \int_0^H F(\xi)d\xi \right), \tag{3.11}$$

where A is the normalization constant such that $\int_{-\infty}^{+\infty} \int_{-\infty}^{+\infty} p(x, \dot{x}) dx d\dot{x} = 1$.

It can be seen that Eq. (3.11) satisfies all the requirements for a probability density, and that it also satisfies Eq.(3.6). Because of its exponential nature, the above solution belongs to a class of well-behaved stationary solutions and for that reason it is the unique steady-state solution of Eq. (3.6) [8,9].

In the foregoing, $H(y, x)$ can be interpreted as the system Hamiltonian from which the energy-based envelope process, $\alpha(t)$, is defined [8,9,12,27] by $H(0, \alpha) = H(y, x)$, having the following probability density function,

$$
\begin{aligned}
p_e(\alpha) &= 4 \frac{\partial}{\partial \alpha} \int_0^\alpha \left(\int_0^{[2(H(0,\alpha)-H(0,x))]^{\frac{1}{2}}} p(x, \dot{x}) d\dot{x} \right) dx \\
&= A H_x(0, \alpha) T(\alpha) \exp \left(-\int_0^{H(0,\alpha)} F(\xi) d\xi \right),
\end{aligned}
\tag{3.12}
$$

where

$$
T(\alpha) = 4 \int_0^\alpha \frac{dx}{[2(H(0, \alpha) - H(0, x))]^{\frac{1}{2}}}
\tag{3.13}
$$

is the period of the deterministic oscillator

$$
\ddot{x} + \frac{H_x}{H_y} = 0.
\tag{3.14}
$$

The above results are further particularized in order to develop some additional results that will be used in the application of the Method of Equivalent

Nonlinearization. Consider a case of Eq. (3.1) of practical interest having nonlinear damping and nonlinear stiffness of the form

$$\ddot{x} + f(H)\dot{x} + g(x) = w(t). \tag{3.15}$$

By comparison with Eq. (3.1), find $H_y = 1$, $H_x = g(x)$ and $F(H) = f(H)/D$. Substituting these values into Eq. (3.11) yields the joint probability density function of displacement and velocity as

$$p(x, \dot{x}) = A \exp\left(-\frac{1}{D} \int_0^H f(\xi)d\xi\right), \tag{3.16}$$

where H is given by

$$H(y, x) = y + \int_0^x g(\eta)d\eta. \tag{3.17}$$

Further consider the case in which $g(x) = \omega_n^2 x$, that is, a system with linear stiffness. For this case the joint probability density function of displacement and velocity is still given by Eq. (3.16) but now H is given by

$$H(y, x) = y + \frac{\omega_n^2}{2}x^2. \tag{3.18}$$

In addition, the probability density function of the energy-based envelope is obtained from Eqs. (3.12) and (3.13) as

$$p_e(\alpha) = 2\pi A \omega_n \alpha \exp\left(-\frac{1}{D} \int_0^{\omega_n^2 \alpha^2/2} f(\xi) d\xi\right), \qquad (3.19)$$

where α is defined by

$$\alpha = \sqrt{x^2 + \frac{\dot{x}^2}{\omega_n^2}}. \qquad (3.20)$$

The Method of Equivalent Nonlinearization is next applied to nonlinear SDOF systems for which there are no exact solutions. The approximate joint probability density function of displacement and velocity and the (corresponding) probability density function of the energy-based envelope are obtained based on the known solutions for the class of nonlinear systems just presented.

3.2 The Approximate Solution for a Class of SDOF Systems with Nonlinear Damping and Linear Stiffness

Consider the class of nonlinear SDOF systems of the form

$$\ddot{x} + \left(\sum_{i=0}^{n} \sum_{j=0}^{n} b_{ij} \left|x^i \dot{x}^j\right|\right) \text{sgn}(\dot{x}) + x = w(t), \qquad (3.21)$$

where $\text{sgn}(\dot{x})$ is the sign function, taking the value of either $+1$ or -1 according to the sign of the argument $\dot{x}$.

This is a class of SDOF systems that, among others, encompasses systems with $(velocity)^m$ damping, $m = 0, 1, 2, \ldots$, that are obtained by making $b_{0j} = b$, $j = 0, 1, 2, \ldots$, $b_{ij} = 0$ otherwise. For $m = 0$, the system has Coulomb damping; for $m = 1$, the system has viscous damping (linear system); for $m = 2$, the system has velocity-squared damping; etc. In addition, the Van der Pol and the Van der Rayleigh equations are part of this class of SDOF systems, the first being obtained by making $b_{01} = -b$, $b_{21} = b$, $b_{ij} = 0$ otherwise, while the second, by making $b_{01} = -b$, $b_{21} = b$, $b_{03} = b$, $b_{ij} = 0$ otherwise.

Except for the linear damping and the Van der Rayleigh equation, this class of SDOF systems does not possess a closed form solution for the joint probability density function of displacement and velocity, in which case one can resort to the Method of Equivalent Nonlinearization in order to obtain an approximate solution.

An approximate solution for Eq. (3.21) can be obtained by replacing it by

$$\ddot{x} + \left(\sum_{i=0}^{n} \sum_{j=0}^{n} c_{ij} f_{ij}(H) \right) \dot{x} + x = w(t), \qquad (3.22)$$

for which there is a theoretical solution, and by selecting c_{ij} so as to minimize the mean-square deficiency $E\left[\mathcal{D}^2(x, \dot{x}) \right]$ with an appropriate choice of $f_{ij}(H)$ [10].

The deficiency, defined as the difference between Eqs. (3.21) and (3.22), is given by

$$\mathcal{D}(x, \dot{x}) = \sum_{i=0}^{n} \sum_{j=0}^{n} b_{ij} \left| x^i \dot{x}^j \right| \operatorname{sgn}(\dot{x}) - c_{ij} f_{ij}(H) \dot{x}, \qquad (3.23)$$

where for this class of problems, $H = H(y,x) = (y + x^2/2)$, with $y = \dot{x}^2/2$.

A natural choice for $f_{ij}(H)$ is

$$f_{ij}(H) = (2H)^{\frac{(i+j-1)}{2}} \qquad \text{for} \qquad i,j = 0,1,2,\ldots,n, \qquad (3.24)$$

because it will correctly render Eq. (3.22) linear when $i = 0$ and $j = 1$, and will always contain terms that will resemble the corresponding terms in Eq. (3.21).

The mean-square deficiency, which is a function of c_{ij} only, can now be minimized by equating its partial derivatives with respect to c_{ij} to zero, yielding the following set of equations in the coefficients c_{ij}:

$$\frac{\partial}{\partial c_{kl}} E\left[\mathcal{D}^2(x,\dot{x})\right] = E\left[2\mathcal{D}(x,\dot{x})\frac{\partial \mathcal{D}(x,\dot{x})}{\partial c_{kl}}\right]$$

$$= 2\int_{-\infty}^{+\infty}\int_{-\infty}^{+\infty} \mathcal{D}(x,\dot{x})\frac{\partial \mathcal{D}(x,\dot{x})}{\partial c_{kl}}p(x,\dot{x})dxd\dot{x} = 0 \qquad (3.25)$$

$$\text{for} \qquad k,l = 0,1,2,\ldots,n,$$

where $p(x,\dot{x})$ is given by Eq. (3.16) with $f(\xi)$ given by

$$f(\xi) = \sum_{i=0}^{n}\sum_{j=0}^{n} c_{ij}f_{ij}(\xi). \qquad (3.26)$$

The coefficients c_{ij}, solutions for the set of equations given by Eq. (3.25), minimize the mean-square deficiency between the original nonlinear equation (Eq. (3.21))

and its equivalent nonlinear equation (Eq. (3.22)). The solution of the equivalent nonlinear equation with these coefficients will then be an approximate solution for the original nonlinear equation. The remainder of this section will be dedicated to obtaining the solution to the set of equations given by Eq. (3.25) and consequently, to obtaining the solution for the joint probability density function for displacement and velocity and the corresponding probability density function for the energy-based envelope for Eq. (3.22).

The joint probability density function of displacement and velocity is obtained by substituting Eq. (3.24) into Eq. (3.26) and then into Eq. (3.16) and evaluating the integral yielding

$$p(x, \dot{x}) = A \exp \left(-\frac{1}{D} \sum_{i=0}^{n} \sum_{j=0}^{n} \frac{c_{ij}}{(i+j+1)} (x^2 + \dot{x}^2)^{\frac{(i+j+1)}{2}} \right), \qquad (3.27)$$

and the probability density function of the energy-based envelope is obtained by substituting Eq. (3.24) into Eq. (3.26) and then into Eq. (3.19) and evaluating the integral yielding

$$p_e(\alpha) = 2\pi A \alpha \exp \left(-\frac{1}{D} \sum_{i=0}^{n} \sum_{j=0}^{n} \frac{c_{ij}}{(i+j+1)} \alpha^{(i+j+1)} \right). \qquad (3.28)$$

By substituting Eq. (3.24) into (3.23), evaluating its partial derivative with respect to c_{kl}, and substituting both into Eq. (3.25), the set of equations in the coefficients c_{ij} becomes

$$\int_{-\infty}^{+\infty} \int_{-\infty}^{+\infty} \left(\sum_{i=0}^{n} \sum_{j=0}^{n} b_{ij} \left| x^i \dot{x}^j \right| \operatorname{sgn}(\dot{x}) - c_{ij}(x^2 + \dot{x}^2)^{\frac{(i+j-1)}{2}} \dot{x} \right) \times$$

$$(x^2 + \dot{x}^2)^{\frac{(k+l-1)}{2}} \dot{x} p(x, \dot{x}) dx d\dot{x} = 0 \tag{3.29}$$

$$\text{for} \quad k, l = 0, 1, 2, \ldots, n,$$

where use has been made of the fact that $2H = \dot{x}^2 + x^2$.

Substituting Eq. (3.27) into (3.29), applying the following change of variables

$$x = a \cos \theta,$$
$$\dot{x} = a \sin \theta, \tag{3.30}$$

to the resulting equation and simplifying, recalling that the absolute value of the Jacobian of the transformation is $|J| = a$, yields

$$\int_{0}^{2\pi} \int_{0}^{\infty} \sum_{i=0}^{n} \sum_{j=0}^{n} \left(b_{ij} \left| \cos^i \theta \sin^{j+1} \theta \right| - c_{ij} \sin^2 \theta \right) a^{(i+j+k+l)} \lambda(a) da d\theta = 0 \tag{3.31}$$

$$\text{for} \quad k, l = 0, 1, 2, \ldots, n,$$

where $\lambda(a)$ is a function of a only, given by

$$\lambda(a) = a \exp \left(-\frac{1}{D} \sum_{i=0}^{n} \sum_{j=0}^{n} \frac{c_{ij}}{(i+j+1)} a^{(i+j+1)} \right). \tag{3.32}$$

Evaluating the integral in the variable θ in Eq. (3.31) finally yields

$$\sum_{i=0}^{n} \sum_{j=0}^{n} \left(\pi c_{ij} - 2b_{ij} \frac{\Gamma(\frac{i+1}{2})\Gamma(\frac{i+2}{2})}{\Gamma(\frac{i+j+3}{2})} \right) \int_{0}^{\infty} a^{(i+j+k+l)} \lambda(a) da = 0 \tag{3.33}$$

$$\text{for} \quad k, l = 0, 1, 2, \ldots, n.$$

Given a nonlinear SDOF system belonging to the class of systems represented by Eq. (3.21), Eq. (3.33) is the set of equations that will determine the parameters c_{ij} of the approximate solution for its joint probability density function of displacement and velocity, $p(x, \dot{x})$, given by Eq. (3.28) and its probability density function of the energy-based envelope, $p_e(\alpha)$, given by Eq. (3.29). These densities will be the exact solution for the equivalent nonlinear SDOF system represented by Eq. (3.22) with the same coefficients.

A number of examples within this class of SDOF systems will be explicitly solved in Chapter V with the purpose of illustrating and assessing the accuracy of the Method of Equivalent Nonlinearization.

3.3 The Approximate Solution for a Class of SDOF Systems with Nonlinear Damping and Nonlinear Stiffness

In the increasing scale of complexity, consider the class of nonlinear SDOF systems of the form

$$\ddot{x} + \left(\sum_{i=0}^{n} \sum_{j=0}^{n} b_{ij} \left| x^i \dot{x}^j \right| \right) \text{sgn}(\dot{x}) + g(x) = w(t), \tag{3.34}$$

which is similar to Eq. (3.21) except for the stiffness term that is now also non-linear.

As in the case of Eq. (3.21), in general, this class of SDOF systems does not possess a closed form solution for the joint probability density function of displacement and velocity. Again, at least conceptually, one can consider the Method of Equivalent Nonlinearization as a possible means to obtain an approximate solution.

An approximate solution for Eq. (3.34) would be obtained by replacing it by

$$\ddot{x} + \left(\sum_{i=0}^{n} \sum_{j=0}^{n} c_{ij} f_{ij}(H) \right) \dot{x} + g(x) = w(t), \tag{3.35}$$

for which there is a theoretical solution, and selecting c_{ij} so as to minimize the mean-square deficiency $E\left[\mathcal{D}^2(x, \dot{x})\right]$ with an appropriate choice of $f_{ij}(H)$.

The deficiency, defined as the difference between Eqs. (3.34) and (3.35), is identical to the case studied in the previous section, in which the stiffness was linear, and is given by Eq. (3.23). The difference between the two cases resides in the definition of H, which now is

$$H = H(y, x) = y + \int_0^x g(\eta) d\eta, \tag{3.36}$$

where $y = \dot{x}^2/2$.

Once again, f_{ij} can be chosen as before as

$$f_{ij}(H) = (2H)^{\frac{(i+j-1)}{2}} \qquad \text{for} \qquad i,j = 0, 1, 2, \ldots, n, \qquad (3.37)$$

and the mean-square deficiency can be minimized by equating its partial derivatives with respect to c_{ij} to zero, yielding the set of Eqs. (3.25) also reproduced here:

$$\int_{-\infty}^{+\infty} \int_{-\infty}^{+\infty} \mathcal{D}(x, \dot{x}) \frac{\partial \mathcal{D}(x, \dot{x})}{\partial c_{kl}} p(x, \dot{x}) dx d\dot{x} = 0 \quad \text{for} \quad k, l = 0, 1, 2, \ldots, n, \quad (3.38)$$

where

$$\mathcal{D}(x, \dot{x}) = \sum_{i=0}^{n} \sum_{j=0}^{n} b_{ij} \left| x^i \dot{x}^j \right| \operatorname{sgn}(\dot{x}) - c_{ij}(2H)^{\frac{(i+j-1)}{2}} \dot{x}, \qquad (3.39)$$

and

$$p(x, \dot{x}) = A \exp \left(-\frac{1}{D} \sum_{i=0}^{n} \sum_{j=0}^{n} \frac{c_{ij}}{(i + j + 1)} (2H)^{\frac{(i+j+1)}{2}} \right). \qquad (3.40)$$

This is as far as one can get in general terms. Even with the selection of a specific function $g(x)$, the fact that H is now a much more complex function of $\dot{x}$ and x will limit and even preclude the development of general formulas. Solutions of Eq. (3.38), for each specific function $g(x)$, seem to be practical only if obtained numerically as illustrated in the next section.

3.3.1 Nonlinear Stiffness of the *Duffing*-Type

To illustrate the application of the approach in which the solution of the system of equations given by Eq. (3.38) has to be obtained numerically, consider the case in which the nonlinear stiffness is of *Duffing*-type given by

$$g(x) = e_0 x + e_1 x^3. \tag{3.41}$$

In this case,

$$H(\dot{x}, x) = \frac{1}{2}\dot{x}^2 + \frac{e_0}{2}x^2 + \frac{e_1}{4}x^4, \tag{3.42}$$

and therefore the deficiency is given by

$$\mathcal{D}(x, \dot{x}) = \sum_{i=0}^{n}\sum_{j=0}^{n} b_{ij} \left| x^i \dot{x}^j \right| \mathrm{sgn}(\dot{x}) - c_{ij}(\dot{x}^2 + e_0 x^2 + \frac{e_1}{2}x^4)^{\frac{(i+j-1)}{2}} \dot{x}, \tag{3.43}$$

and the joint probability density function of displacement and velocity, by

$$p(x, \dot{x}) = A \exp\left(-\frac{1}{D}\sum_{i=0}^{n}\sum_{j=0}^{n}\frac{c_{ij}}{(i+j+1)}(\dot{x}^2 + e_0 x^2 + \frac{e_1}{2}x^4)^{\frac{(i+j+1)}{2}}\right). \tag{3.44}$$

The probability density function of the energy-based envelope is obtained by substitution of Eqs. (3.42) and (3.44) into Eqs. (3.12) and (3.13) and evaluating the resulting integrals, yielding

$$p_e(\alpha) = A(e_0\alpha + e_1\alpha^3)T(\alpha)\exp\left(-\frac{1}{D}\sum_{i=0}^{n}\sum_{j=0}^{n}\frac{c_{ij}}{(i+j+1)}(e_0\alpha^2 + \frac{e_1}{2}\alpha^4)^{\frac{(i+j+1)}{2}}\right),$$

$$(3.45)$$

where after some manipulation [12,27], $T(\alpha)$ is obtained as

$$T(\alpha) = 4(e_0 + e_1\alpha^2)^{-\frac{1}{2}}\int_0^1 (1-t^2)^{-\frac{1}{2}}\left(1 - \left(\frac{e_1\alpha^2}{2e_0 + 2e_1\alpha^2}\right)t^2\right)^{-\frac{1}{2}} dt. \quad (3.46)$$

In this case, α is given by

$$\alpha = \left(-\left(\frac{e_0}{e_1}\right) + \left(\left(\frac{e_0}{e_1}\right)^2 + \frac{1}{e_1}\left(2\dot{x}^2 + 2e_0x^2 + e_1x^4\right)\right)^{\frac{1}{2}}\right)^{\frac{1}{2}}. \quad (3.47)$$

By substituting Eq. (3.43) and its partial derivative with respect to c_{kl} into Eq. (3.38), the set of equations in the coefficients c_{ij} becomes

$$\int_{-\infty}^{+\infty}\int_{-\infty}^{+\infty}\left(\sum_{i=0}^{n}\sum_{j=0}^{n}b_{ij}\left|x^i\dot{x}^j\right|\operatorname{sgn}(\dot{x}) - c_{ij}(\dot{x}^2 + e_0x^2 + \frac{e_1}{2}x^4)^{\frac{(i+j-1)}{2}}\dot{x}\right) \times$$

$$(\dot{x}^2 + e_0x^2 + \frac{e_1}{2}x^4)^{\frac{(k+l-1)}{2}}\dot{x}p(x,\dot{x})dxd\dot{x} = 0$$

$$\text{for} \quad k,l = 0,1,2,\ldots,n,$$

$$(3.48)$$

where use has been made of the equality $2H = \dot{x}^2 + e_0x^2 + \frac{e_1}{2}x^4$.

Unlike the linear stiffness case, in which the solution of Eq. (3.29) was obtained through a simple change of variables, there is not a change of variables that will attain the same results for Eq. (3.48). The only practical alternative of obtaining the coefficients c_{ij} seems to be the numerical solution of the system of equations given by Eq. (3.48).

It is also noted that, for this particular choice of nonlinear stiffness, $T(\alpha)$ reduced to an expression containing a complete elliptic integral of the first kind. In general, however, while the coefficients c_{ij} can always be obtained numerically, yielding an analytic expression for $p(x, \dot{x})$ of the form given by Eq. (3.40), this is not the case for $p_e(\alpha)$. An analytic expression for $p_e(\alpha)$ will depend on whether or not it is possible to obtain an analytic expression for $T(\alpha)$ given by Eq. (3.13).

Again, a number of examples will be explicitly solved in Chapter V to demonstrate the application of the Method of Equivalent Nonlinearization when the coefficients c_{ij} require numerical evaluation.

CHAPTER IV

SIMULATION CONCEPTS

4.1 Random Number Generation

The extensive computational time required to perform each of the time-domain simulations required in this work prompted the use of all available computing resources at Caltech. These ranged from microcomputers of several makes to super minicomputers.

If on one hand this approach allowed for several simulations to be carried out at the same time, on the other hand, it also required the capability of generating the same random forcing function time history across all machines. In other words, the random number generator to be used in the generation of the time history had to be portable.

In addition, since the length of each time-domain simulation was to be of approximately 500,000 points, the random number generator had to be capable of generating considerably more points without repeating itself; that is, its period had to be much greater than 500,000 points.

The requirements of portability and long periods simply precluded the use of the so-called intrinsic random number generators, that is, random number generators that can be accessed through systems functions or subroutines. In fact, the intrinsic random number generator of some microcomputers are not able to generate more than 65,536 numbers without repetition [31,38], and the intrinsic random number generator of minicomputers and main frames place too stringent requirements to be ported down to present microcomputers [19]. The alternative was to search for a random number generator that would satisfy the requirements of period set forth among the so-called portable random number generators.

Even though the expression "random number" was and will be used throughout this work what is meant by it is "pseudorandom number." The reason for this distinction resides in the fact that the process by which these numbers are generated is entirely deterministic, and therefore questions about true randomness may well arise. This section concerns itself with the definition of such a deterministic process and with the tests performed to assure that the sequence generated possesses the atributes to be considered a random sequence sampled from a certain distribution.

4.1.1 Uniformly Distributed Random Numbers

The linear congruential random number generator, the most widely used generator of recent times [25], is of the following form:

$$x_{i+1} = (ax_i + c) \bmod m \qquad \text{for all } i \geq 0, \tag{4.1}$$

where a, c, m and x_i are integer numbers with the following characteristics:

$$
\begin{aligned}
&m, \text{ modulus,} && m > 0; \\
&a, \text{ multiplier,} && 0 \le a < m; \\
&c, \text{ increment,} && 0 \le c < m; \\
&x_0, \text{ seed,} && 0 \le x_0 < m.
\end{aligned}
\tag{4.2}
$$

The sequence of integer numbers generated by Eq. (4.1) will be between zero and m, and therefore random numbers, uniformly distributed in the interval $(0,1)$, are obtained by

$$
u_i = x_i/m. \tag{4.3}
$$

Depending on the choices for parameters (4.2) above, the sequences generated by Eq. (4.1) will have a period of at most m numbers [25,26]. Because these sequences will always have a period [25], and because good statistical properties for the generated sequences are closely related to the length of their period, the main objective in designing linear congruential random number generators reduces to choosing parameters to make the period of the generated sequence as long as possible.

In recent years a number of theoretical developments in the area of congruential random number generators [25] has made it possible to define sets of parameters (4.2) so that the sequence generated by Eq. (4.1) has the desired period

and also passes a series of statistical tests that all good random sequences should pass. Several such sets are provided in [34].

The basic problem faced during this work was that none of the available sets of parameters (4.2) would produce a sequence long enough (of the order of at least 1,000,000 numbers), and those that would, would not be in the machine range of the 16-bit microcomputers that were going to be used in part of the simulations.

As opposed to developing a new set of parameters (4.2), which in turn would require extensive testing, the alternative of combining two or more good congruential random number generators with smaller periods to produce a random number with a longer period seemed very attractive. The author came across at least two of such schemes: (a) an algorithm by which the most significant part and the least significant part of a random number are generatad by two independent random number generators [25], and (b) an algorithm by which a random number is generated by taking the fractional part of the sum of three independent, random number generators [39].

The author chose to implement the second algorithm because: (a) it is very simple; (b) it was developed as a portable random number generator; (c) its period exceeds 6.95×10^{12}; (d) it works well for extreme values; and (e) it was extensively tested, showing excellent characteristics as random number generator.

The characteristics of the three congruential random number generators used in the algorithm are presented in Table 4.1.

Table 4.1 Generator Parameters		
m	a	c
30,269	171	0
30,307	172	0
30,323	170	0

The algorithm was coded as the subroutine RANDU and was imbedded in the computer code for the time-domain simulations included in Appendix A.

4.1.1.1 Empirical Testing of the Random Number Generator

There is a fairly large number of empirical tests that could be used to test a random number generator [25,26], and new tests could be developed to determine whether a random number generator is suitable for a particular application. However, because the random number generator is just a tool in the present work, and because the one chosen to be used in this work had been the object of other studies [39], the author presents in this section the few tests that were used only as a means of confirming the good properties of the generator. The tests used have been adapted from [26].

(a) Frequency Test

The first test, and also the simplest, is the frequency test. The frequency test is used to determine whether the random sequence generated has numbers uniformly distributed in the interval $(0, 1)$. The test is applied by dividing the interval $(0, 1)$ in a number of k equal subintervals (cells) and counting the number of numbers x_i, out of n generated numbers, that fall in each cell. The histogram generated is tested with a chi-square test with $(k-1)$ degrees of freedom against the hypothesis that the numbers belong to a uniform distribution with theoretical frequency of (n/k) for each cell. The following statistics is generated:

$$\chi^2_{k-1} = \sum_{i=1}^{k} \frac{(x_i - \frac{n}{k})^2}{(\frac{n}{k})}. \tag{4.4}$$

This test was applied to the histograms, with 100 cells, obtained by generating 250,000, 500,000, 1,000,000 and 2,000,000 numbers. The hypothesis that these numbers are uniformly distributed could not be rejected at a level of significance of 0.05. Table 4.2 shows the computed chi-square statistics.

Table 4.2 Frequency Test Results	
n	χ^2
250,000	87.1
500,000	100.9
1,000,000	100.5
2,000,000	86.1

The chi-square value for 99 degrees of freedom and a level of significance of 0.05 is 123.2.

(b) Serial Test

As the second requirement, the random number generator should be able to generate not only single numbers that are uniformly distributed over the domain $(0, 1)$, but also pairs of numbers that are uniformly distributed, over the two-dimensional domain $[(0, 1), (0, 1)]$. This test is particularly important in the present work because, as will be seen in the next section, normally distributed random numbers will be obtained by transforming a pair of uniformly distributed random numbers.

The test is applied by dividing the two-dimensional domain in a number of k equal subintervals in each direction and counting the number of pairs of successive numbers $x_{i,j}$, out of n generated numbers, that fall in each cell. A chi-square test with $(k^2 - 1)$ degrees of freedom and theoretical frequency of (n/k^2) for each cell is applied, generating the following statistics:

$$\chi^2_{k^2-1} = \sum_{i=1}^{k} \sum_{j=1}^{k} \frac{\left(x_{i,j} - \frac{n}{k^2}\right)^2}{\left(\frac{n}{k^2}\right)}. \tag{4.5}$$

This test was applied to the histograms, with 30 cells in each direction, obtained by generating 250,000, 500,000, 1,000,000 and 2,000,000 numbers. The hypothesis that these numbers are uniformly distributed

could not be rejected at a level of significance of 0.05. Table 4.3 shows the computed chi-square statistics.

Table 4.3 Serial Test Results	
n	χ^2
250,000	945.0
500,000	908.9
1,000,000	904.5
2,000,000	879.9

The chi-square value for 899 degrees of freedom and a level of significance of 0.05 is 969.7.

(c) Gap Test

The gap test examines the length of gaps between occurrences of u_i in a certain subinterval of $(0, 1)$. The gap test is applied by dividing the interval $(0, 1)$ in a number of k equal subintervals, and counting the length of gaps between occurrences for a particular subinterval. A chi-square test is applied to the histogram of gap distribution, generating the following statistics:

$$\chi^2_{l-1} = \sum_{i=1}^{l} \frac{(g_i - np_i)^2}{np_i}, \tag{4.6}$$

where l is the number of cells chosen for the histogram of gap lengths, g_i is the count for gap with length i, n is the total number of points

generated, and p_i is the probability of occurrence of a gap with length i. This probability p_i is the geometric distribution and is given by:

$$p_i = \left(1 - \frac{1}{k}\right)^i \left(\frac{1}{k}\right). \tag{4.7}$$

This test was applied to the histograms of gaps with 40 cells generated from numbers that fall in the interval ($0.01 \leq u_i < 0.02$) out of 250,000, 500,000, 1,000,000 and 2,000,000 numbers. The hypothesis that these numbers are uniformly distributed could not be rejected at a level of significance of 0.05. Table 4.4 shows the computed chi-square statistics.

Table 4.4 Gap Test Results	
n	χ^2
250,000	35.8
500,000	32.0
1,000,000	32.4
2,000,000	32.6

The chi-square value for 39 degrees of freedom and a level of significance of 0.05 is 54.6. Note that since, in this case, the length of the subinterval is 0.01, there are another 99 subintervals that should also be used in applying this test. It is expected, however, that the gap test will be passed for all subintervals.

(d) The Maximum- (Minimum-) of-t

The maximum- (minimum-) of-t test examines the distribution of maxima or minima obtained from all subsequences of length t, out of the sequence of n generated random numbers. It can be shown [25,26] that if r_j is the maximum of the subsequence j, from an underlying uniform sequence, then the distribution of r_j^t is also uniform in $(0,1)$. If r_j is the minimum, then $(1 - r_j)^t$ is also uniform in $(0,1)$. A frequency test as in (a) above is then applied to the sequence of r_j^t or of $(1 - r_j)^t$.

This test was applied to subsequences of 5 numbers out of 250,000, 500,000, 1,000,000 and 2,000,000 numbers. Histograms of maxima and minima with 100 cells were then formed. The hypothesis that the random numbers are uniformly distributed could not be rejected at a level of significance of 0.05. Table 4.5 shows the computed chi-square statistics.

Table 4.5 Max/Min-of-t Test Results		
n	Max-t χ^2	Min-t χ^2
250,000	95.2	87.6
500,000	101.1	116.0
1,000,000	95.9	103.7
2,000,000	106.9	76.2

The chi-square value for 99 degrees of freedom and a level of significance of 0.05 is 123.2. Note that with this test one has the freedom to choose the length of the subsequence, and more appropriately, a number of these subsequences should be tested. Again, it is expected that

the random number generator will pass this test for subsequences of any length.

In addition to the above tests, the random number generator in discussion also passed the "poker test," the "coupon collector's test," and the "runs-up-and-down test" as reported by [39]. A thorough discussion of these and other tests, including the relative merit of each one is contained in [25].

4.1.2 Normally Distributed Random Numbers

There are a number of methods of obtaining normally distributed random numbers [25,26]. Common to practically all of them is the fact that they are obtained through a transformation of uniformly distributed random numbers.

4.1.2.1 General Method

Define $p(u)$ as the uniform probability density function; that is,

$$p(u) = \begin{cases} 1 & \text{if } 0 < u < 1; \\ 0 & \text{elsewhere.} \end{cases} \tag{4.8}$$

Also, define $p(z)$ as the normal probability density function with zero mean and standard deviation one; that is,

$$p(z) = \frac{1}{\sqrt{2\pi}} e^{-z^2} \qquad -\infty < z < +\infty. \tag{4.9}$$

Theoretically [20], the transformation between the two probability density functions is given by:

$$p(z) = p(u) \left| \frac{du}{dz} \right|. \tag{4.10}$$

Substituting Eqs. (4.8) and (4.9) into Eq. (4.10) and integrating yields

$$u = F(z) = \frac{1}{\sqrt{2\pi}} \int_{-\infty}^{z} e^{-t^2} dt. \tag{4.11}$$

Therefore, the desired transformation, the one that takes u, a uniformly distributed random number, into z, a normally distributed random number, is given by

$$z = F^{-1}(u), \tag{4.12}$$

where F^{-1} is the inverse function of F. The fact that F^{-1} is not easy to compute directly has given rise to a number of other indirect methods to obtain the desired transformation. The author in the present work adopted one of such methods.

4.1.2.2 Polar Method

The main advantage of this method, as is shown below, is that it is exact; that is, no approximations are involved in the transformation. Thus, the distribution is accurate also in the tails, making it suitable for studying extreme response. Disadvantages, if any, are of computational nature only.

This method generates two independent, normally distributed random numbers, (z_1, z_2), given two independent, uniformly distributed random numbers, (u_1, u_2), through the following transformation:

$$z_1 = \sqrt{-2 \ln u_1} \cos 2\pi u_2,$$
$$z_2 = \sqrt{-2 \ln u_1} \sin 2\pi u_2. \tag{4.13}$$

That z_1 and z_2 are independent and normally distributed random variables can be seen by calculating the joint probability density function $p(z_1, z_2)$. To that end, consider the extension of Eq. (4.10) in two dimensions [20]:

$$p(z_1, z_2) = p(u_1, u_2) |J|, \tag{4.14}$$

where $|J|$ is the absolute value of the Jacobian of the inverse of the transformation defined by Eq. (4.13); that is,

$$J = \begin{vmatrix} \frac{\partial u_1}{\partial z_1} & \frac{\partial u_1}{\partial z_2} \\ \frac{\partial u_2}{\partial z_1} & \frac{\partial u_2}{\partial z_2} \end{vmatrix}. \tag{4.15}$$

Solving for u_1 and u_2 as functions of z_1 and z_2 from Eq. (4.13), evaluating Eq. (4.15) and substituting into Eq. (4.14) yields

$$p(z_1, z_2) = \left(\frac{1}{\sqrt{2\pi}} \exp\left(-\frac{z_1^2}{2}\right) \right) \left(\frac{1}{\sqrt{2\pi}} \exp\left(-\frac{z_2^2}{2}\right) \right), \tag{4.16}$$

which in itself says that z_1 and z_2 are independent and normally distributed random variables.

In order to improve efficiency, the transformation defined by Eq. (4.13) is implemented in a slightly different fashion as discussed by [25]:

$$z_1 = v_1 \sqrt{\frac{-2\ln s}{s}} \qquad \text{and} \qquad z_2 = v_2 \sqrt{\frac{-2\ln s}{s}}, \qquad (4.17)$$

where

$$v_1 = 1 - 2u_1, \qquad v_2 = 1 - 2u_2, \qquad \text{and} \qquad s = (v_1^2 + v_2^2) < 1, \qquad (4.18)$$

or, in other words, generate pairs of uniform random numbers (u_1, u_2) from $(0, 1)$, and transform them into (v_1, v_2) in $(-1, 1)$. Keep only values (v_1, v_2) inside the unit circle, discarding all the other pairs. The pair of numbers (z_1, z_2), obtained with Eq. (4.17), will be normally distributed with zero mean and standard deviation one. Again, Eqs. (4.14) and (4.15) are used to show that (z_1, z_2) are indeed normally distributed random numbers.

The procedure outlined above was implemented in the subroutine RANDZ, also imbedded in the computer code included in Appendix A.

Fig. 4.1 shows the histogram obtained by generating 300,000 points with RANDZ and sampling them in 100 cells. It can be seen that the agreement of the numerical and theoretical curves is excellent.
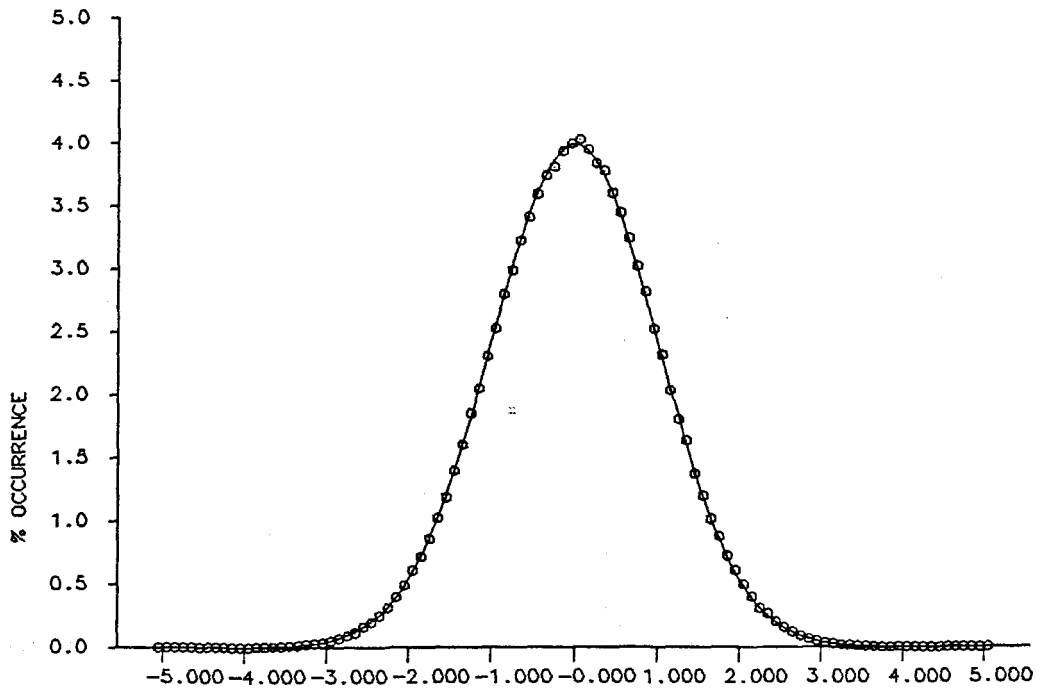
Figure 4-1

Normally Distributed Random Numbers

4.2 The Gaussian White Noise Random Process

Of interest to this work is the class of random processes that are stationary and ergodic and whose independent variable is time. Stationarity is the property by which the process probability structure, that is, the probability density functions of all orders, is invariant under a time shift, and ergodicity is the property by which statistical properties, for instance moments (mean, variance, etc), calculated in time with one realization of the process are the same as if they were calculated based on an ensemble of several realizations of the process [27].

A stationary Gaussian or normal random process is a stationary random process whose first- and second-order probability density functions are given respectively by [15]:

$$p(z_1) = \frac{1}{\sqrt{2\pi}\sigma} \exp\left[-\frac{(z_1 - \mu)^2}{2\sigma^2}\right] \quad \text{for} \quad -\infty < z_1 < +\infty, \quad (4.19)$$

and

$$p(z_1, z_2) = \frac{1}{2\pi\sigma^2\sqrt{1 - \rho_{12}^2}}$$

$$\times \exp\left\{\frac{-1}{2\sigma^2(1 - \rho_{12}^2)}\left[(z_1 - \mu)^2 - 2\rho_{12}(z_1 - \mu)(z_2 - \mu) + (z_2 - \mu)^2\right]\right\}$$

$$\text{for} \quad -\infty < z_1, z_2 < +\infty,$$

$$(4.20)$$

where z_1 and z_2 are understood as being $z(t_1)$ and $z(t_2)$, the value of the process $z(t)$ at time t_1 and t_2, respectively. The parameters μ, σ and ρ_{12} are the mean, standard deviation and correlation coefficient of the distribution, defined as

$$\mu = E[z],$$

$$\sigma^2 = E[z^2] - \mu^2, \quad (4.21)$$

$$\rho_{12}^2 = \frac{E[(z_1 - \mu)(z_2 - \mu)]}{\sigma^2},$$

where $E[*]$ is the expectation operator. Because the process is stationary, the correlation coefficient is a function only of the time-lag $\tau = (t_2 - t_1)$, not of the individual times.

The autocorrelation function $R(\tau)$ of a stationary (and ergodic in the present application) random process is defined by

$$R(\tau) = E[z_1 z_2] = E[z(t)z(t + \tau)]$$
$$= \int_{-\infty}^{+\infty} S(\omega)e^{i\omega\tau}d\omega, \tag{4.22}$$

where ω is the circular frequency in radians-per-second (rad/s). The double-sided power spectral density function $S(\omega)$ is related to the autocorrelation function by

$$S(\omega) = \frac{1}{2\pi}\int_{-\infty}^{+\infty} R(\tau)e^{-i\omega\tau}d\tau. \tag{4.23}$$

Eqs. (4.22) and (4.23) relating $R(\tau)$ and $S(\omega)$ are the so-called Wiener-Khintchine relations.

In general, the complete specification of a random process would require the specification of probability density functions of all orders and therefore the specification of an infinite set of functions [27]. For the stationary Gaussian process, however, the knowledge of the mean and the autocorrelation function or the power spectral density function completely specifies the process [15].

A stationary random process in general, and a stationary Gaussian random process in particular, whose power spectral density function is uniform over the entire frequency range,

$$S(\omega) = S_0 \qquad \text{for } -\infty < \omega < +\infty, \qquad (4.24)$$

is called white noise [15,29]. This process, however, is physically unatainable because its mean square, which is the area under the power spectral density function curve, is infinite–hence the name "ideal" white noise.

It can be seen from Eq.(4.22) that the ideal white noise also possesses the property of being correlated only at the origin of the time-lags, because for $S(\omega) = S_0$, the autocorrelation function $R(\tau) = 2\pi S_0 \delta(\tau)$ where $\delta(\tau)$ is the Dirac delta function.

In practice, only the so-called "band-limited" white noise, whose power spectral density function is constant over certain bands of frequencies, is attainable:

$$S(\omega) = \begin{cases} S_0 & \text{if} & -\omega_2 < \omega < -\omega_1, \\ S_0 & \text{if} & +\omega_1 < \omega < +\omega_2, \\ 0 & \text{otherwise.} \end{cases} \qquad (4.25)$$

Of interest for the present application is the case of $\omega_1 = 0$ and $\omega_2 = \omega_c$, where ω_c is a cut-off frequency chosen so that the power spectral density function is approximately constant over all frequencies of interest.

Finally, having briefly reviewed the basic concepts of random vibrations, the forcing function for the simulations used in this work is defined as the stationary ergodic Gaussian white-noise random process $w(t)$ such that

$$E[w(t)] = 0$$

$$E[w(t)w(t + \tau)] = 2D\delta(\tau).$$

$$(4.26)$$

This forcing function is numerically realized by generating normally distributed random numbers at regular intervals of time Δt_1, using subroutine RANDZ. Because these simulations involve the time-domain integration of a nonlinear single degree-of-freedom oscillator, at regular discrete intervals of time Δt_2 ($\Delta t_2 \leq \Delta t_1$), the cut-off frequency ω_c will effectively be the Nyquist frequency $\omega_c = \pi/\Delta t$, where Δt is the lesser of Δt_1 or Δt_2. Although not necessary, in the present application the author chose to have $\Delta t_2 = \Delta t_1$.

The problem of choosing a cut-off frequency now reduces to the problem of choosing the time-step for the integration, and therefore one needs to address not only questions of accurate representation of the white noise over the band-width of the oscillator, but also questions of accuracy and stability of the numerical scheme being employed in the step-by-step integration procedure.

4.3 The Numerical Step-by-Step Integration Procedure

There are currently available a very large number of schemes for the solution of initial value problems composed of a single, second-order, nonlinear differential equation with constant coefficients [1,34]. The author chose to implement the Newmark method in association with the Newton-Raphson method. The Newmark method when applied to linear systems: (a) is second order accurate; (b)

does not exhibit amplitude decay; (c) exhibits period elongation that can be made very small by appropriate choice of Δt; and (d) can be made unconditionally stable; that is, the stability of the solutions can be made independent of the size of the time-step Δt, by appropriate choices of the method parameters. The Newton-Raphson method, on the other hand, is also second order accurate and therefore, the combination should produce a good integration scheme.

In addition, because a single second-order equation is being solved, the scheme was made explicit before implementation by solving for displacement and velocity at time-step $(n + 1)$ as functions of displacement, velocity, acceleration and force at time-step (n) and force at time-step $(n + 1)$. The result was a fast and efficient computer code.

Although the scheme is second order accurate, there is no means of controlling the error at each time-step. Because of the concern that this local error could accumulate and grow unbounded after a very large number of time-steps, the author, as a means of verification, also used a higher order integration scheme that allowed the control of local errors. The results, as will be seen in the next chapter, indicate that the Newmark/Newton-Raphson scheme is sufficiently accurate with the added advantage of being more than an order of magnitude faster than the more accurate method.

4.3.1 The Newmark Method

Consider that the single degree-of-freedom (SDOF) nonlinear system of interest has the corresponding second-order differential equation of the form

$$\ddot{x} + f(\dot{x}, x) = w(t), \qquad (4.27)$$

where x, $\dot{x}$ and $\ddot{x}$ are the displacement, velocity and acceleration, respectively; $f(\dot{x}, x)$ is a nonlinear function of $\dot{x}$ and x, and $w(t)$ is the stationary Gaussian white noise forcing function defined in the previous sections.

The numerical integration scheme will satisfy Eq. (4.27), at least approximately, at discrete time intervals Δt apart. The discrete counterpart of Eq. (4.27), then, is

$$a_{n+1} + f(v_{n+1}, d_{n+1}) = w_{n+1}, \qquad (4.28)$$

where d_{n+1}, v_{n+1} and a_{n+1} are the approximate displacement, velocity and acceleration of the system defined by Eq. (4.27) at the discrete time-step $(n + 1)$, and w_{n+1} is the forcing function at the same time.

The following assumptions are used by the Newmark method to solve for the discrete displacements and velocities

$$d_{n+1} = d_n + \Delta t v_n + (\Delta t)^2 [(\frac{1}{2} - \alpha)a_n + \alpha a_{n+1}],$$

$$v_{n+1} = v_n + \Delta t [(1 - \delta)a_n + \delta a_{n+1}],$$

(4.29)

where the subscripts n and $(n + 1)$ indicate quantities at time-step n and $(n + 1)$, respectively, and α and δ are parameters that govern the stability and accuracy of the method. For the present application the author chose $\alpha = 1/4$ and $\delta = 1/2$, which render the method unconditionally stable [1]. Substitution of these values into Eq. (4.29) yields

$$d_{n+1} = d_n + \Delta t v_n + \left(\frac{\Delta t}{2}\right)^2 (a_n + a_{n+1}),$$

$$v_{n+1} = v_n + \left(\frac{\Delta t}{2}\right)(a_n + a_{n+1}).$$

(4.30)

Solving for d_{n+1} and v_{n+1} as functions of d_n, v_n, a_n, w_n and w_{n+1} from Eqs. (4.28), (4.30) and Eq. (4.28) evaluated at time step n yields

$$d_{n+1} + \left(\frac{\Delta t}{2}\right)^2 f(v_{n+1}, d_{n+1}) = d_n + \Delta t v_n + \left(\frac{\Delta t}{2}\right)^2 (a_n + w_{n+1}),$$

$$v_{n+1} + \left(\frac{\Delta t}{2}\right) f(v_{n+1}, d_{n+1}) = v_n + \left(\frac{\Delta t}{2}\right)(a_n + w_{n+1}).$$

(4.31)

The coupled nonlinear set of difference Eqs. (4.31) will be solved at each time-step with the aid of the Newton-Raphson procedure. Once d_{n+1} and v_{n+1} are obtained, a_{n+1} is obtained with Eq. (4.28).

Because the method, with the chosen parameters is unconditionally stable, the only concern in choosing Δt is with accuracy. Some authors [1] recommend that $\frac{\Delta t}{T} \leq \frac{1}{10}$, where T is the minimum period of the system to be integrated. In the present application, the author chose $\frac{\Delta t}{T} = \frac{1}{20\pi}$, assuring that period elongation is virtually negligible [1].

4.3.2 The Newton-Raphson Method

Consider that the system of Eqs. (4.31) can be symbolically written in the following form

$$\mathbf{N(d)} = \mathbf{F}, \tag{4.32}$$

where $\mathbf{N}$ is the vector composed of the left-hand side of Eq. (4.31), whose components are nonlinear functions of $\mathbf{d}$, the vector composed of d_{n+1} and v_{n+1}, and $\mathbf{F}$ is the load vector composed of the right-hand side of Eq. (4.31).

The basic idea behind the Newton-Raphson method, and any other method for solving nonlinear equations, is:

(1) Initialization: guess an approximate solution, $\mathbf{d}^0$, for Eq. (4.32);

(2) Iteration: from $\mathbf{d}^i$ calculate an improved approximation $\mathbf{d}^{i+1}$;

(3) Test: test for convergence of $\mathbf{d}^{i+1}$, if converged set $\mathbf{d} = \mathbf{d}^{i+1}$, otherwise, go to step (2).

The following iteration procedure is used by the Newton-Raphson method

$$DN(\mathbf{d}^i)(\mathbf{d}^{i+1} - \mathbf{d}^i) = \mathbf{F} - \mathbf{N}(\mathbf{d}^i), \qquad (4.33)$$

$$\vdots$$

where DN is the Jacobian matrix given by

$$DN = \left[\frac{\partial N_p}{\partial d_q}\right] \qquad \text{for } 1 \leq p, q \leq n_{eq}. \qquad (4.34)$$

Applying the Newton-Raphson method to Eq. (4.31), considering that in this case $n_{eq} = 2$, and solving for d_{n+1}^{i+1} and v_{n+1}^{i+1} leads to

$$d_{n+1}^{i+1} = d_{n+1}^i + \frac{1}{\Delta_{n+1}^i}\left[(F_{1,n+1} - N_{1,n+1})\frac{\partial N_{2,n+1}}{\partial v_{n+1}} - (F_{2,n+1} - N_{2,n+1})\frac{\partial N_{1,n+1}}{\partial v_{n+1}}\right]^i,$$

$$v_{n+1}^{i+1} = v_{n+1}^i + \frac{1}{\Delta_{n+1}^i}\left[(F_{1,n+1} - N_{1,n+1})\frac{\partial N_{2,n+1}}{\partial d_{n+1}} - (F_{2,n+1} - N_{2,n+1})\frac{\partial N_{1,n+1}}{\partial d_{n+1}}\right]^i,$$

$$(4.35)$$

where the components of the vector $\mathbf{N}$ are given by

$$N_{1,n+1} = d_{n+1} + \left(\frac{\Delta t}{2}\right)^2 f(v_{n+1}, d_{n+1}),$$

$$(4.36)$$

$$N_{2,n+1} = v_{n+1} + \left(\frac{\Delta t}{2}\right) f(v_{n+1}, d_{n+1});$$

the components of the vector $\mathbf{F}$ are given by

$$F_{1,n+1} = d_n + \Delta t v_n + \left(\frac{\Delta t}{2}\right)^2 (a_n + w_{n+1}),$$

$$F_{2,n+1} = v_n + \left(\frac{\Delta t}{2}\right)(a_n + w_{n+1});$$

(4.37)

the components of the Jacobian matrix $D\mathbf{N}$ are given by

$$\frac{\partial N_{1,n+1}}{\partial d_{n+1}} = 1 + \left(\frac{\Delta t}{2}\right)^2 \frac{\partial f(v_{n+1}, d_{n+1})}{\partial d_{n+1}},$$

$$\frac{\partial N_{1,n+1}}{\partial v_{n+1}} = \left(\frac{\Delta t}{2}\right)^2 \frac{\partial f(v_{n+1}, d_{n+1})}{\partial v_{n+1}},$$

$$\frac{\partial N_{2,n+1}}{\partial d_{n+1}} = \left(\frac{\Delta t}{2}\right) \frac{\partial f(v_{n+1}, d_{n+1})}{\partial d_{n+1}},$$

$$\frac{\partial N_{2,n+1}}{\partial v_{n+1}} = 1 + \left(\frac{\Delta t}{2}\right) \frac{\partial f(v_{n+1}, d_{n+1})}{\partial v_{n+1}};$$

(4.38)

and Δ_{n+1}, the determinant of the Jacobian matrix $D\mathbf{N}$, is

$$\Delta_{n+1} = \frac{\partial N_{1,n+1}}{\partial d_{n+1}} \frac{\partial N_{2,n+1}}{\partial v_{n+1}} - \frac{\partial N_{1,n+1}}{\partial v_{n+1}} \frac{\partial N_{2,n+1}}{\partial d_{n+1}}.$$

(4.39)

Eqs. (4.35) were implemented in the subroutine DESOL that is part of the code included in the Appendix A, used for the time-domain simulations that will be discussed in the next chapter.

CHAPTER V

CASE STUDIES

In this chapter the accuracy of the Method of Equivalent Nonlinearization will be investigated with the simulation of the reponse, to white-noise random excitation of several single degree-of-freedom (SDOF) systems with varying degrees of different nonlinearities.

To this end, a computer program was developed to compute the simulated steady-state probability density functions (histograms) for the displacement, velocity and energy-based envelope responses for each system considered. The program, included in Appendix A, uses the subroutines RANDU, RANDZ and DESOL, whose algorithms were discussed in the previous chapter. The program also has logic for the comparison of the simulated histograms with their corresponding approximate probability density functions (histograms) obtained by the Method of Equivalent Nonlinearization.

Initially, the response histograms of a linear SDOF system are compared with the corresponding well-known theoretical histograms. The purpose of this exercise is to determine the minimum time-history length necessary to obtain adequate representation for each of the histograms. The accuracy of the subroutine DESOL is also assessed at this time, by comparing the responses obtained with DESOL with

the responses obtained with the more accurate subroutine MODDEQ. Once the accuracy of the computer code and the length of the time-histories are ascertained, the simulations for the nonlinear systems are then performed.

5.1 Linear SDOF Systems

Consider the linear SDOF system of the form

$$\ddot{x} + 2\zeta\omega_n\dot{x} + \omega_n^2 x = w(t), \tag{5.1}$$

where x, $\dot{x}$ and $\ddot{x}$ are displacement, velocity and acceleration, respectively. $w(t)$ is the random stationary zero mean Gaussian white-noise forcing function defined in the previous chapter, and ζ and ω_n are the damping ratio and natural frequency of the system.

In this case, the Hamiltonian is $H(y, x) = y + \frac{\omega_n^2}{2}x^2$, and $f(H) = 2\zeta\omega_n$; therefore, applying Eq. (3.16), and evaluating the normalization constant A, yields the well-known joint probability density function of displacement and velocity for this system as

$$p(x, \dot{x}) = \frac{1}{2\pi\sigma_{\dot{x}}\sigma_x} \exp\left[-\frac{1}{2}\left(\frac{\dot{x}^2}{\sigma_{\dot{x}}^2} + \frac{x^2}{\sigma_x^2}\right)\right], \tag{5.2}$$

where

$$\sigma_{\dot{x}}^2 = \frac{D}{2\zeta\omega_n},$$

$$\sigma_x^2 = \frac{D}{2\zeta\omega_n^3}. \tag{5.3}$$

The (marginal) probability density function of $\dot{x}$ and x are, respectively,

$$p(\dot{x}) = \frac{1}{\sqrt{2\pi}\sigma_{\dot{x}}} \exp\left(-\frac{\dot{x}^2}{2\sigma_{\dot{x}}^2}\right),$$

$$p(x) = \frac{1}{\sqrt{2\pi}\sigma_x} \exp\left(-\frac{x^2}{2\sigma_x^2}\right). \tag{5.4}$$

In addition, the probability density function of the energy-based envelope α is given by the Rayleigh distribution, obtained from Eq. (3.19),

$$p_e(\alpha) = \frac{\alpha}{\sigma_x^2} \exp\left(-\frac{\alpha^2}{2\sigma_x^2}\right), \tag{5.5}$$

where at each instant in time α is defined as

$$\alpha = \sqrt{x^2 + \frac{\dot{x}^2}{\omega_n^2}}. \tag{5.6}$$

Figs. 5.1 through 5.3 show the comparison of theoretical and simulated histograms for the displacement, velocity and energy-based envelope, for different simulation lengths. Without loss of generality, the natural frequency of the system, ω_n, was chosen equal to 1.0, and for the purpose of comparison, the damping ratio, ζ, was taken equal to 0.01, typical of a narrow band process. The histograms with 100 cells were obtained for 100,000, 300,000 and 500,000 points
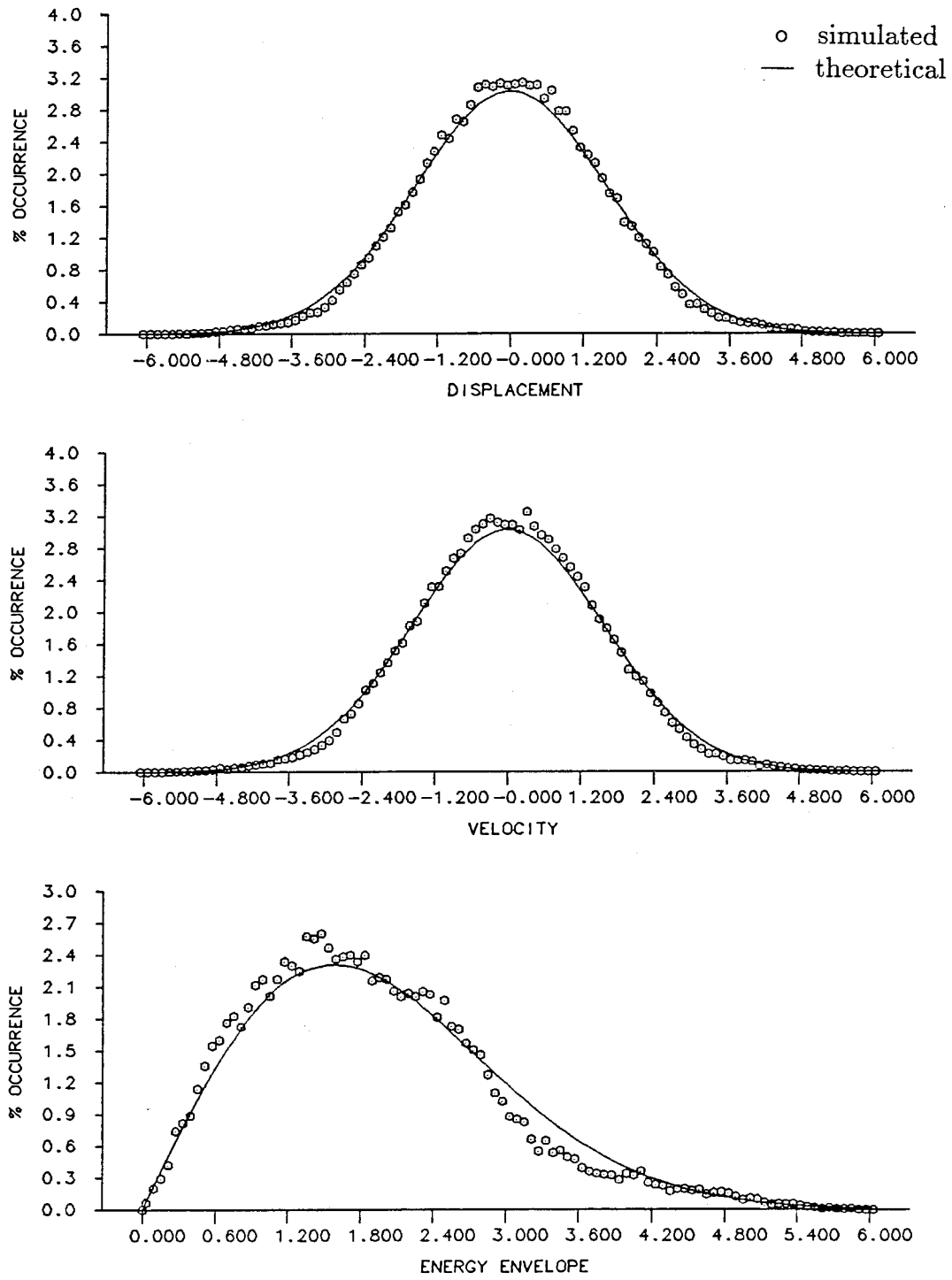
Figure 5.1

Linear Damping: $b_{01}\dot{x}$

$b_{01} = 0.02, \quad D = 0.05, \quad NPTS = 100,000$
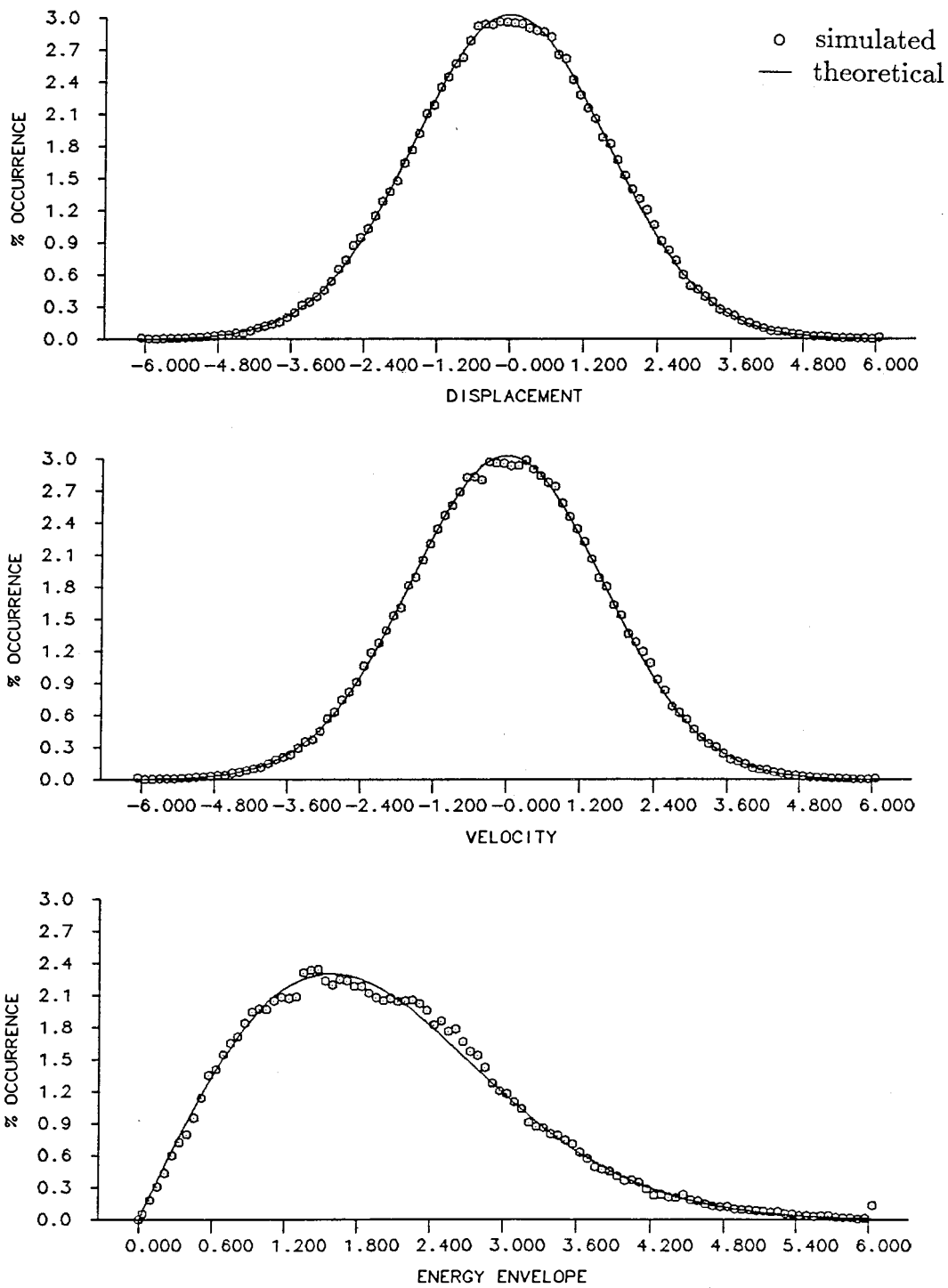
Figure 5.2

Linear Damping: $b_{01}\dot{x}$

$b_{01} = 0.02$, $D = 0.05$, $NPTS = 300,000$
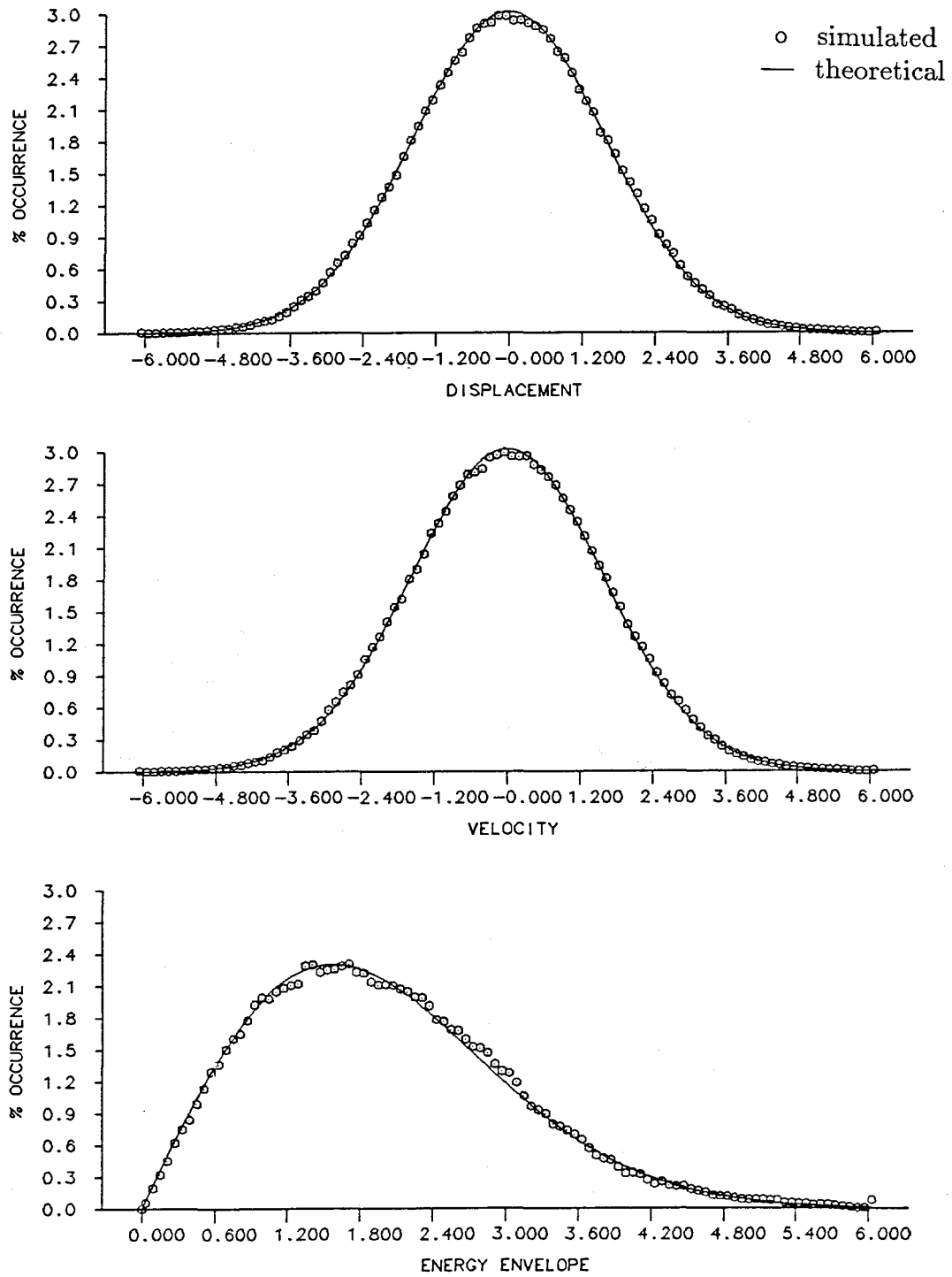
Figure 5.3

Linear Damping: $b_{01}\dot{x}$

$b_{01} = 0.02, \quad D = 0.05, \quad NPTS = 500,000$

spaced $\Delta t = 0.1$ s apart. An additional 20,000 points were used and discarded at the beginning of each simulation to insure that only the steady-state response was considered. Figs. 5.4 through 5.6 show the same comparison for a similar system with damping ratio equal to 0.20, typical of a wide-band process.

From these comparisons we can conclude that the length of time required to produce reasonable match between simulated and theoretical histograms depends on the characteristics of the system. The wide-band response required lengths of the order of 300,000 points (4,800 natural periods) while the narrow-band process required on the order of 500,000 points (7,900 natural periods). The length adopted henceforth, for all simulations, will be 500,000 points, with an additional 20,000 points discarded upfront to assure that only the steady-state response is considered in the computation of the histograms. Here, the implicit assumption is that this length is also sufficient for characterizing the histograms of nonlinear systems, the main object of this thesis.

Another important aspect surfacing from these comparisons is that even though the simulated histograms for displacement and velocity of a linear system have an exact theoretical solution, the agreement between the two is not perfect. Therefore, in principle, one may conclude that, for a nonlinear system, this would also be the best level of agreement to be expected between the simulated and the approximate solutions.

Fig. 5.7 shows results obtained using the more accurate subroutine MODDEQ for the same parameters as used for Fig. 5.2. In both cases a time-history length of 300,000 points was used. The subroutine MODDEQ was developed at Caltech in
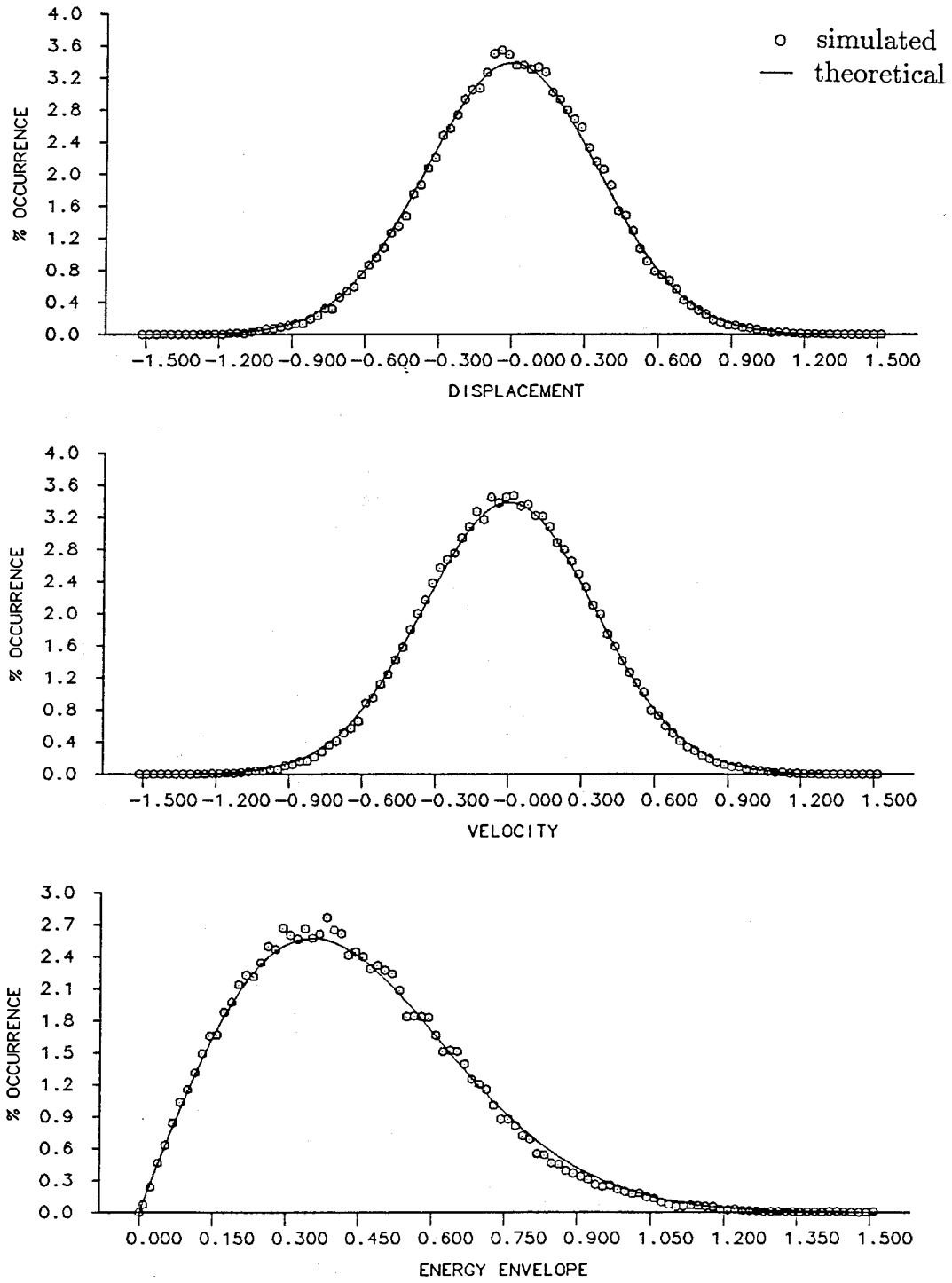
Figure 5.4

Linear Damping: $b_{01}\dot{x}$

$b_{01} = 0.40$, $D = 0.05$, $NPTS = 100,000$
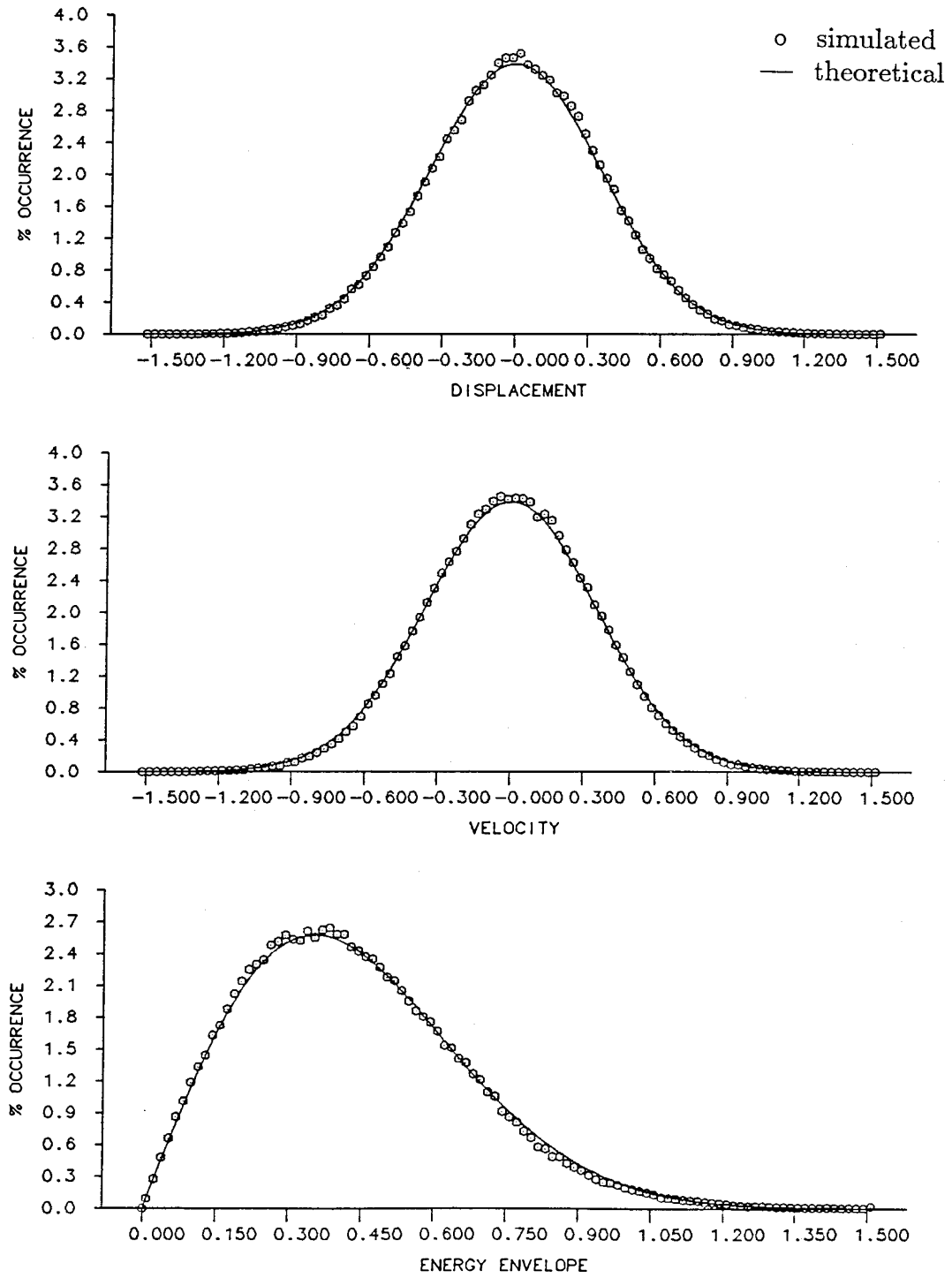
Figure 5.5

Linear Damping: $b_{01}\dot{x}$

$b_{01} = 0.40, \quad D = 0.05, \quad NPTS = 300,000$
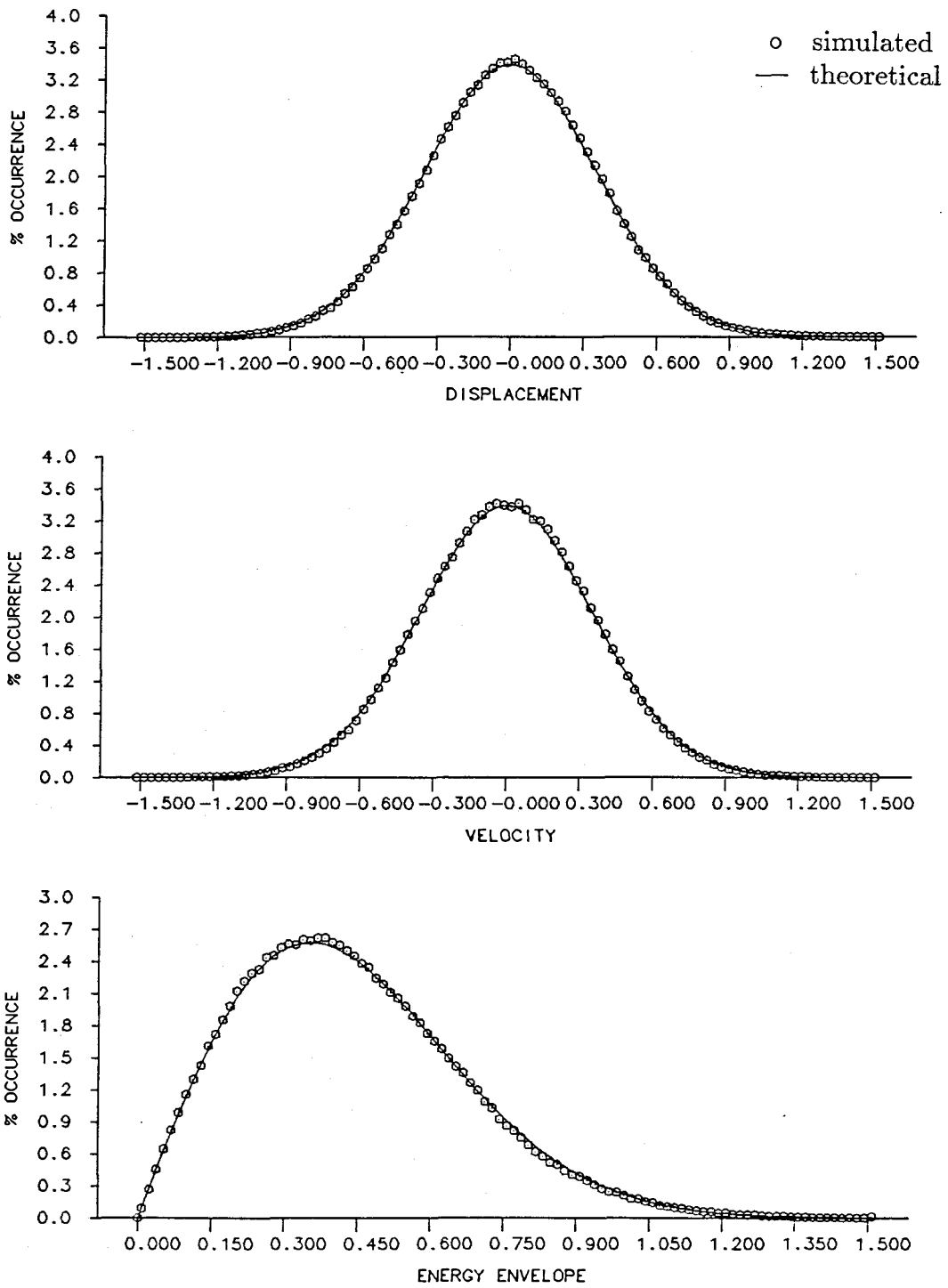
Figure 5.6

Linear Damping: $b_{01}\dot{x}$

$b_{01} = 0.40, \quad D = 0.05, \quad NPTS = 500,000$
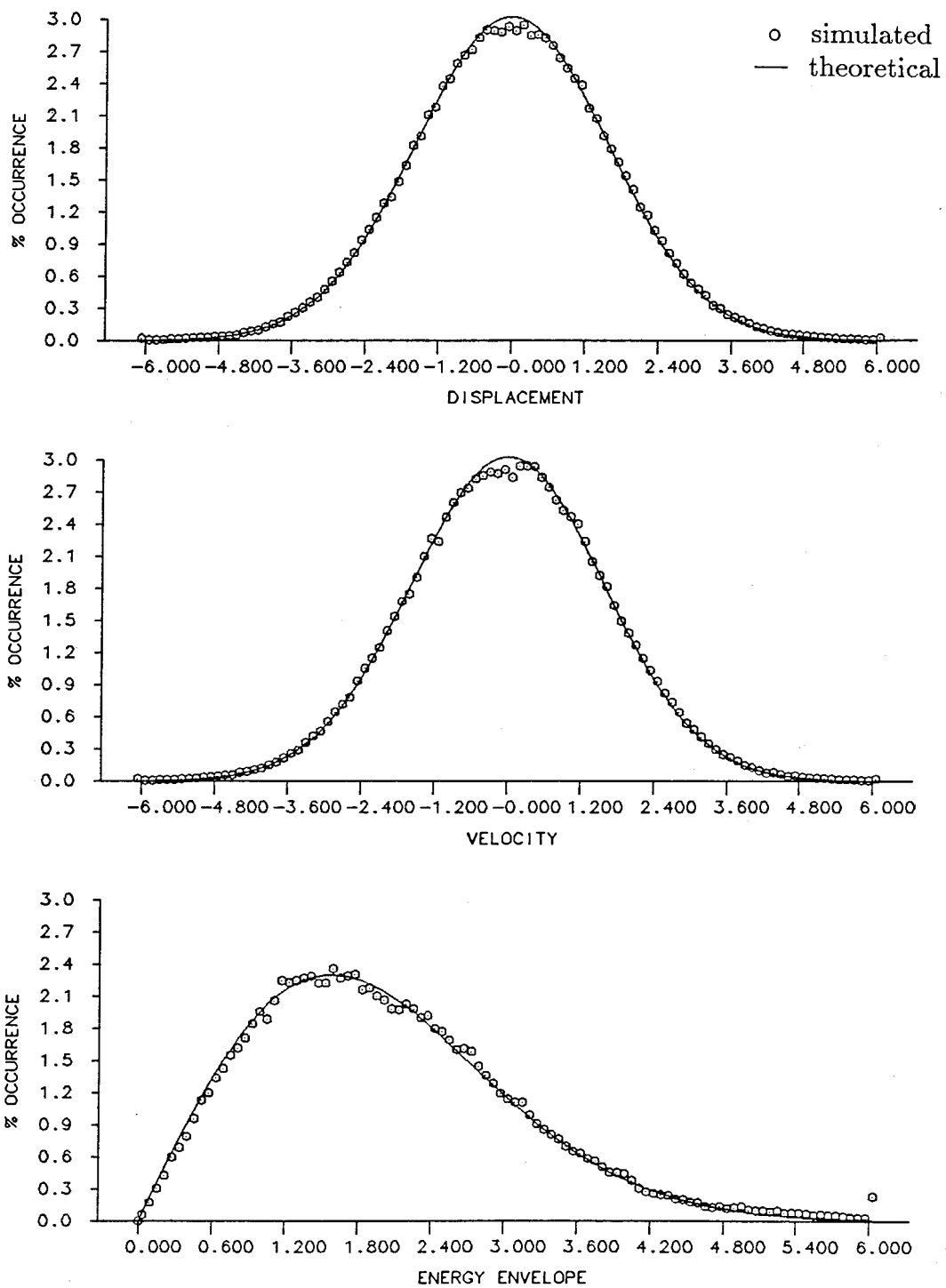
Figure 5.7

Linear Damping: $b_{01}\dot{x}$

$b_{01} = 0.02, \quad D = 0.05, \quad NPTS = 300,000$

the mid 70's and is based on the Adams-Moulton predictor corrector formulas using the Runge-Kutta-Gill method to start or restart the integration process. A write-up for the subroutine is included in Appendix B. The subroutine allows control over the local truncation error, which is achieved by subdividing the initial time-interval and restarting the integration process whenever local accuracy is not satisfied. Both sets of histograms were obtained with the same forcing function, which in the case of MODDEQ was linearly interpolated in order to allow subdivision of the initial time interval.

The comparison indicates that there are differences between the two results; however, these differences are minor overall (within the range of approximately 3 standard deviations from the mean) and do not justify the considerable expense to achieve higher accuracy. For this particular example of response simulation of a linear system, the program with MODDEQ took about 13 times longer to run than the program with DESOL. For a benchmark test, using a system with velocity fifth damping nonlinearity, this ratio was approximately the same. It is also noted that when interest lies in statistics of extremes, where the tail of the distribution is important, the differences between both subroutines become larger, and therefore more important. Under these circumstances the use of MODDEQ is more advisable in spite of the longer computational time required. For the purpose of this thesis, DESOL was used because it possesses the required accuracy and has the advantage of being considerably faster.

5.2 A Class of SDOF Systems with Linear Stiffness and Nonlinear Damping

A number of examples within this class of SDOF systems, discussed in Chapter III, are now solved with the purpose of illustrating and assessing the accuracy of the Method of Equivalent Nonlinearization. The joint probability density function of x and $\dot{x}$ and the probability density function of the energy-based envelope are generated and then compared with numerically simulated histograms.

5.2.1 Systems with Coulomb Damping

Consider the nonlinear SDOF system with Coulomb damping given by

$$\ddot{x} + b\,\text{sgn}(\dot{x}) + x = w(t), \tag{5.7}$$

which is obtained from Eq. (3.21) by making $b_{00} = b$, $b_{ij} = 0$ otherwise.

The following equivalent nonlinear equation replaces Eq. (5.7)

$$\ddot{x} + c_{00}f_{00}(H)\dot{x} + x = w(t), \tag{5.8}$$

which is obtained from Eq. (3.22) by making $c_{ij} = 0$ for all $i, j \neq 0$. The only f_{ij} term of interest is f_{00} obtained from Eq. (3.24) and given by

$$f_{00} = \frac{1}{a}. \tag{5.9}$$

The unknown coefficient c_{00} is the solution of

$$\pi c_{00} - 2b_{00}\frac{\Gamma(\frac{1}{2})\Gamma(1)}{\Gamma(\frac{3}{2})} = 0, \qquad (5.10)$$

obtained by direct substitution of the appropriate values in Eq. (3.33). Solving Eq. (5.10) yields $c_{00} = 4b_{00}/\pi$.

Recalling that $b_{00} = b$, direct substitution on Eq. (3.27) and evaluation of the normalization constant, A, yields the steady-state joint probability density function of x and $\dot{x}$ as

$$p(x, \dot{x}) = \left(\frac{1}{2\pi}\right)\left(\frac{4b}{\pi D}\right)^2 \exp\left[-\left(\frac{4b}{\pi D}\right)(x^2 + \dot{x}^2)^{\frac{1}{2}}\right], \qquad (5.11)$$

and substitution in Eq. (3.28) yields the probability density function of the energy-based envelope as

$$p_e(\alpha) = \left(\frac{4b}{\pi D}\right)^2 \alpha \exp\left[-\left(\frac{4b}{\pi D}\right)\alpha\right]. \qquad (5.12)$$

The expected value of α^2, $E[\alpha^2]$, then, is

$$E[\alpha^2] = \int_0^\infty \alpha^2 p_e(\alpha)d\alpha = \frac{6}{\left(\frac{4b}{\pi D}\right)^2}, \qquad (5.13)$$

and because of the symmetry of $p(x, \dot{x})$ with respect of x and $\dot{x}$ and because of the definition of α^2 $\left(= x^2 + \dot{x}^2\right)$, $E[x^2] = E[\dot{x}^2] = E[\alpha^2]/2$.

The response of the original nonlinear equation, Eq. (5.7), in principle, is a function of the two parameters b and D, the damping term coefficient and the parameter that controls the forcing function level. The response to the equivalent nonlinear equation, on the other hand, is a function of the ratio b/D. In order to assess the effect of b and D on the response of the original equation, two series of simulations were performed. In the first, D was kept constant and b varied over a fairly wide range of values in order to encompass cases of practical interest. In the second series, b was kept constant and D varied in such a way that the ratio b/D was the same in both series.

Figs. 5.8 through 5.11 show the results for the first series, which are the comparisons of theoretical and simulated histograms for the displacement, velocity and energy-based envelope. In these figures b was made equal to 0.02, 0.05, 0.10 and 0.20, respectively, and D was kept constant and equal to 0.05. This value of D produced a random forcing function with unit standard deviation. Fig. 5.10 and Figs. 5.12 through 5.14 show the results for the second series, for $b = 0.10$ and D equal to 0.05, 0.25, 0.10 and 0.025. As mentioned before, the histograms, with 100 cells, were obtained by sampling 500,000 points spaced $\Delta t = 0.1$ s apart. Steady-state response was assured by skipping an additional 20,000 points at the beginning of the simulations.

A number of conclusions can be drawn from this comparison:

(a) the response is indeed a function of the individual parameters b and D;

(b) the histograms of displacements and velocities tend to be equal, as predicted by theory, except that for large values of b/D (say, $\frac{b}{D} \geq 2.00$), the

distribution of displacements tend to be lower than predicted around zero and the distribution of velocities higher than predicted around the same region. These unbalances tend to compensate each other and produce a reasonably well-matched envelope;

(c) even though, in general, the equivalent nonlinear solutions follow the simulated results, it can be seen that the method works best for intermediate values of the damping coefficient (say, for $0.07 \leq b \leq 0.12$); and

(d) for intermediate to high values of the damping coefficient, the tails of the histograms are very long as evidenced by the points in the overflow cells outside the range considered.

Fig. 5.15 shows the comparison of the simulated and theoretical results for the $E[x^2]$, $E[\dot{x}^2]$ and the $E[\alpha^2]$ as functions of the ratio b/D. The solid line represents the theoretical results and the symbols,the simulated results, one set of symbols representing the points obtained with fixed D and the other with fixed b. Some of the observations that can be made based on this figure are:

(a) the theoretical results diverge from the simulated ones for low values of b/D (say, $\frac{b}{D} \leq 0.60$);

(b) given a low value for b/D, the response will be smaller for very small damping than for very large forcing; and

(c) the divergence between simulated and predicted responses for low values of b/D, coupled with the fact that the histograms are reasonably well matched, indicates that the tails of the response distributions for the original system is not being accurately modeled by the approximate theoretical solution.

It should be noted, however, that the approximate solution models the actual behavior quite well for values larger than $\frac{b}{D} = 0.40$ and overpredicts for smaller values of this ratio, therefore being on the conservative side.
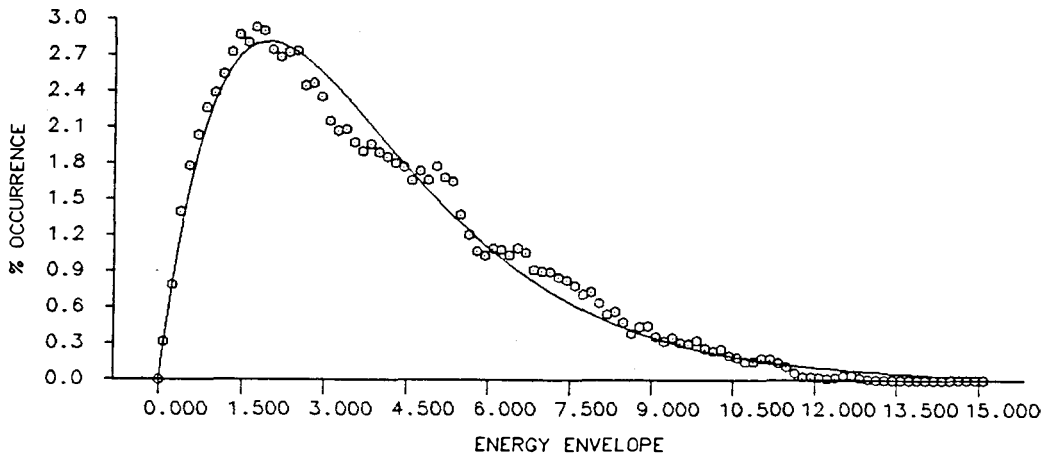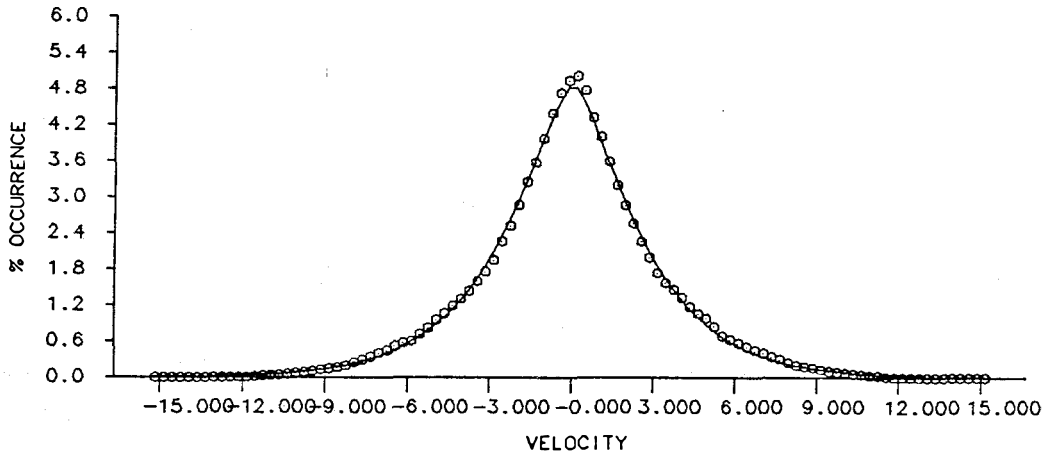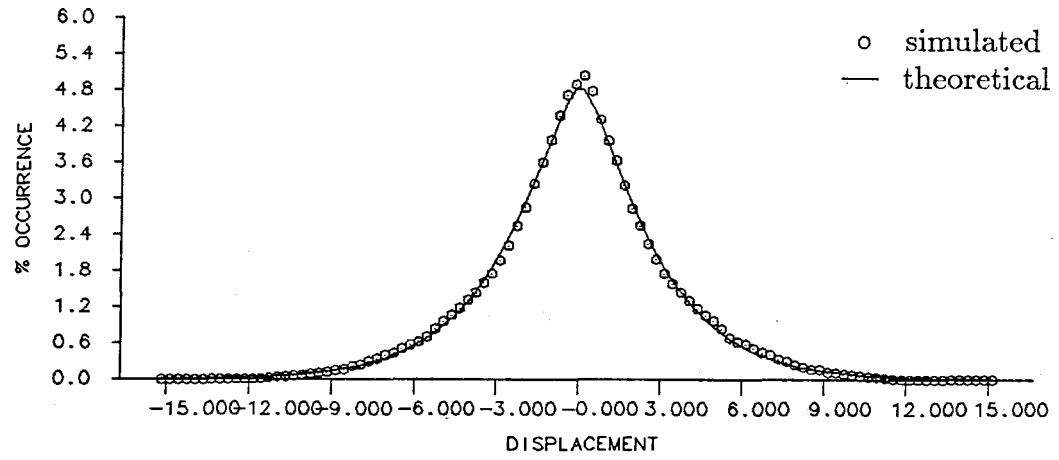
Figure 5.8

Coulomb Damping: b_{00} sgn($\dot{x}$)

$b_{00} = 0.02$, $D = 0.05$
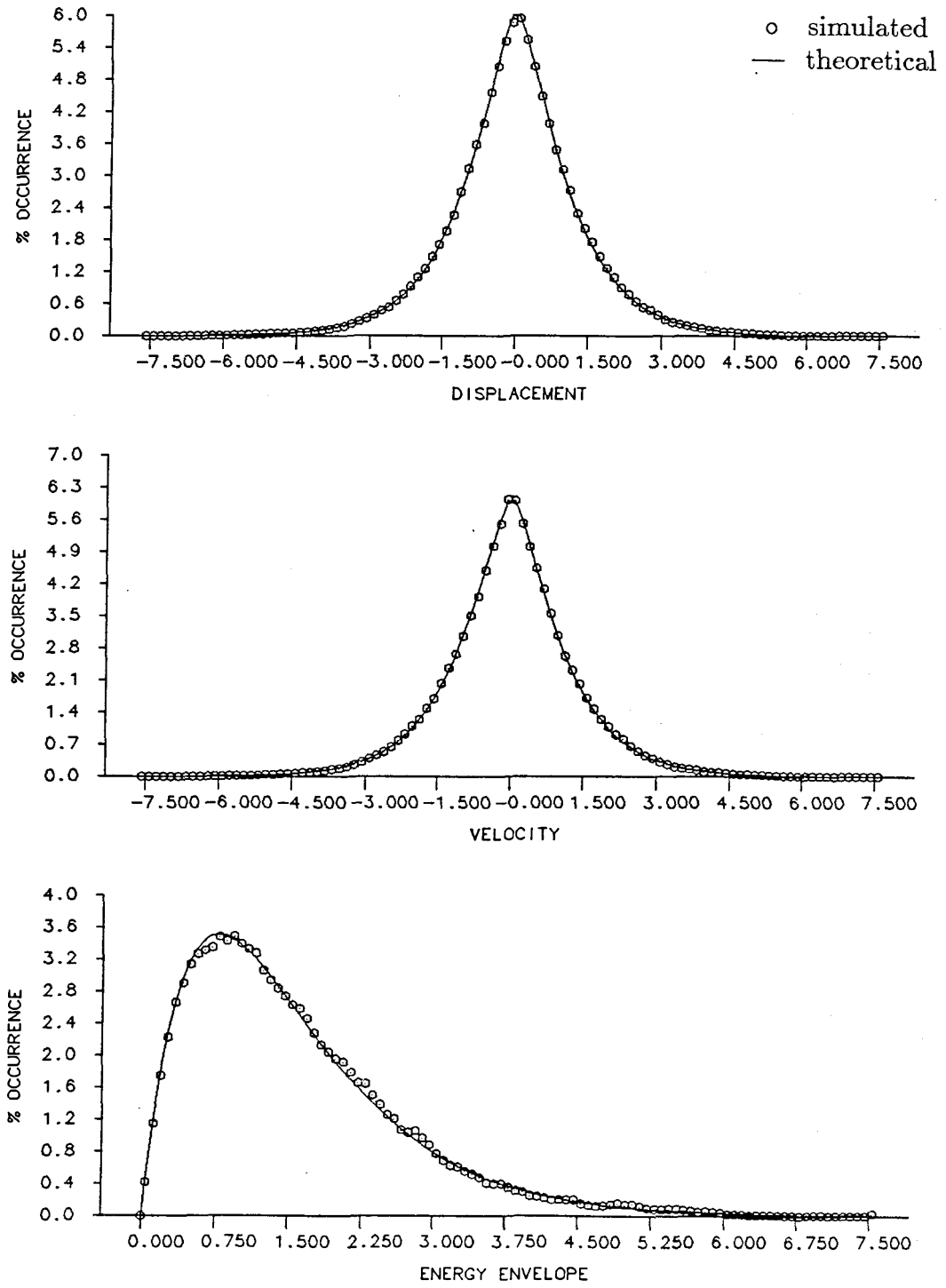
Figure 5.9

Coulomb Damping: b_{00} sgn$(\dot{x})$

$b_{00} = 0.05$, $D = 0.05$
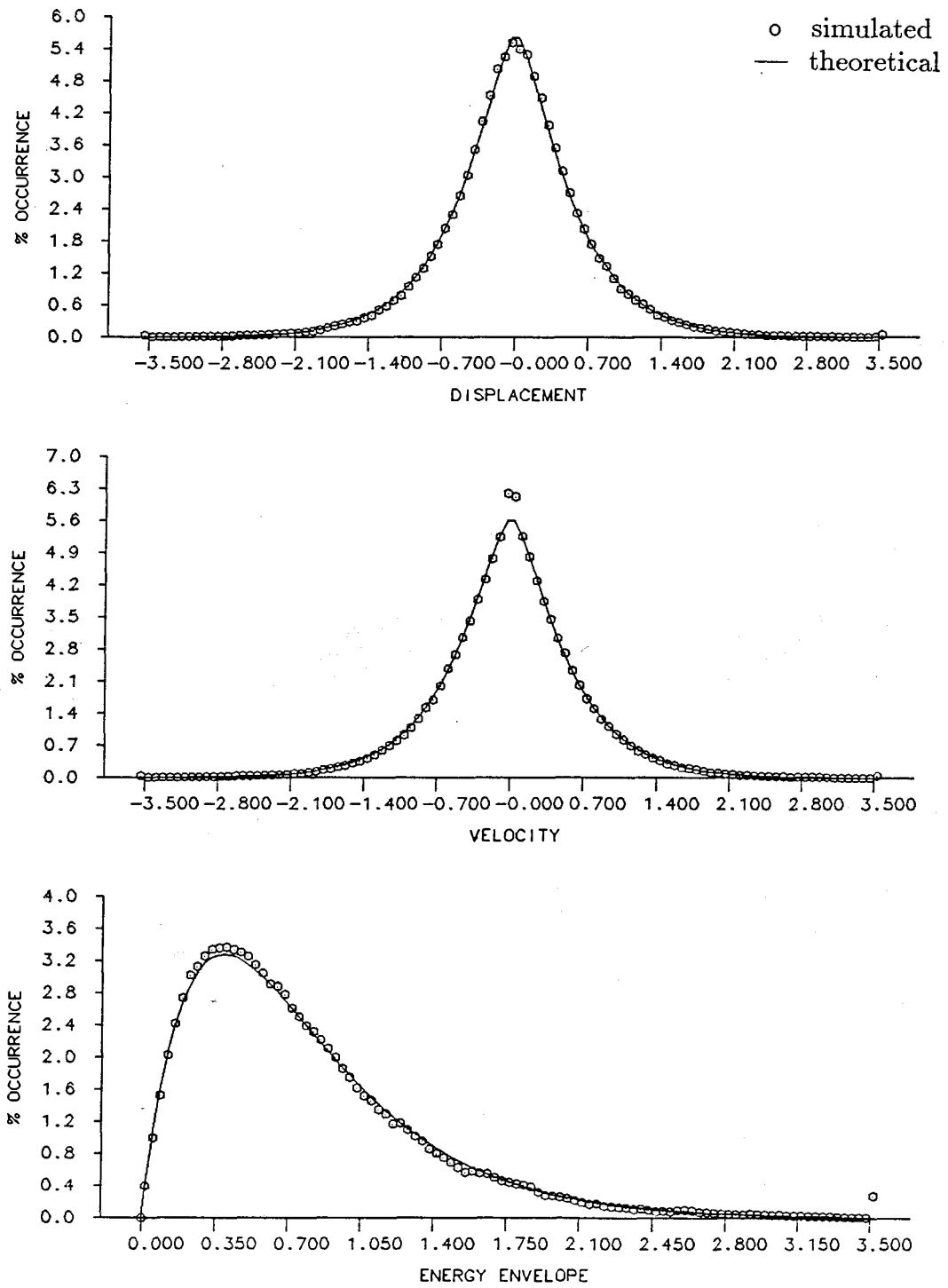
Figure 5.10

Coulomb Damping: b_{00} sgn$(\dot{x})$

$b_{00} = 0.10, \quad D = 0.05$
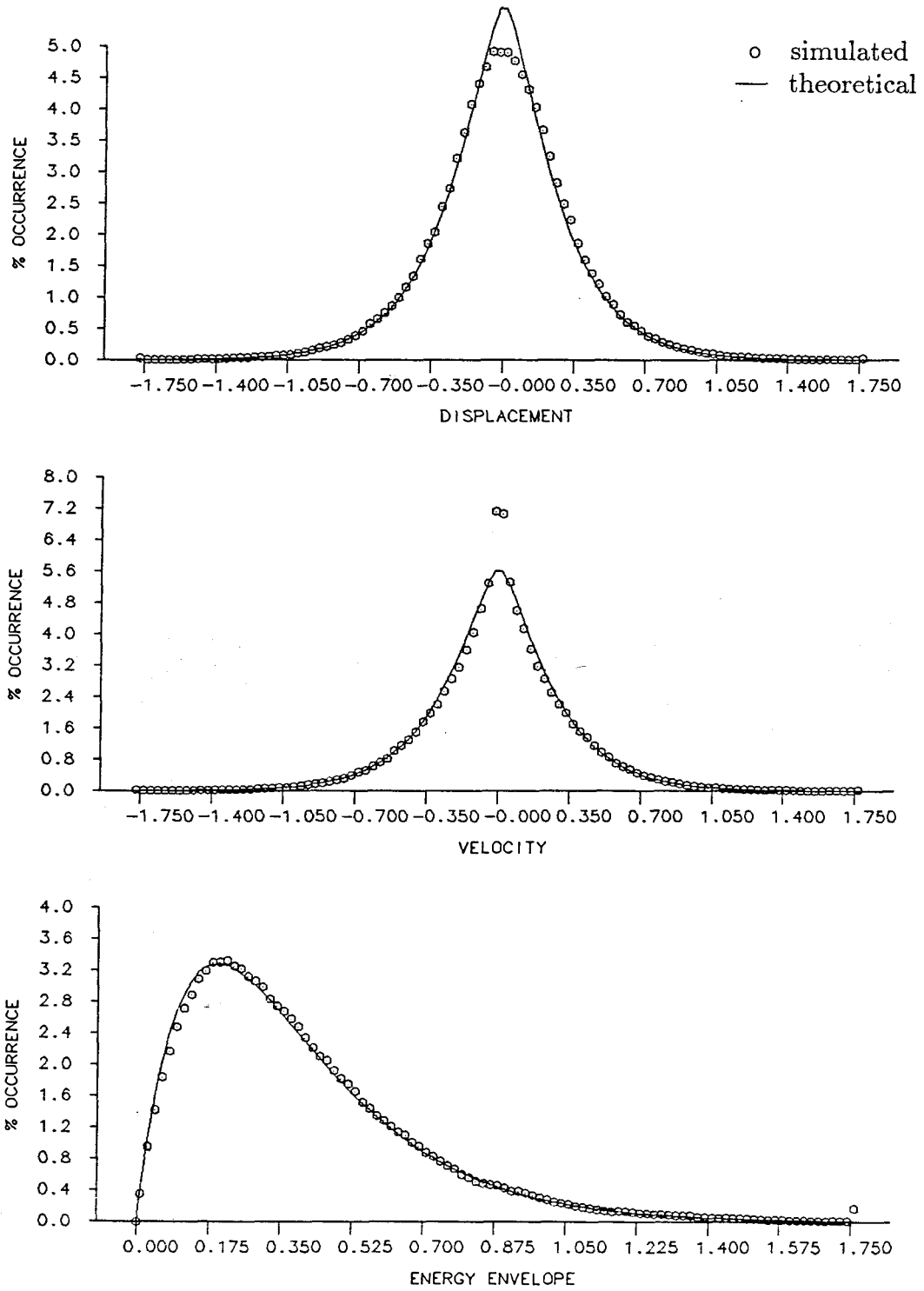
Figure 5.11

Coulomb Damping: b_{00} sgn($\dot{x}$)

$b_{00} = 0.20$, $D = 0.05$
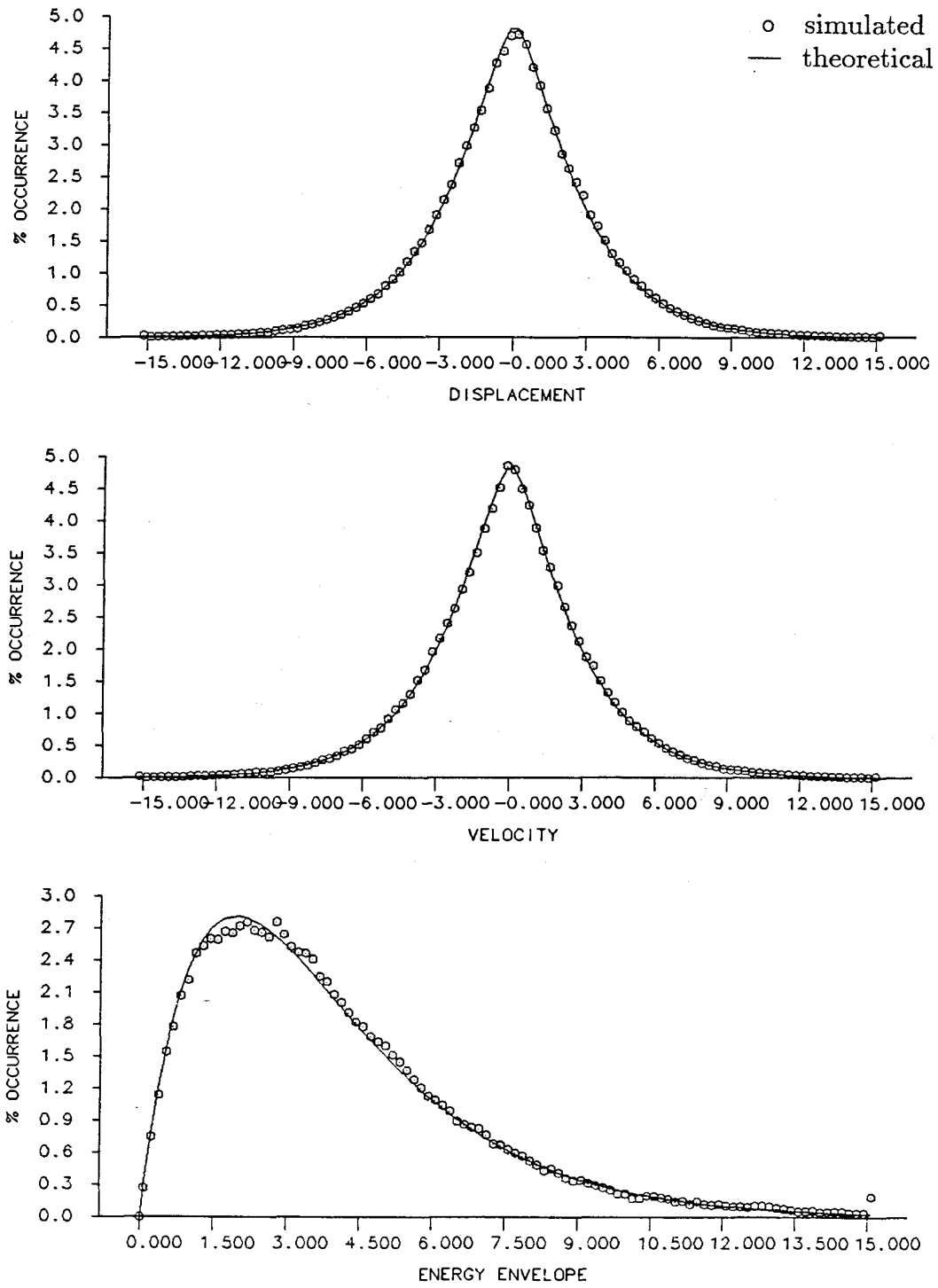
Figure 5.12

Coulomb Damping: b_{00} sgn($\dot{x}$)

$b_{00} = 0.10, \quad D = 0.25$
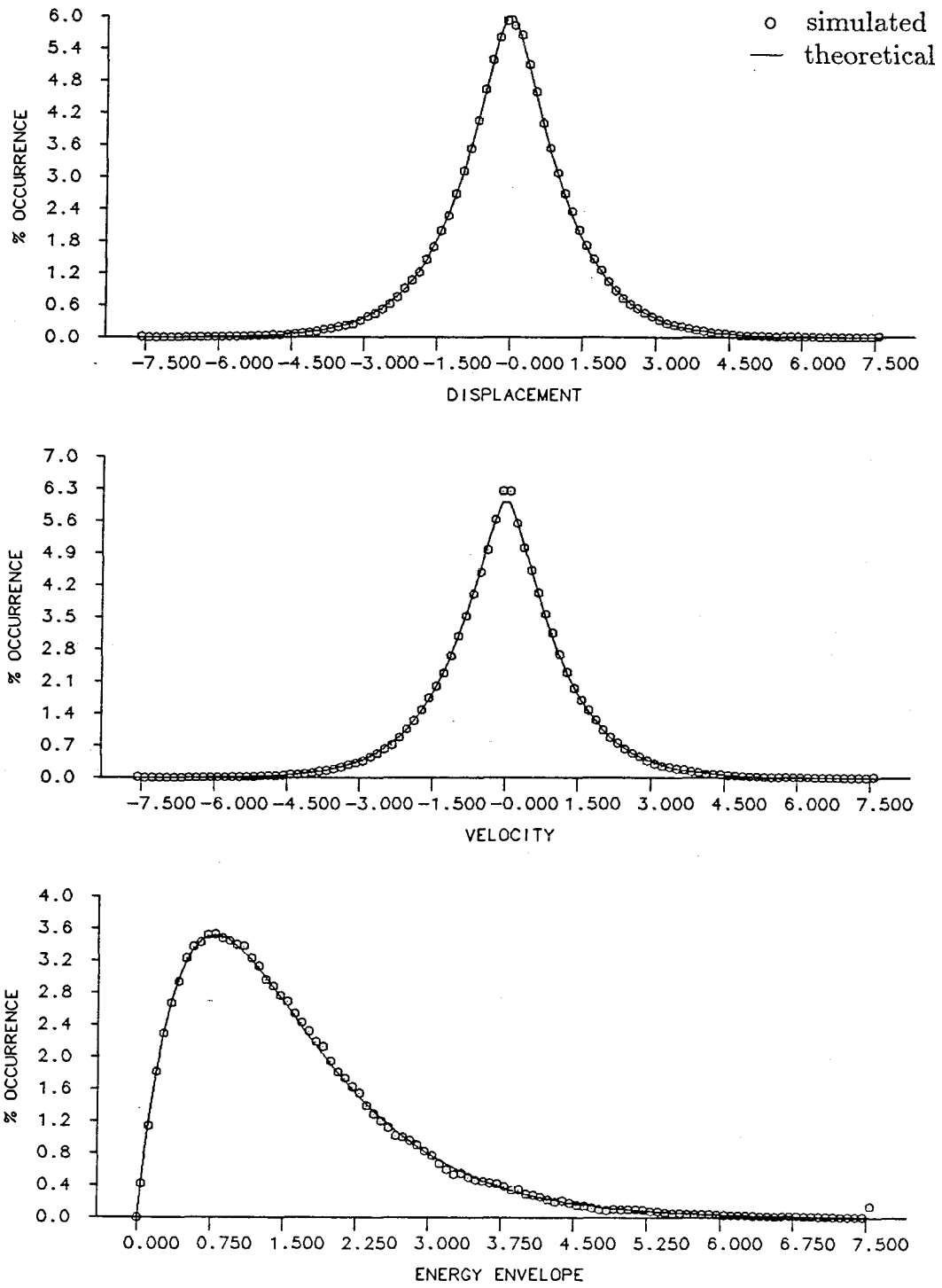
Figure 5.13

Coulomb Damping: b_{00} sgn$(\dot{x})$

$b_{00} = 0.10, \quad D = 0.10$
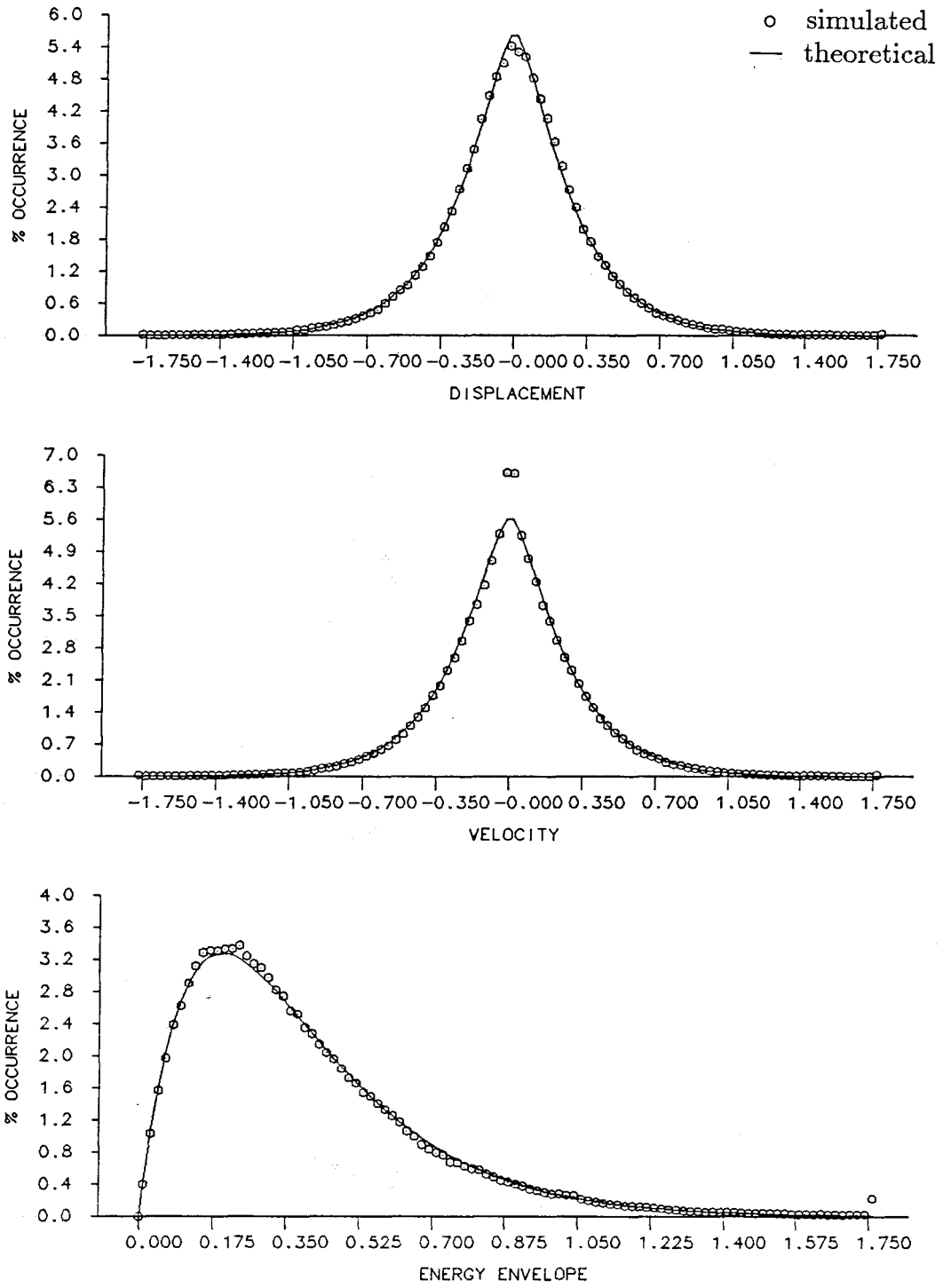
Figure 5.14

Coulomb Damping: b_{00} sgn($\dot{x}$)

$b_{00} = 0.10$, $D = 0.025$
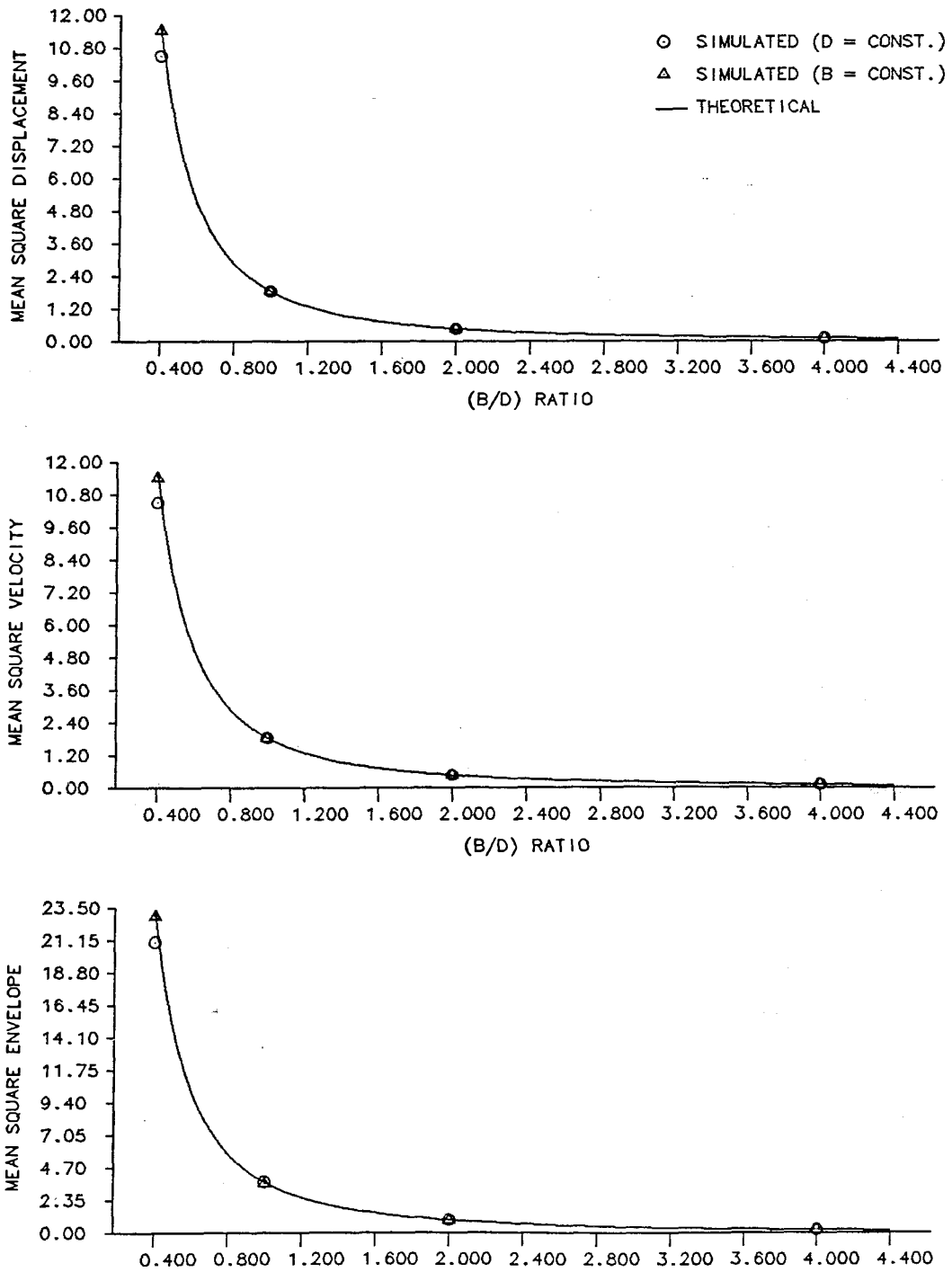
Figure 5.15

Mean-Square Response for Coulomb Damping

5.2.2 Systems with $(velocity)^m$-Damping

Consider the nonlinear SDOF system with $(velocity)^m$-damping given by

$$\ddot{x} + b\,|\dot{x}^m|\mathrm{sgn}(\dot{x}) + x = w(t), \qquad (5.14)$$

which is obtained from Eq. (3.21) by making $b_{0m} = b$, $b_{ij} = 0$ otherwise. The Coulomb damping case and the linear damping case previously studied are particular cases of Eq. (5.14), obtained by making $m = 0$ and $m = 1$, respectively.

The following equivalent nonlinear equation replaces Eq. (5.14):

$$\ddot{x} + c_{0m}f_{0m}(H)\dot{x} + x = w(t), \qquad (5.15)$$

which is obtained from Eq. (3.22) by making $c_{ij} = 0$ for all $i \neq 0$ and $j \neq m$. The only f_{ij} term of interest is f_{0m} obtained from Eq. (3.24) and given by

$$f_{0m} = a^{m-1}. \qquad (5.16)$$

The unknown coefficient c_{0m} is the solution of

$$\pi c_{0m} - 2b_{0m}\frac{\Gamma(\frac{1}{2})\Gamma(\frac{m+2}{2})}{\Gamma(\frac{m+3}{2})} = 0, \qquad (5.17)$$

obtained by direct substitution of the appropriate values in Eq. (3.33). Solving Eq. (5.17), recalling that $b_{0m} = b$, yields

$$c_{0m} = \frac{2}{\pi} \frac{\Gamma(\frac{1}{2})\Gamma(\frac{m+2}{2})}{\Gamma(\frac{m+3}{2})} b. \tag{5.18}$$

(a) Case of $(velocity)^2$-Damping

Evaluation of Eqs. (5.16) and (5.18) for $m = 2$ yields $f_{02} = a$ and $c_{02} = 8b/3\pi$, respectively.

Direct substitution of these values on Eq. (3.27) and evaluation of the normalization constant, A, yields the steady-state joint probability density function of x and $\dot{x}$ as

$$p(x, \dot{x}) = \left(\frac{1}{2\pi}\right) \left(\frac{3}{\Gamma(\frac{2}{3})}\right) \left(\frac{8b}{9\pi D}\right)^{\frac{2}{3}} \exp\left[-\left(\frac{8b}{9\pi D}\right)(x^2 + \dot{x}^2)^{\frac{3}{2}}\right], \tag{5.19}$$

and substitution in Eq. (3.28) yields the probability density function of the energy-based envelope as

$$p_e(\alpha) = \left(\frac{3}{\Gamma(\frac{2}{3})}\right) \left(\frac{8b}{9\pi D}\right)^{\frac{2}{3}} \alpha \exp\left[-\left(\frac{8b}{9\pi D}\right)\alpha^3\right]. \tag{5.20}$$

The expected value of α^2, $E[\alpha^2]$, then is

$$E[\alpha^2] = \int_0^\infty \alpha^2 p_e(\alpha) d\alpha = \frac{\Gamma(\frac{4}{3})}{\Gamma(\frac{2}{3})} \frac{1}{\left(\frac{8b}{9\pi D}\right)^{\frac{2}{3}}}. \tag{5.21}$$

(b) Case of $(velocity)^3$-Damping

Evaluation of Eqs. (5.16) and (5.18) for $m = 3$ yields $f_{03} = a^2$ and $c_{03} = 3b/4$, respectively.

Direct substitution of these values on Eq. (3.27) and evaluation of the normalization constant, A, yields the steady-state joint probability density function of x and $\dot{x}$ as

$$p(x, \dot{x}) = \left(\frac{1}{2\pi} \right) \left(\frac{4}{\Gamma(\frac{1}{2})} \right) \left(\frac{3b}{16D} \right)^{\frac{1}{2}} \exp \left[- \left(\frac{3b}{16D} \right) (x^2 + \dot{x}^2)^2 \right],$$

$$(5.22)$$

and substitution in Eq. (3.28) yields the probability density function of the energy-based envelope as

$$p_e(\alpha) = \left(\frac{4}{\Gamma(\frac{1}{2})} \right) \left(\frac{3b}{16D} \right)^{\frac{1}{2}} \alpha \exp \left[- \left(\frac{3b}{16D} \right) \alpha^4 \right].$$

$$(5.23)$$

The expected value of α^2, $E[\alpha^2]$, then is

$$E[\alpha^2] = \int_0^\infty \alpha^2 p_e(\alpha) d\alpha = \frac{1}{\Gamma(\frac{1}{2})} \frac{1}{\left(\frac{3b}{16D} \right)^{\frac{1}{2}}}.$$

$$(5.24)$$

(c) Case of $(velocity)^5$-Damping

Evaluation of Eqs. (5.16) and (5.18) for $m = 5$ yields $f_{05} = a^4$ and $c_{05} = 5b/8$, respectively.

Direct substitution of these values on Eq. (3.27) and evaluation of the normalization constant, A, yield the steady-state joint probability density function of x and $\dot{x}$ as

$$p(x, \dot{x}) = \left(\frac{1}{2\pi}\right) \left(\frac{6}{\Gamma(\frac{1}{3})}\right) \left(\frac{5b}{48D}\right)^{\frac{1}{3}} \exp\left[-\left(\frac{5b}{48D}\right)(x^2 + \dot{x}^2)^3\right],$$

(5.25)

and substitution in Eq. (3.28) yields the probability density function of the energy-based envelope as

$$p_e(\alpha) = \left(\frac{6}{\Gamma(\frac{1}{3})}\right) \left(\frac{5b}{48D}\right)^{\frac{1}{3}} \alpha \exp\left[-\left(\frac{5b}{48D}\right)\alpha^6\right].$$

(5.26)

The expected value of α^2, $E[\alpha^2]$, then, is

$$E[\alpha^2] = \int_0^\infty \alpha^2 p_e(\alpha)d\alpha = \frac{\Gamma(\frac{2}{3})}{\Gamma(\frac{1}{3})} \frac{1}{\left(\frac{5b}{48D}\right)^{\frac{1}{3}}}.$$

(5.27)

Cases (a), (b) and (c) above, because of the symmetry of $p(x, \dot{x})$ with respect to x and $\dot{x}$ and because of the definition of α^2 $\left(= x^2 + \dot{x}^2\right)$, will also have $E[x^2] = E[\dot{x}^2] = E[\alpha^2]/2$.

As in the Coulomb damping case, the response of the original nonlinear equation, Eq. (5.14), in principle, is a function of the two parameters b and D, the damping term coefficient and the parameter that controls the forcing function level. The response to the equivalent nonlinear equation, Eq. (5.15), on the other hand, is a function of the ratio b/D. In order to assess the effect of b and D on the response of the original equation, again, the two series of simulations performed

for the Coulomb damping case are repeated here for cases (a), (b) and (c) above, that is, for the $(velocity)^2$-, $(velocity)^3$- and $(velocity)^5$-damping cases. In the first series, D was kept constant and b varied over a fairly wide range of values in order to encompass cases of practical interest. In the second series, b was kept constant and D varied in such a way that the ratio b/D was the same in both series.

Figs. 5.16 through 5.19 show the comparison of theoretical and simulated histograms for the displacement, velocity and energy-based envelope, for the first series applied to the $(velocity)^2$-damping case. In these figures b was made equal to 0.02, 0.05, 0.10 and 0.20, respectively, and D was kept constant and equal to 0.05. This value of D produced a random forcing function with unit standard deviation. Fig. 5.18 and Figs. 5.20 through 5.22 show the results for the second series, for $b = 0.10$ and D equal to 0.05, 0.25, 0.10 and 0.025.

Fig. 5.23 shows the comparison of the simulated and theoretical results for the $E[x^2]$, $E[\dot{x}^2]$ and the $E[\alpha^2]$ as functions of the ratio b/D, for the $(velocity)^2$-damping case. The solid line represents the theoretical results and the symbols, the simulated results, one set of symbols representing the points obtained with fixed D and the other with fixed b.

Figs. 5.24 through 5.27 show the results for the first series applied to the $(velocity)^3$-damping case. Fig. 5.26 and Figs. 5.28 through 5.30 show the results for the second series. In these figures all parameters were kept the same as in the $(velocity)^2$-damping case.

Fig. 5.31 shows the comparison of the simulated and theoretical results for the $E[x^2]$, $E[\dot{x}^2]$ and the $E[\alpha^2]$ as functions of the ratio b/D, for the $(velocity)^3$-damping case.

Figs. 5.32 through 5.35 show the results for the first series applied to the $(velocity)^5$-damping case. Fig. 5.34 and Figs. 5.36 through 5.38 show the results for the second series. In these figures all parameters were kept the same as in the $(velocity)^2$-damping case.

Fig. 5.39 shows the comparison of the simulated and theoretical results for the $E[x^2]$, $E[\dot{x}^2]$ and the $E[\alpha^2]$ as functions of the ratio b/D, for the $(velocity)^5$-damping case.

Some of the conclusions that can be drawn from these comparisons are:

(a) the matching between predicted and simulated distributions is considerably better for this series of cases than for the Coulomb damping case;

(b) the response is indeed a function of the individual parameters b and D, but not as pronounced as in the Coulomb damping case;

(c) the histograms of displacements and velocities tend to be equal, as predicted by theory;

(d) for small values of b, the displacement, velocity and envelope distributions tend to be overpredicted around the zero region with a corresponding underprediction of the tail regions; this effect remains but is smaller for

larger damping values, and is particularly pronounced for the $(velocity)^5$-damping case, in which the crossover of the predicted and simulated distributions is clearly seen; and

(e) analysis of the mean-squared results indicate that there is a tendency of overprediction, as exaggerated by the $(velocity)^5$-damping case, but the differences between simulated and predicted results are within the range of the random uncertainty. This last statement is fully supported by the results obtained with the Van der Rayleigh equation, which are discussed in Section 5.2.4. An evaluation of any bias would require averaging of the results obtained from the realization of several simulations in order to eliminate any random errors.
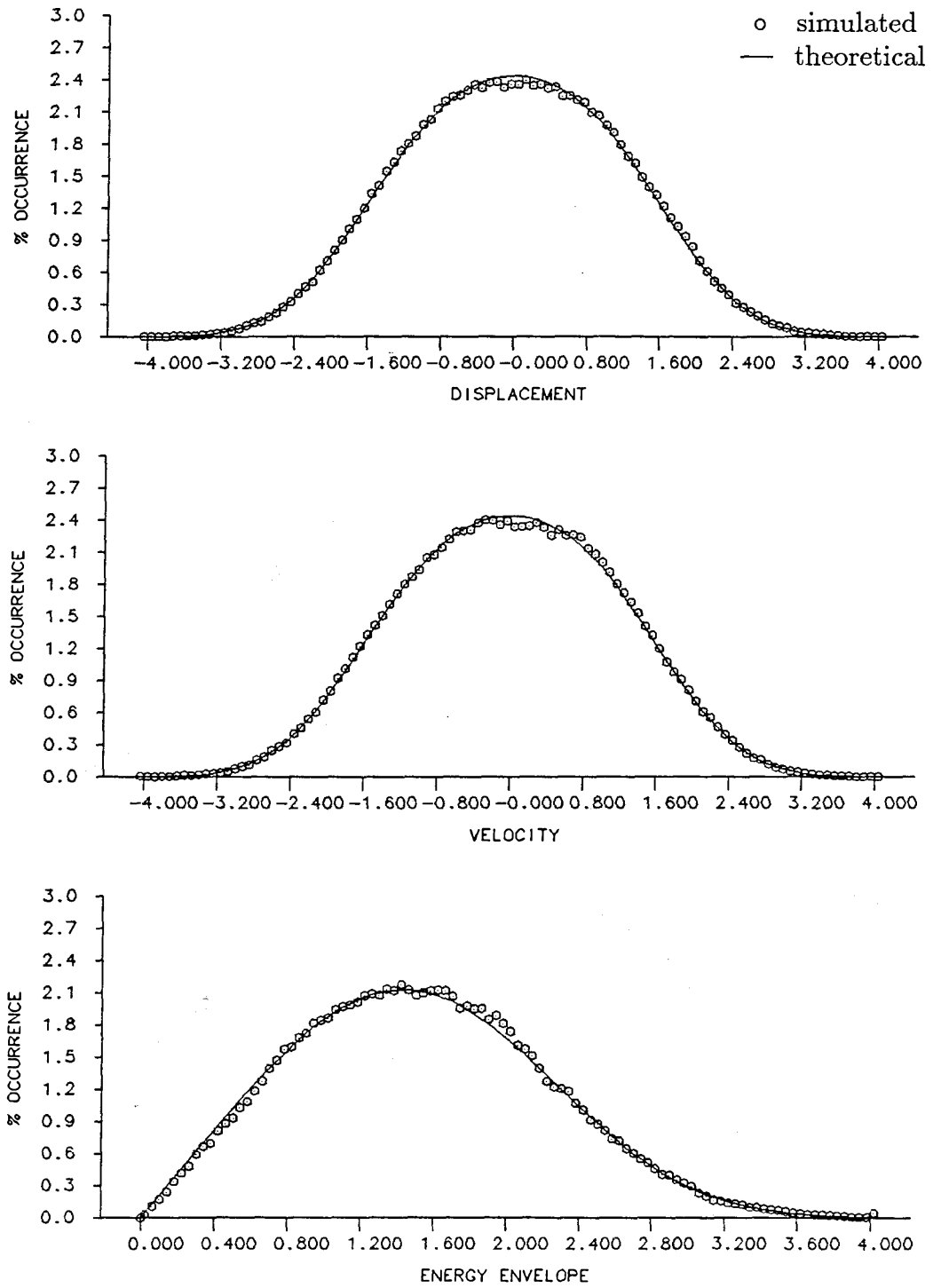
Figure 5.16

$(Velocity)^2$-Damping: $b_{02}\dot{x}^2 \, \text{sgn}(\dot{x})$

$b_{02} = 0.02, \quad D = 0.05$
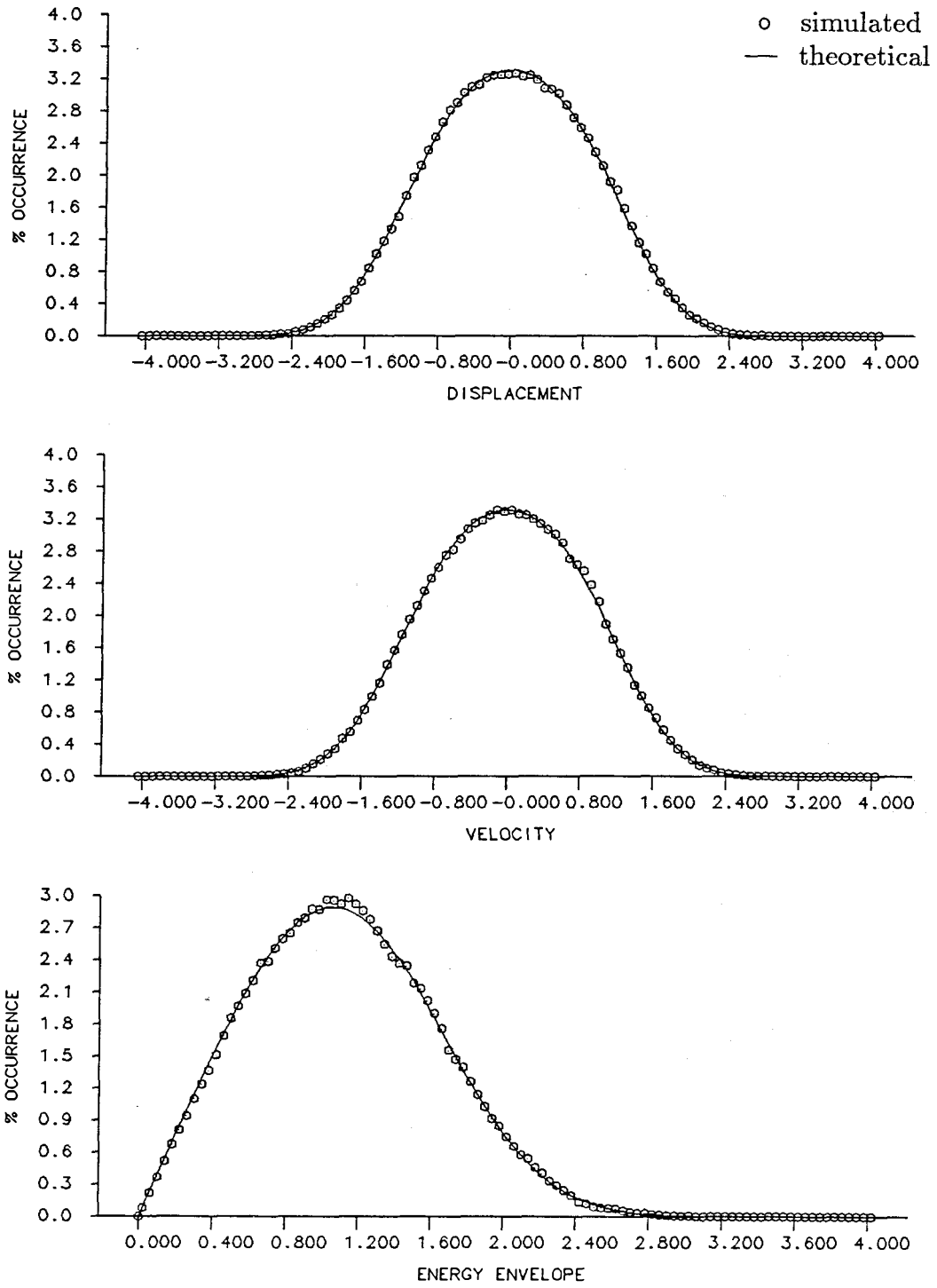
Figure 5.17

$(Velocity)^2$-Damping: $b_{02}\dot{x}^2$ sgn$(\dot{x})$

$b_{02} = 0.05$ $D = 0.05$
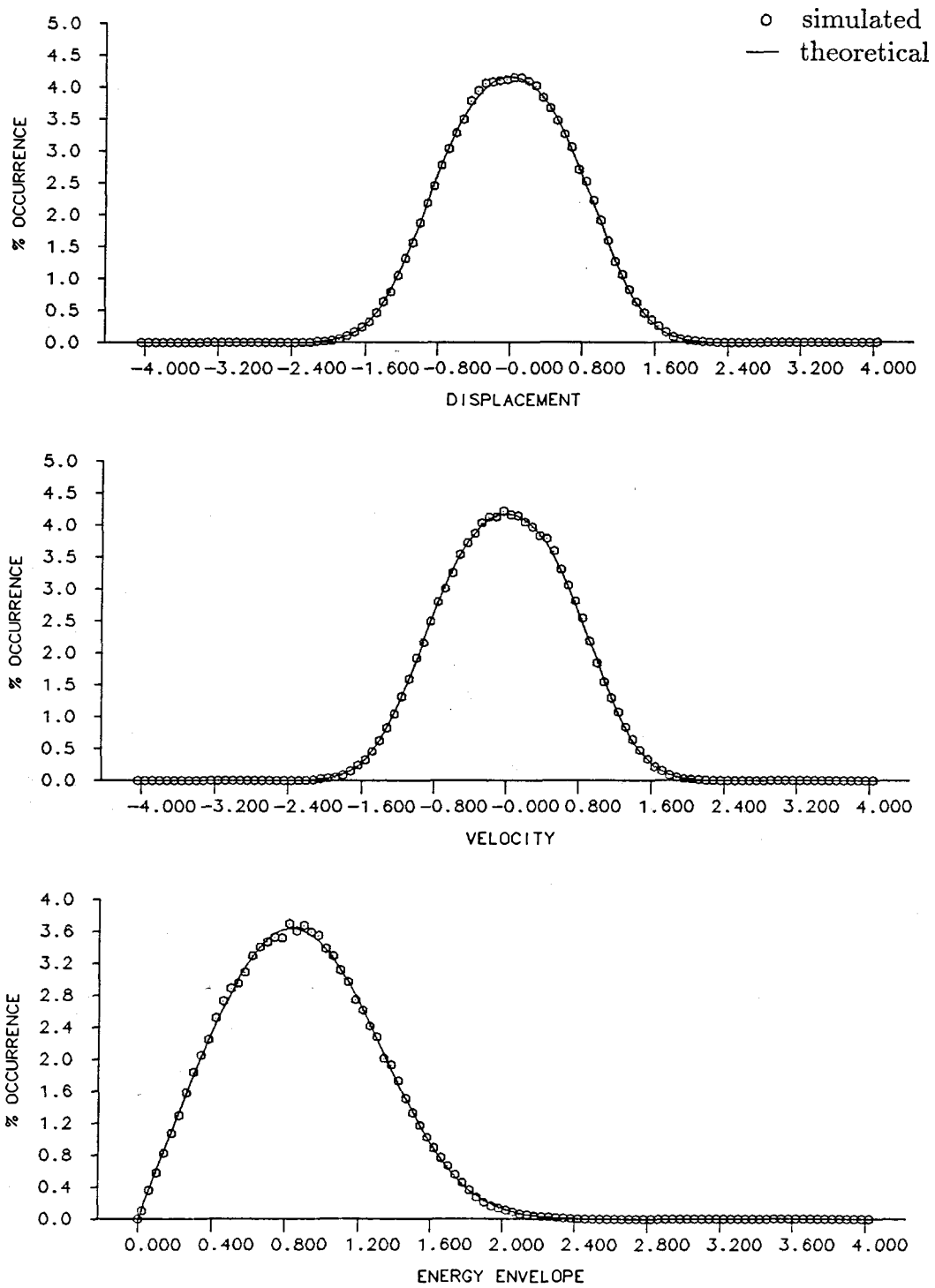
Figure 5.18

$(Velocity)^2$-Damping: $b_{02}\dot{x}^2 \, \mathrm{sgn}(\dot{x})$

$b_{02} = 0.10 \; D = 0.05$
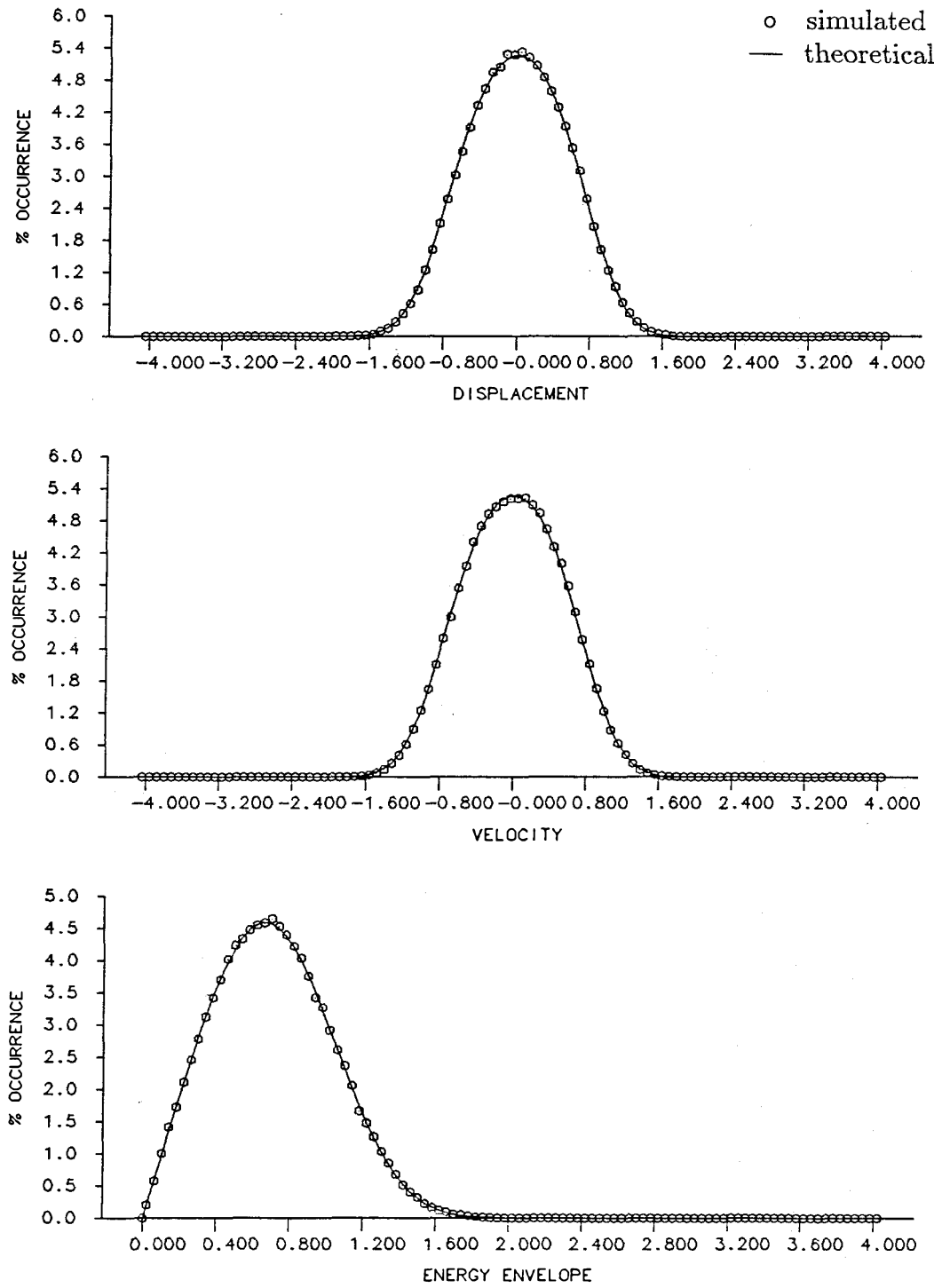
Figure 5.19

$(Velocity)^2$-Damping: $b_{02}\dot{x}^2$ sgn$(\dot{x})$

$b_{02} = 0.20$ $D = 0.05$
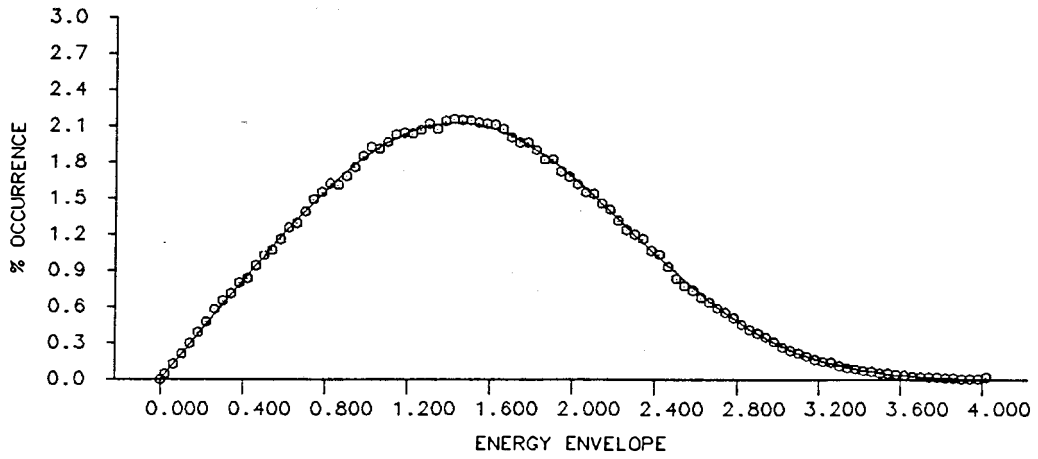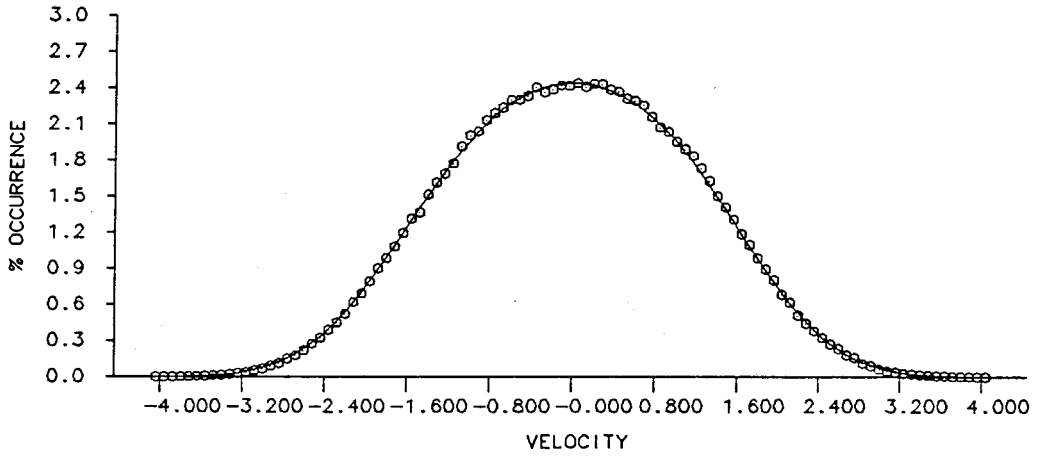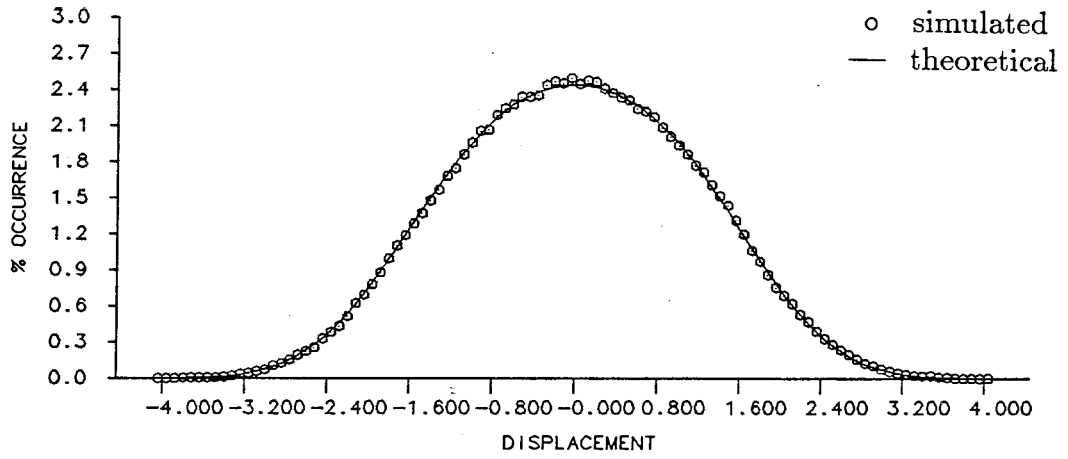
Figure 5.20

$(Velocity)^2$-Damping: $b_{02}\dot{x}^2 \, \text{sgn}(\dot{x})$

$b_{02} = 0.10 \; D = 0.25$
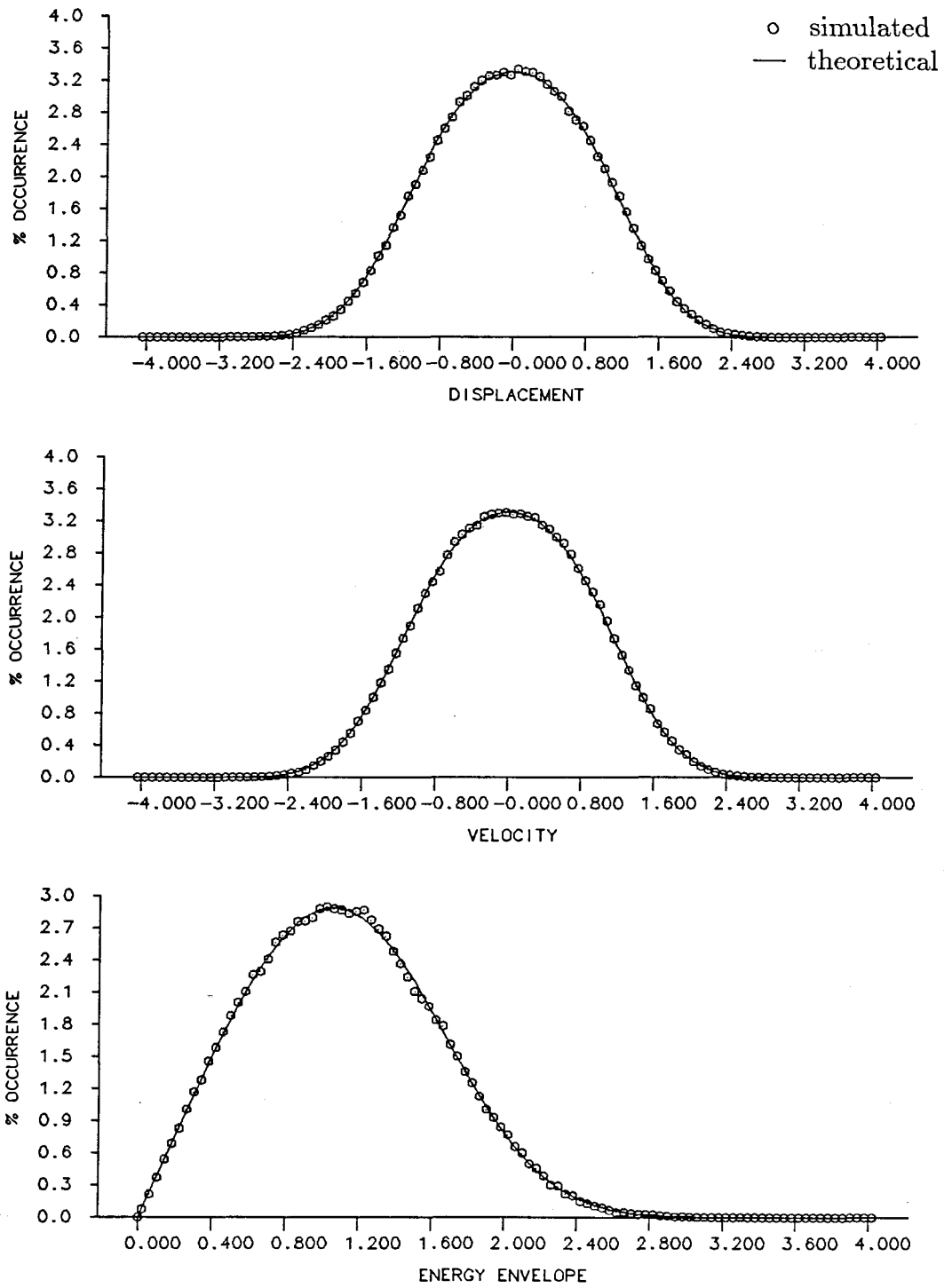
Figure 5.21

$(Velocity)^2$-Damping: $b_{02} \dot{x}^2 \operatorname{sgn}(\dot{x})$

$b_{02} = 0.10 \; D = 0.10$
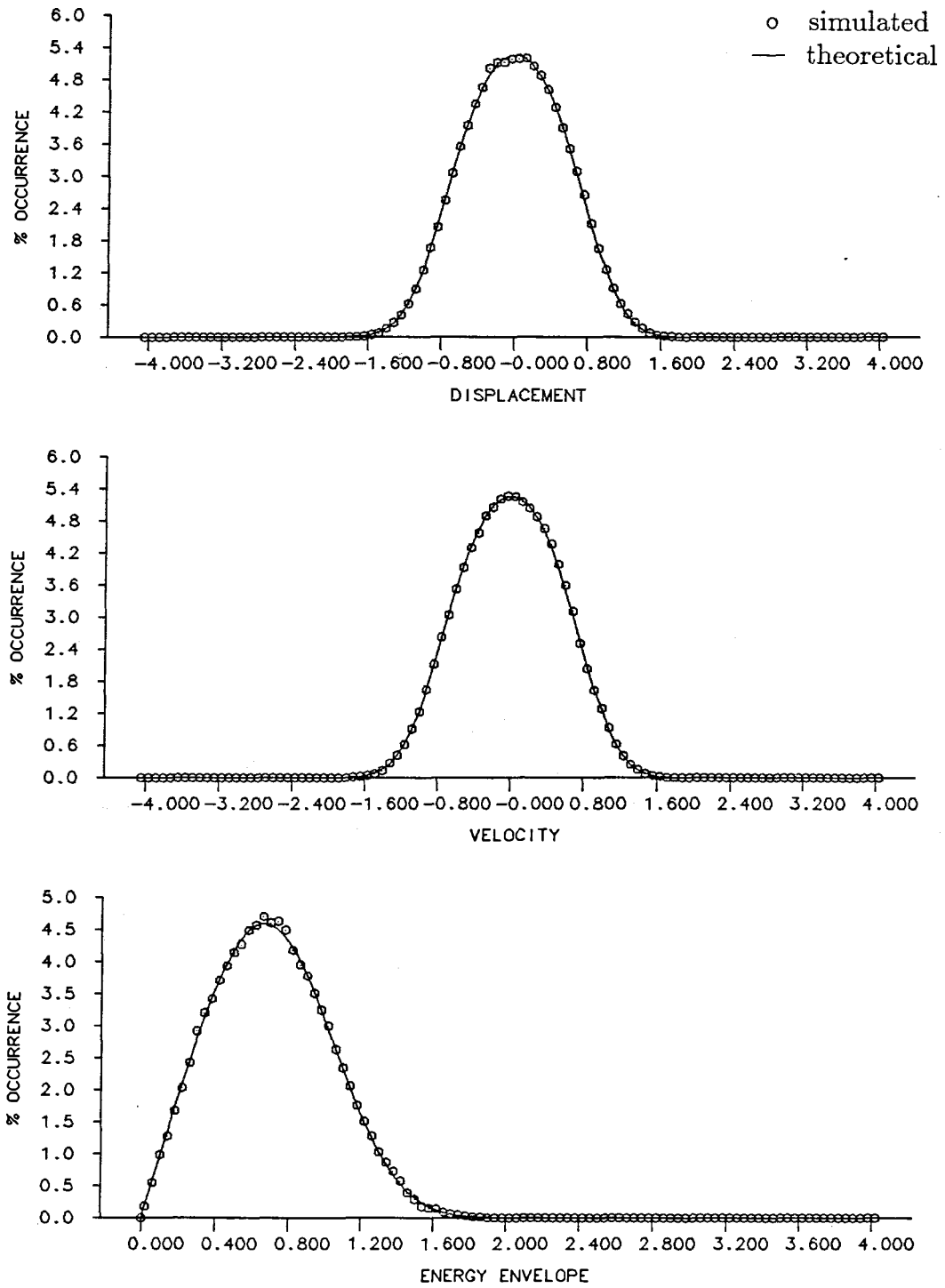
Figure 5.22

$(Velocity)^2$-Damping: $b_{02}\dot{x}^2 \; \text{sgn}(\dot{x})$

$b_{02} = 0.10 \; D = 0.025$
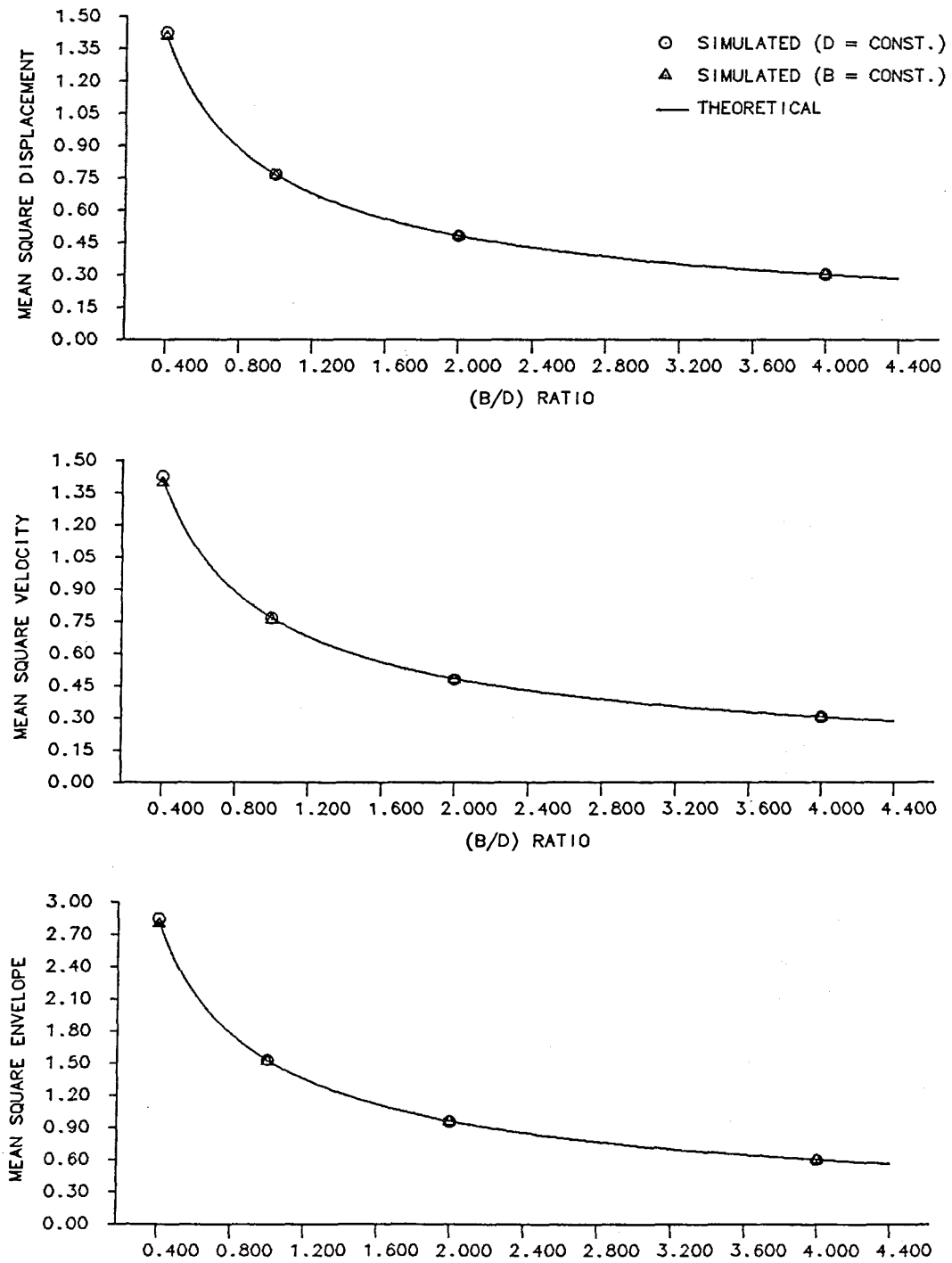
Figure 5.23

Mean-Square Response for $(Velocity)^2$-Damping
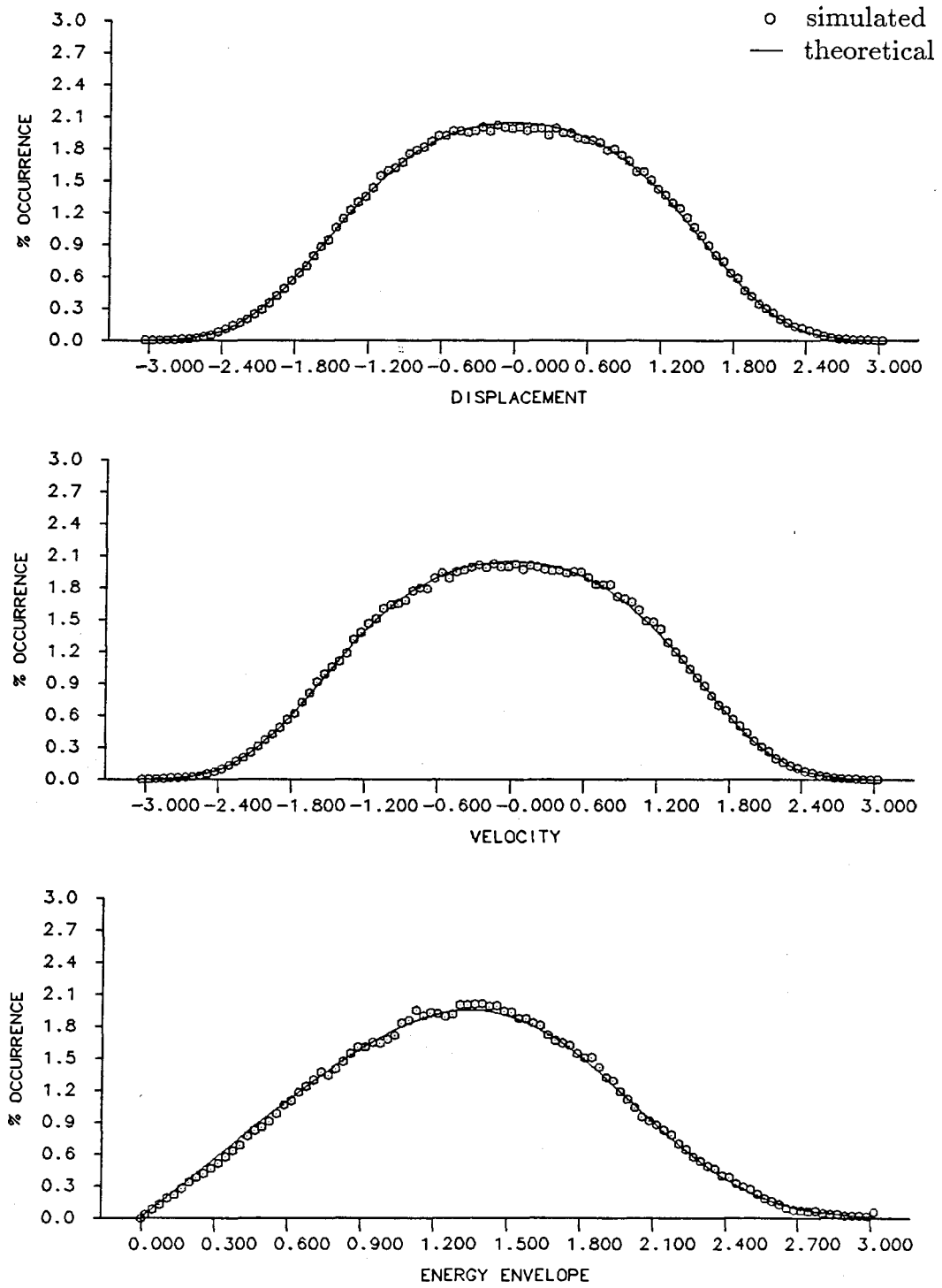
Figure 5.24

$(Velocity)^3$-Damping: $b_{03}\dot{x}^3$

$b_{03} = 0.02 \ D = 0.05$
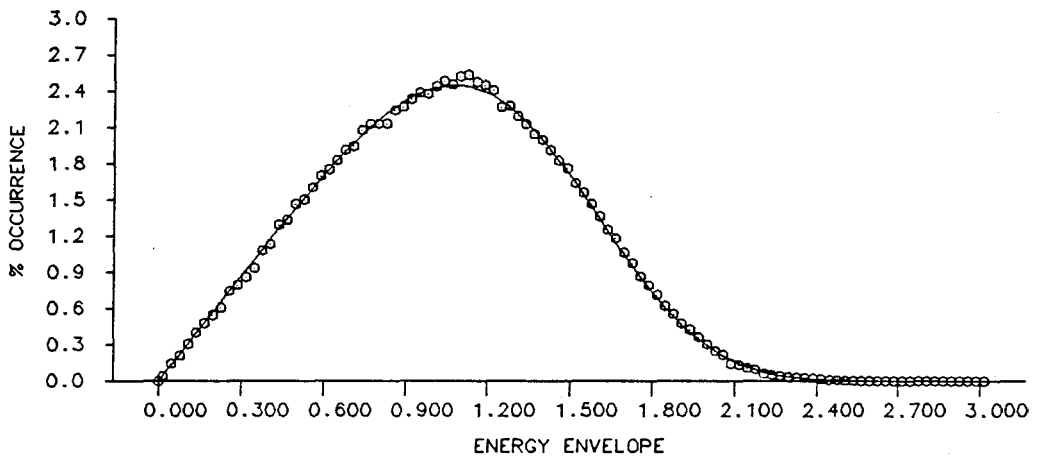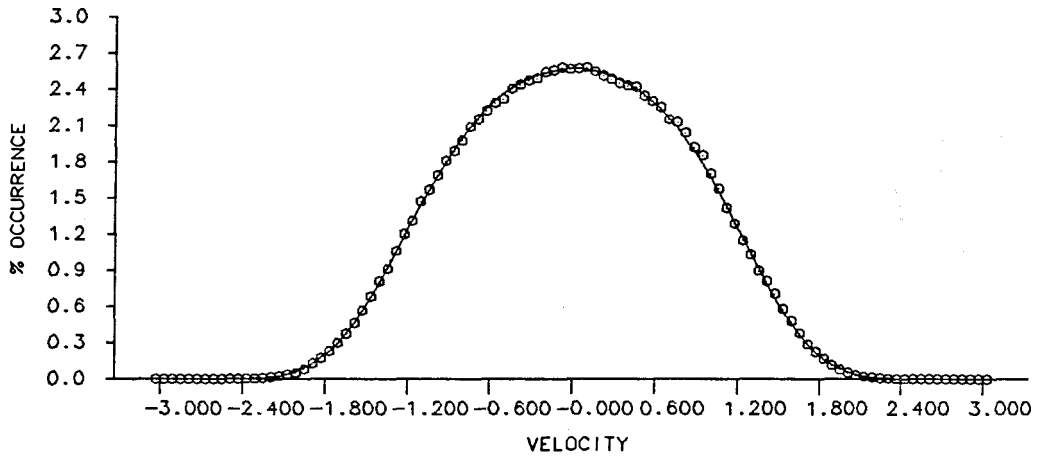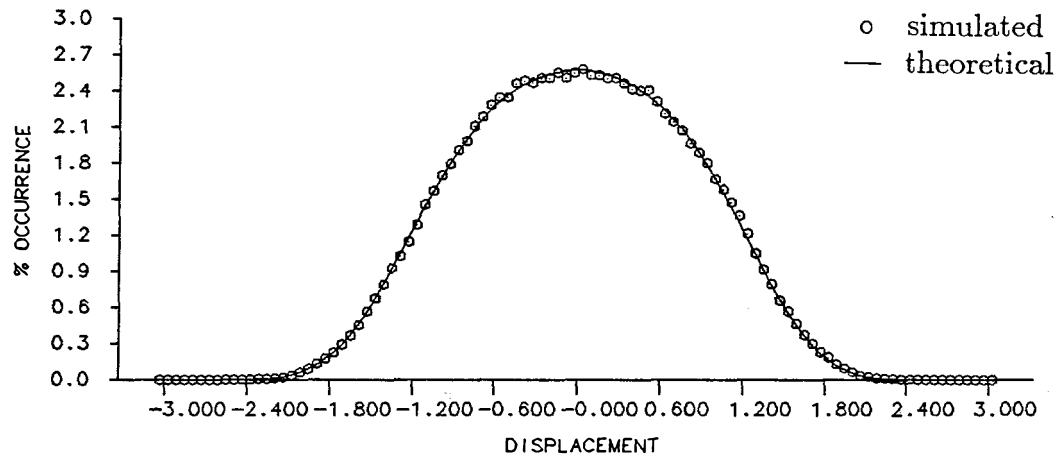
Figure 5.25

$(Velocity)^3$-Damping: $b_{03} \dot{x}^3$

$b_{03} = 0.05$ $D = 0.05$
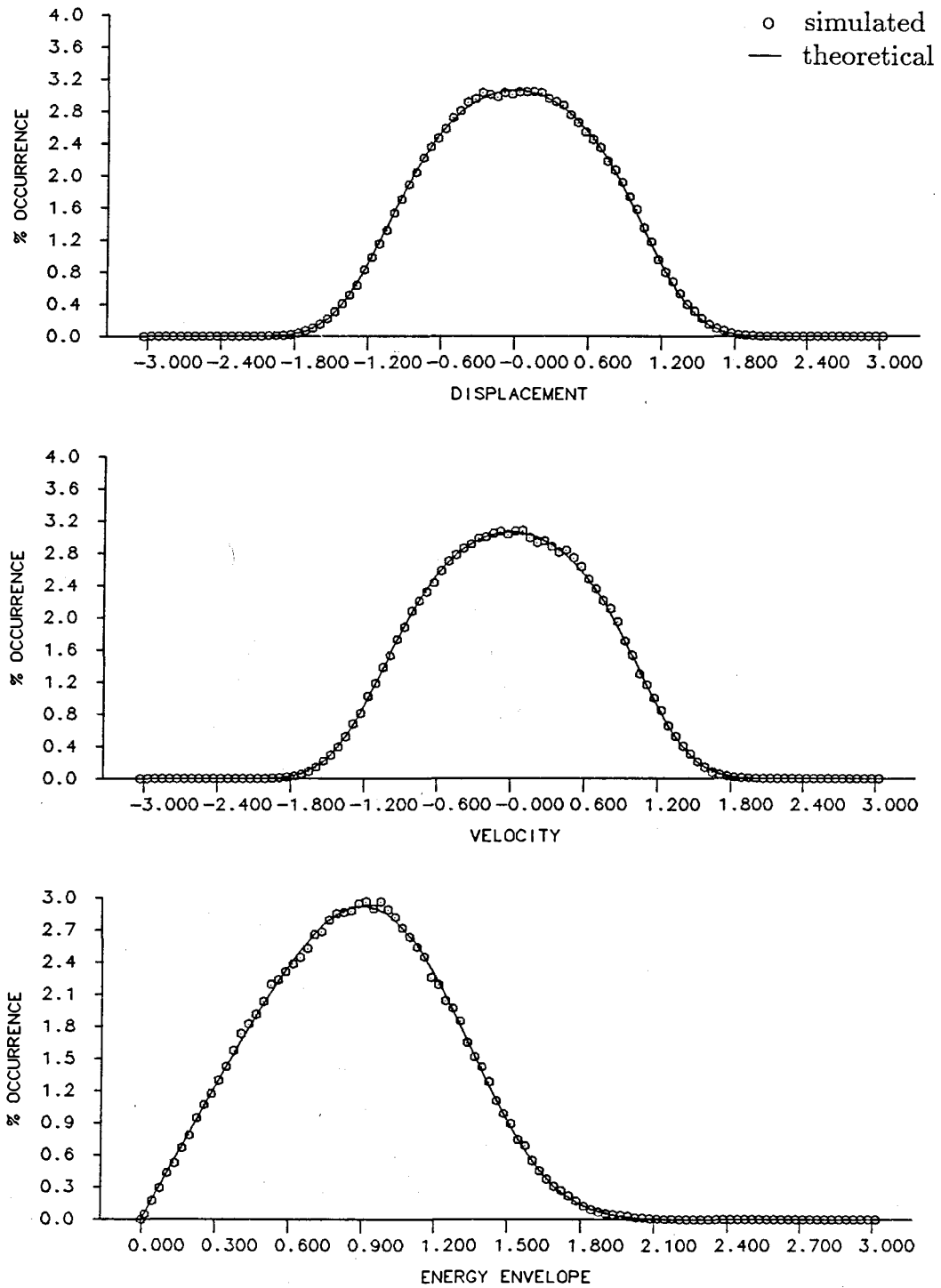
Figure 5.26

$(Velocity)^3$-Damping: $b_{03}\dot{x}^3$

$b_{03} = 0.10 \ D = 0.05$
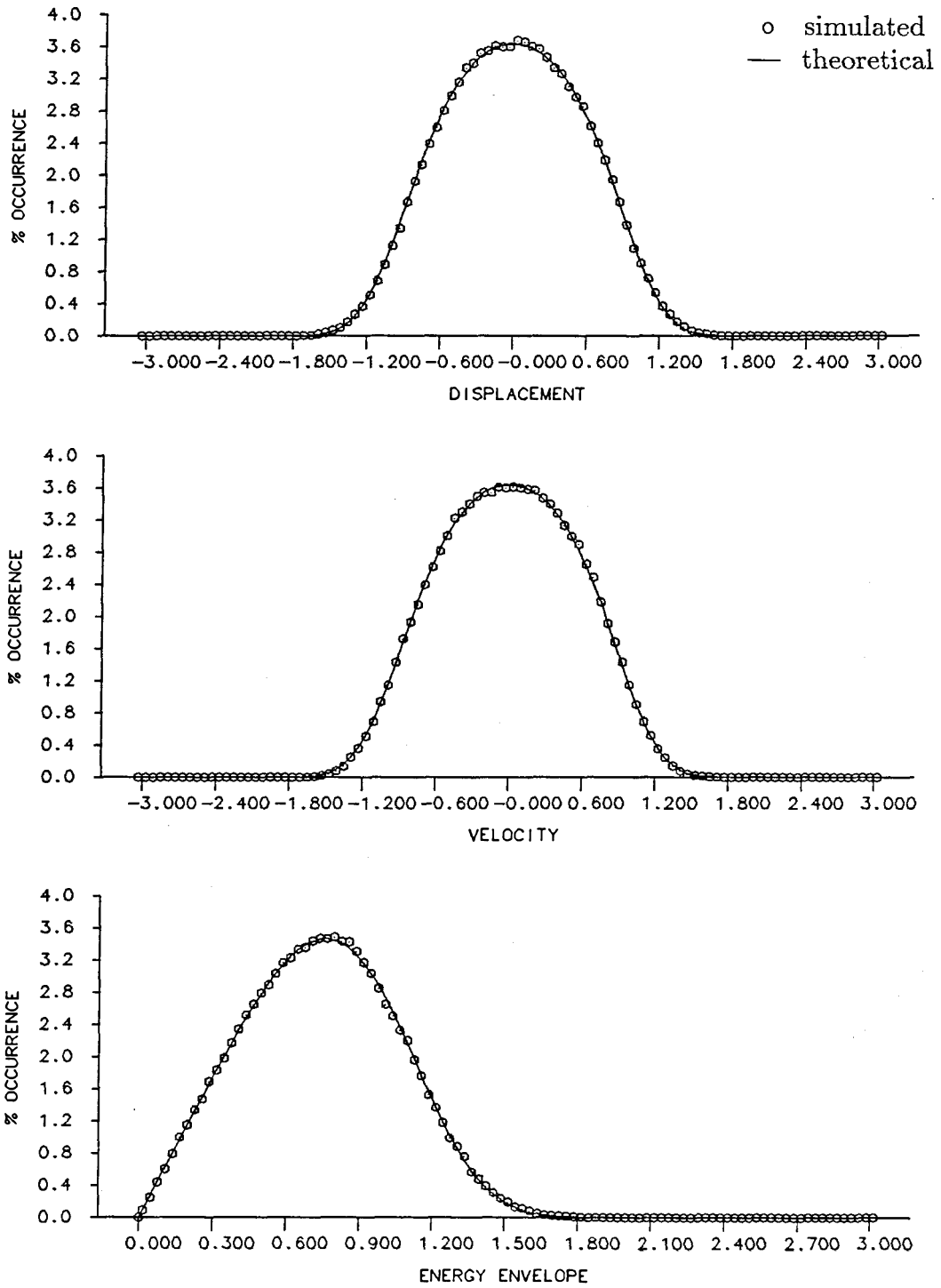
Figure 5.27

$(Velocity)^3$-Damping: $b_{03}\dot{x}^3$

$b_{03} = 0.20$ $D = 0.05$
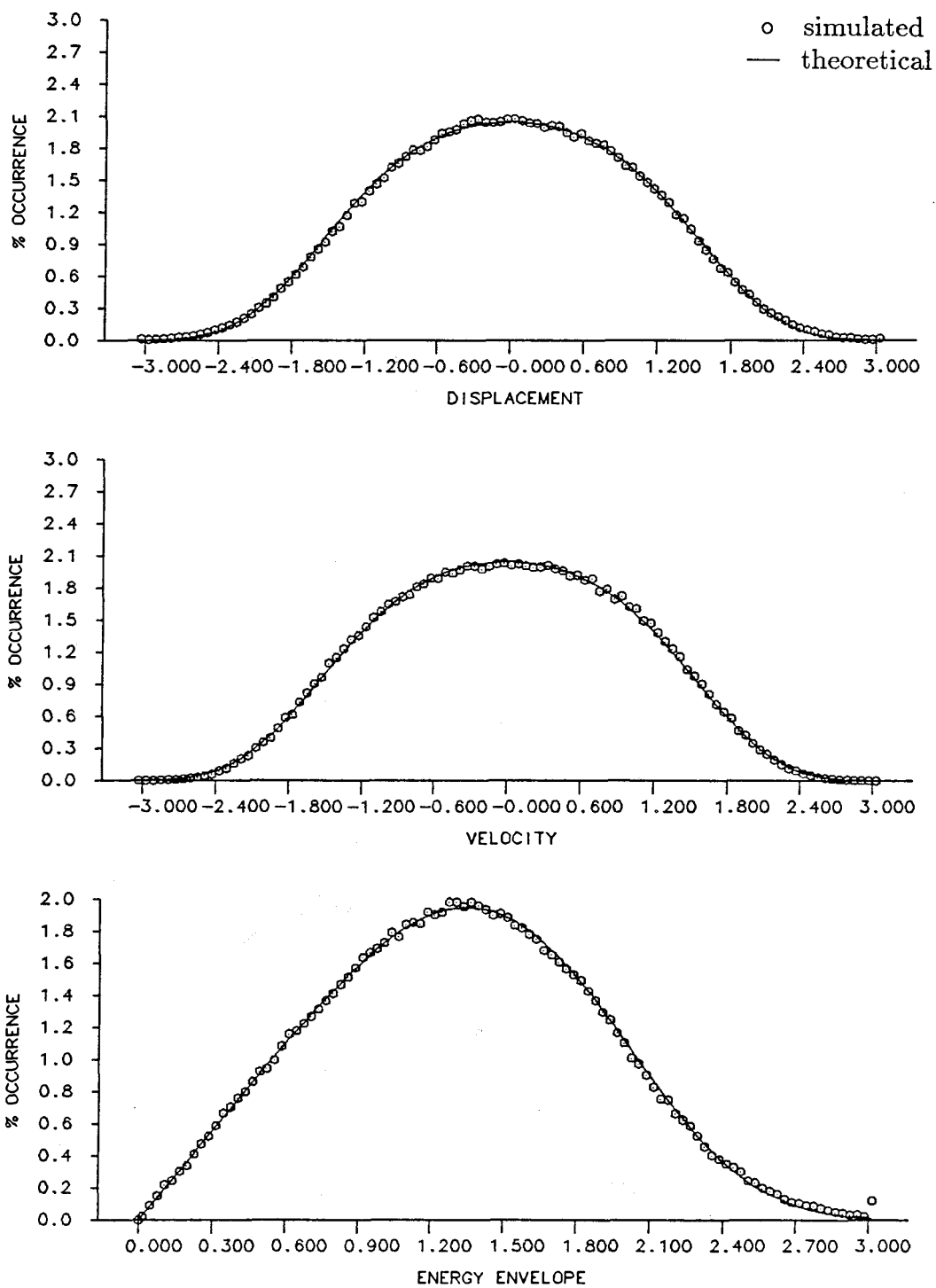
Figure 5.28

$(Velocity)^3$-Damping: $b_{03}\dot{x}^3$

$b_{03} = 0.10\ D = 0.25$
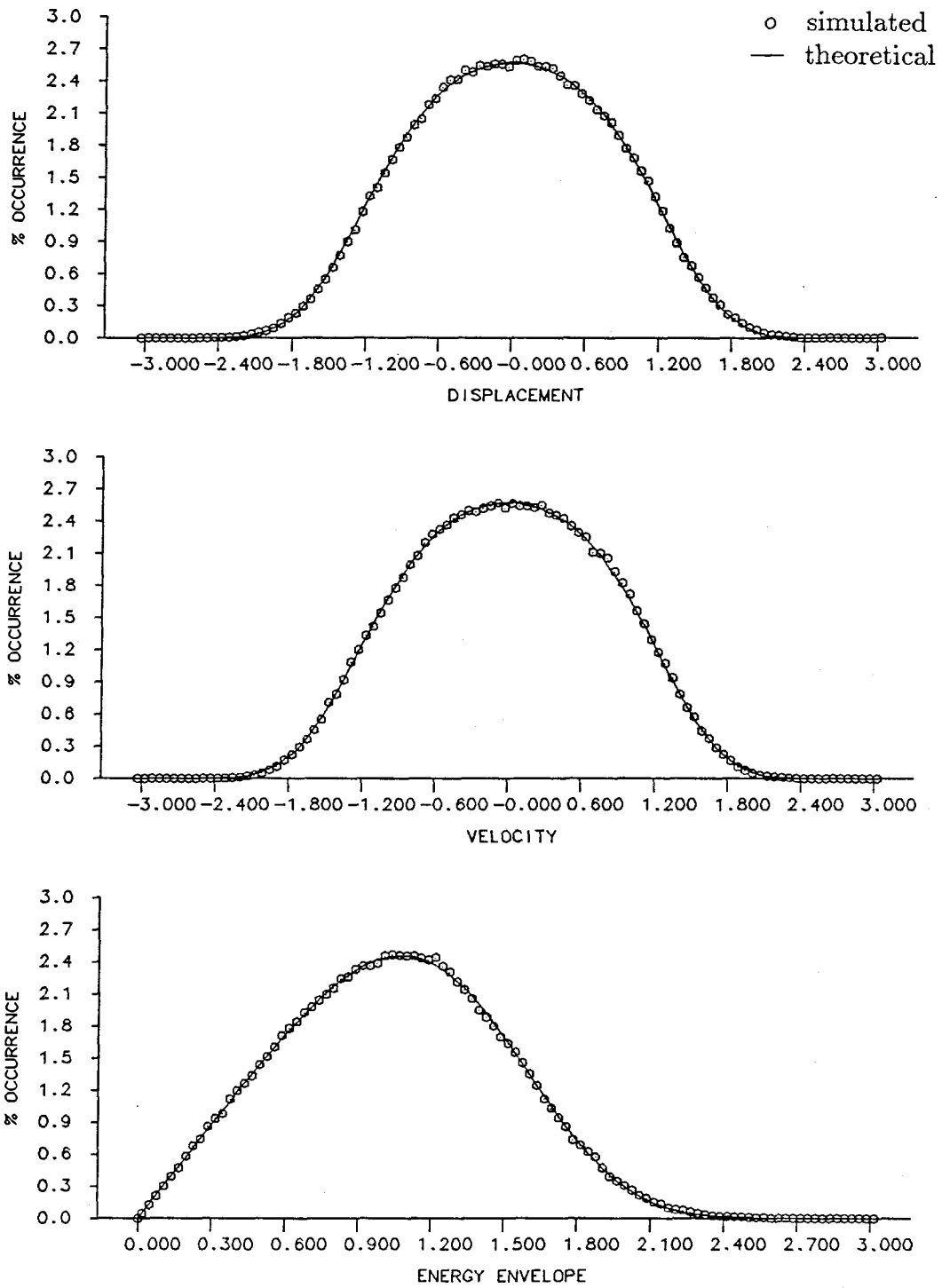
Figure 5.29

$(Velocity)^3$-Damping: $b_{03}\dot{x}^3$

$b_{03} = 0.10 \; D = 0.10$
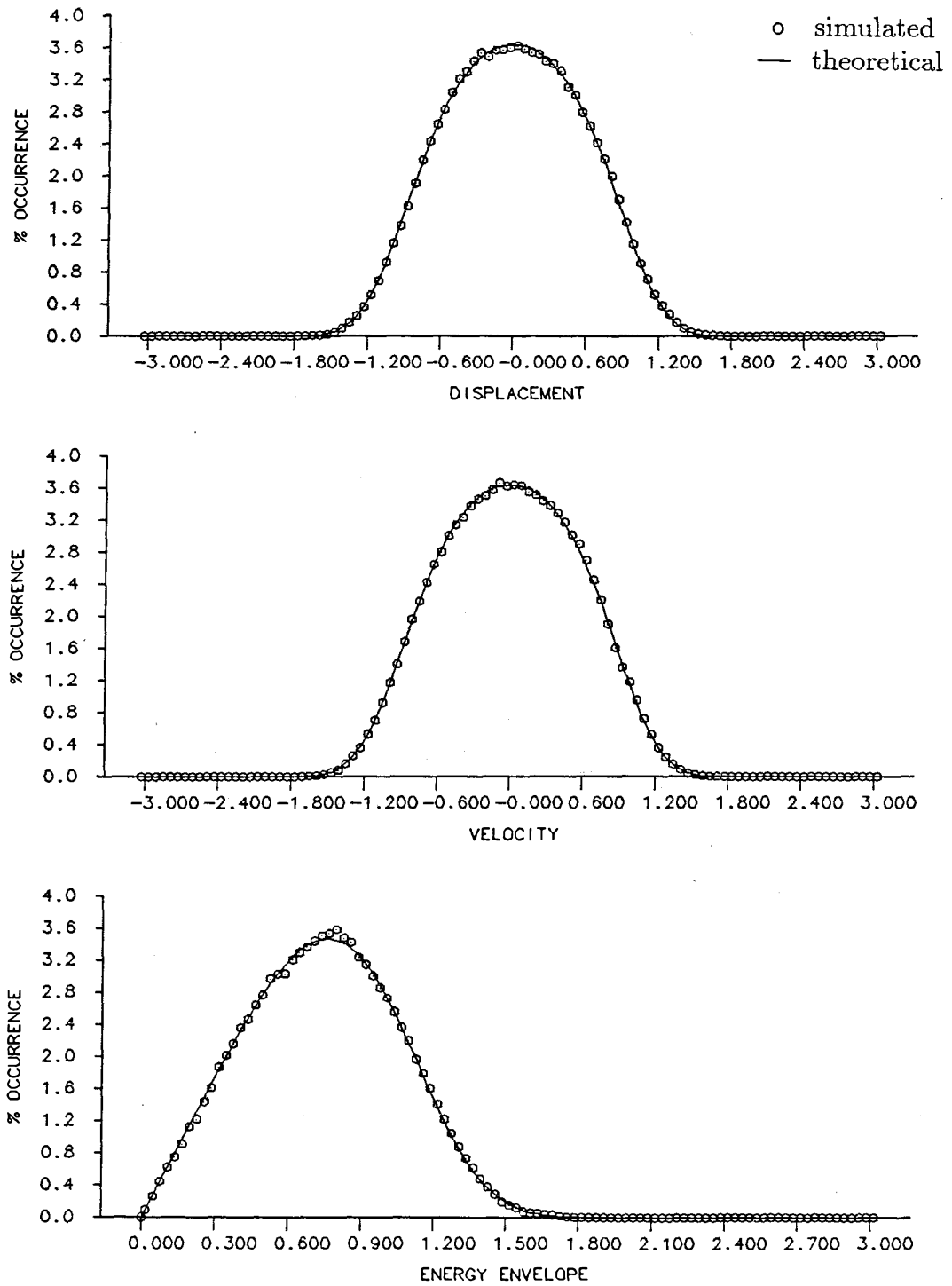
Figure 5.30

$(Velocity)^3$-Damping: $b_{03}\dot{x}^3$

$b_{03} = 0.10$ $D = 0.025$
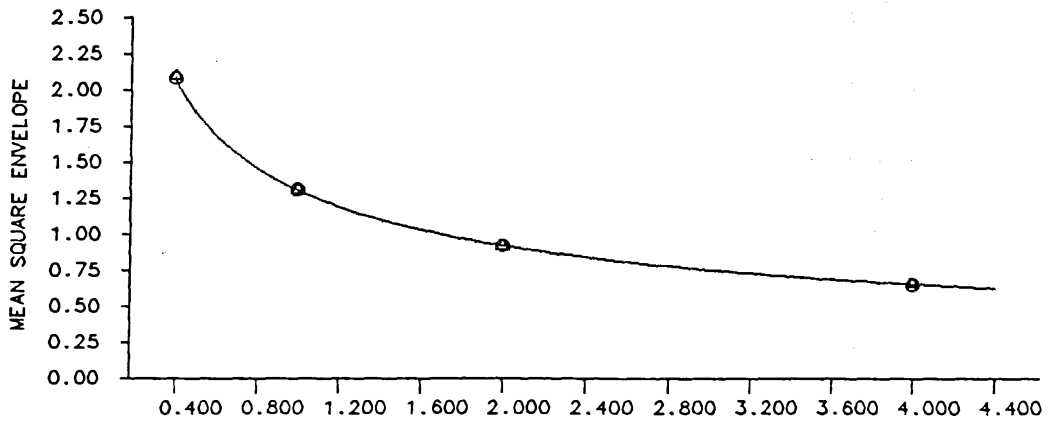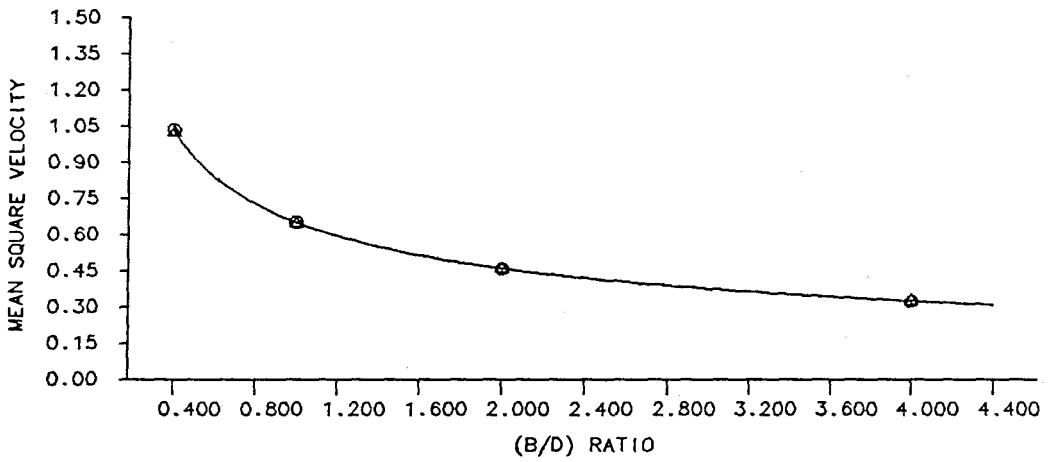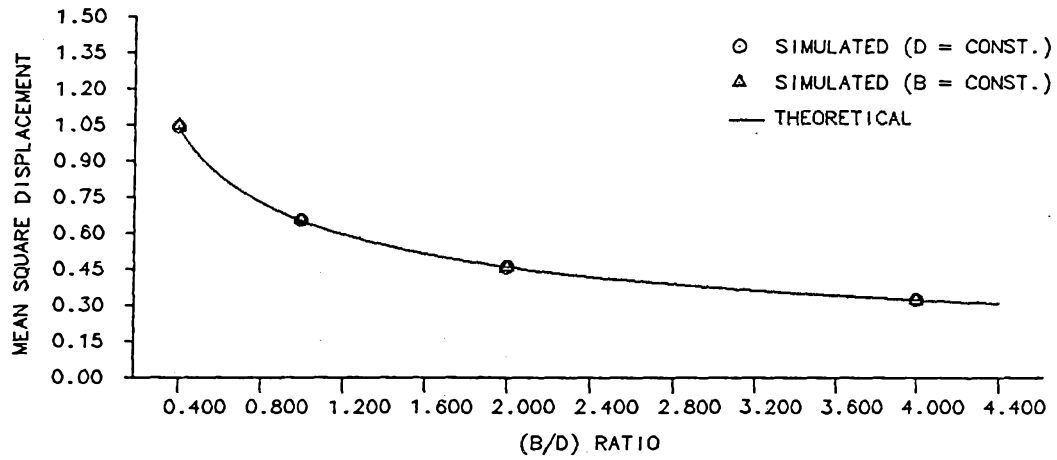
Figure 5.31

Mean-Square Response for $(Velocity)^3$-Damping
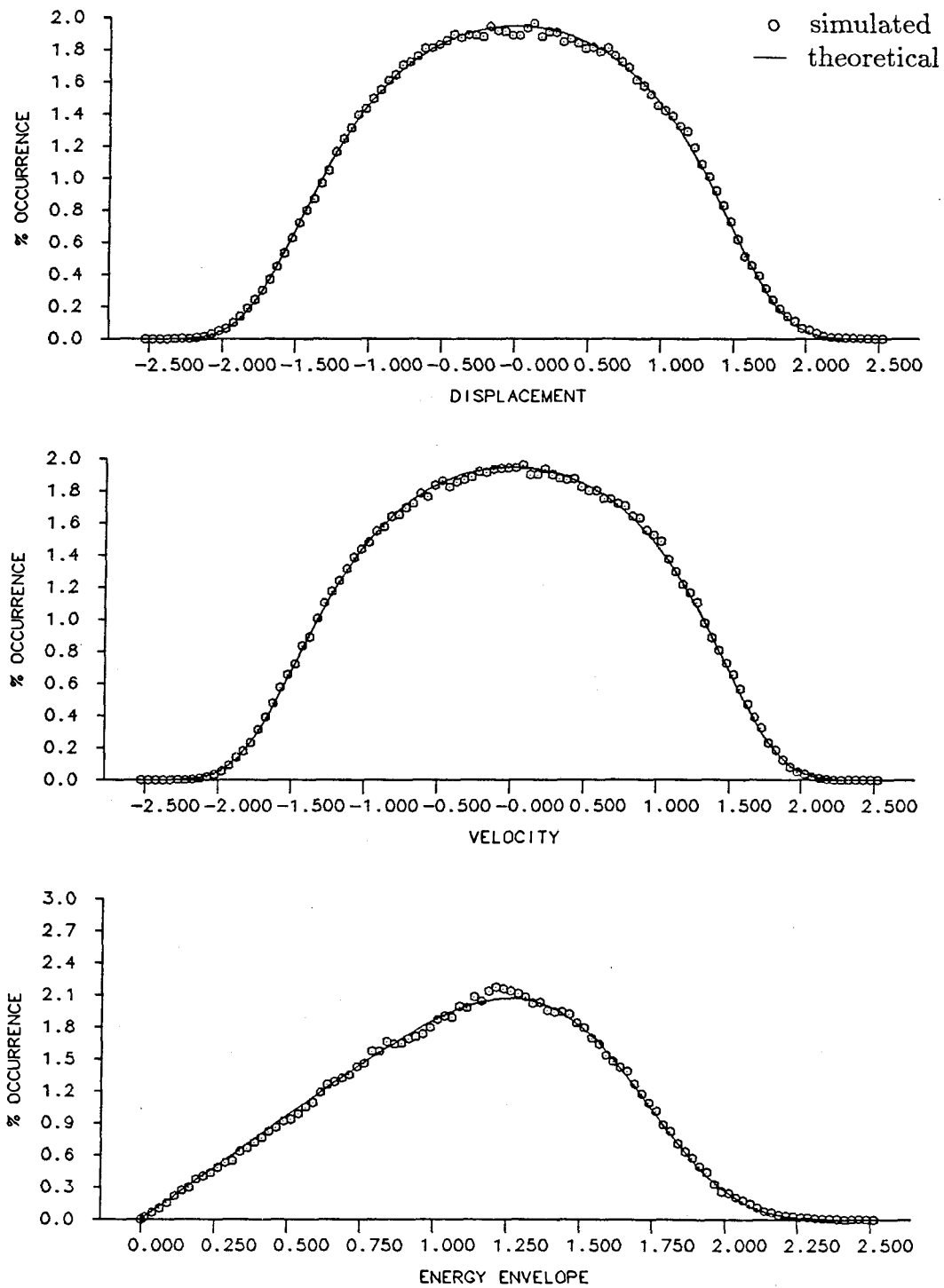
Figure 5.32

$(Velocity)^5$-Damping: $b_{05}\dot{x}^5$

$b_{05} = 0.02 \ D = 0.05$
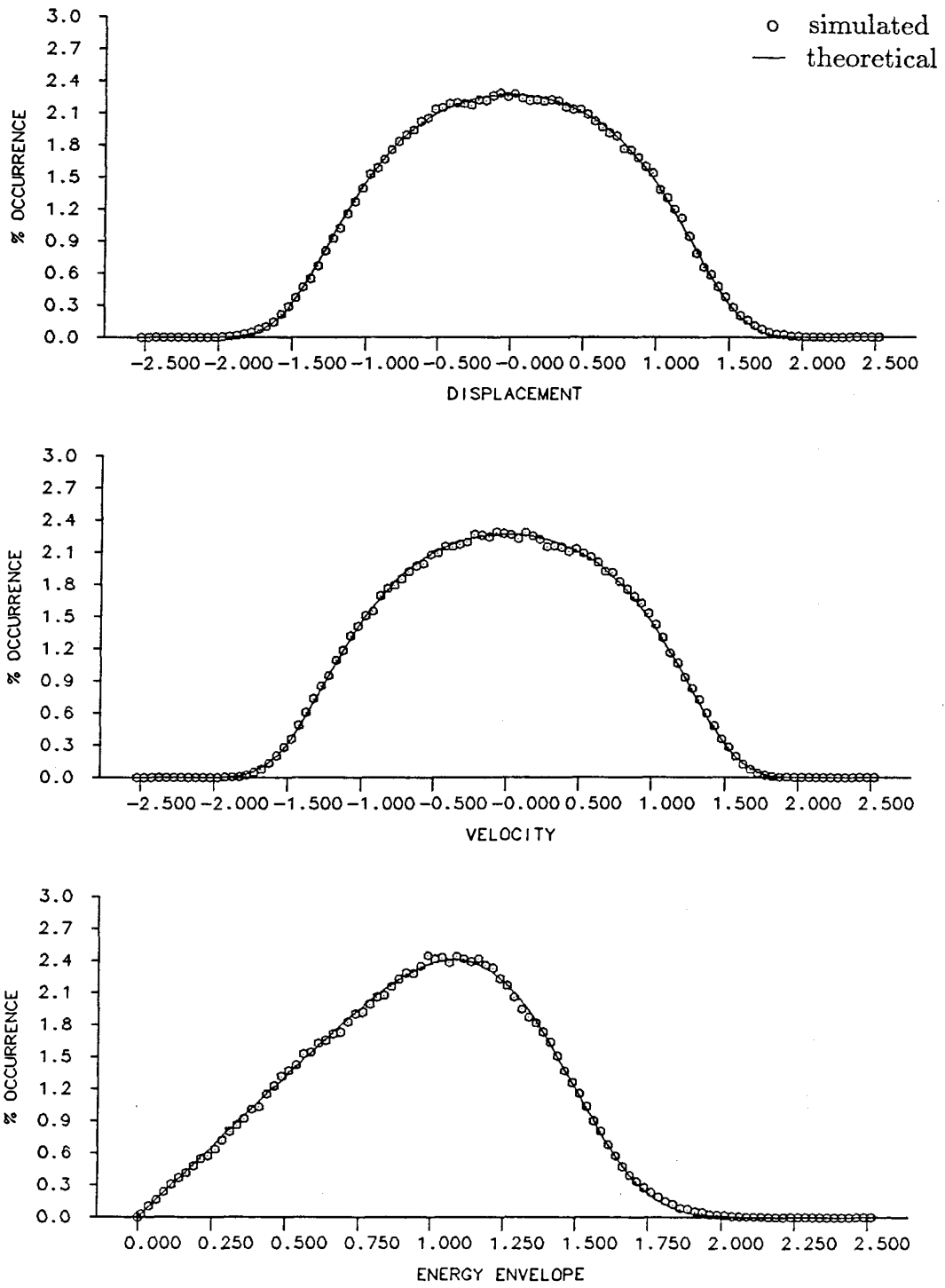
Figure 5.33

$(Velocity)^5$-Damping: $b_{05}\dot{x}^5$

$b_{05} = 0.05\ D = 0.05$
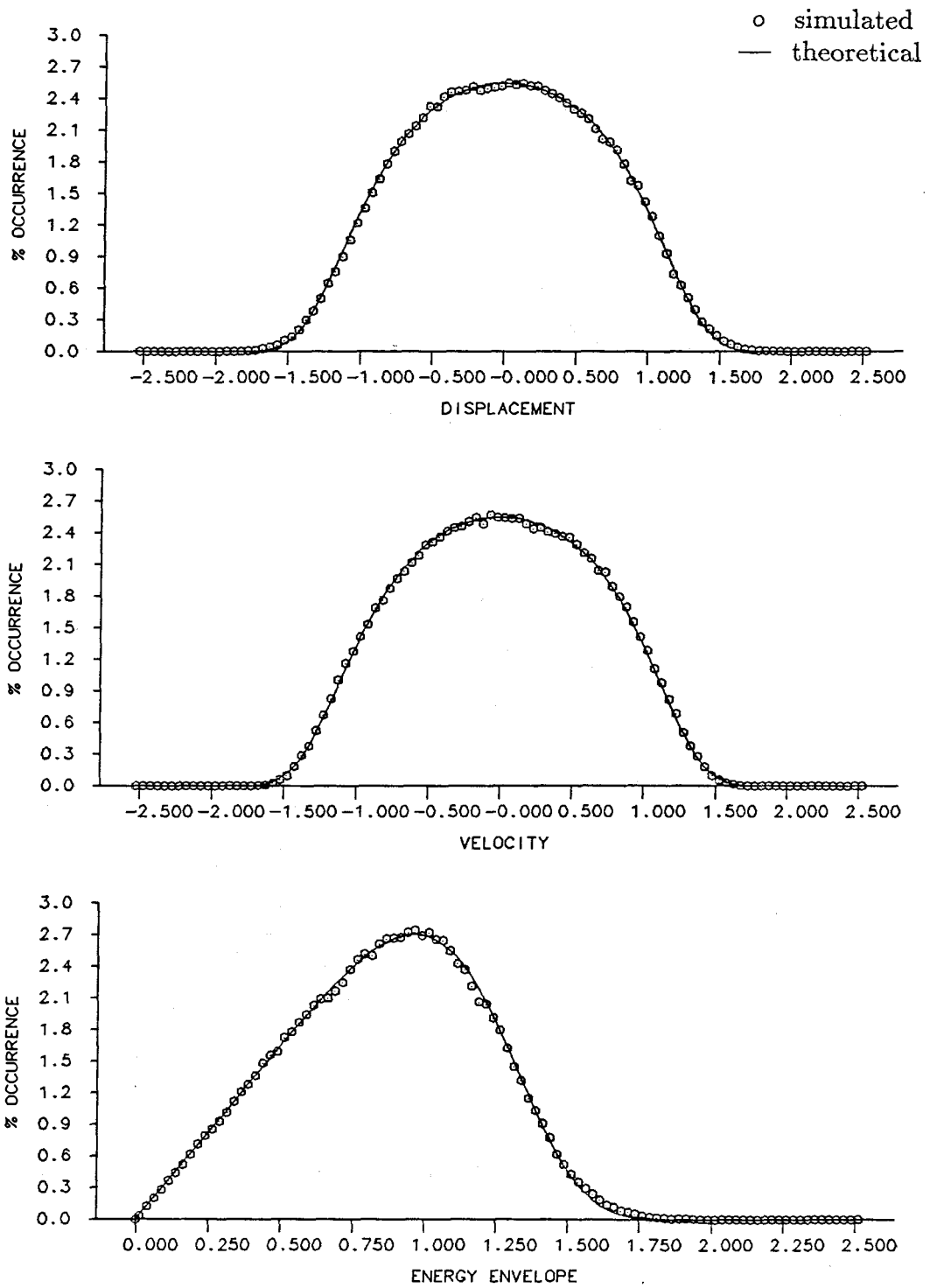
Figure 5.34

$(Velocity)^5$-Damping: $b_{05}\dot{x}^5$

$b_{05} = 0.10 \ D = 0.05$
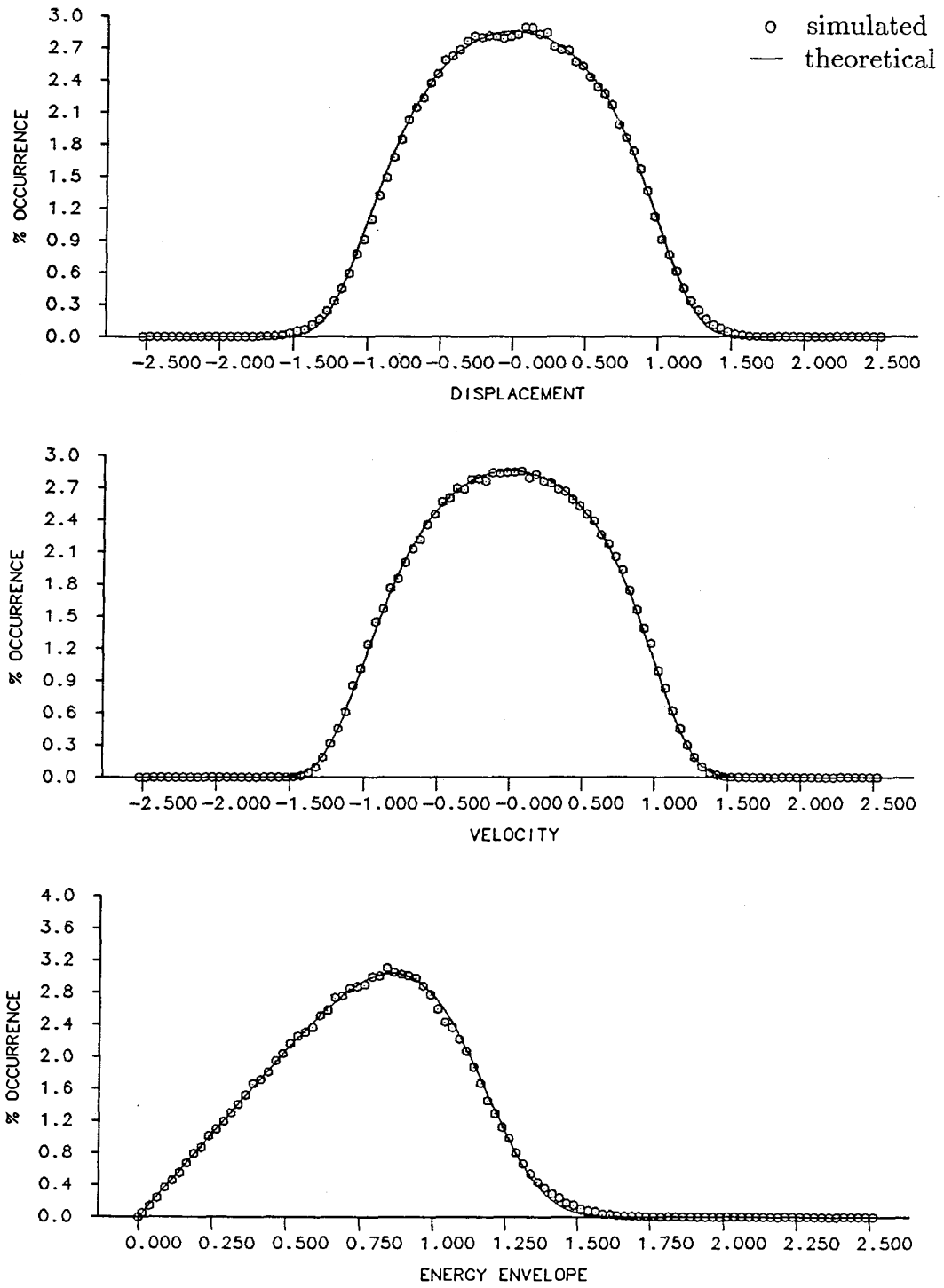
Figure 5.35

$(Velocity)^5$-Damping: $b_{05}\dot{x}^5$

$b_{05} = 0.20 \; D = 0.05$
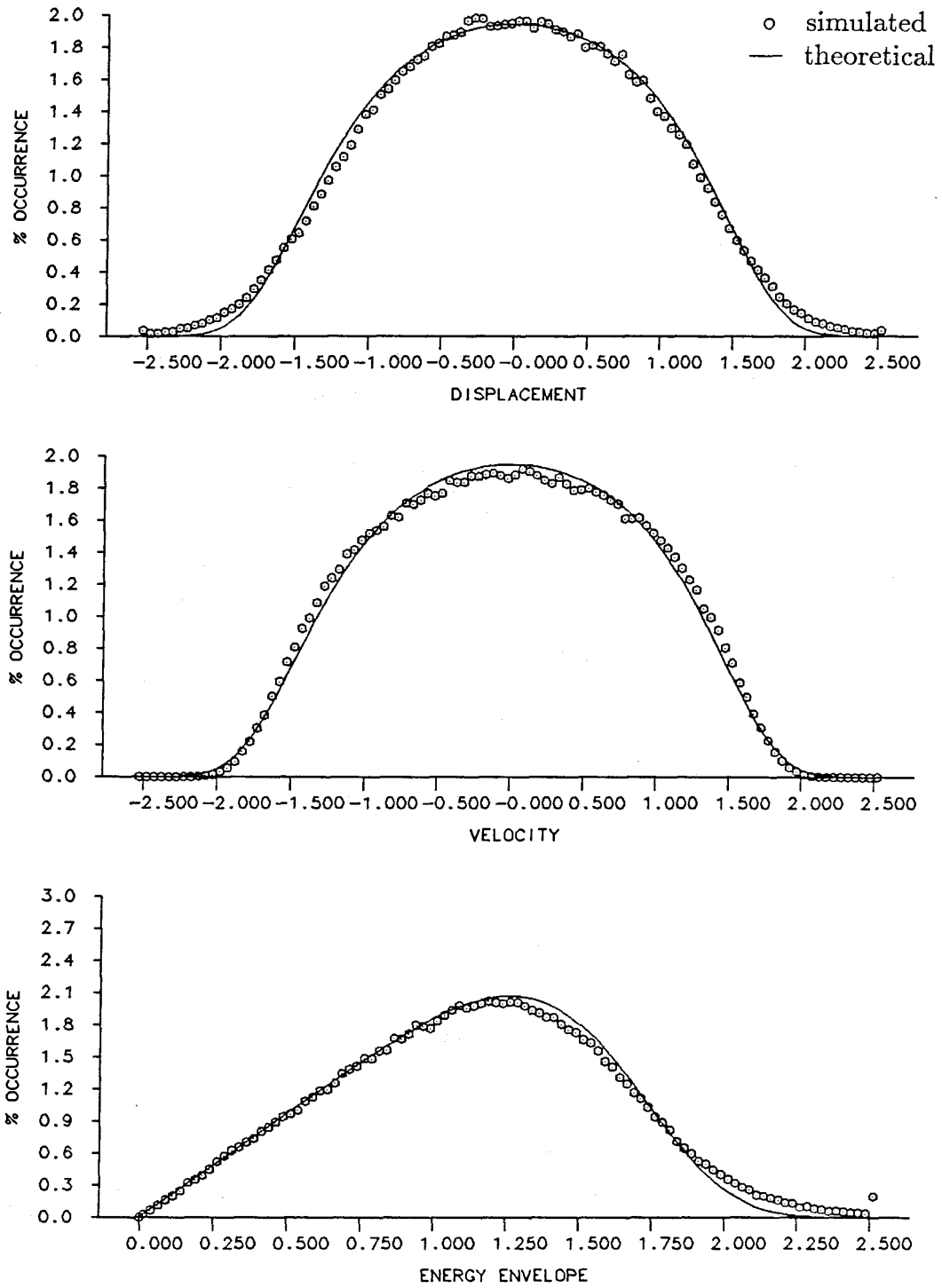
Figure 5.36

$(Velocity)^5$-Damping: $b_{05}\dot{x}^5$

$b_{05} = 0.10$ $D = 0.25$
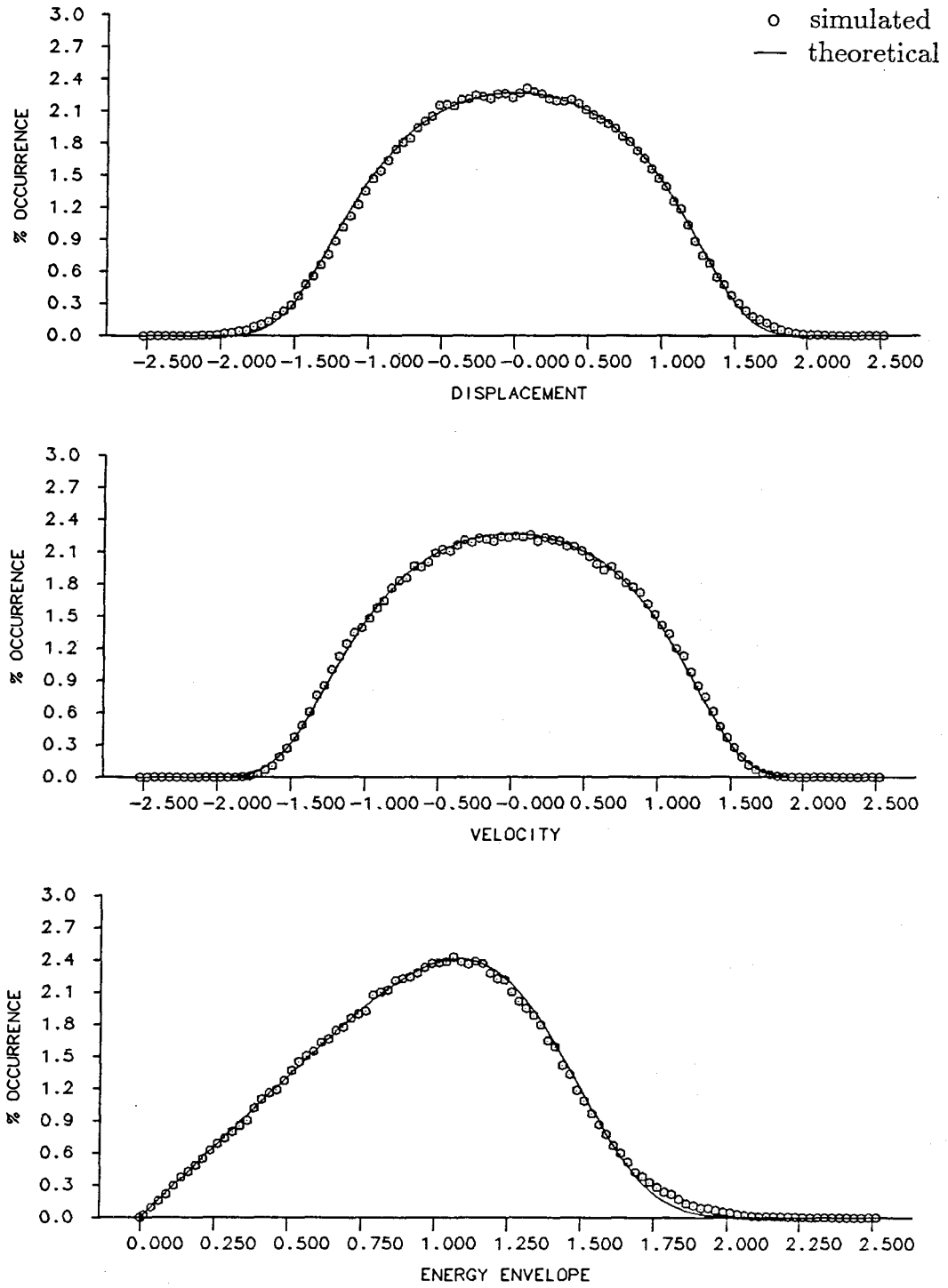
Figure 5.37

$(Velocity)^5$-Damping: $b_{05}\dot{x}^5$

$b_{05} = 0.10 \ D = 0.10$
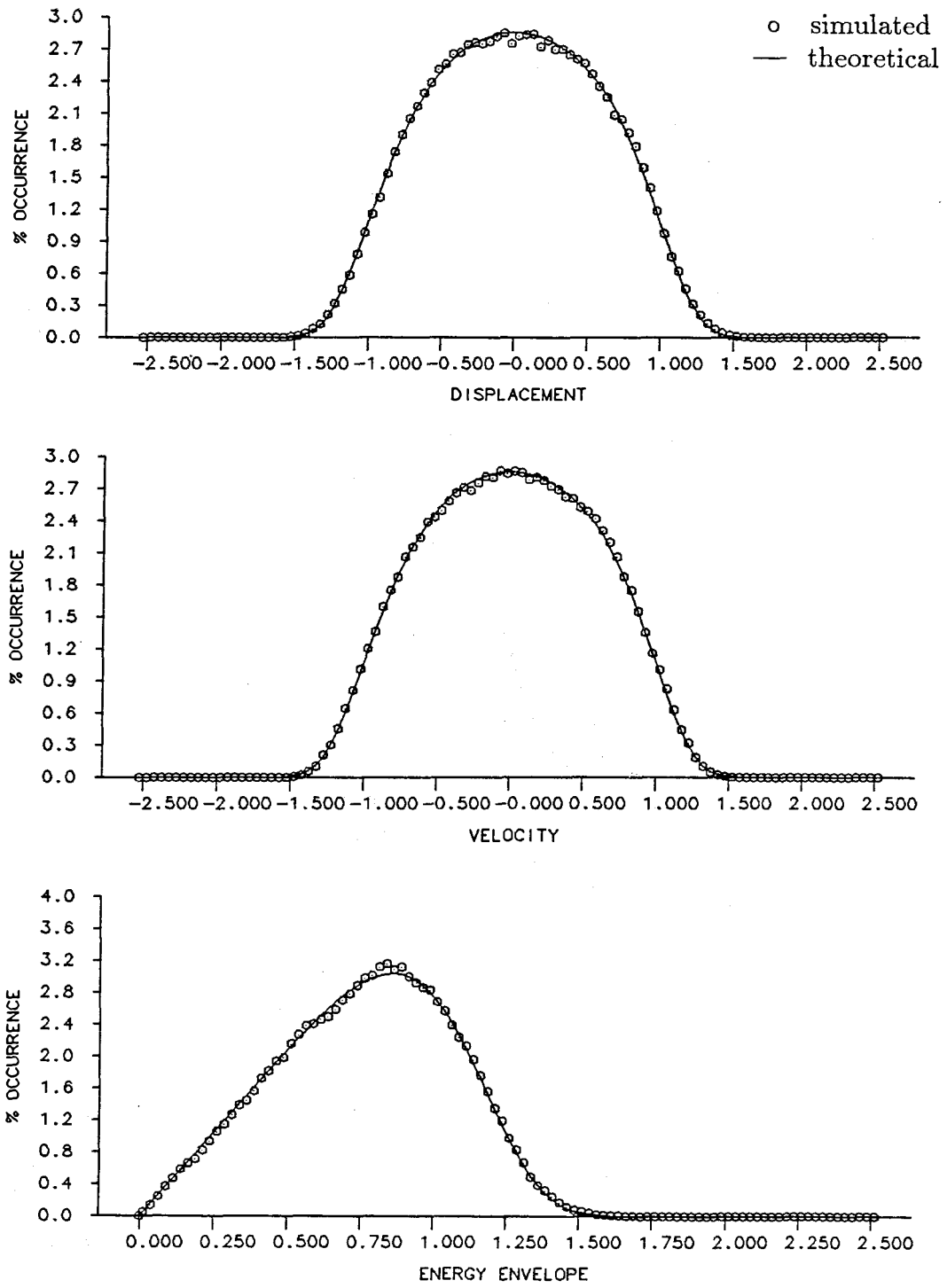
Figure 5.38

$(Velocity)^5$-Damping: $b_{05}\dot{x}^5$

$b_{05} = 0.10 \ D = 0.025$
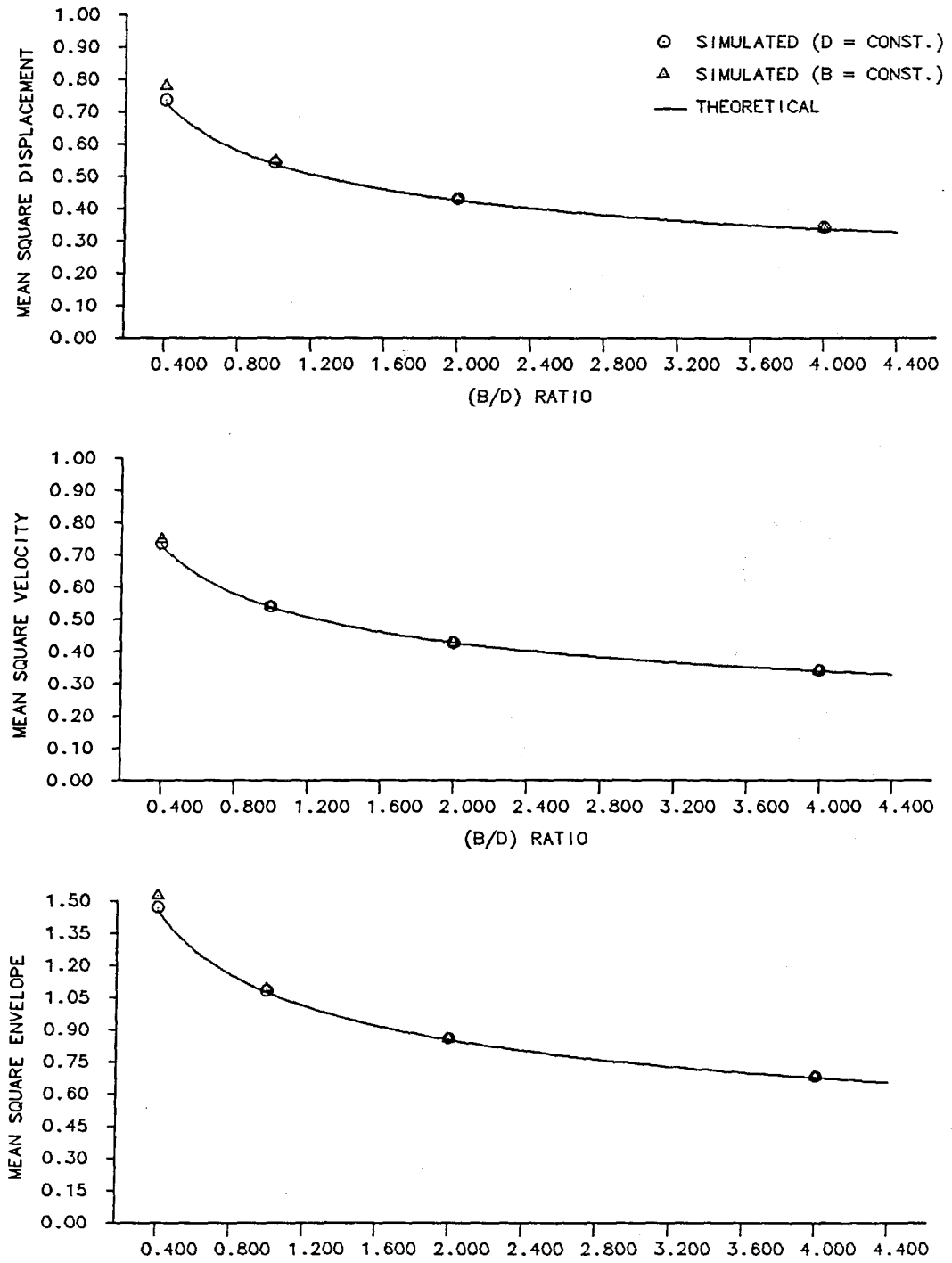
Figure 5.39

Mean-Square Response for $(Velocity)^5$-Damping

5.2.3 Van der Pol Equation

Consider the Van der Pol equation

$$\ddot{x} - b \left(1 - x^2\right) \dot{x} + x = w(t), \tag{5.28}$$

which is obtained from Eq. (3.21) by making $b_{01} = -b$, $b_{21} = b$, $b_{ij} = 0$ otherwise.

The following equivalent nonlinear equation replaces Eq. (5.28),

$$\ddot{x} + (c_{01} f_{01}(H) + c_{21} f_{21}(H)) \dot{x} + x = w(t), \tag{5.29}$$

which is obtained from Eq. (3.22) by making $c_{ij} = 0$ except for c_{01} and c_{21}. The only f_{ij} terms of interest are f_{01} and f_{21}, obtained from Eq. (3.24) and given by

$$f_{01} = 1 \quad \text{and} \quad f_{21} = a^2. \tag{5.30}$$

The unknown coefficients c_{01} and c_{21} are the solutions of the following set of equations:

$$\left(\pi c_{01} - 2b_{01}\frac{\Gamma(\frac{1}{2})\Gamma(\frac{3}{2})}{\Gamma(2)}\right)\int_0^\infty a^2\lambda(a)da+$$

$$\left(\pi c_{21} - 2b_{21}\frac{\Gamma(\frac{3}{2})\Gamma(\frac{3}{2})}{\Gamma(3)}\right)\int_0^\infty a^4\lambda(a)da = 0,$$

and $\hfill (5.31)$

$$\left(\pi c_{01} - 2b_{01}\frac{\Gamma(\frac{1}{2})\Gamma(\frac{3}{2})}{\Gamma(2)}\right)\int_0^\infty a^4\lambda(a)da+$$

$$\left(\pi c_{21} - 2b_{21}\frac{\Gamma(\frac{3}{2})\Gamma(\frac{3}{2})}{\Gamma(3)}\right)\int_0^\infty a^6\lambda(a)da = 0,$$

obtained from Eq. (3.33) by first making $k, l = 0, 1$ and varying i, j, and then $k, l = 2, 1$ and varying i, j. A solution for Eq. (5.31) is $c_{01} = b_{01}$ and $c_{21} = b_{21}/4$.

Recalling that $b_{01} = -b$ and $b_{21} = b$, direct substitution on Eq. (3.27) and evaluation of the normalization constant, A, yields the steady-state joint probability density function of x and $\dot{x}$ as

$$p(x, \dot{x}) = \left(\frac{1}{2\pi}\right)\left(\frac{(\frac{b}{D})^{\frac{1}{2}}}{\sqrt{\pi}\,\mathrm{erfc}\left[-(\frac{b}{D})^{\frac{1}{2}}\right]}\right)\exp\left[-\left(\frac{b}{D}\right)\left(1 - \frac{(x^2 + \dot{x}^2)}{4}\right)^2\right],$$

$$(5.32)$$

and substitution in Eq. (3.28) yields the probability density function of the energy-based envelope as

$$p_e(\alpha) = \left(\frac{(\frac{b}{D})^{\frac{1}{2}}}{\sqrt{\pi}\,\mathrm{erfc}\left[-(\frac{b}{D})^{\frac{1}{2}}\right]}\right)\alpha\exp\left[-\left(\frac{b}{D}\right)\left(1 - \frac{\alpha^2}{4}\right)^2\right], \hfill (5.33)$$

The expected value of α^2, $E[\alpha^2]$, then is

$$E[\alpha^2] = \int_0^\infty \alpha^2 p_e(\alpha)d\alpha = 4 + \frac{4}{\left(\frac{b}{D}\right)^{\frac{1}{2}}\sqrt{\pi}\,\text{erfc}\left[-\left(\frac{b}{D}\right)^{\frac{1}{2}}\right]}\frac{\exp\left[-\left(\frac{b}{D}\right)\right]}{} \qquad (5.34)$$

and again, because of the symmetry of $p(x,\dot{x})$ with respect to x and $\dot{x}$ and because of the definition of α^2 $(= x^2 + \dot{x}^2)$, $E[x^2] = E[\dot{x}^2] = E[\alpha^2]/2$.

As before, the response of the original nonlinear equation, Eq. (5.28), in principle, is a function of the two independent parameters b and D. The response to the equivalent nonlinear equation, however, is a function of the ratio b/D. In order to assess the effect of b and D on the response of the original equation, the two series of simulations previously discussed were performed. In the first, D was kept constant and b varied over a fairly wide range of values in order to encompass cases of practical interest. In the second series, b was kept constant and D varied in such a way that the ratio b/D was the same in both series.

Figs. 5.40 through 5.43 show the results for the first series, which is the comparison of theoretical and simulated histograms for the displacement, velocity and energy-based envelope. In these figures b was made equal to 0.02, 0.05, 0.10 and 0.20, respectively, and D was kept constant and equal to 0.05. This value of D produced a random forcing function with unit standard deviation. Fig. 5.42 and Figs. 5.44 through 5.46 show the results for the second series, for $b = 0.10$ and D equal to 0.05, 0.25, 0.10 and 0.025.

The agreement between simulated and predicted response histograms is excellent for all but Fig. 5.43 for $b = 0.20$ and $D = 0.05$, in which the histogram of velocities tends to be overpredicted in the region of the two crests. This can be explained by the fact that the resulting equivalent nonlinear equation (Eq. (5.29)) has a limit-cycle that is symmetric with respect to x and $\dot{x}$, regardless of the value of the coeffient b. The Van der Pol equation, on the other hand, possesses a limit-cycle that is symmetric only for small values of b. What is being observed in Fig. 5.43 is the effect of the the limit-cycle distortion. As a result, it is expected that the matching between predicted and simulated responses will probably only get worse. It is important to note, however, that the matching of the energy-based envelope is still very good.

A close examination of the curves also indicates a systematic overprediction for small values of the envelope, which, as will be seen in the next section, may be due to random error or a small bias in the integration scheme used. In any case it indicates that the agreement is in reality better than what these figures convey.

Fig. 5.47 shows the comparison of the simulated and theoretical results for the $E[x^2]$, $E[\dot{x}^2]$ and the $E[\alpha^2]$ as functions of the ratio b/D. In this figure, although by a small margin, all of the mean-squared values are systematically underpredicted. However, it is important to realize that the underprediction is at most of the order of a few percent and therefore for all practical purposes is negligible.
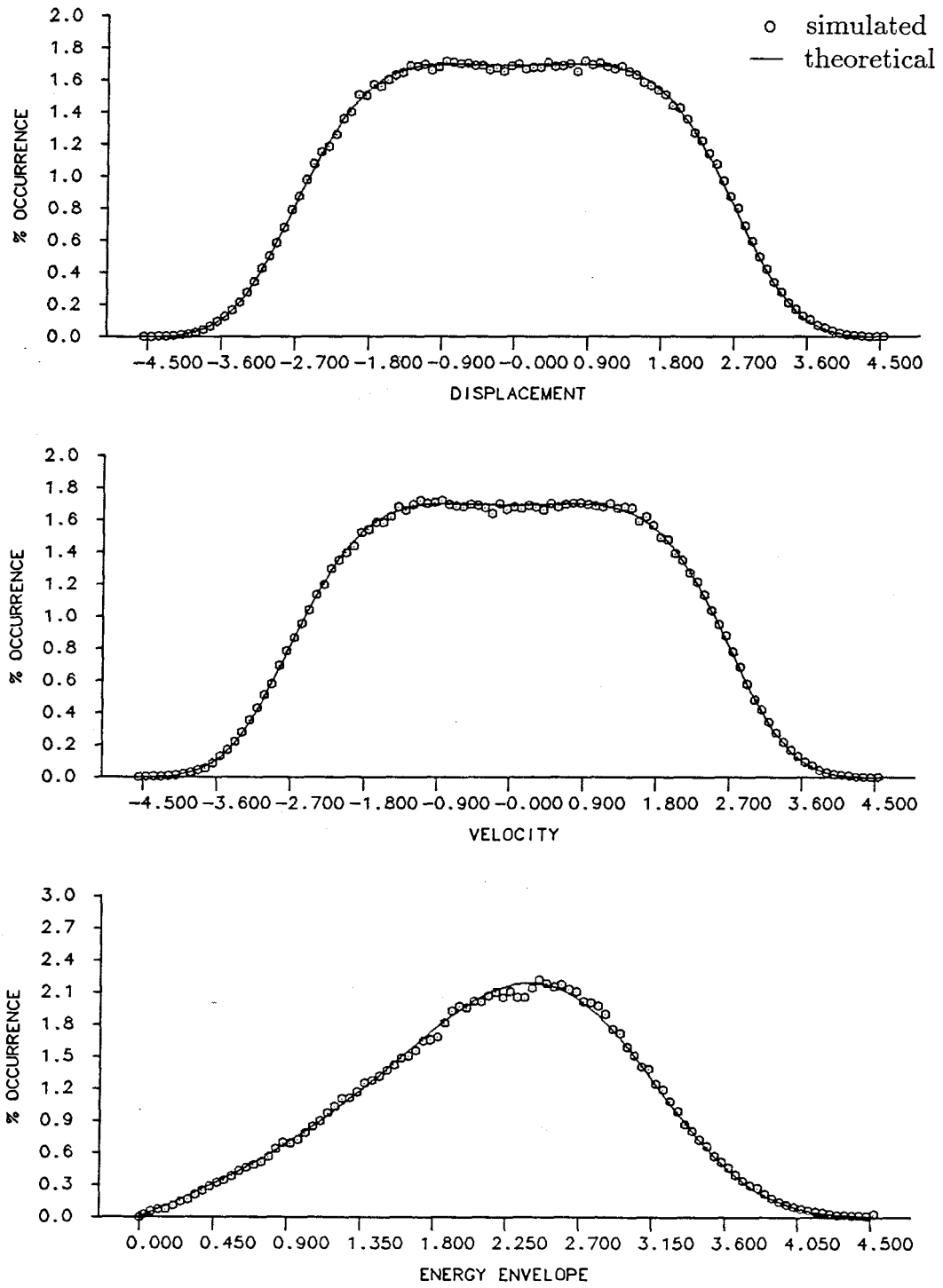
Figure 5.40

Van der Pol Equation: $\left(b_{01}|\dot{x}| + b_{21}|x^2\dot{x}|\right)\operatorname{sgn}(\dot{x})$

$b_{01} = -0.02, \quad b_{21} = 0.02, \quad D = 0.05$
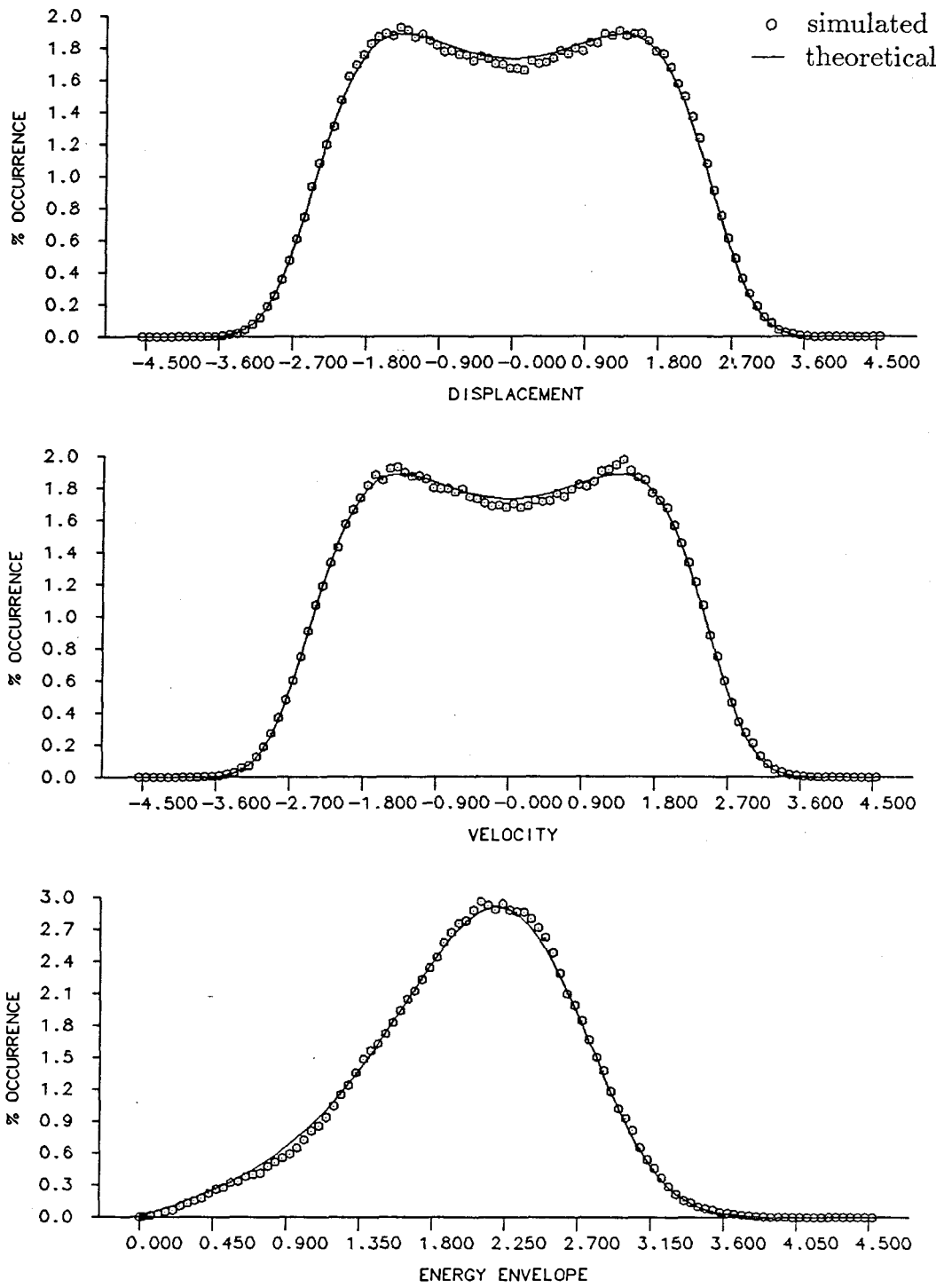
Figure 5.41

Van der Pol Equation: $\left(b_{01}|\dot{x}| + b_{21}|x^2\dot{x}|\right)\text{sgn}(\dot{x})$

$b_{01} = -0.05, \quad b_{21} = 0.05, \quad D = 0.05$
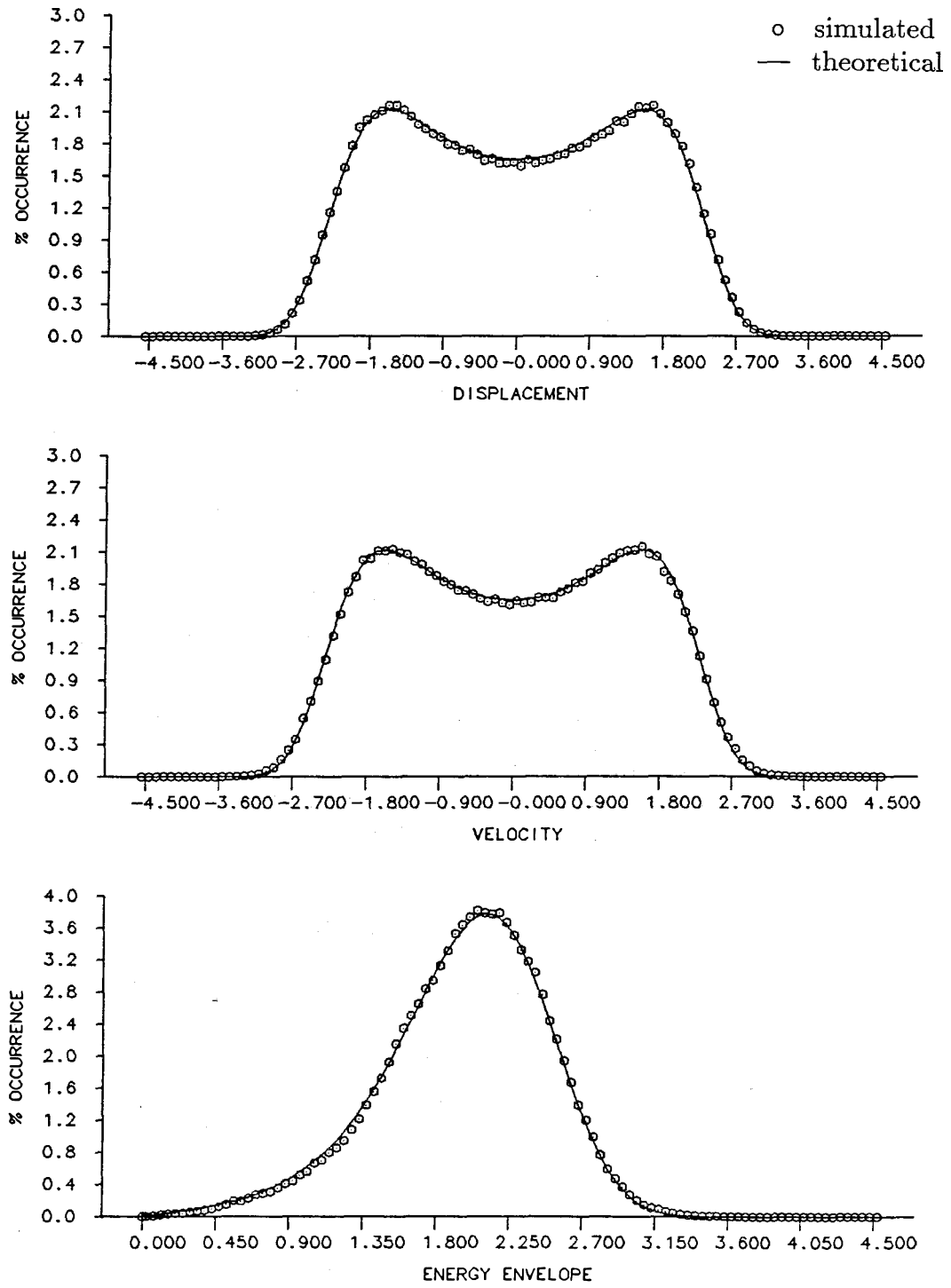
Figure 5.42

Van der Pol Equation: $\left(b_{01}|\dot{x}| + b_{21}|x^2\dot{x}|\right)\mathrm{sgn}(\dot{x})$

$b_{01} = -0.10, \quad b_{21} = 0.10, \quad D = 0.05$
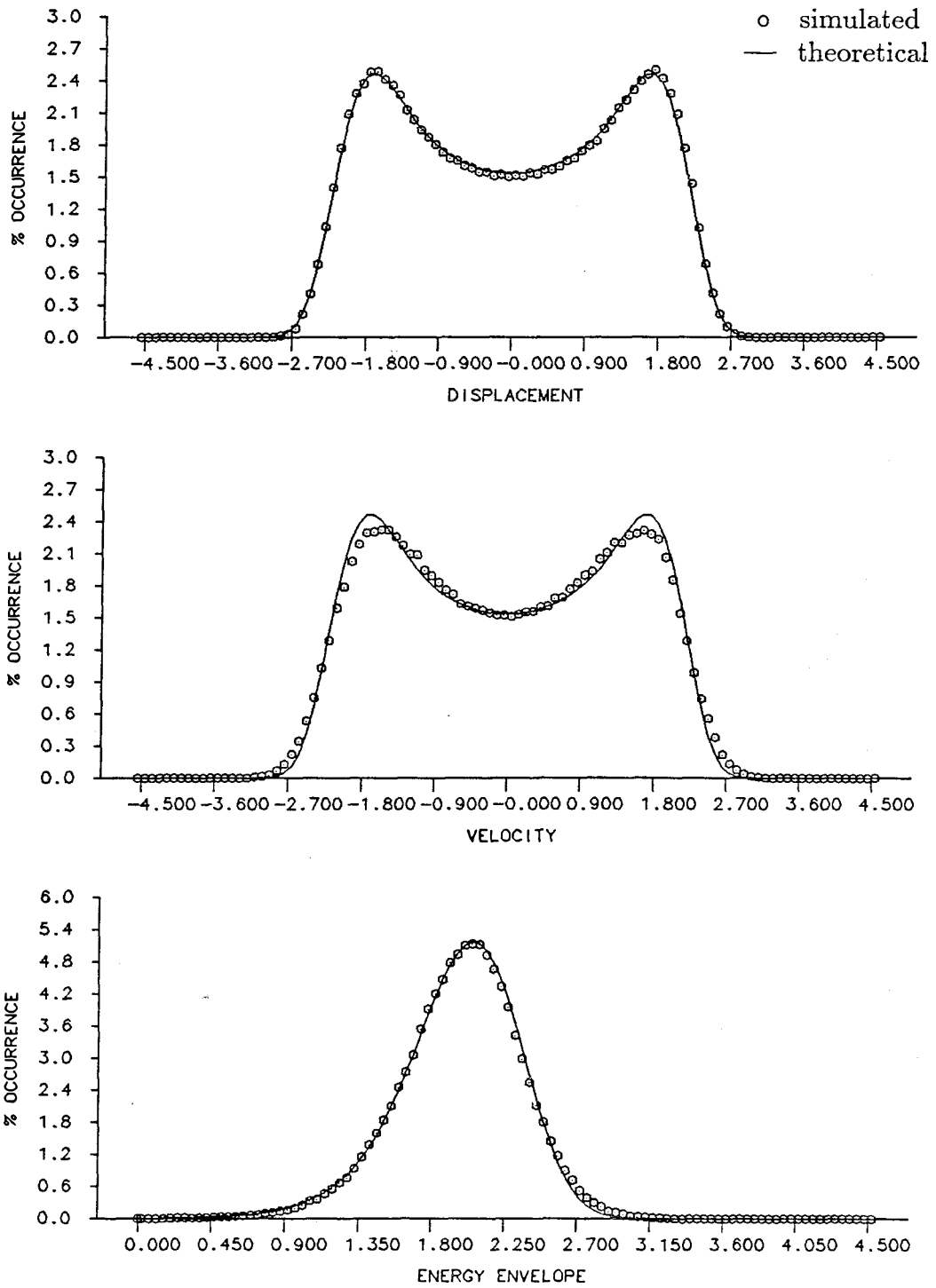
Figure 5.43

Van der Pol Equation: $\left(b_{01}|\dot{x}| + b_{21}|x^2\dot{x}|\right) \mathrm{sgn}(\dot{x})$

$b_{01} = -0.20, \quad b_{21} = 0.20, \quad D = 0.05$
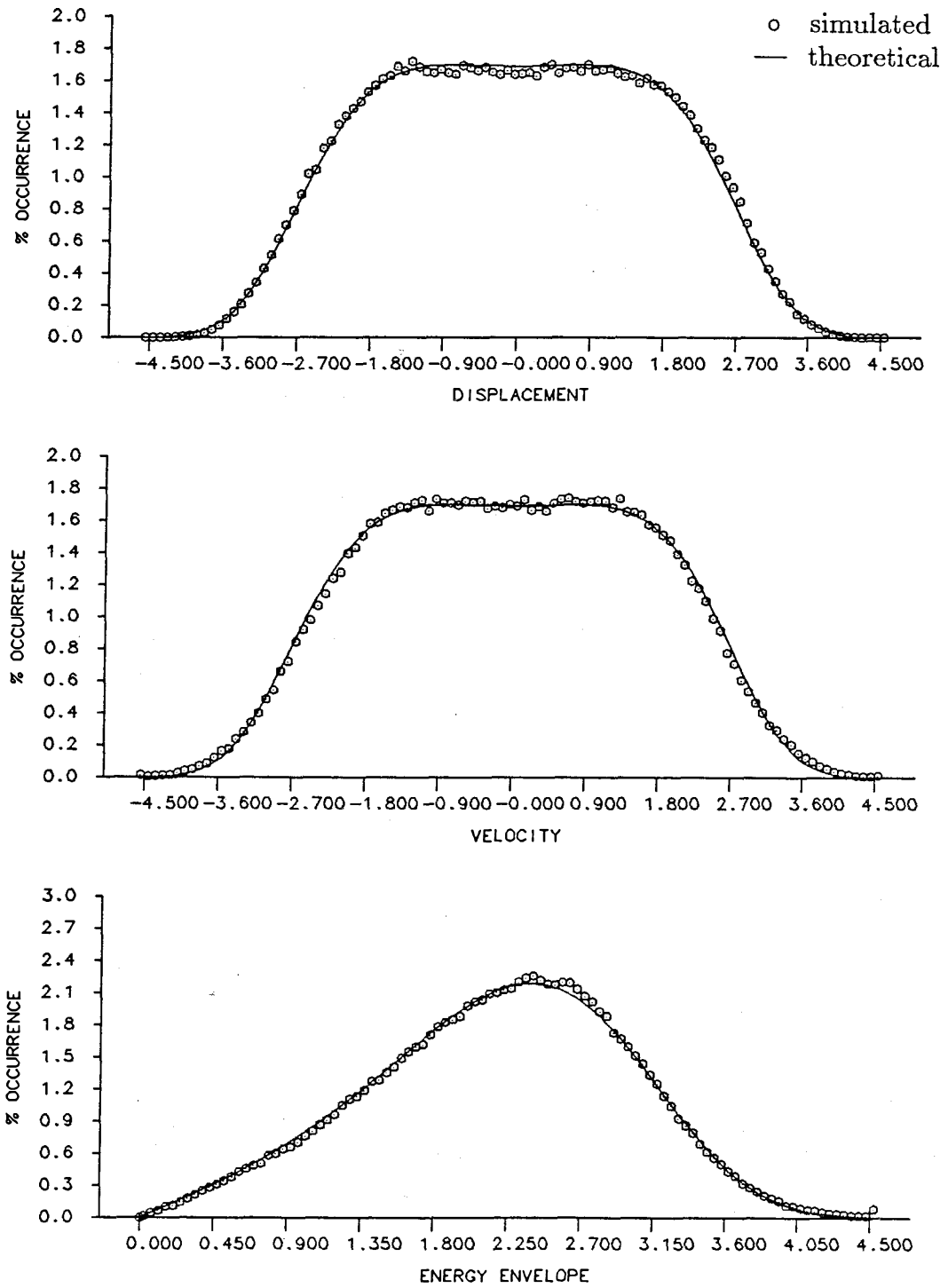
Figure 5.44

Van der Pol Equation: $\left(b_{01}|\dot{x}| + b_{21}|x^2\dot{x}|\right)\mathrm{sgn}(\dot{x})$
$b_{01} = -0.10, \quad b_{21} = 0.10, \quad D = 0.25$
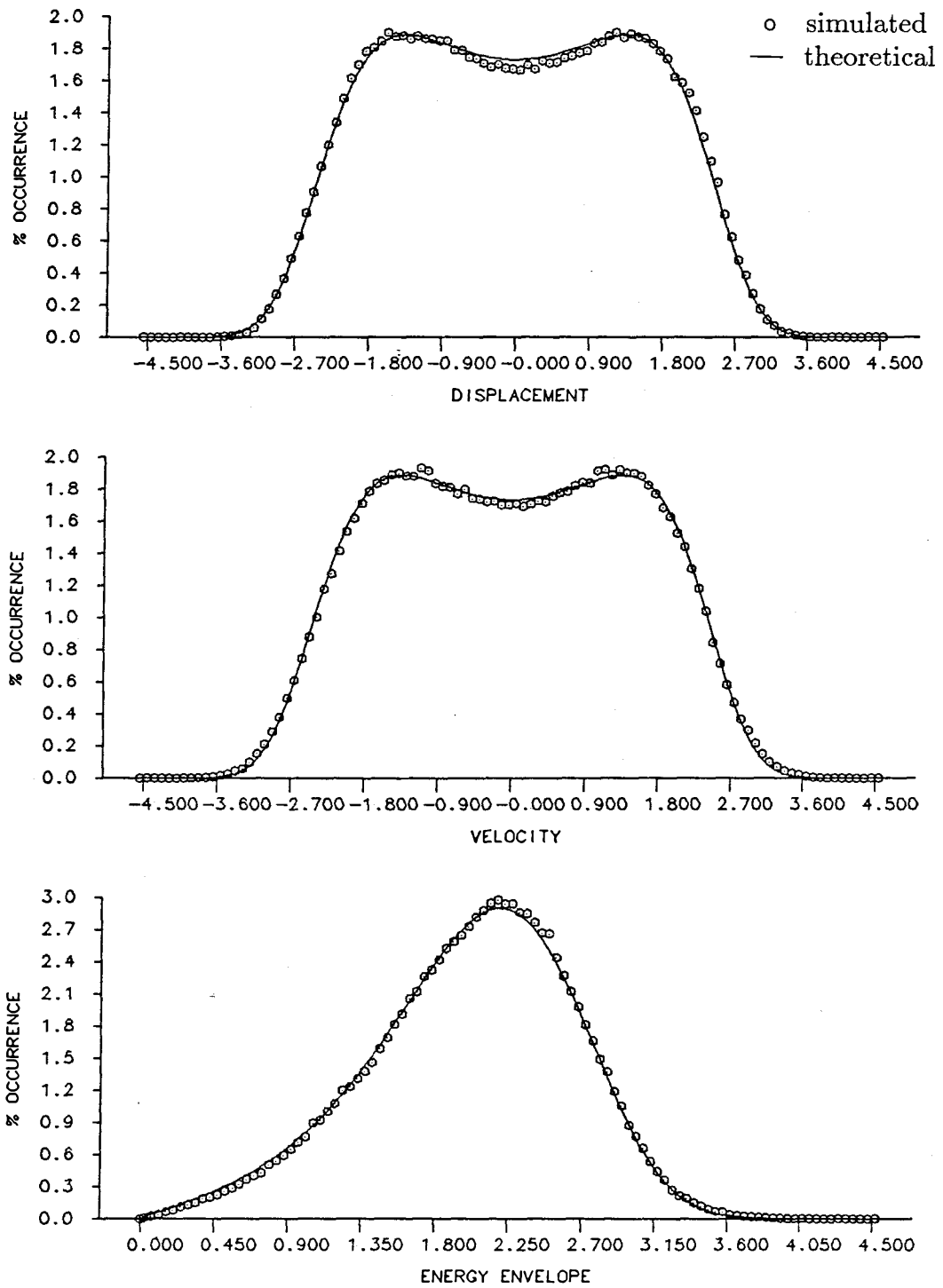
Figure 5.45

Van der Pol Equation: $\left(b_{01}|\dot{x}| + b_{21}|x^2\dot{x}|\right) \operatorname{sgn}(\dot{x})$

$b_{01} = -0.10, \quad b_{21} = 0.10, \quad D = 0.10$
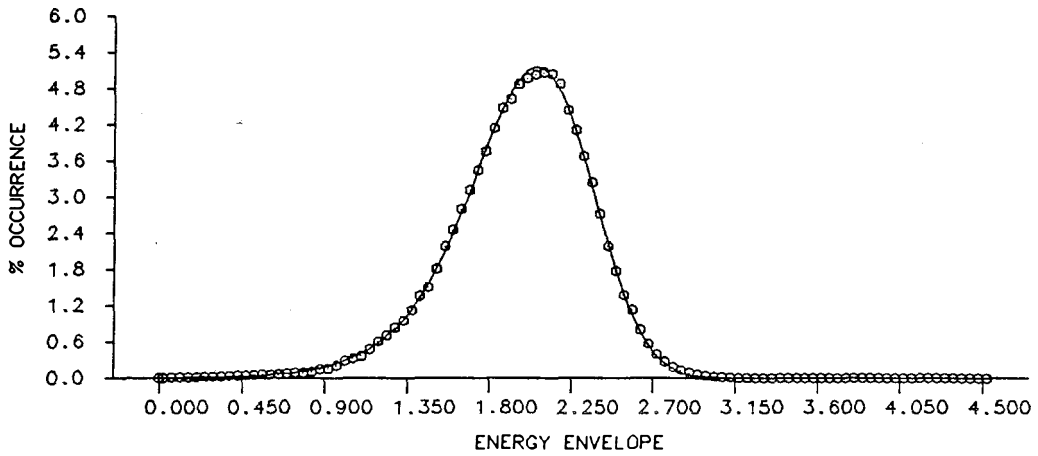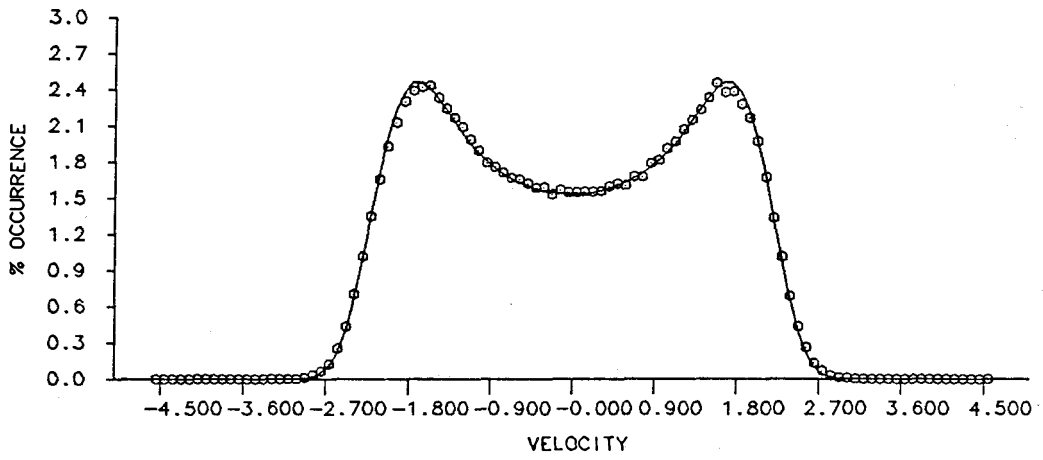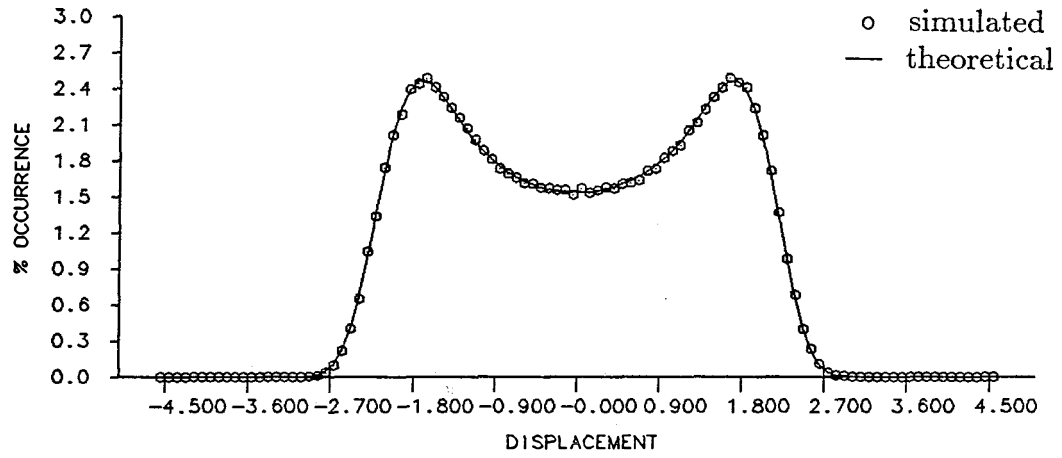
Figure 5.46

Van der Pol Equation: $\left(b_{01}|\dot{x}| + b_{21}|x^2\dot{x}|\right)\text{sgn}(\dot{x})$

$b_{01} = -0.10, \quad b_{21} = 0.10, \quad D = 0.025$
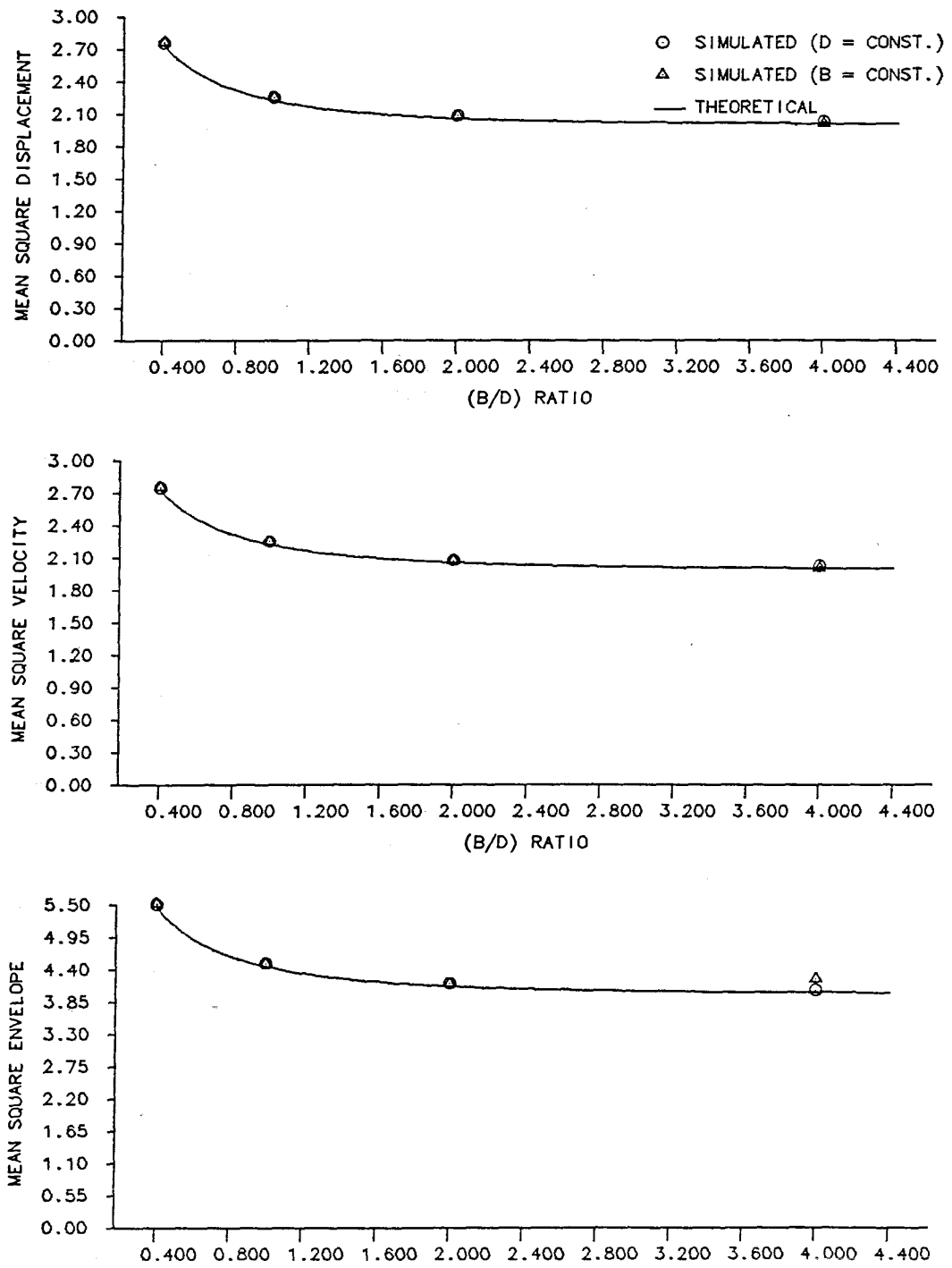
Figure 5.47

Mean-Square Response for Van der Pol Equation

5.2.4 Van der Rayleigh Equation

Consider the Van der Rayleigh equation

$$\ddot{x} - b\left(1 - \left(x^2 + \dot{x}^2\right)\right)\dot{x} + x = w(t), \tag{5.35}$$

which is obtained from Eq. (3.21) by making $b_{01} = -b$, $b_{03} = b$, $b_{21} = b$, $b_{ij} = 0$ otherwise.

First, it is noted that the Van der Rayleigh equation possesses an exact solution for its steady-state probability density function. However, it is still included here because it is an example of a nonlinear equation that can be generated from Eq. (3.21), requiring more than two coefficients, and because it is a good verification example for the numerical procedures used in this thesis. The same procedure will be followed here as if the Van der Rayleigh equation did not possess an exact solution.

The following nonlinear equation replaces Eq. (5.35),

$$\ddot{x} + \left(c_{01}f_{01}(H) + c_{03}f_{03}(H) + c_{21}f_{21}(H)\right)\dot{x} + x = w(t), \tag{5.36}$$

which is obtained from Eq. (3.22) by making $c_{ij} = 0$ except for c_{01}, c_{03} and c_{21}. The only f_{ij} terms of interest are f_{01}, f_{03} and f_{21}, obtained from Eq. (3.24) and given by

$$f_{01} = 1, \quad f_{03} = a^2 \quad \text{and} \quad f_{21} = a^2. \tag{5.37}$$

The unknown coefficients c_{01}, c_{03} and c_{21} are the solutions of the following set of equations:

$$\left(\pi c_{01} - 2b_{01} \frac{\Gamma(\frac{1}{2})\Gamma(\frac{3}{2})}{\Gamma(2)} \right) \int_0^\infty a^2 \lambda(a) da +$$

$$\left(\pi c_{03} - 2b_{03} \frac{\Gamma(\frac{1}{2})\Gamma(\frac{5}{2})}{\Gamma(3)} \right) \int_0^\infty a^4 \lambda(a) da +$$

$$\left(\pi c_{21} - 2b_{21} \frac{\Gamma(\frac{3}{2})\Gamma(\frac{3}{2})}{\Gamma(3)} \right) \int_0^\infty a^4 \lambda(a) da = 0,$$

and

$$\left(\pi c_{01} - 2b_{01} \frac{\Gamma(\frac{1}{2})\Gamma(\frac{3}{2})}{\Gamma(2)} \right) \int_0^\infty a^4 \lambda(a) da +$$

$$\left(\pi c_{03} - 2b_{03} \frac{\Gamma(\frac{1}{2})\Gamma(\frac{5}{2})}{\Gamma(3)} \right) \int_0^\infty a^6 \lambda(a) da + \tag{5.38}$$

$$\left(\pi c_{21} - 2b_{21} \frac{\Gamma(\frac{3}{2})\Gamma(\frac{3}{2})}{\Gamma(3)} \right) \int_0^\infty a^6 \lambda(a) da = 0,$$

and

$$\left(\pi c_{01} - 2b_{01} \frac{\Gamma(\frac{1}{2})\Gamma(\frac{3}{2})}{\Gamma(2)} \right) \int_0^\infty a^4 \lambda(a) da +$$

$$\left(\pi c_{03} - 2b_{03} \frac{\Gamma(\frac{1}{2})\Gamma(\frac{5}{2})}{\Gamma(3)} \right) \int_0^\infty a^6 \lambda(a) da +$$

$$\left(\pi c_{21} - 2b_{21} \frac{\Gamma(\frac{3}{2})\Gamma(\frac{3}{2})}{\Gamma(3)} \right) \int_0^\infty a^6 \lambda(a) da = 0,$$

obtained from Eq. (3.33) by sequentially making $k, l = 0, 1$, $k, l = 0, 3$ and $k, l = 2, 1$ and varying i, j over the same range. A solution for Eq. (5.38) is $c_{01} = b_{01}$, $c_{03} = 3b_{03}/4$ and $c_{21} = b_{21}/4$.

Recalling that $b_{01} = -b$, $b_{03} = b$ and $b_{21} = b$, direct substitution on Eq. (3.27) and evaluation of the normalization constant, A, yield the steady-state joint probability density function of x and $\dot{x}$ as

$$p(x, \dot{x}) = \left(\frac{1}{2\pi}\right) \left(\frac{4\left(\frac{b}{4D}\right)^{\frac{1}{2}}}{\sqrt{\pi}\ \mathrm{erfc}\left[-\left(\frac{b}{4D}\right)^{\frac{1}{2}}\right]}\right) \exp\left[-\left(\frac{b}{4D}\right)(1 - (x^2 + \dot{x}^2))^2\right],$$

$$(5.39)$$

and substitution in Eq. (3.28) yields the probability density function of the energy-based envelope as

$$p_e(\alpha) = \left(\frac{4\left(\frac{b}{4D}\right)^{\frac{1}{2}}}{\sqrt{\pi}\ \mathrm{erfc}\left[-\left(\frac{b}{4D}\right)^{\frac{1}{2}}\right]}\right) \alpha \exp\left[-\left(\frac{b}{4D}\right)(1 - \alpha^2)^2\right]. \qquad (5.40)$$

The expected value of α^2, $E[\alpha^2]$, then, is

$$E[\alpha^2] = \int_0^\infty \alpha^2 p_e(\alpha)d\alpha = 1 + \frac{1}{\left(\frac{b}{4D}\right)^{\frac{1}{2}}} \frac{\exp\left[-\left(\frac{b}{4D}\right)\right]}{\sqrt{\pi}\ \mathrm{erfc}\left[-\left(\frac{b}{4D}\right)^{\frac{1}{2}}\right]}, \qquad (5.41)$$

and again, because of the symmetry of $p(x, \dot{x})$ with respect to x and $\dot{x}$ and because of the definition of α^2 $(= x^2 + \dot{x}^2)$, $E[x^2] = E[\dot{x}^2] = E[\alpha^2]/2$.

Because the purpose of the comparisons between theoretical and simulated results is now to assess the performance of the numerical scheme employed in this work, only the first of the two series of simulations previously discussed was performed. In this series, D was kept constant and b varied over a fairly wide range of values in order to encompass cases of practical interest.

Figs. 5.48 through 5.51 show the results for the first series, which is the comparison of theoretical and simulated histograms for the displacement, velocity and energy-based envelope. In these figures b was made equal to 0.02, 0.05, 0.10 and 0.20, respectively, and D was kept constant and equal to 0.05.

These figures show a small overprediction of the histograms for small values of damping in the region of small values of displacement, velocity and envelope. This bias decreases with increasing damping. With this exception, the agreement between simulated and predicted response histograms is excellent, indicating that the numerical integration scheme with the chosen parameters and simulation length were appropriate.

Fig. 5.52 shows the comparison of the simulated and theoretical results for the $E[x^2]$, $E[\dot{x}^2]$ and the $E[\alpha^2]$ as functions of the ratio b/D. These figures show a sytematic underprediction, which indicates either or both of a small bias in the numerical integration process or a random error associated with the forcing function time-history used, which was the same for all cases. The realization of more simulations with subsequent averaging of the results would either quantify the bias or eliminate this error. This, however, is outside the scope of this work.
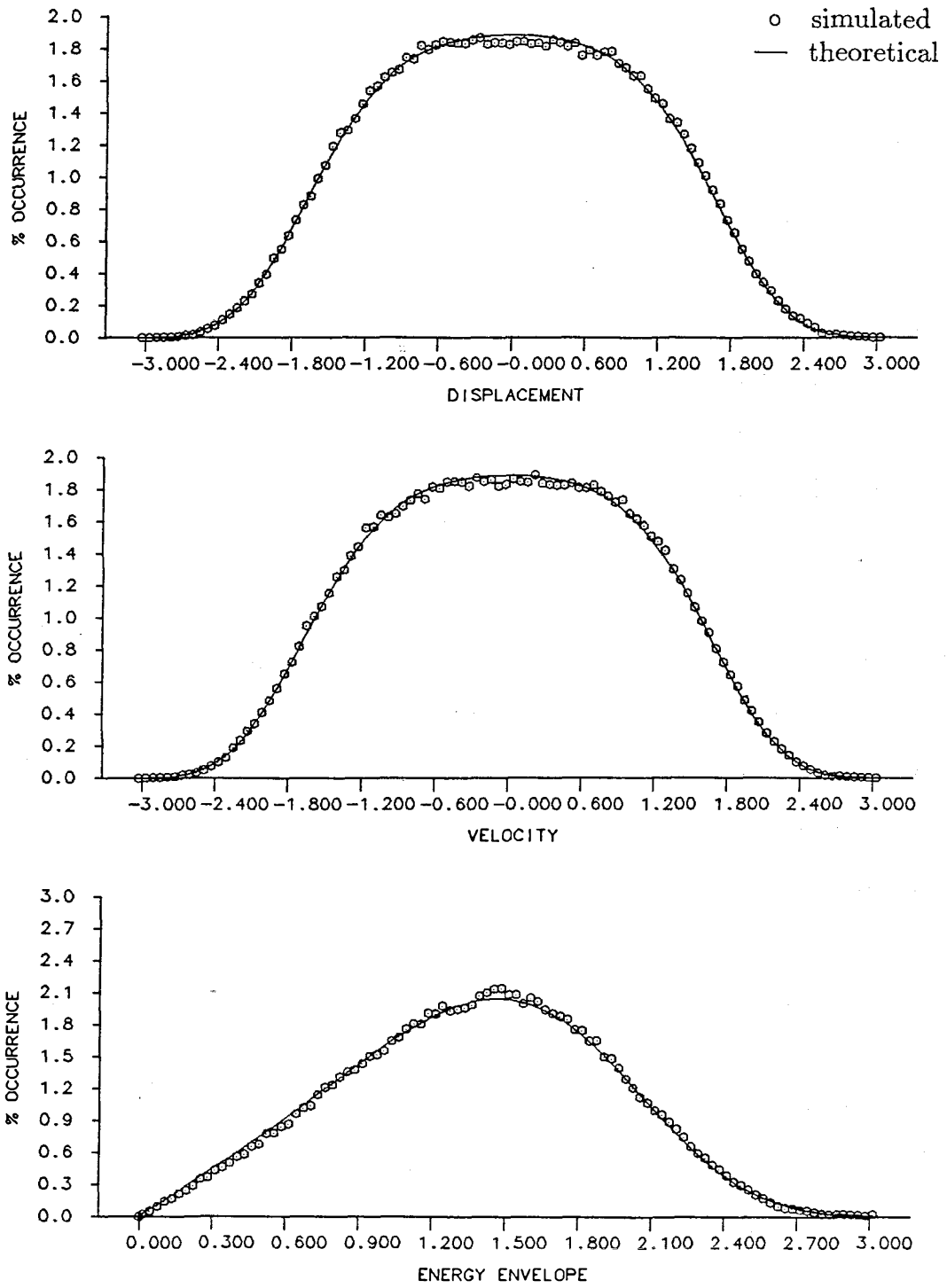
Figure 5.48

Van der Rayleigh Equation: $\left(b_{01}|\dot{x}| + b_{03}|\dot{x}^3| + b_{21}|x^2\dot{x}|\right)\text{sgn}(\dot{x})$

$b_{01} = -0.02, \quad b_{03} = 0.02, \quad b_{21} = 0.02, \quad D = 0.05$
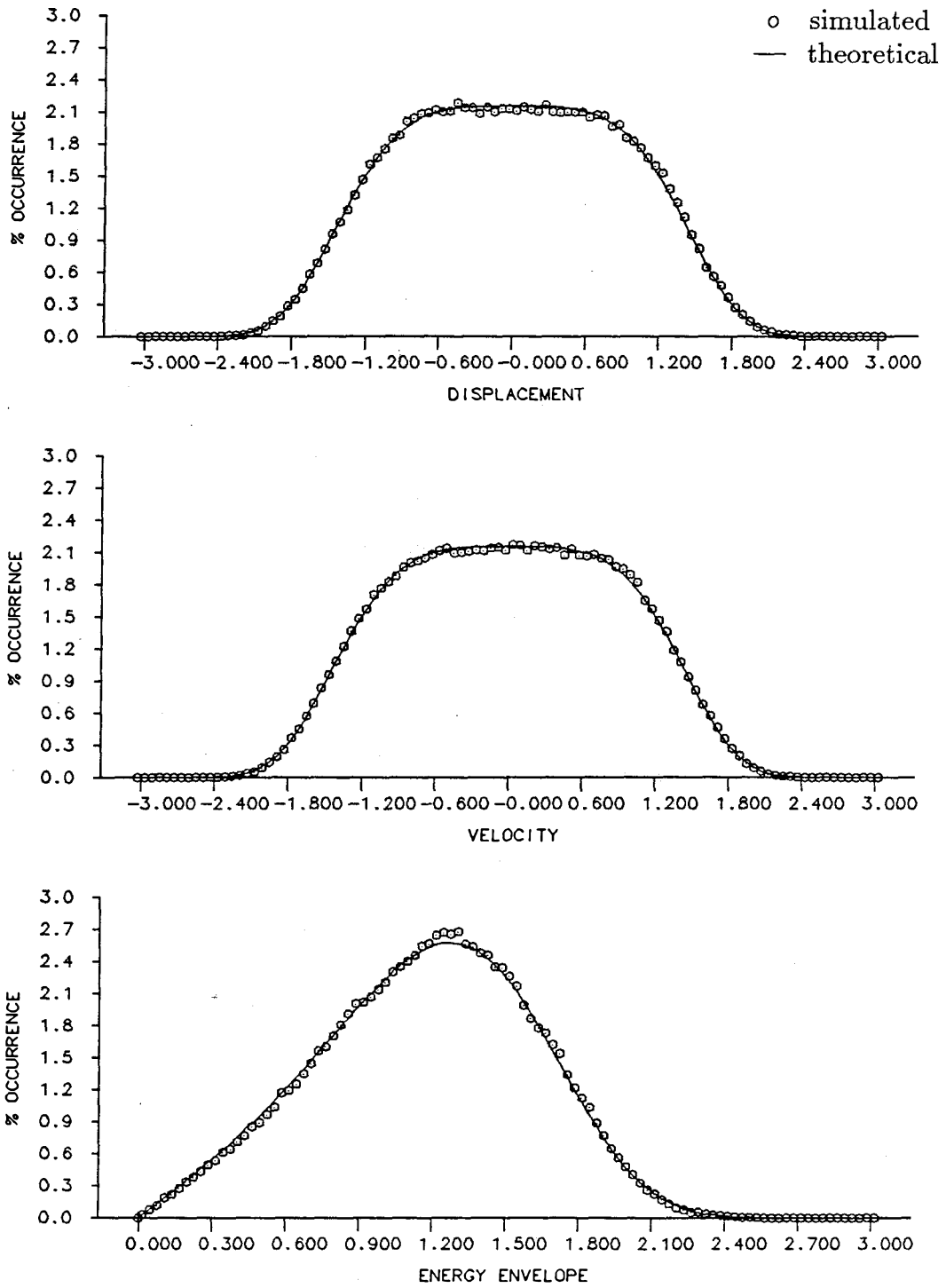
Figure 5.49

Van der Rayleigh Equation: $\left(b_{01}|\dot{x}| + b_{03}|\dot{x}^3| + b_{21}|x^2\dot{x}|\right)\operatorname{sgn}(\dot{x})$

$b_{01} = -0.05,\ \ b_{03} = 0.05,\ \ b_{21} = 0.05,\ \ D = 0.05$
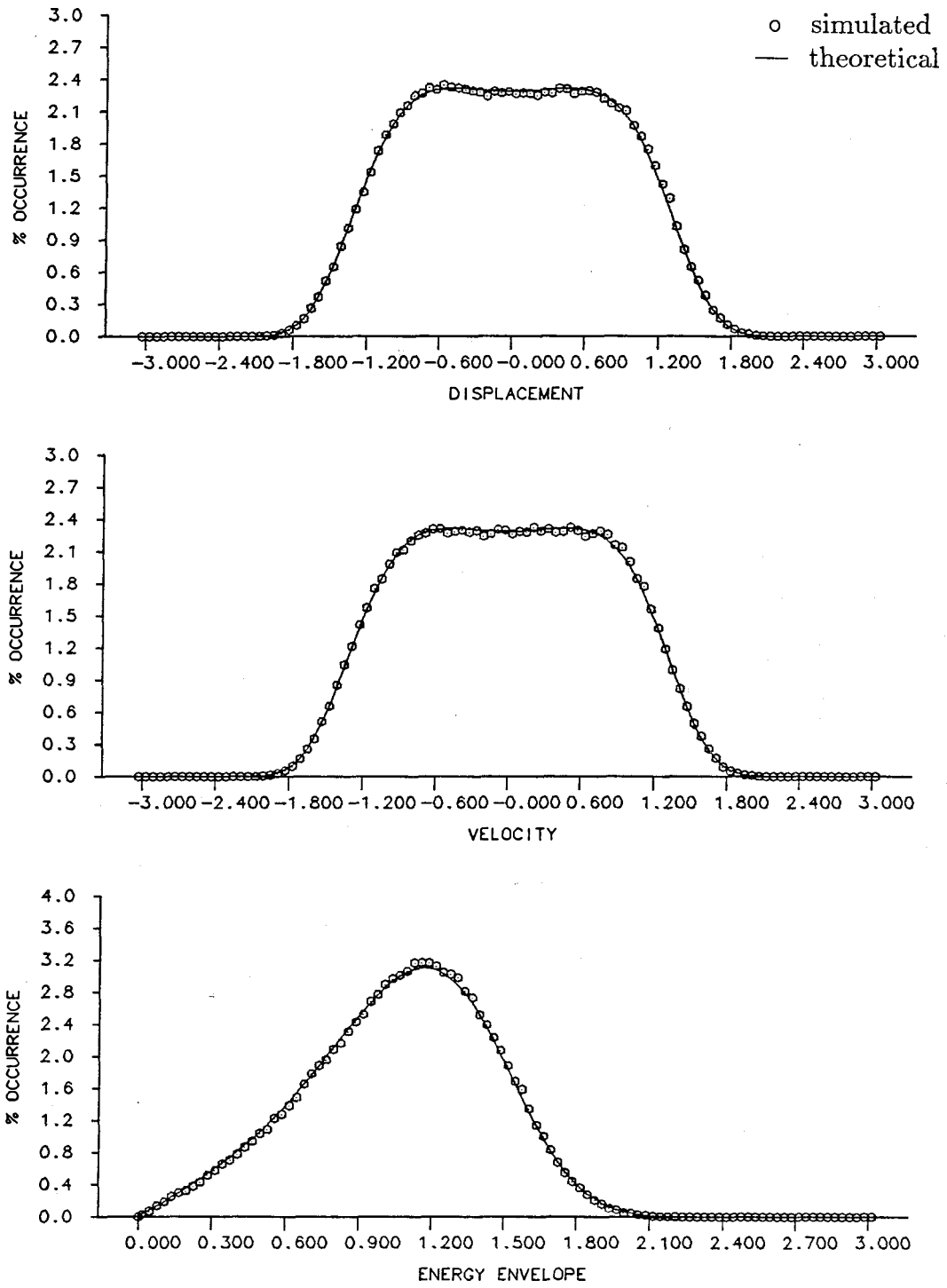
Figure 5.50

Van der Rayleigh Equation: $\left(b_{01}|\dot{x}| + b_{03}|\dot{x}^3| + b_{21}|x^2\dot{x}|\right)\mathrm{sgn}(\dot{x})$

$b_{01} = -0.10, \quad b_{03} = 0.10, \quad b_{21} = 0.10, \quad D = 0.05$
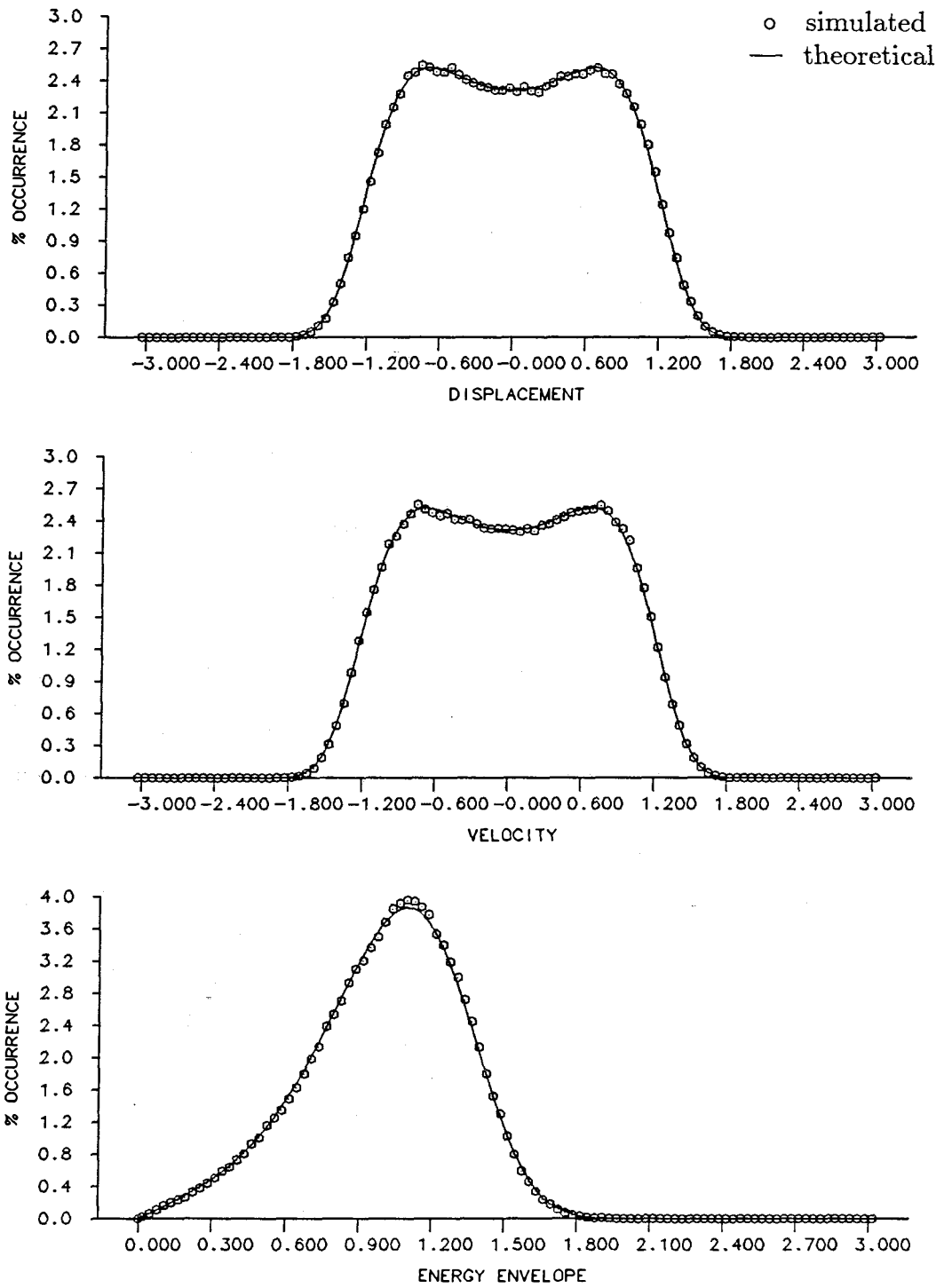
Figure 5.51

Van der Rayleigh Equation: $\left(b_{01}|\dot{x}| + b_{03}|\dot{x}^3| + b_{21}|x^2\dot{x}|\right)\mathrm{sgn}(\dot{x})$
$b_{01} = -0.20, \quad b_{03} = 0.20, \quad b_{21} = 0.20, \quad D = 0.05$
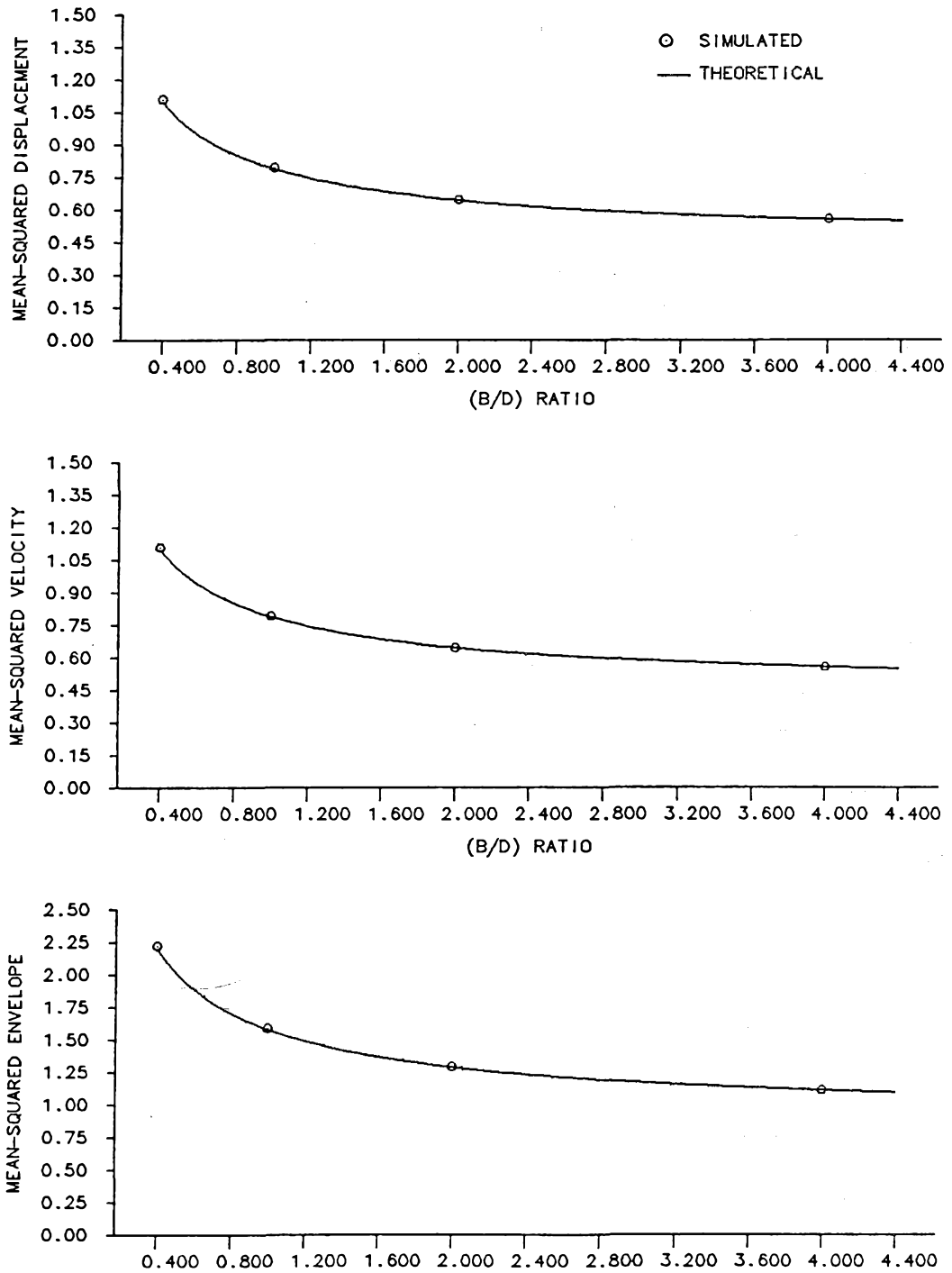
Figure 5.52

Mean-Square Response for Van der Rayleigh Equation

5.2.5 Systems with $(bx^2\dot{x})$-Damping

Consider the SDOF system with damping involving displacement and velocity terms of the form

$$\ddot{x} + b\,x^2\dot{x} + x = w(t), \qquad (5.42)$$

which is obtained from Eq. (3.21) by making $b_{21} = b$, $b_{ij} = 0$ otherwise.

The following nonlinear equation replaces Eq. (5.42),

$$\ddot{x} + c_{21}f_{21}(H)\dot{x} + x = w(t), \qquad (5.43)$$

which is obtained from Eq. (3.22) by making $c_{ij} = 0$ except for c_{21}. The only f_{ij} term of interest is f_{21}, obtained from Eq. (3.24) and given by

$$f_{21} = a^2. \qquad (5.44)$$

The unknown coefficient c_{21} is the solution of the following equation,

$$\pi c_{21} - 2b_{21}\frac{\Gamma(\frac{3}{2})\Gamma(\frac{3}{2})}{\Gamma(3)} = 0, \qquad (5.45)$$

obtained from Eq. (3.33) by making $k, l = 2, 1$, and $i, j = 2, 1$. A solution for Eq. (5.45) is $c_{21} = b_{21}/4$.

Recalling that $b_{21} = b$, direct substitution on Eq. (3.27) and evaluation of the normalization constant, A, yields the steady-state joint probability density function of x and $\dot{x}$ as

$$p(x, \dot{x}) = \left(\frac{1}{2\pi}\right) \left(\frac{4}{\sqrt{\pi}}\right) \left(\frac{b}{16D}\right)^{\frac{1}{2}} \exp\left[-\left(\frac{b}{16D}\right)(x^2 + \dot{x}^2)^2\right], \qquad (5.46)$$

and substitution in Eq. (3.28) yields the probability density function of the energy-based envelope as

$$p_e(\alpha) = \left(\frac{4}{\sqrt{\pi}}\right) \left(\frac{b}{16D}\right)^{\frac{1}{2}} \alpha \exp\left[-\left(\frac{b}{16D}\right)\alpha^4\right]. \qquad (5.47)$$

The expected value of α^2, $E[\alpha^2]$, then is

$$E[\alpha^2] = \int_0^\infty \alpha^2 p_e(\alpha)d\alpha = \frac{1}{\sqrt{\pi}} \frac{1}{\left(\frac{b}{16D}\right)^{\frac{1}{2}}}, \qquad (5.48)$$

and again, because of the symmetry of $p(x, \dot{x})$ with respect to x and $\dot{x}$ and because of the definition of α^2 $\left(= x^2 + \dot{x}^2\right)$, $E[x^2] = E[\dot{x}^2] = E[\alpha^2]/2$.

As before, the response of the original nonlinear equation, Eq. (5.42), in principle, is a function of the two independent parameters b and D. The response to the equivalent nonlinear equation, however, is a function of the ratio b/D. In order to assess the effect of b and D on the response of the original equation, the two series of simulations were again performed. In the first, D was kept constant and b varied over a fairly wide range of values in order to encompass cases of

practical interest. In the second series, b was kept constant and D varied in such a way that the ratio b/D was the same in both series.

Figs. 5.53 through 5.56 show the results for the first series, which are the comparisons of theoretical and simulated histograms for the displacement, velocity and energy-based envelope. In these figures b was made equal to 0.02, 0.05, 0.10 and 0.20, respectively, and D was kept constant and equal to 0.05. This value of D produced a random forcing function with unit standard deviation. Fig. 5.55 and Figs. 5.57 through 5.59 show the results for the second series, for $b = 0.10$ and D equal to 0.05, 0.25, 0.10 and 0.025. Fig. 5.60 shows the comparison of the simulated and theoretical results for the $E[x^2]$, $E[\dot{x}^2]$ and the $E[\alpha^2]$ as functions of the ratio b/D.

In general, the agreement between simulated and predicted response histograms is excellent. A close examination of the curves also indicates a small systematic overprediction for small values of the envelope which, as pointed out in the previous section, may be due, in part, to a bias in the integration procedure used to obtain the simulated results.
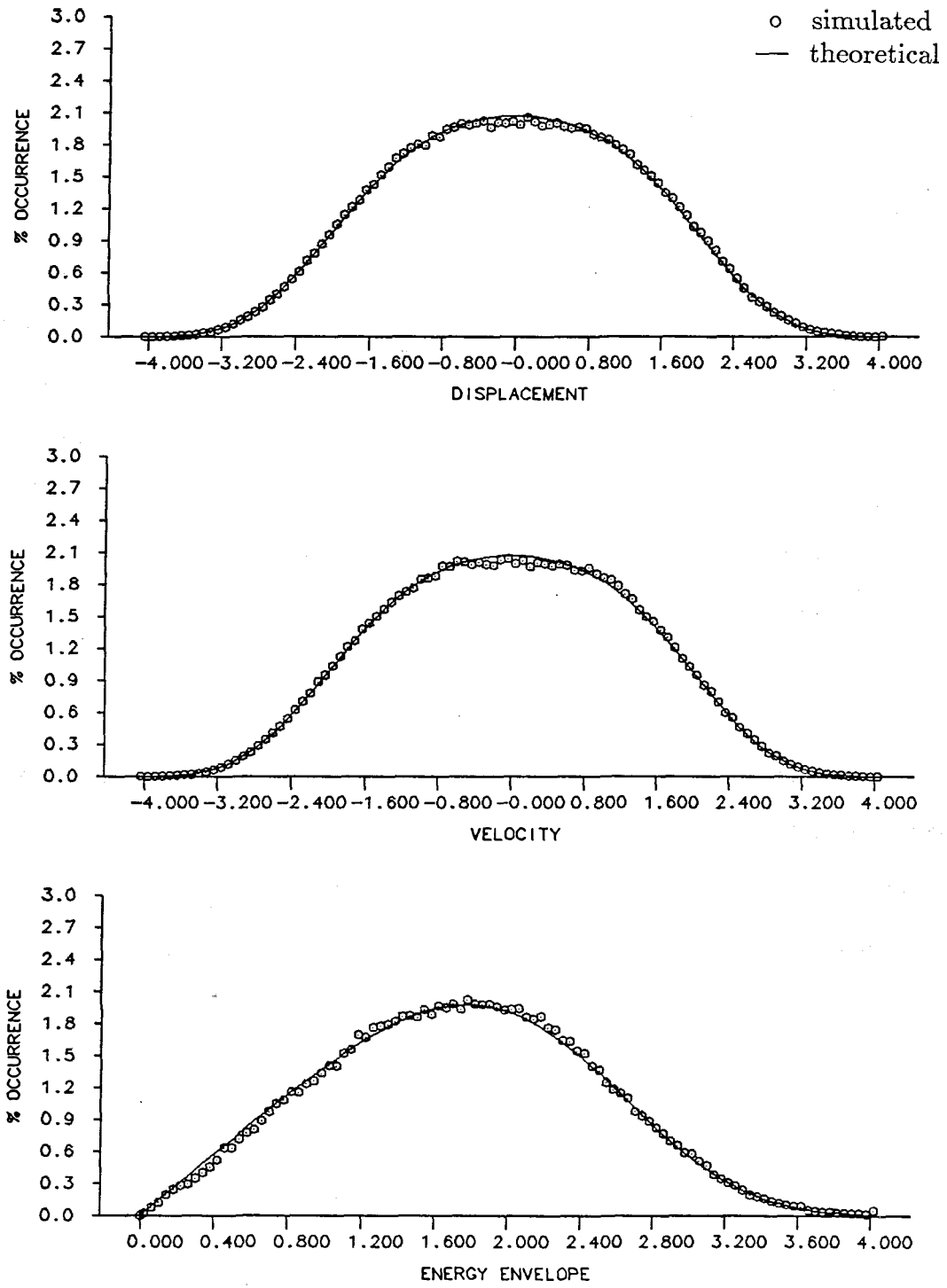
Figure 5.53

Composite Damping: $b_{21}x^2\dot{x}$

$b_{21} = 0.02, \quad D = 0.05$
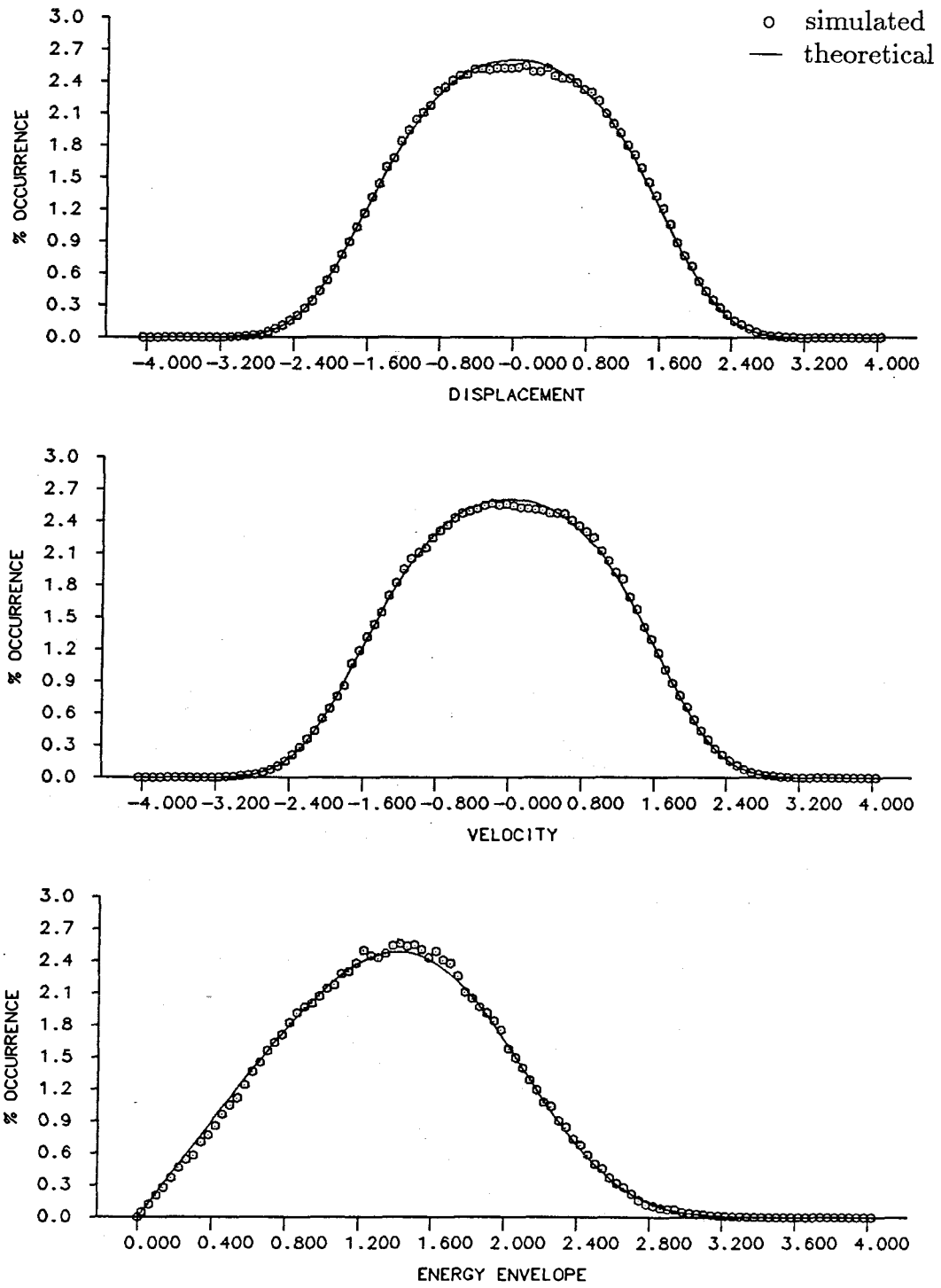
Figure 5.54

Composite Damping: $b_{21}x^2\dot{x}$

$b_{21} = 0.05, \quad D = 0.05$
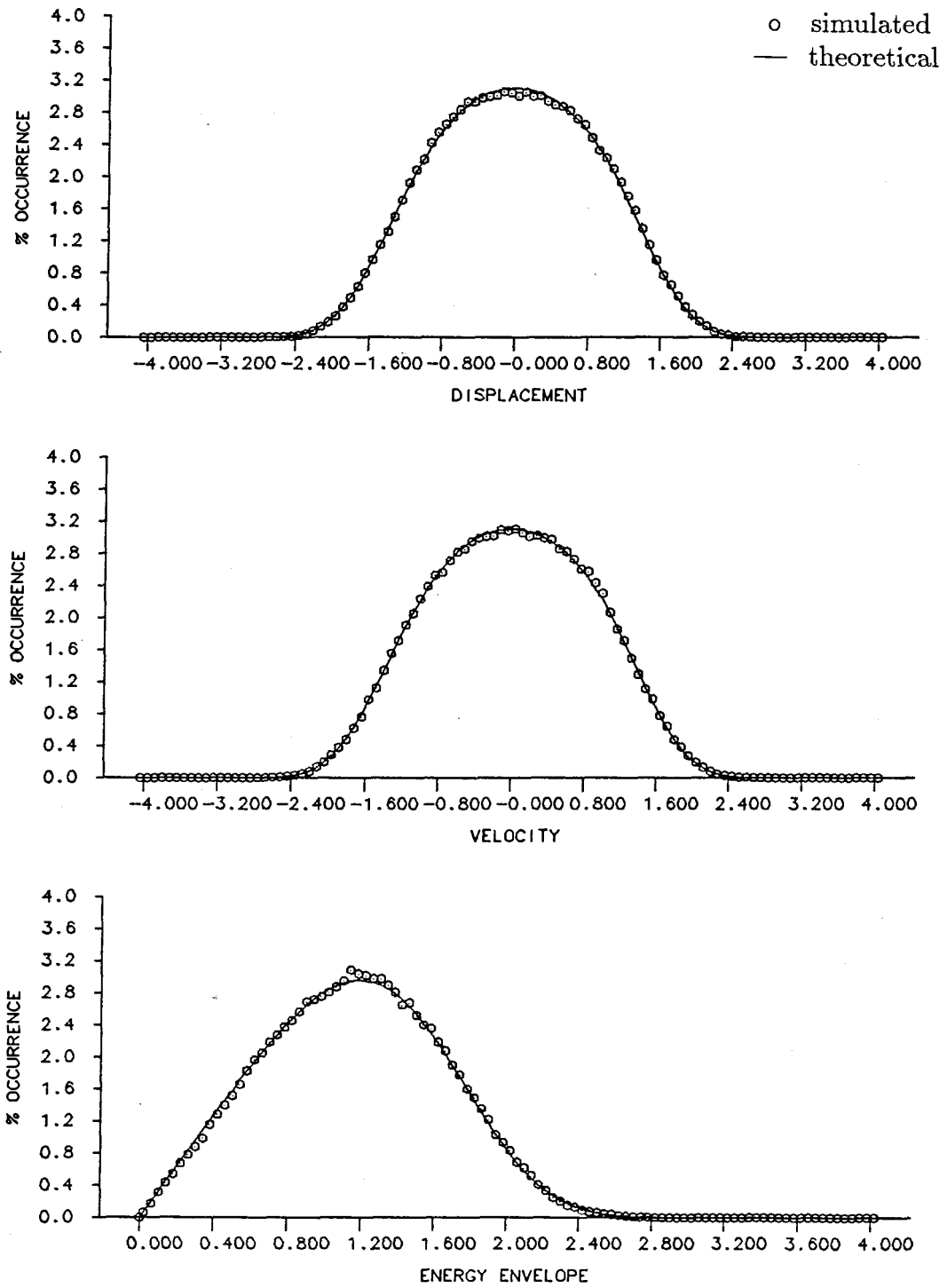
Figure 5.55

Composite Damping: $b_{21} x^2 \dot{x}$

$b_{21} = 0.10, \quad D = 0.05$
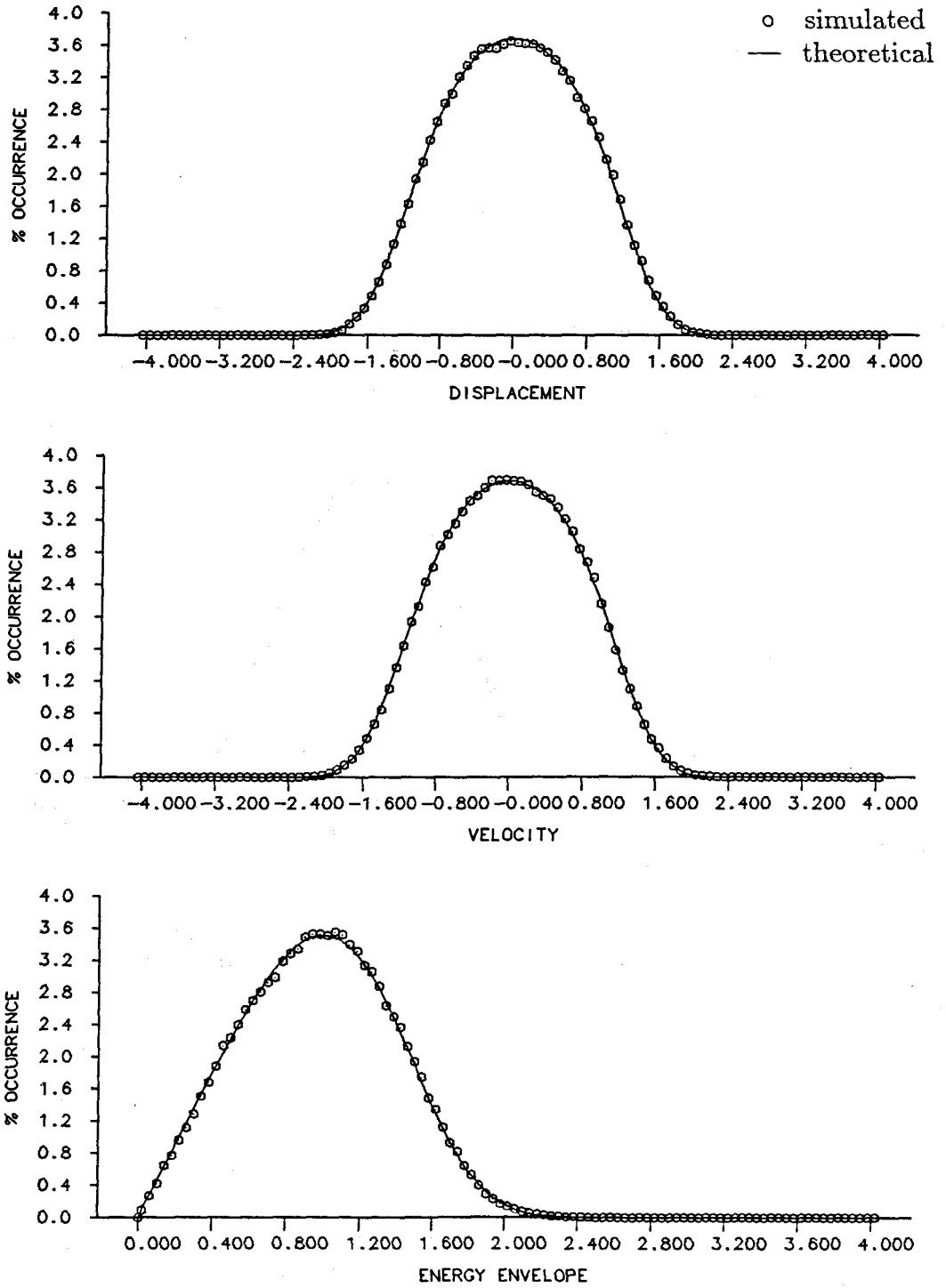
Figure 5.56

Composite Damping: $b_{21}x^2\dot{x}$

$b_{21} = 0.20, \quad D = 0.05$
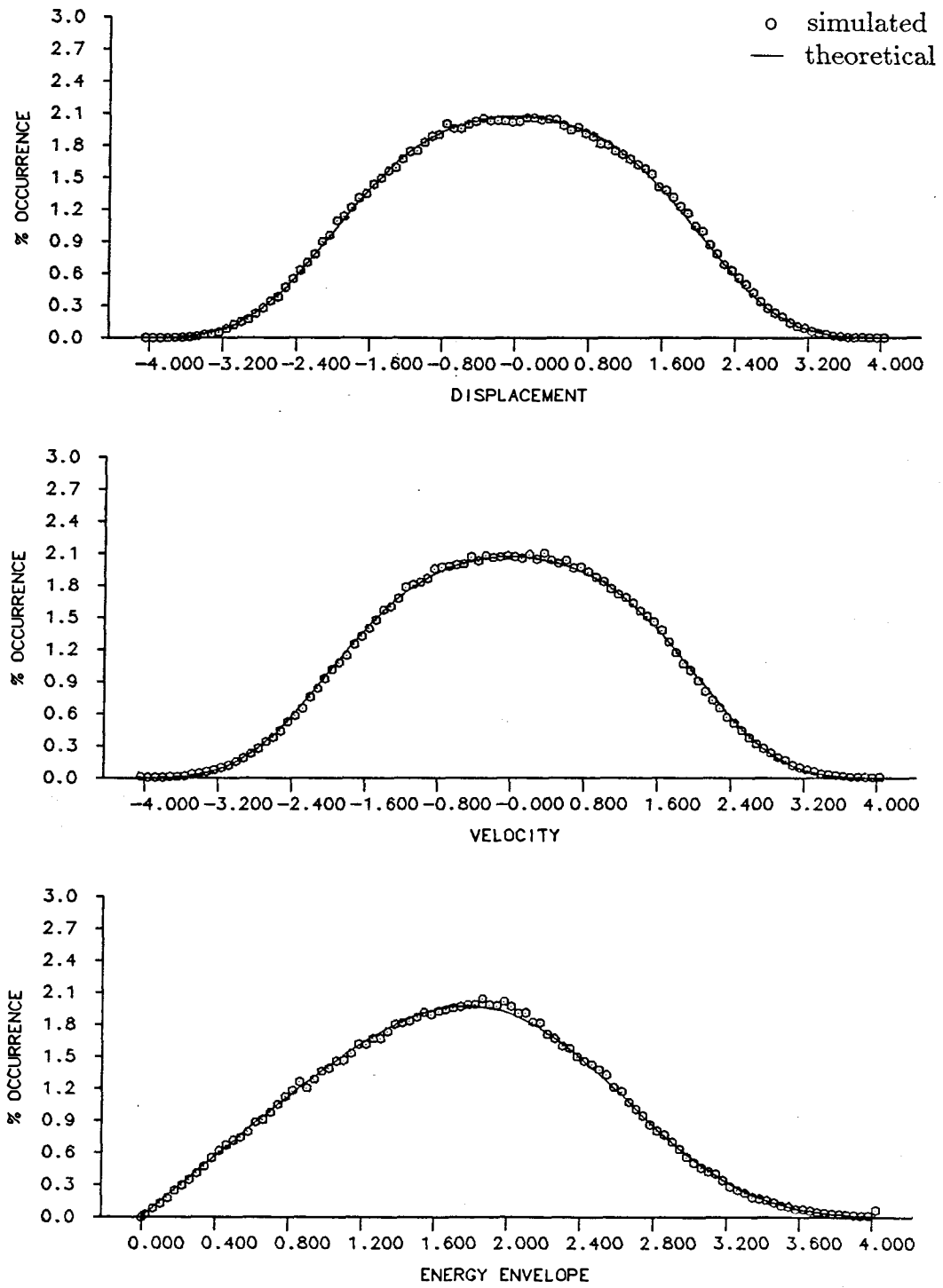
Figure 5.57

Composite Damping: $b_{21}x^2\dot{x}$

$b_{21} = 0.10, \quad D = 0.25$
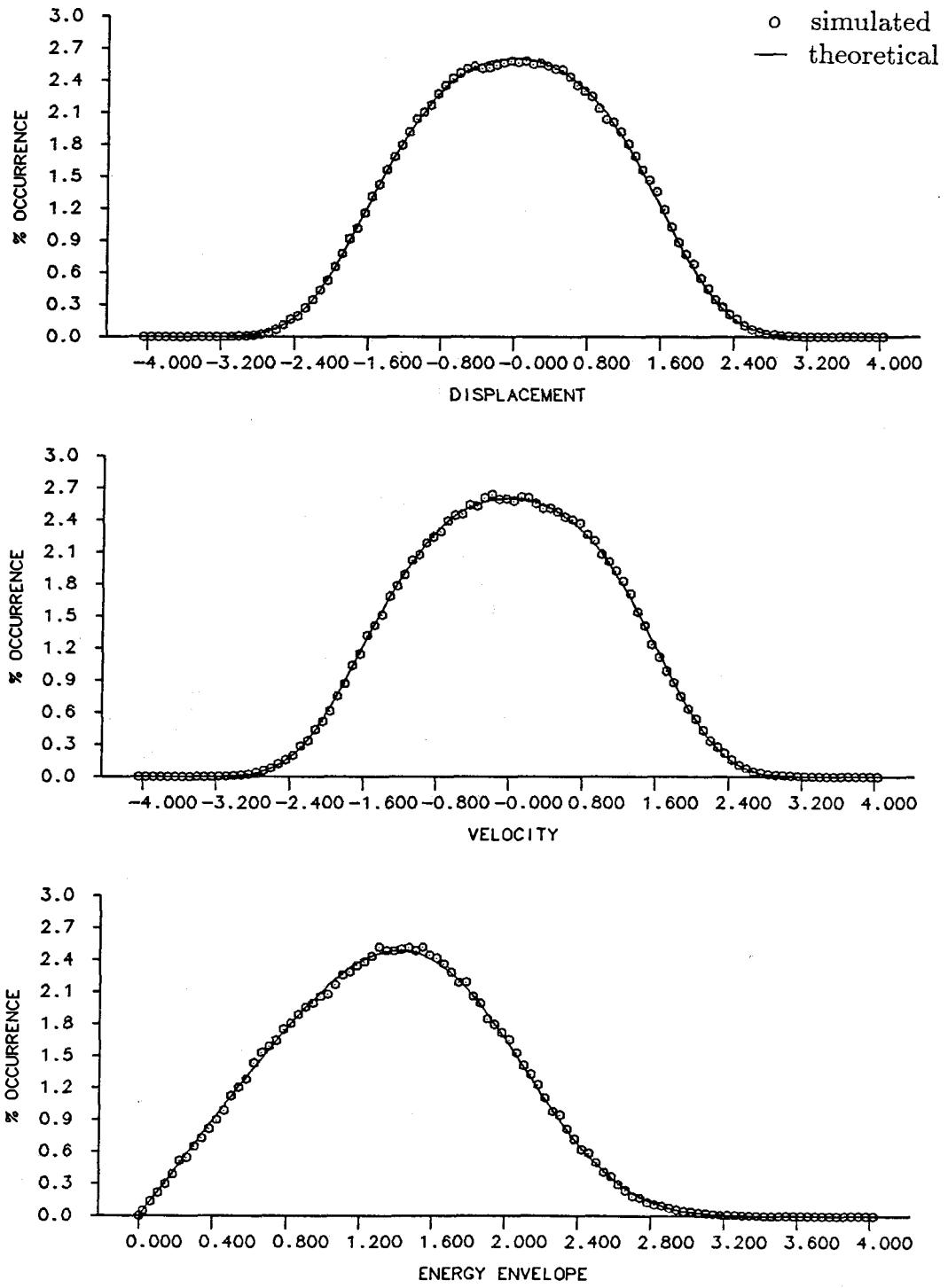
Figure 5.58

Composite Damping: $b_{21}x^2\dot{x}$
$b_{21} = 0.10, \quad D = 0.10$
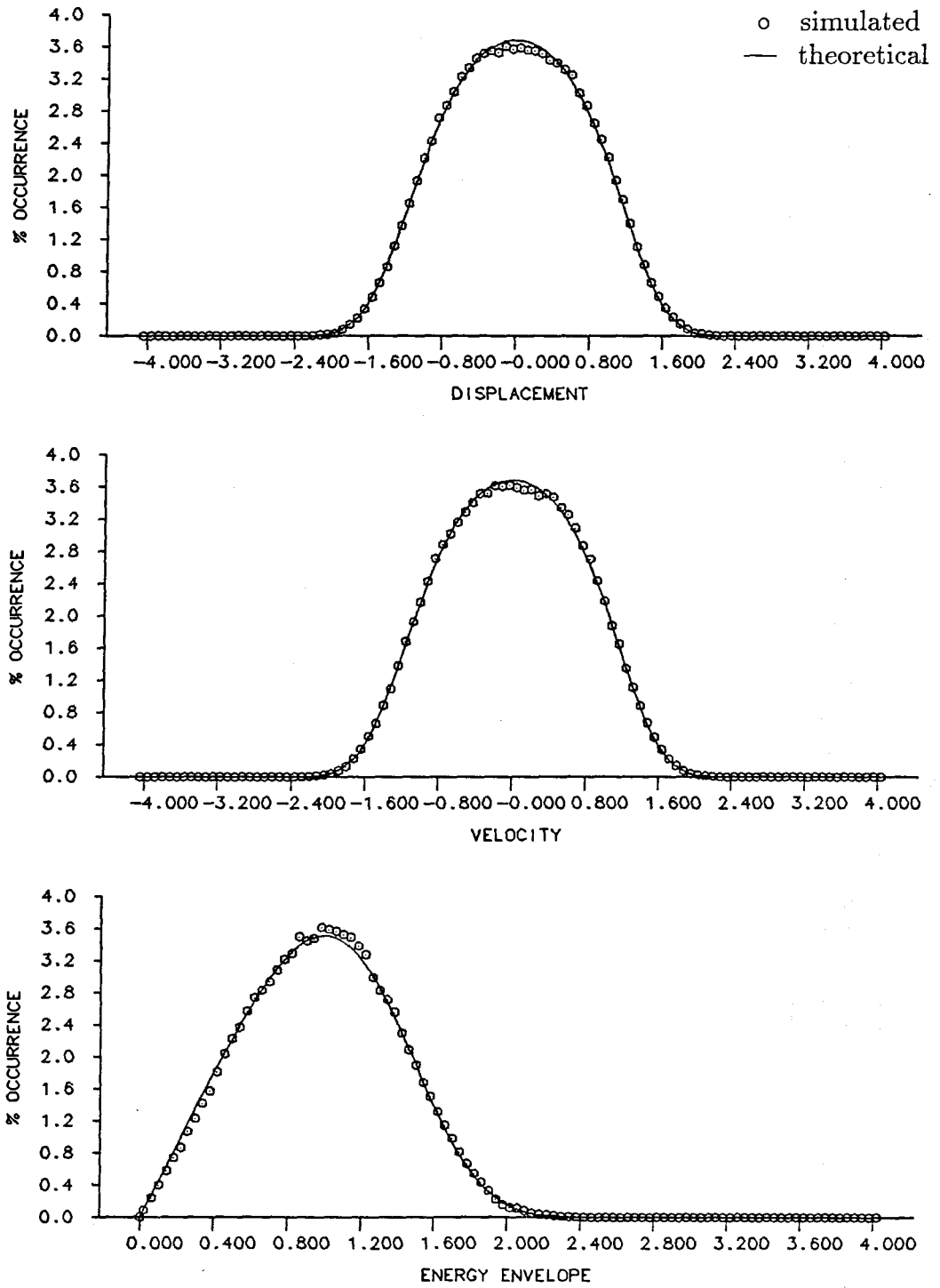
Figure 5.59

Composite Damping: $b_{21} x^2 \dot{x}$

$b_{21} = 0.10, \quad D = 0.025$
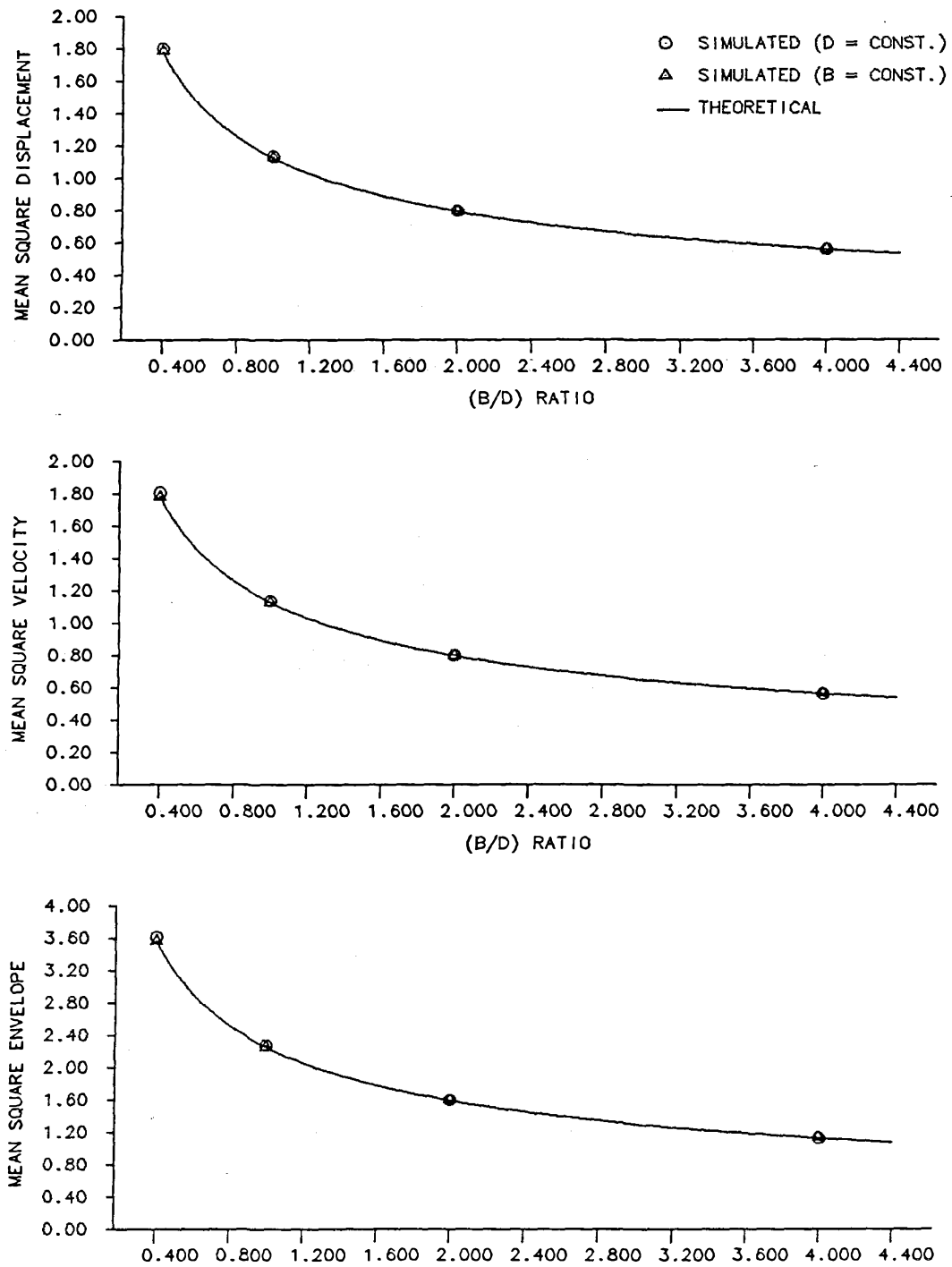
Figure 5.60

Mean-Square Response for $(b_{21} x^2 \dot{x})$-Damping

5.2.6 Systems with $\big((a\dot{x}^2 + bx^2)\text{sgn}(\dot{x})\big)$-Damping

Consider the SDOF system with damping involving other displacement and velocity terms of the form

$$\ddot{x} + (a\dot{x}^2 + bx^2)\text{sgn}(\dot{x}) + x = w(t), \qquad (5.49)$$

which is obtained from Eq. (3.21) by making $b_{02} = a$, $b_{20} = b$, $b_{ij} = 0$ otherwise.

The following equivalent nonlinear equation replaces Eq. (5.49),

$$\ddot{x} + (c_{02}f_{02}(H) + c_{20}f_{20}(H))\,\dot{x} + x = w(t), \qquad (5.50)$$

which is obtained from Eq. (3.22) by making $c_{ij} = 0$ except for c_{02} and c_{20}. The only f_{ij} terms of interest are f_{02} and f_{20}, obtained from Eq. (3.24) and given by

$$f_{02} = f_{20} = a, \qquad (5.51)$$

The unknown coefficients c_{02} and c_{20} are the solutions of the following set of equations:

$$\left(\pi c_{02} - 2b_{02} \frac{\Gamma(\frac{1}{2})\Gamma(2)}{\Gamma(\frac{5}{2})} \right) \int_0^\infty a^4 \lambda(a) da +$$

$$\left(\pi c_{20} - 2b_{20} \frac{\Gamma(\frac{3}{2})\Gamma(3)}{\Gamma(\frac{5}{2})} \right) \int_0^\infty a^4 \lambda(a) da = 0,$$

and $\qquad\qquad\qquad\qquad\qquad\qquad\qquad\qquad\qquad$ (5.52)

$$\left(\pi c_{02} - 2b_{02} \frac{\Gamma(\frac{1}{2})\Gamma(2)}{\Gamma(\frac{5}{2})} \right) \int_0^\infty a^4 \lambda(a) da +$$

$$\left(\pi c_{20} - 2b_{20} \frac{\Gamma(\frac{3}{2})\Gamma(3)}{\Gamma(\frac{5}{2})} \right) \int_0^\infty a^4 \lambda(a) da = 0,$$

obtained from Eq. (3.33) by first making $k, l = 0, 2$ and varying i, j, and then $k, l = 2, 0$ and varying i, j. A solution for Eq. (5.52) is $c_{02} = 8b_{02}/3\pi$ and $c_{21} = 4b_{20}/3\pi$.

Recalling that $b_{02} = a$ and $b_{20} = b$, direct substitution on Eq. (3.27) and evaluation of the normalization constant, A, yield the steady-state joint probability density function of x and $\dot{x}$ as

$$p(x, \dot{x}) = \left(\frac{1}{2\pi} \right) \left(\frac{3}{\Gamma(\frac{2}{3})} \right) \left(\frac{8\left(a + \frac{b}{2}\right)}{9\pi D} \right)^{\frac{2}{3}} \exp\left[-\left(\frac{8\left(a + \frac{b}{2}\right)}{9\pi D} \right) \left(x^2 + \dot{x}^2\right)^{\frac{3}{2}} \right],$$

$$(5.53)$$

and substitution in Eq. (3.28) yields the probability density function of the energy-based envelope as

$$p_e(\alpha) = \left(\frac{3}{\Gamma(\frac{2}{3})} \right) \left(\frac{8\left(a + \frac{b}{2}\right)}{9\pi D} \right)^{\frac{2}{3}} \alpha \exp\left[-\left(\frac{8\left(a + \frac{b}{2}\right)}{9\pi D} \right) \alpha^3 \right]. \qquad (5.54)$$

The expected value of α^2, $E[\alpha^2]$, then is

$$E[\alpha^2] = \int_0^\infty \alpha^2 p_e(\alpha)d\alpha = \frac{\Gamma(\frac{4}{3})}{\Gamma(\frac{2}{3})} \frac{1}{\left(\frac{8\left(a+\frac{b}{2}\right)}{9\pi D}\right)^{\frac{2}{3}}}, \qquad (5.55)$$

and again, because of the symmetry of $p(x, \dot{x})$ with respect to x and $\dot{x}$ and because of the definition of α^2 $\left(= x^2 + \dot{x}^2\right)$, $E[x^2] = E[\dot{x}^2] = E[\alpha^2]/2$.

The response of the original nonlinear equation, Eq. (5.49), now is a function of three independent parameters a, b and D. The response of the equivalent nonlinear equation, however, is a function of the ratio $(a + \frac{b}{2})/D$. In order to assess the effect of a, b and D on the response of the original equation, four series of simulations were performed. Because for $b = 0$ the system has $(velocity)^2$-damping, already studied in Section 5.2.2(a), the simulations concentrated on the other extreme where $a = 0$, and on the region where a and $b/2$ have approximately the same values. For the first series of simulations $a = 0$, D was kept constant and $b/2$ was varied over the same range as for the previous simulations, encompassing cases of practical interest. For the second series, $a = 0$, $b/2$ was kept constant and D was varied in such a way that the ratio $(b/2)/D$ was the same as in the first series. For the third series of simulations, D was kept constant and a and $b/2$ were varied with the same values in such a way that $a + \frac{b}{2}$ varied over the same range as $b/2$ in the previous simulations. Finally, in the fourth series a and $b/2$ were kept constant and D was varied in such a way that the ratio $(a + \frac{b}{2})/D$ was the same as in the third series.

The comparison of theoretical and simulated histograms for the displacement, velocity and energy-based envelope, resulting from the first and second series of simulations are shown in Figs. 5.61 through 5.67. In Figs. 5.61 through 5.67, $b/2$ was made equal to 0.02, 0.05, 0.10 and 0.20, respectively, and D was kept constant and equal to 0.05. Fig. 5.63 and Figs. 5.65 through 5.67 show the results for the second series, for $\frac{b}{2} = 0.10$ and D equal to 0.05, 0.25, 0.10 and 0.025. The same comparison for the third and fourth series of simulations are shown in Figs. 5.68 through 5.74. In Figs. 5.68 through 5.71, a was made equal to 0.01, 0.02, 0.05 and 0.10, respectively, $b/2$ was made equal to 0.01, 0.03, 0.05 and 0.10, respectively, and D was kept constant and equal to 0.05. Fig. 5.67 and Figs. 5.72 through 5.74 show the results for the fourth series, for $a = 0.05$, $\frac{b}{2} = 0.05$ and D equal to 0.05, 0.25, 0.10 and 0.025.

The agreement between the simulated and predicted response histograms for the first two series of simulations is not as good as in previous simulations. It is, nonetheless, quite reasonable. There is an overprediction ocurring for small displacements and small values of the envelope that increases with increasing values of $b/2$ and D. At least in part, however, the overprediction is due to the precision of the integration process that, in this case history as well as in the Coulomb damping case history, required a less stringent accuracy in order to yield a solution. The agreement for the velocity histograms is excellent throughout for all cases.

The agreement between the simulated and predicted response histograms for the second two series of simulations is as good as any of the previous case histories. The discrepancies pointed out on the first two series are also in the second two

but are much less accentuated. The agreement for the velocity histograms is, as before, excellent throughout for all cases.

Figs. 5.75 and 5.76 show the comparison of the simulated and theoretical results for the $E[x^2]$, $E[\dot{x}^2]$ and the $E[\alpha^2]$ as functions of the ratio $(a + \frac{b}{2})/D$ for the first two and last two series of simulations, respectively. In Fig. 5.75, although by a small margin, all of the mean-squared values are systematically underpredicted, with the underprediction increasing with decreasing values of the ratio $(a + \frac{b}{2})/D$. In Fig. 5.76, on the other hand, the agreement is almost perfect. It is clear from both pictures that the respose is a function of the three independent parameters a, b and D; however, as in previous case histories, this dependence is not very strong, and can be disregarded for practical purposes.
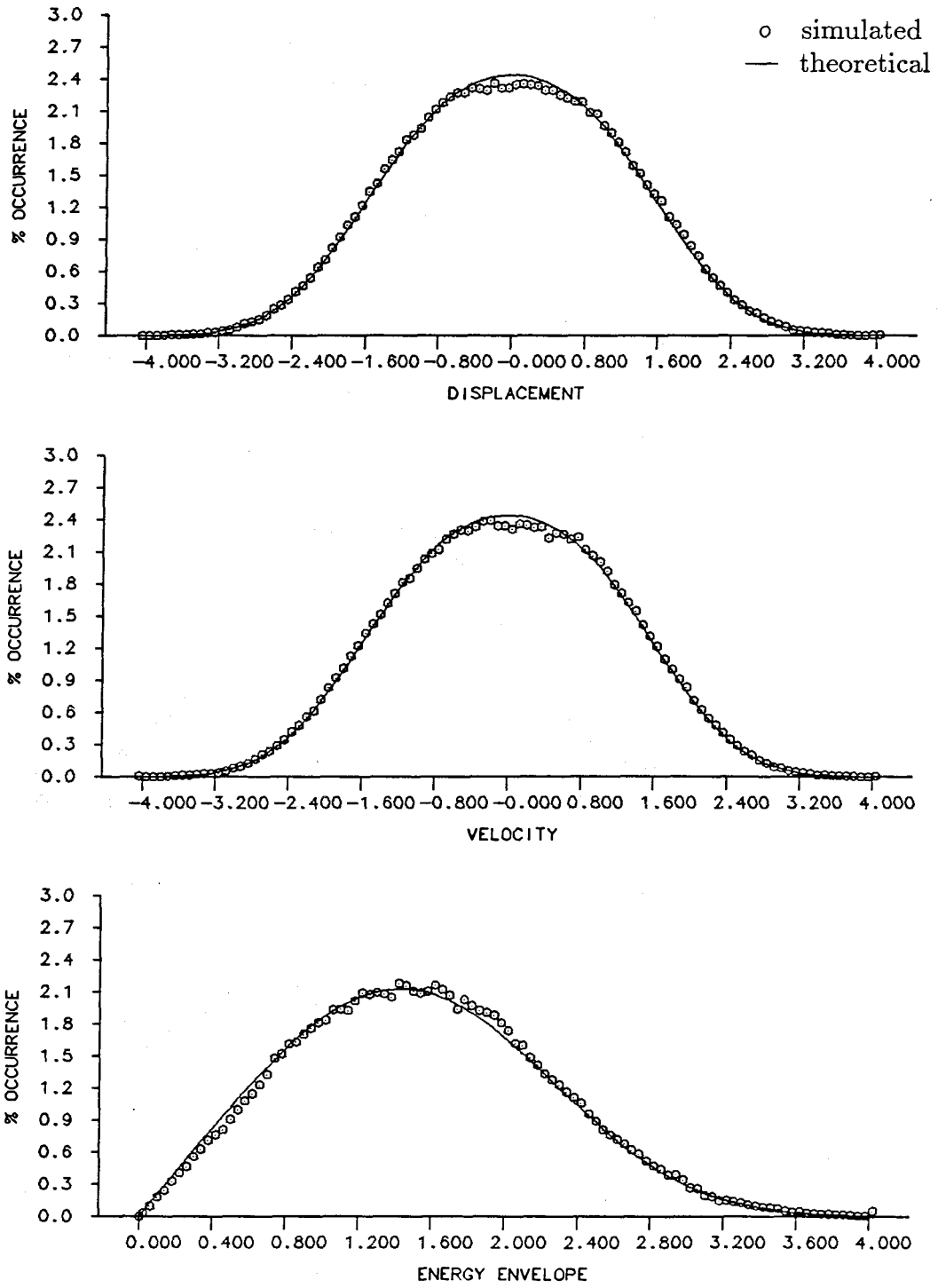
Figure 5.61

Composite Damping: $(b_{02}\dot{x}^2 + b_{20}x^2)\,\mathrm{sgn}(\dot{x})$
$b_{02} = 0.00, \quad b_{20} = 0.04, \quad D = 0.05$
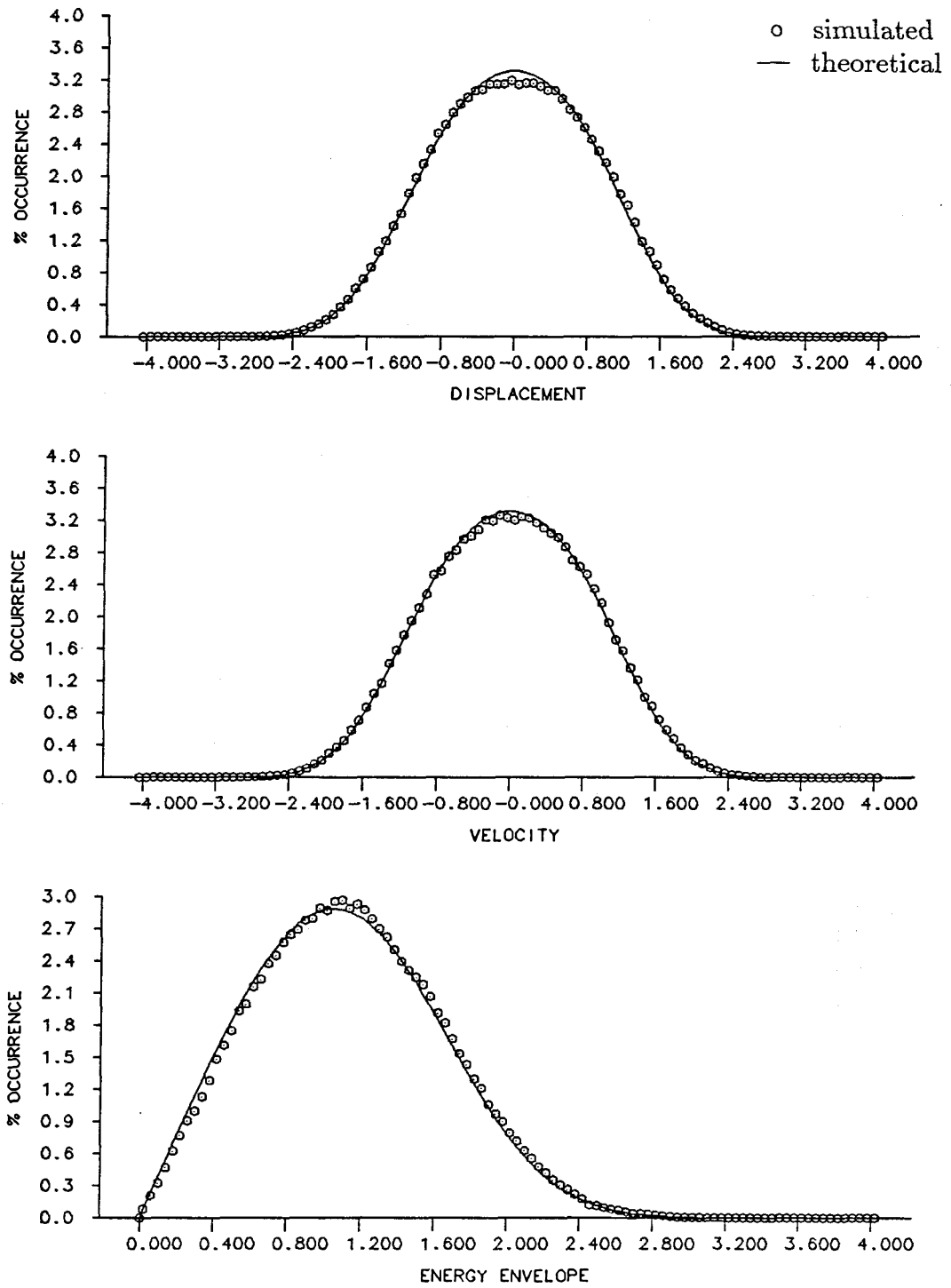
Figure 5.62

Composite Damping: $(b_{02}\dot{x}^2 + b_{20}x^2)\,\mathrm{sgn}(\dot{x})$
$b_{02} = 0.00,\ b_{20} = 0.10,\ D = 0.05$
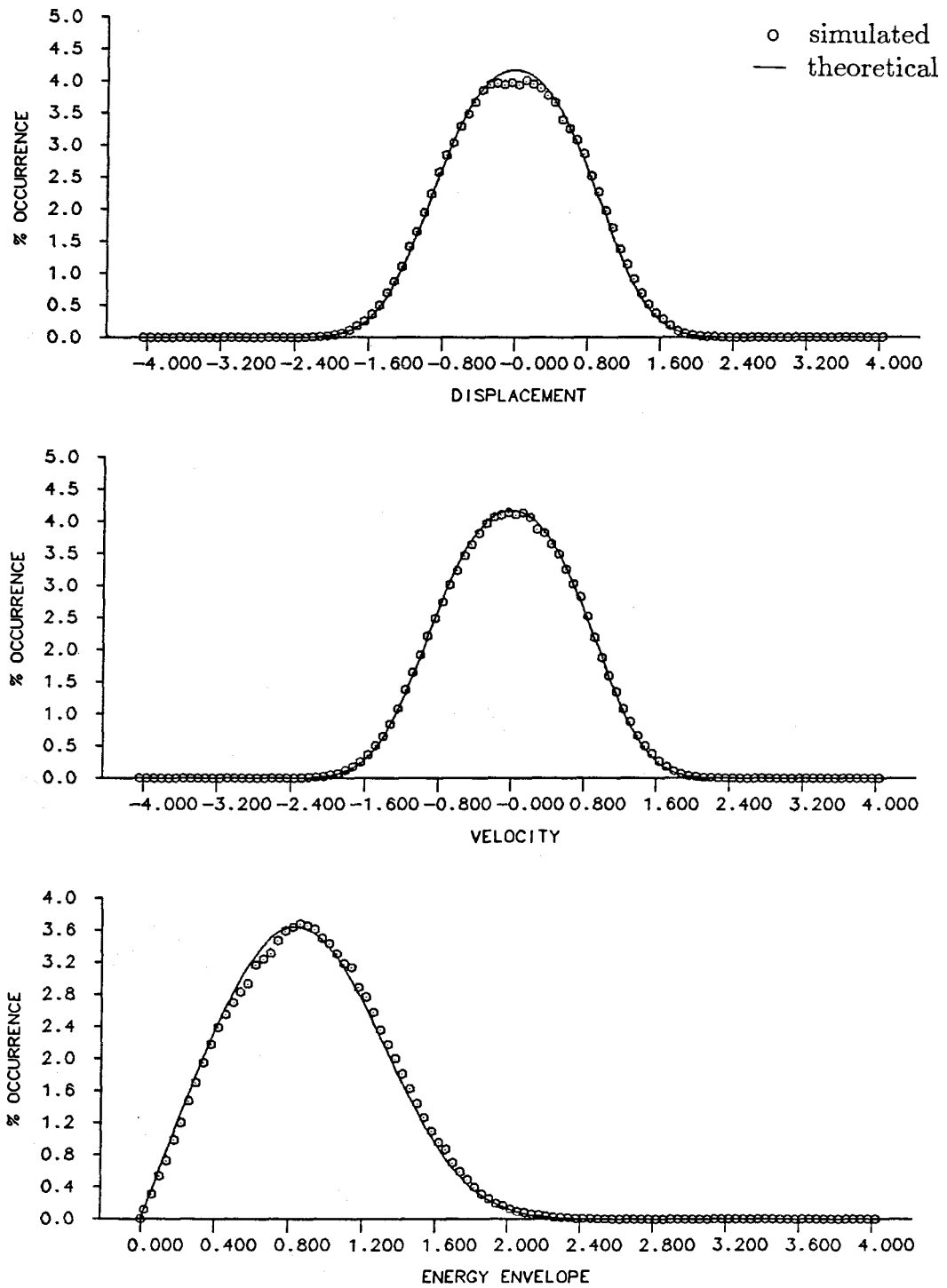
Figure 5.63

Composite Damping: $(b_{02}\dot{x}^2 + b_{20}x^2)\,\text{sgn}(\dot{x})$

$b_{02} = 0.00,\quad b_{20} = 0.20,\quad D = 0.05$
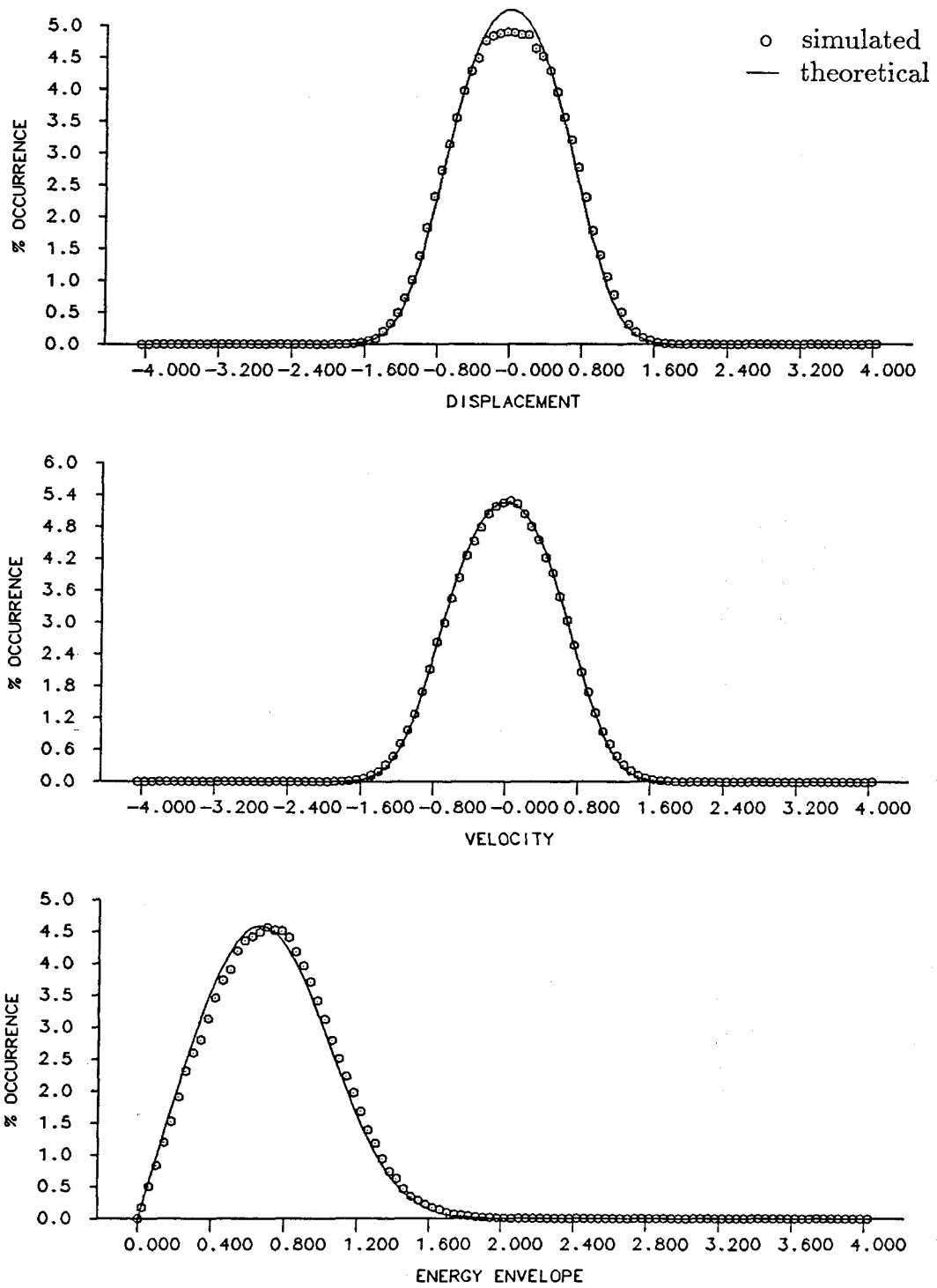
Figure 5.64

Composite Damping: $(b_{02}\dot{x}^2 + b_{20}x^2)\,\mathrm{sgn}(\dot{x})$

$b_{02} = 0.00,\quad b_{20} = 0.40,\quad D = 0.05$
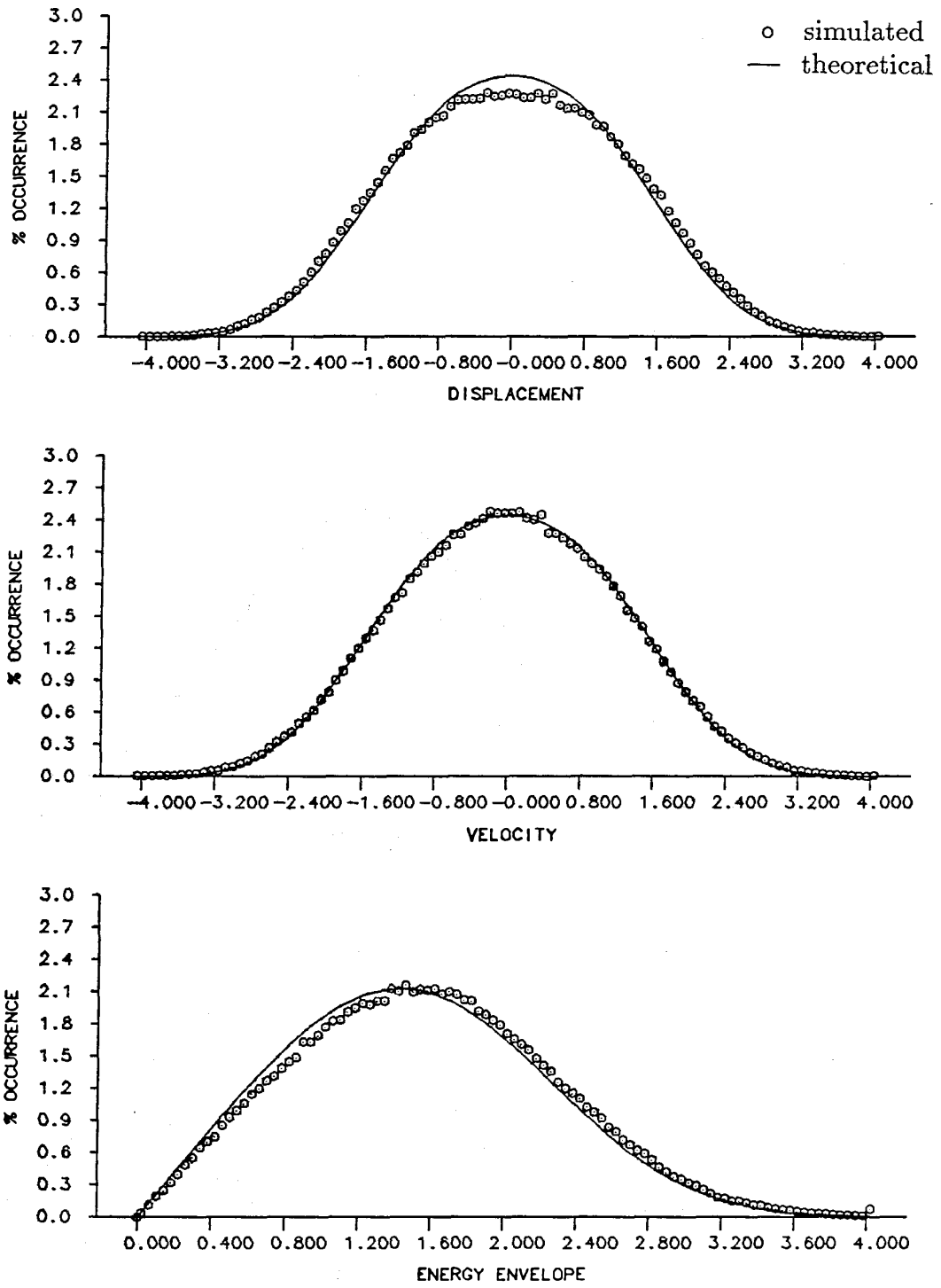
Figure 5.65

Composite Damping: $(b_{02}\dot{x}^2 + b_{20}x^2)\,\text{sgn}(\dot{x})$
$b_{02} = 0.00,\quad b_{20} = 0.20,\quad D = 0.25$
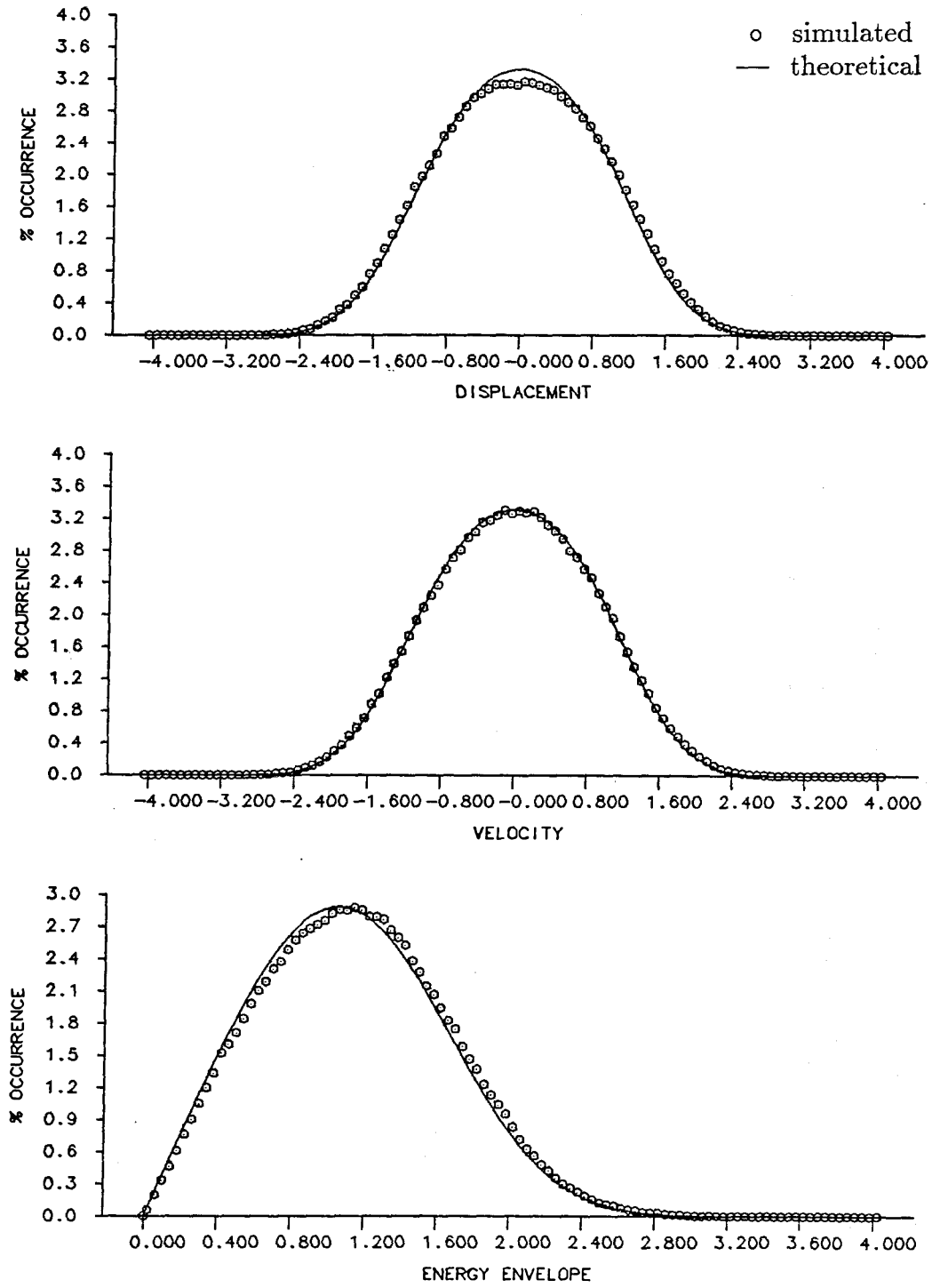
Figure 5.66

Composite Damping: $(b_{02}\dot{x}^2 + b_{20}x^2)\,\mathrm{sgn}(\dot{x})$

$b_{02} = 0.00,\quad b_{20} = 0.20,\quad D = 0.10$
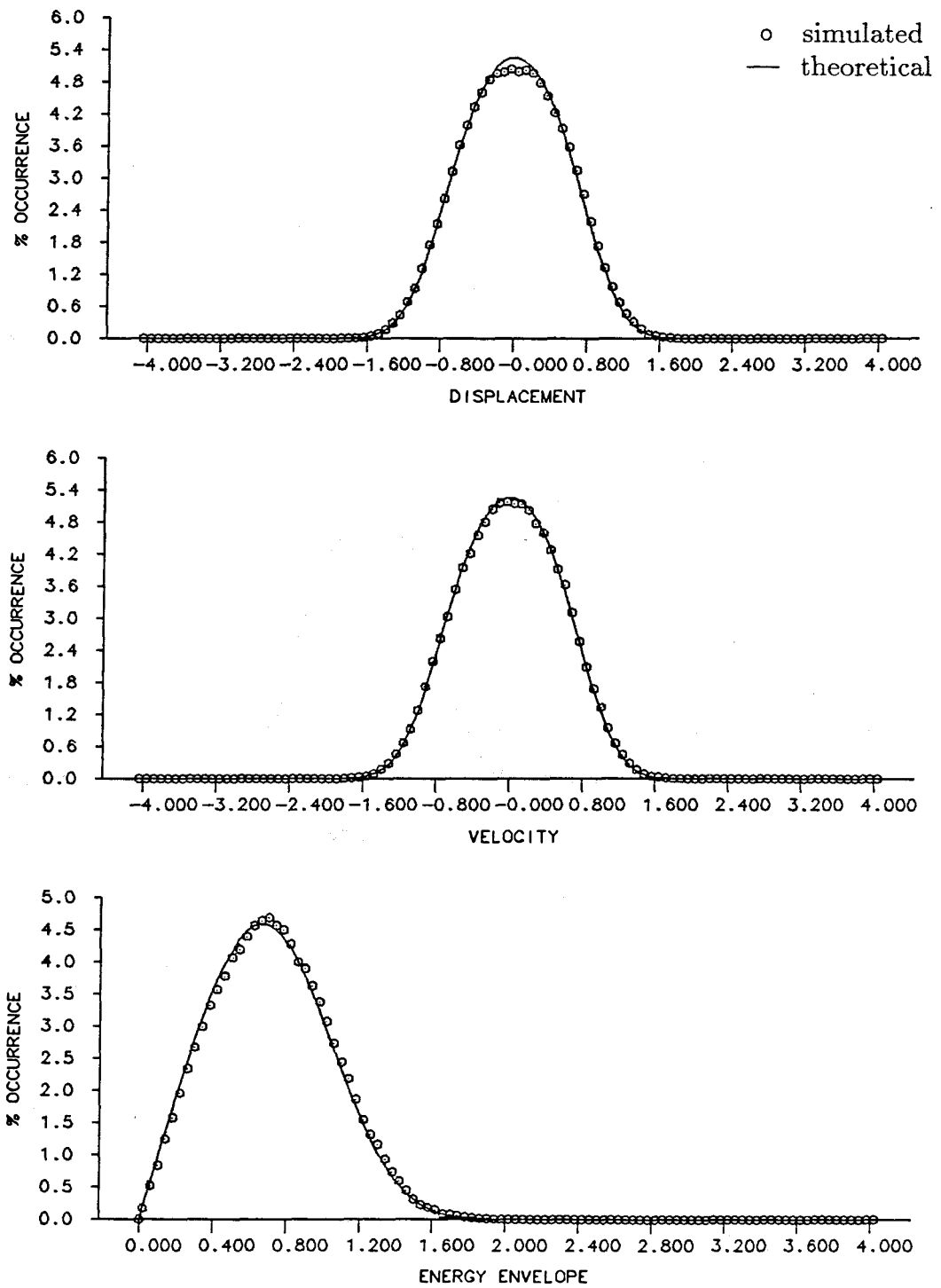
Figure 5.67

Composite Damping: $(b_{02}\dot{x}^2 + b_{20}x^2)\,\text{sgn}(\dot{x})$
$b_{02} = 0.00,\ b_{20} = 0.20,\ D = 0.025$
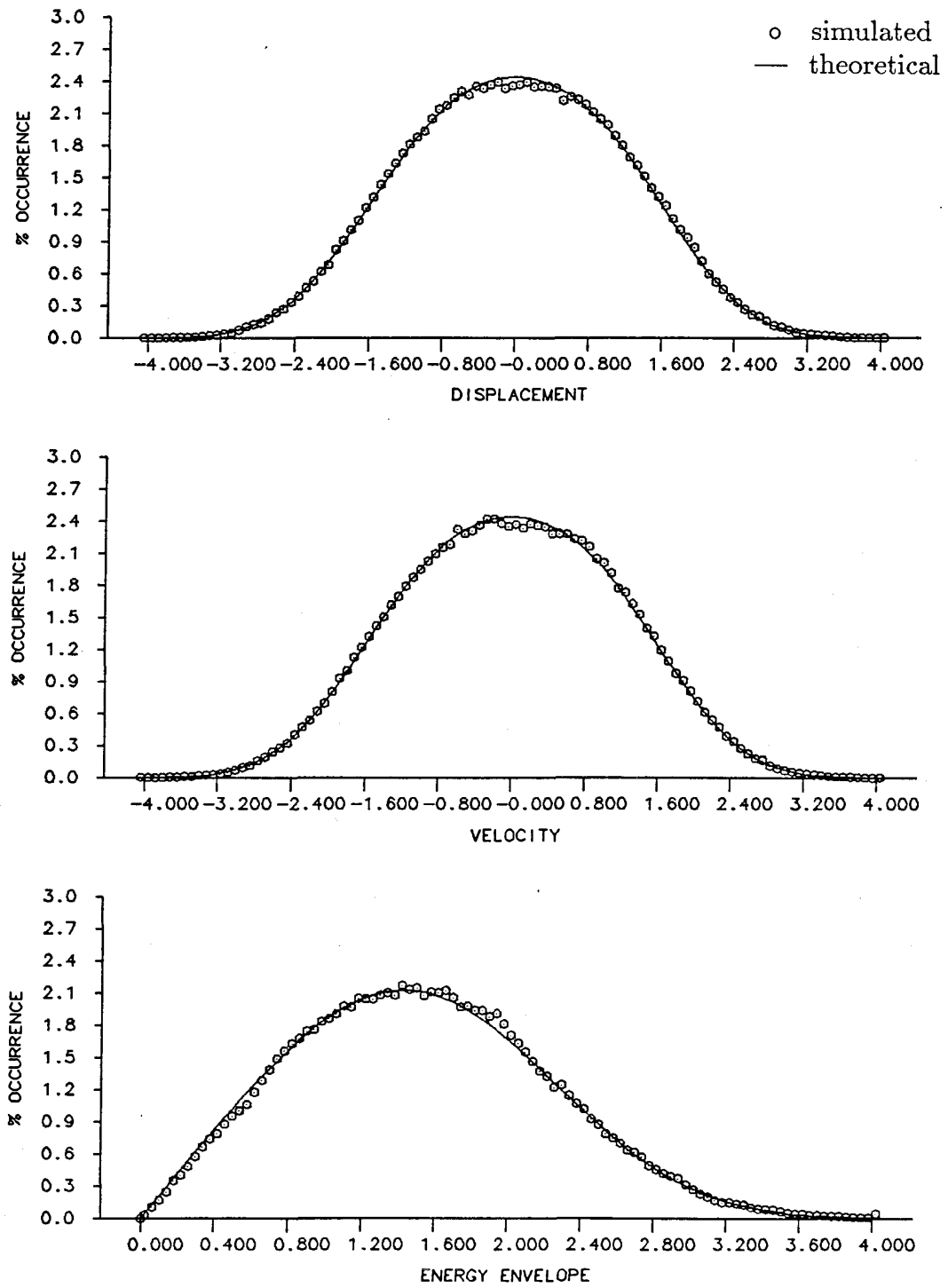
Figure 5.68

Composite Damping: $\left(b_{02}\dot{x}^2 + b_{20}x^2\right) \text{sgn}(\dot{x})$

$b_{02} = 0.01$, $b_{20} = 0.02$, $D = 0.05$
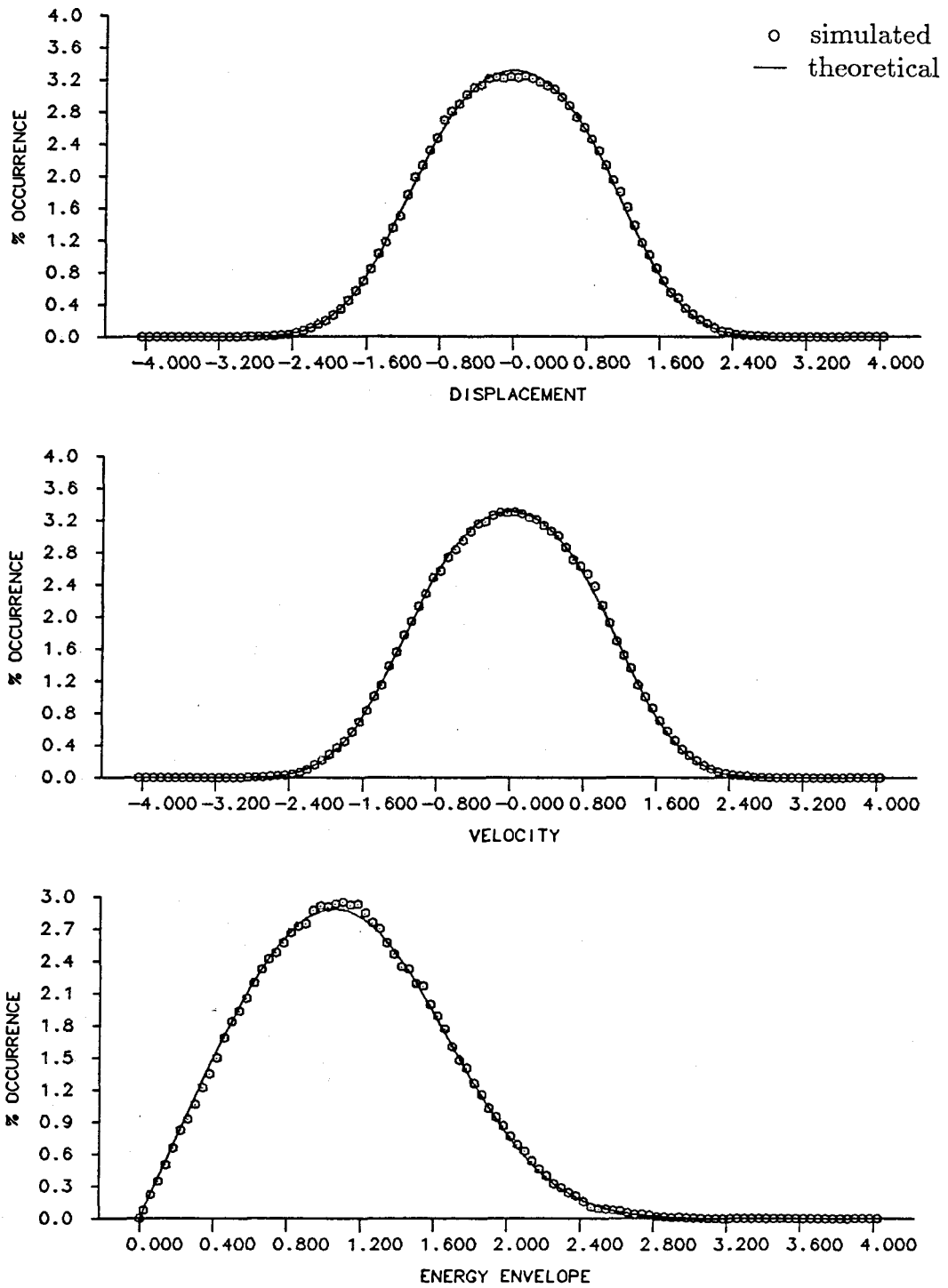
Figure 5.69

Composite Damping: $(b_{02}\dot{x}^2 + b_{20}x^2)\,\mathrm{sgn}(\dot{x})$
$b_{02} = 0.02,\ \ b_{20} = 0.06,\ \ D = 0.05$
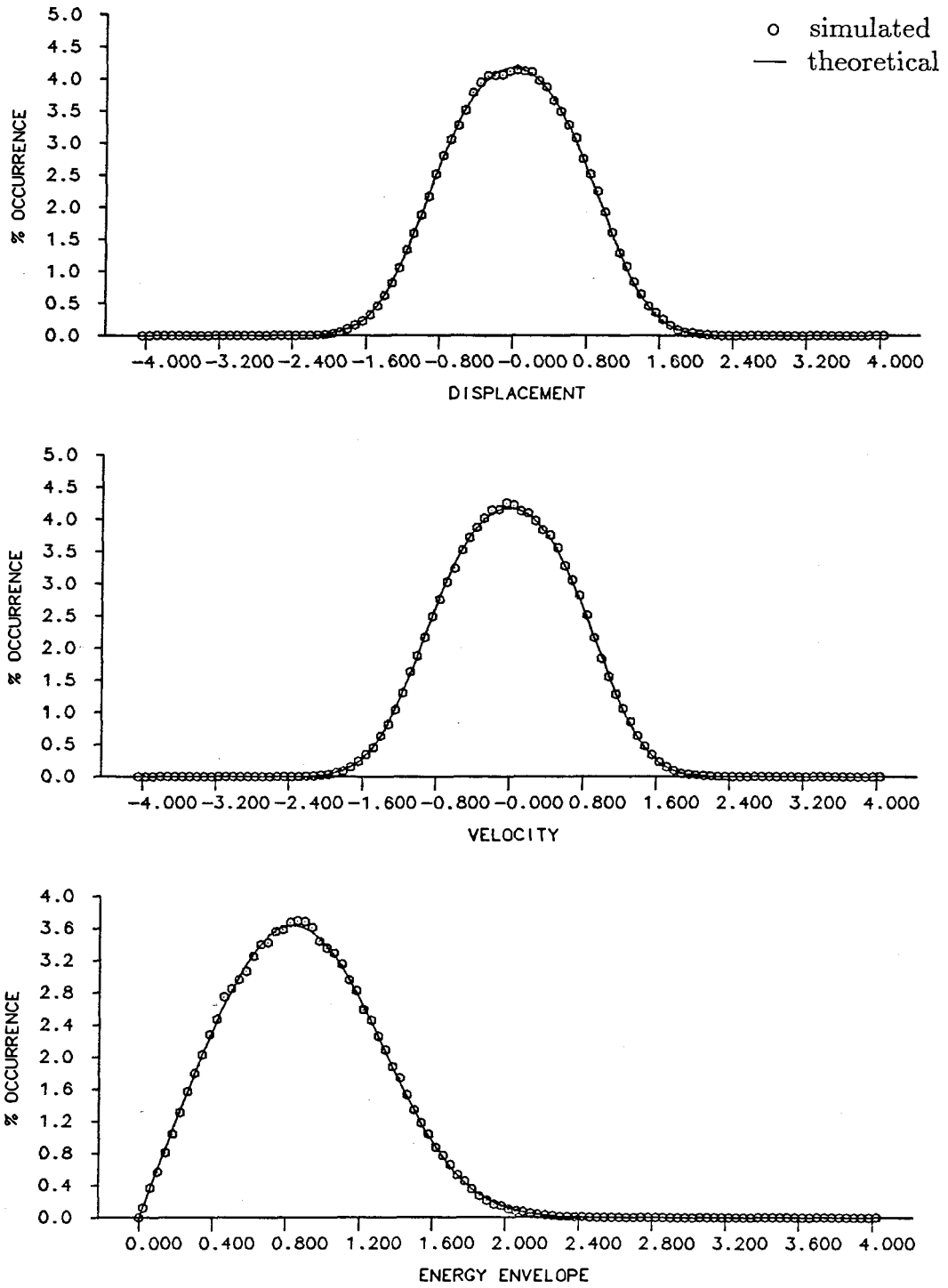
Figure 5.70

Composite Damping: $(b_{02}\dot{x}^2 + b_{20}x^2)\,\mathrm{sgn}(\dot{x})$

$b_{02} = 0.05, \quad b_{20} = 0.10, \quad D = 0.05$
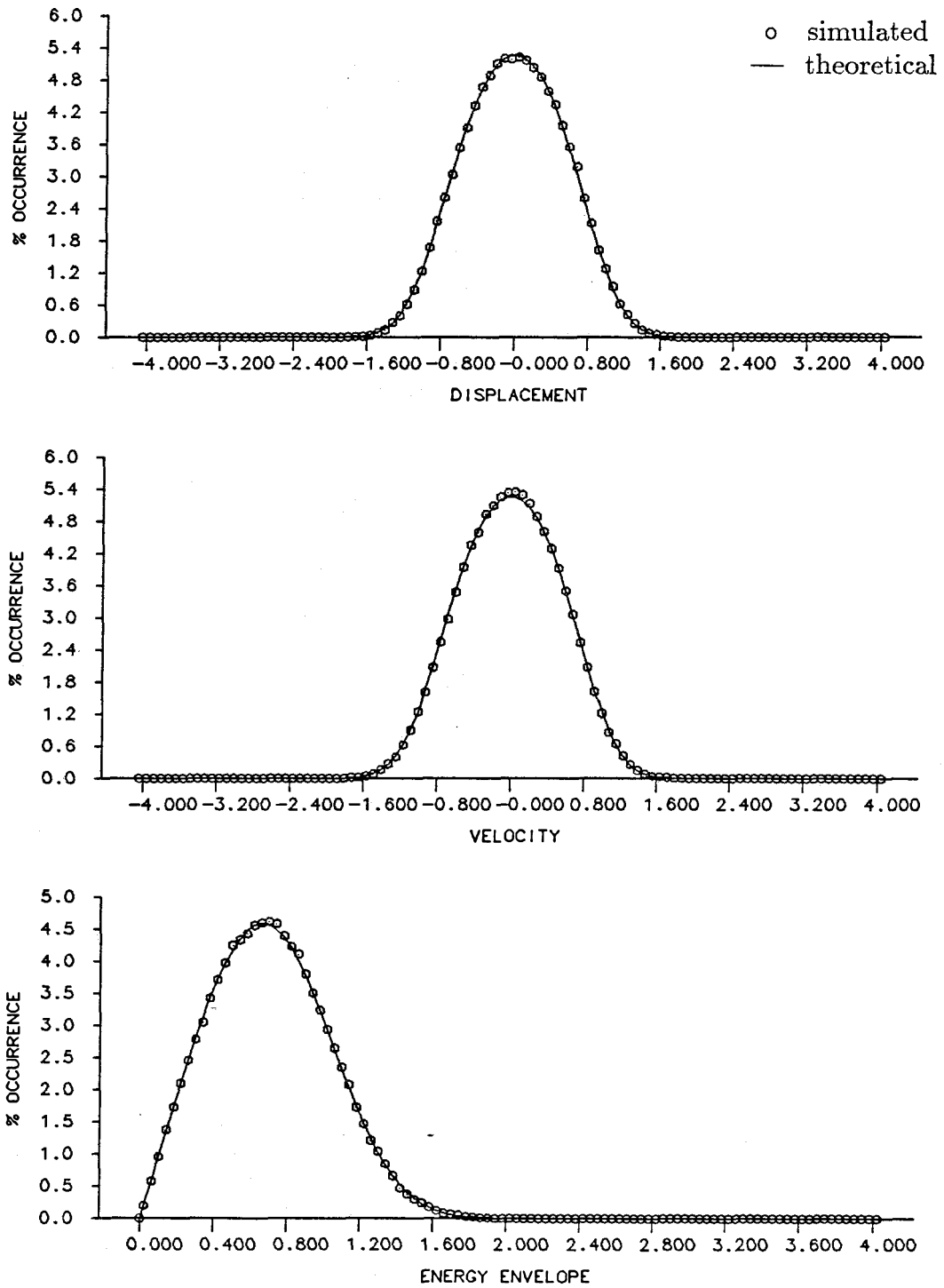
Figure 5.71

Composite Damping: $(b_{02}\dot{x}^2 + b_{20}x^2)\,\mathrm{sgn}(\dot{x})$

$b_{02} = 0.10,\quad b_{20} = 0.20,\quad D = 0.05$
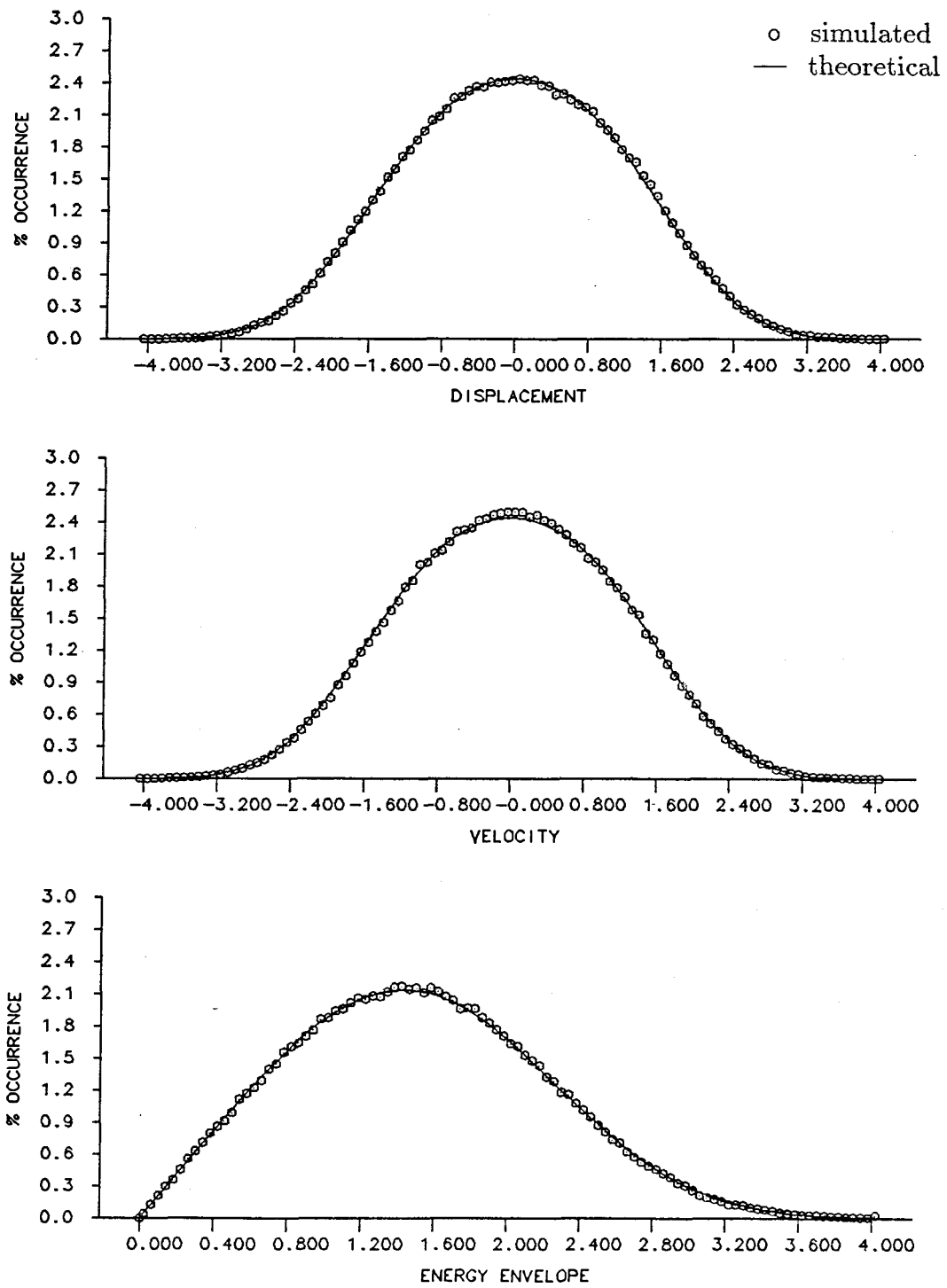
Figure 5.72

Composite Damping: $(b_{02}\dot{x}^2 + b_{20}x^2)\,\mathrm{sgn}(\dot{x})$
$b_{02} = 0.05,\quad b_{20} = 0.10,\quad D = 0.25$
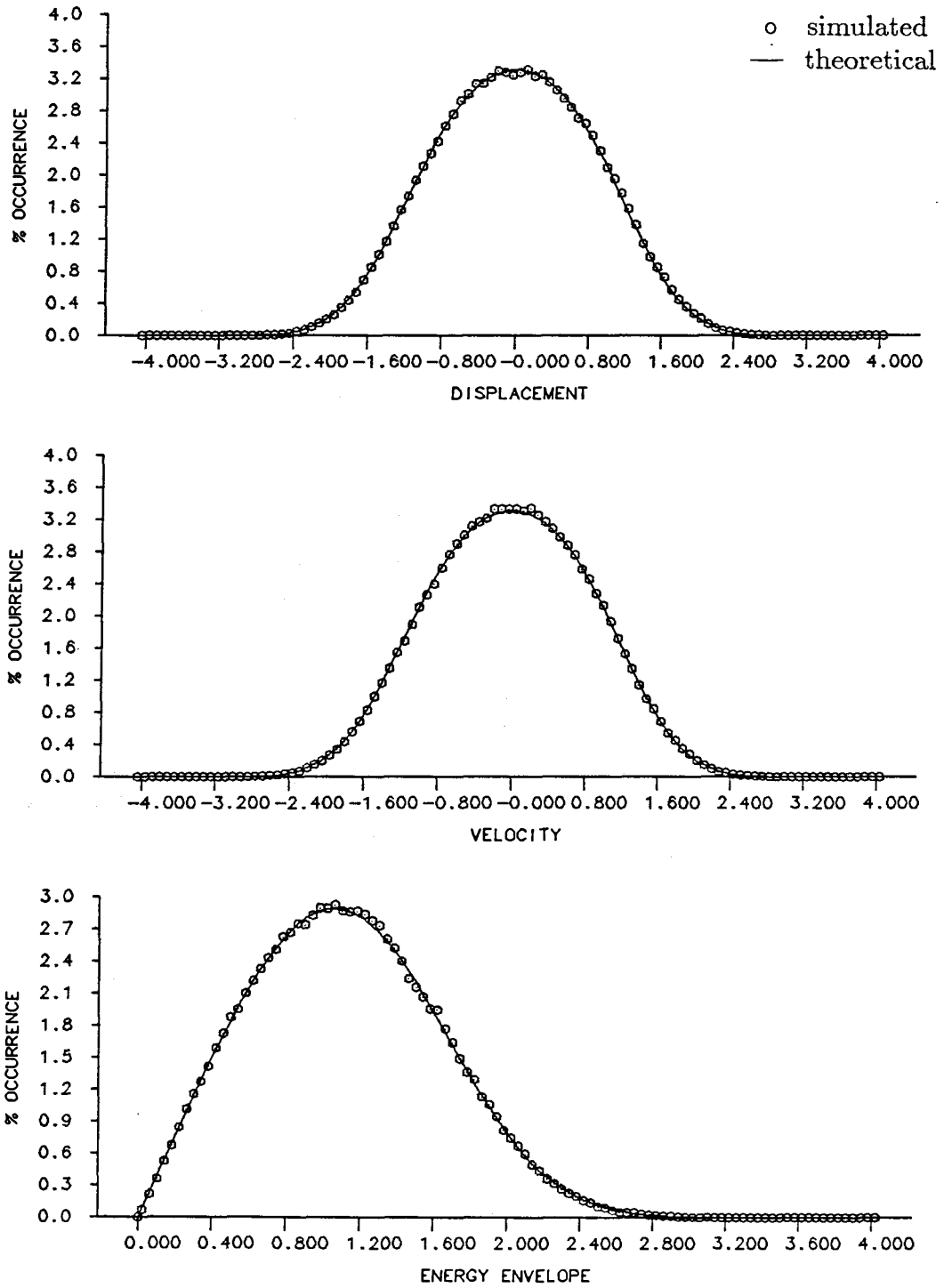
Figure 5.73

Composite Damping: $(b_{02}\dot{x}^2 + b_{20}x^2)\,\mathrm{sgn}(\dot{x})$

$b_{02} = 0.05,\quad b_{20} = 0.10,\quad D = 0.10$
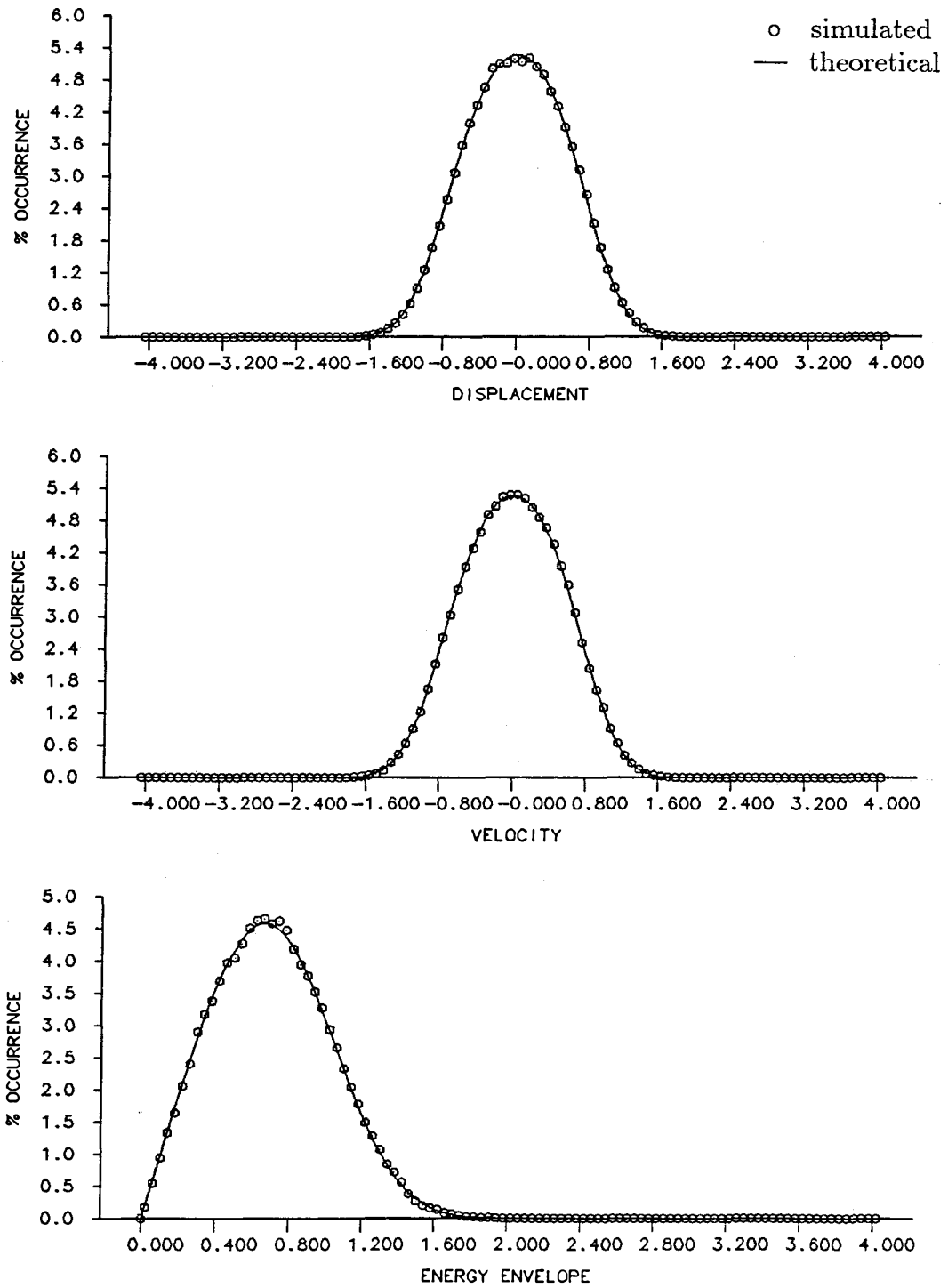
Figure 5.74

Composite Damping: $(b_{02}\dot{x}^2 + b_{20}x^2)\,\mathrm{sgn}(\dot{x})$
$b_{02} = 0.05, \quad b_{20} = 0.10, \quad D = 0.025$
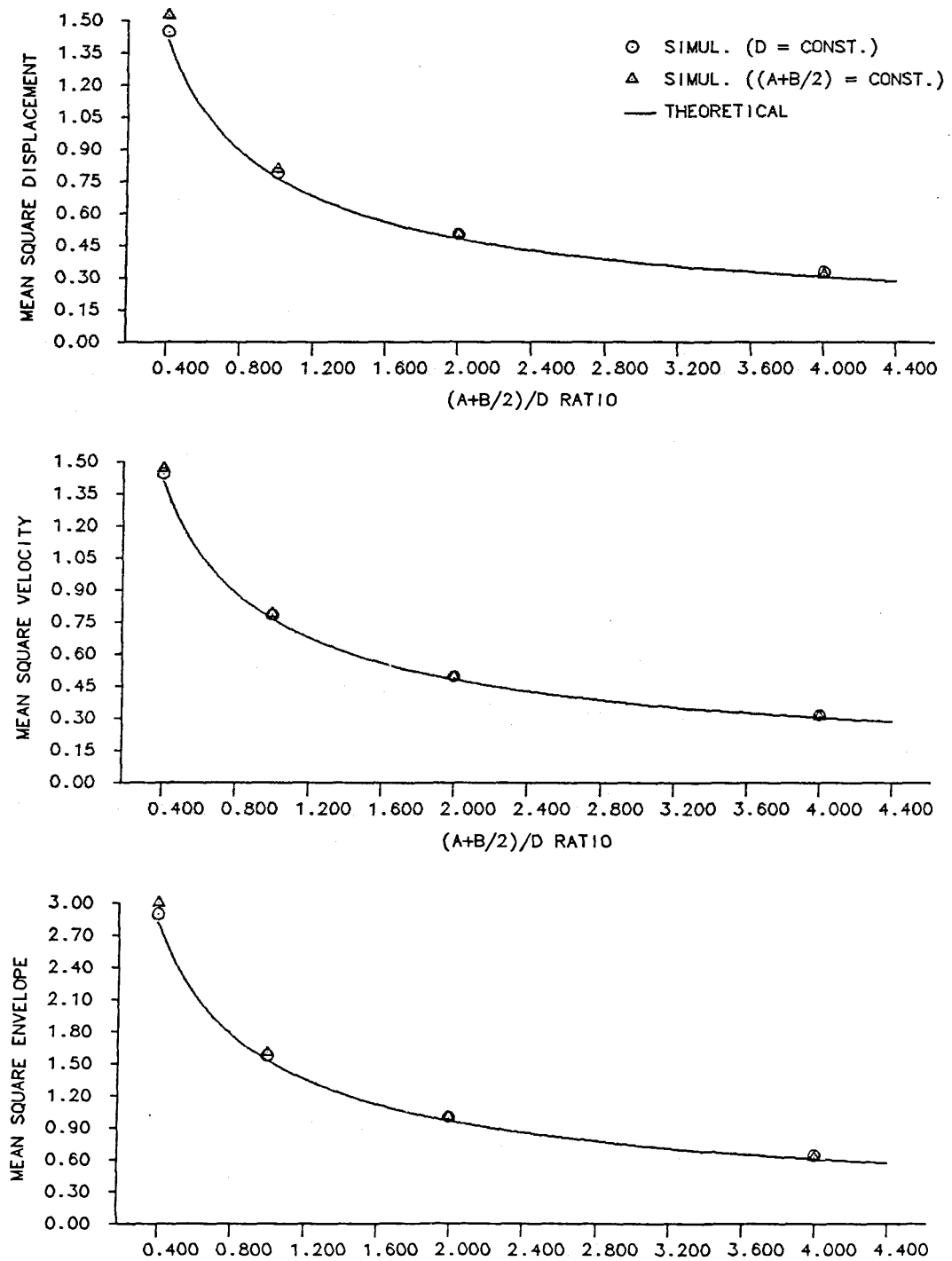
Figure 5.75

Mean-Square Response for $((b_{02}\dot{x}^2 + b_{20}x^2)\, \text{sgn}(\dot{x}))$-Damping
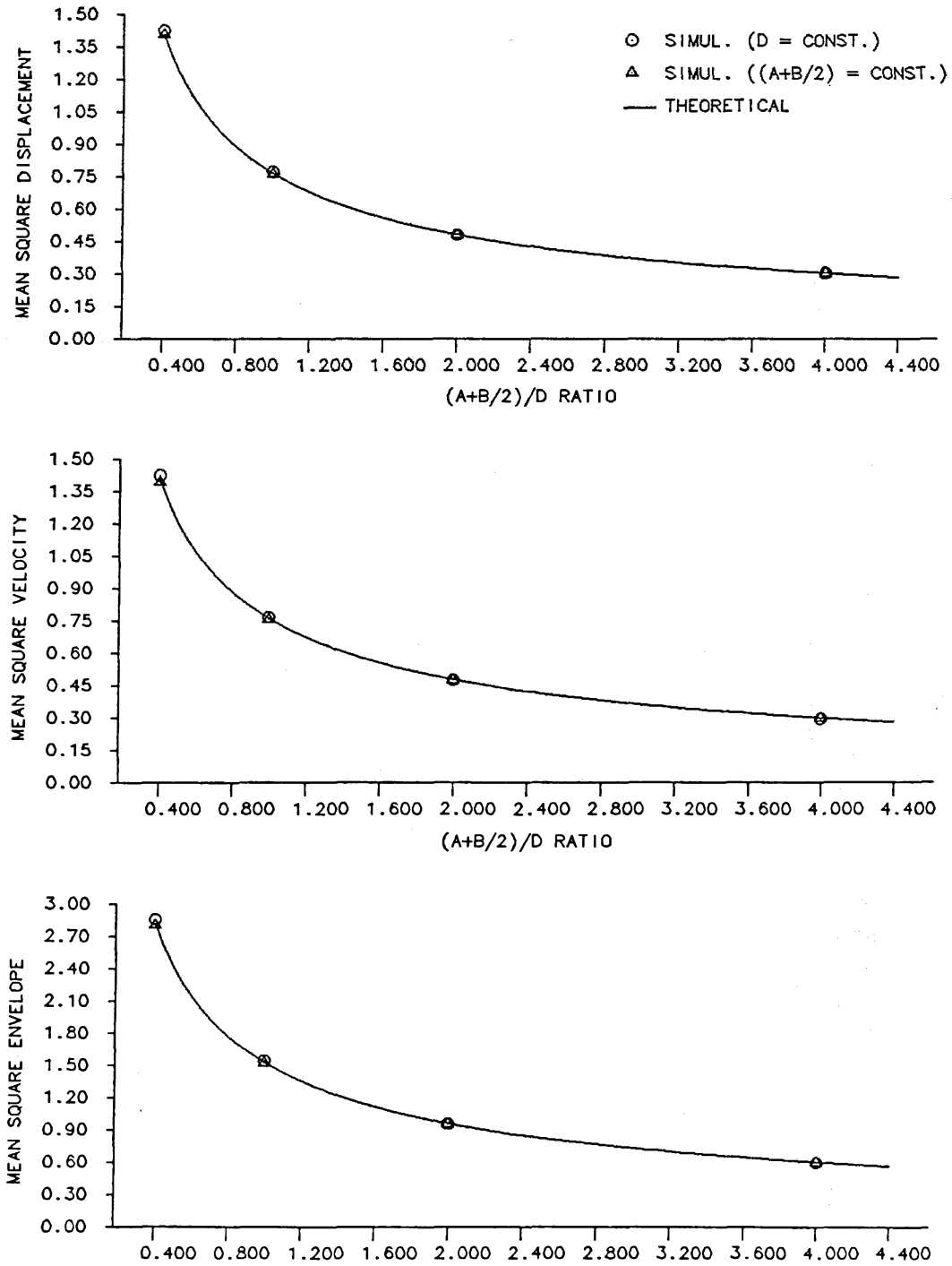
Figure 5.76

Mean-Square Response for $((b_{02}\dot{x}^2 + b_{20}x^2)\,\mathrm{sgn}(\dot{x}))$-Damping

5.3 SDOF Systems with *Duffing*-Type Stiffness and Nonlinear Damping

A few examples within this class of SDOF systems, discussed in Chapter III, are now solved with the purpose of illustrating and assessing the accuracy of the Method of Equivalent Nonlinearization, when the coefficients c_{ij} can be determined only numerically. The joint probability density function of x and $\dot{x}$ and the probability density function of the energy-based envelope are generated and then compared with numerically simulated histograms.

5.3.1 Systems with $(velocity)^m$-Damping

Consider the nonlinear SDOF system with $(velocity)^m$-damping and *Duffing*-type stiffness given by

$$\ddot{x} + b\,|\dot{x}^m|\mathrm{sgn}(\dot{x}) + e_0 x + e_1 x^3 = w(t), \tag{5.56}$$

which is obtained by substituting Eq. (3.41) into (3.34) and making $b_{0m} = b$, $b_{ij} = 0$ otherwise.

The following equivalent nonlinear equation replaces Eq. (5.56),

$$\ddot{x} + c_{0m} f_{0m}(H)\dot{x} + e_0 x + e_1 x^3 = w(t), \tag{5.57}$$

which is obtained from Eq. (3.35) by making $c_{ij} = 0$ for all $i \neq 0$ and $j \neq m$. The only f_{ij} term of interest is f_{0m} obtained from Eq. (3.37) and given by

$$f_{0m} = (\dot{x}^2 + e_0 x^2 + \frac{e_1}{2} x^4)^{\frac{(m-1)}{2}}.$$
(5.58)

The unknown coefficient c_{0m} is the solution of

$$\int_{-\infty}^{+\infty} \int_{-\infty}^{+\infty} \left(b_{0m} |\dot{x}^m| \operatorname{sgn}(\dot{x}) - c_{0m}(\dot{x}^2 + e_0 x^2 + \frac{e_1}{2} x^4)^{\frac{(m-1)}{2}} \dot{x} \right) \times$$

$$(\dot{x}^2 + e_0 x^2 + \frac{e_1}{2} x^4)^{\frac{(m-1)}{2}} \dot{x} \exp \left(-\frac{c_{0m}}{(m+1)D}(\dot{x}^2 + e_0 x^2 + \frac{e_1}{2} x^4)^{\frac{(m+1)}{2}} \right) dx d\dot{x} = 0,$$
(5.59)

obtained by direct substitution of the appropriate values in Eq. (3.48). Factoring b_{0m} on Eq. (5.59) and defining $\rho_{0m} = c_{0m}/b_{0m}$ yield

$$\int_{-\infty}^{+\infty} \int_{-\infty}^{+\infty} \left(|\dot{x}^m| \operatorname{sgn}(\dot{x}) - \rho_{0m}(\dot{x}^2 + e_0 x^2 + \frac{e_1}{2} x^4)^{\frac{(m-1)}{2}} \dot{x} \right) \times$$

$$(\dot{x}^2 + e_0 x^2 + \frac{e_1}{2} x^4)^{\frac{(m-1)}{2}} \dot{x} \exp \left(-\frac{\rho_{0m} b_{0m}}{(m+1)D}(\dot{x}^2 + e_0 x^2 + \frac{e_1}{2} x^4)^{\frac{(m+1)}{2}} \right) dx d\dot{x} = 0.$$
(5.60)

As pointed out before, the solution of Eq. (5.60) for the unknown ρ_{0m} can be obtained only numerically. Once ρ_{0m} is determined, the joint probability density function of displacement and velocity is given by

$$p(x, \dot{x}) = A_m \exp \left[-\frac{\rho_{0m}}{(m+1)} \left(\frac{b_{0m}}{D} \right) (\dot{x}^2 + e_0 x^2 + \frac{e_1}{2} x^4)^{\frac{(m+1)}{2}} \right],$$
(5.61)

and the probability density function of the energy-based envelope is given by

$$p_e(\alpha) = A_m(e_0\alpha + e_1\alpha^3)T(\alpha)\exp\left[-\frac{\rho_{0m}}{(m+1)}\left(\frac{b_{0m}}{D}\right)\left(e_0\alpha^2 + \frac{e_1}{2}\alpha^4\right)^{\frac{(m+1)}{2}}\right].$$

(5.62)

$T(\alpha)$ is given by Eq. (3.46) and A_m is the normalization which also has to be obtained numerically. Unlike all previous cases, $p(x, \dot{x})$ is not symmetric with respect to x and $\dot{x}$ anymore, and, in addition, $E[x^2]$, $E[\dot{x}^2]$ and $E[\alpha^2]$ are not as simply related as before. The net result is that each of these values also requires numerical evaluation. Next, ρ_{0m} and A_m are determined for different values of m, b_{0m}/D and e_1, and the corresponding theoretical histograms are compared with the simulated ones.

(a) Case of $(velocity)^2$-Damping

The numerical solution of Eq. (5.60) for $m = 2$ and $e_0 = 1$ yields values for ρ_{02} tabulated in Table 5.1.

Table 5.1 Numerical Values for ρ_{02}					
$\frac{b_{02}}{D}\backslash e_1$	0.00	0.05	0.10	0.15	0.20
0.40	0.8488	0.8564	0.8612	0.8647	0.8675
1.00	0.8488	0.8535	0.8569	0.8596	0.8619
2.00	0.8488	0.8519	0.8544	0.8565	0.8584
4.00	0.8488	0.8509	0.8526	0.8542	0.8556

The corresponding values for the normalization constant, A_2, are obtained from the numerical evaluation of $\int_{-\infty}^{+\infty} \int_{-\infty}^{+\infty} p(x, \dot{x}) dx d\dot{x} = 1$. using Eq. (5.61) and are given in Table 5.2.

Table 5.2 Numerical Values for A_2					
$\frac{b_{02}}{D} \backslash e_1$	0.00	0.05	0.10	0.15	0.20
0.40	0.0825	0.0867	0.0899	0.0926	0.0950
1.00	0.1520	0.1565	0.1603	0.1636	0.1665
2.00	0.2412	0.2459	0.2500	0.2537	0.2572
4.00	0.3829	0.3877	0.3921	0.3962	0.4001

(b) Case of $(velocity)^5$-Damping

The numerical solution of Eq. (5.60) for $m = 5$ and $e_0 = 1$ yields values for ρ_{05} tabulated in Table 5.3.

Table 5.3 Numerical Values for ρ_{05}					
$\frac{b_{05}}{D} \backslash e_1$	0.00	0.05	0.10	0.15	0.20
0.40	0.6250	0.6337	0.6406	0.6462	0.6510
1.00	0.6250	0.6317	0.6372	0.6419	0.6480
2.00	0.6250	0.6304	0.6351	0.6391	0.6427
4.00	0.6250	0.6299	0.6337	0.6371	0.6402

As before, the corresponding values for the normalization constant, A_5, are obtained from the numerical evaluation of $\int_{-\infty}^{+\infty} \int_{-\infty}^{+\infty} p(x, \dot{x}) dx d\dot{x} = 1$, using Eq. (5.61), and are given in Table 5.4.

Table 5.4 Numerical Values for A_5					
$\frac{b_0^2}{D} \backslash e_1$	0.00	0.05	0.10	0.15	0.20
0.40	0.1236	0.1273	0.1304	0.1332	0.1358
1.00	0.1677	0.1715	0.1748	0.1779	0.1807
2.00	0.2113	0.2115	0.2186	0.2218	0.2247
4.00	0.2662	0.2703	0.2737	0.2771	0.2802

For all of these tables, the value of e_1, the coefficient of the nonlinear stiffness term, is increased from left to right, starting with the value corresponding to a system with linear stiffness on the left and increasing to the maximum value studied of $e_1 = 0.20$.

As in previous cases, the response of the original nonlinear equation, Eq. (5.56), in principle, is a function of the two parameters b and D, the damping term coefficient and the parameter that controls the forcing function level. The response to the equivalent nonlinear equation, Eq. (5.57), on the other hand, is a function of the ratio b/D. In order to assess the effect of b and D on the response of the original equation, again, the two series of simulations performed in previous cases are repeated here for cases (a) and (b) above, that is, for the $(velocity)^2$- and $(velocity)^5$-damping cases. In the first series, D was kept constant and b varied over a fairly wide range of values in order to encompass cases of practical interest.

In the second series, b was kept constant and D varied in such a way that the ratio b/D was the same in both series. For both of the series, e_1 was also kept constant and equal to 0.20. In this manner, an idea of the accuracy, for $0.00 \leq e_1 \leq 0.20$, can be obtained by comparing these results with results obtained in Section 5.2.2.

Figs. 5.77 through 5.80 show the comparison of theoretical and simulated histograms for the displacement, velocity and energy-based envelope for the first series applied to the $(velocity)^2$-damping case. In these figures b was made equal to 0.02, 0.05, 0.10 and 0.20, respectively, and D was kept constant and equal to 0.05. This value of D produced a random forcing function with unit standard deviation. Fig. 5.79 and Figs. 5.81 through 5.83 show the results for the second series, for $b = 0.10$ and D equal to 0.05, 0.25, 0.10 and 0.025.

Figs. 5.84 through 5.87 show the results for the first series applied to the $(velocity)^5$-damping case. Fig. 5.86 and Figs. 5.88 through 5.90 show the results for the second series. In these figures all parameters are kept the same as in the $(velocity)^2$-damping case.

Tables 5.5 and 5.6 show the comparison of the simulated and theoretical results for the $E[\dot{x}^2]$ and $E[x^2]$, respectively, for $m = 2$, $e_1 = 0.20$ and for the values of the ratio b/D corresponding to each one of the Figs. 5.77 through 5.83 described above. Tables 5.7 and 5.8 show the corresponding results for $m = 5$ and Figs. 5.84 through 5.90.

Table 5.5 Comparison of $E[\dot{x}^2]$ for $m = 2$			
$\frac{b_{02}}{D}$	Theoretical	Simulated $D = constant$	Simulated $b = constant$
0.40	1.4100	1.3598	1.3873
1.00	0.7651	0.7443	0.7529
2.00	0.4820	0.4742	0.4742
4.00	0.3037	0.3002	0.3019

Table 5.6 Comparison of $E[x^2]$ for $m = 2$			
$\frac{b_{02}}{D}$	Theoretical	Simulated $D = constant$	Simulated $b = constant$
0.40	0.9723	0.9452	0.9691
1.00	0.5963	0.5843	0.5921
2.00	0.4035	0.4002	0.4002
4.00	0.2684	0.2680	0.2683

Table 5.7 Comparison of $E[\dot{x}^2]$ for $m = 5$			
$\frac{b_{05}}{D}$	Theoretical	Simulated $D = constant$	Simulated $b = constant$
0.40	0.7330	0.7324	0.7488
1.00	0.5396	0.5392	0.5437
2.00	0.4278	0.4288	0.4288
4.00	0.3392	0.3410	0.3415

Table 5.8 Comparison of $E[x^2]$ for $m = 5$			
$\frac{b_{os}}{D}$	Theoretical	Simulated $D = constant$	Simulated $b = constant$
0.40	0.5870	0.5888	0.6113
1.00	0.4524	0.4545	0.4606
2.00	0.3694	0.3729	0.3729
4.00	0.3005	0.3049	0.3038

In general, the matching between predicted and simulated results is very good. As expected, and by comparing the present results with results of Section 5.2.2, roughly the same level of agreement is attained with nonlinear stiffness as it is with the linear stiffness. The same trends in the matching encountered there are also found here and therefore the same comments also apply.
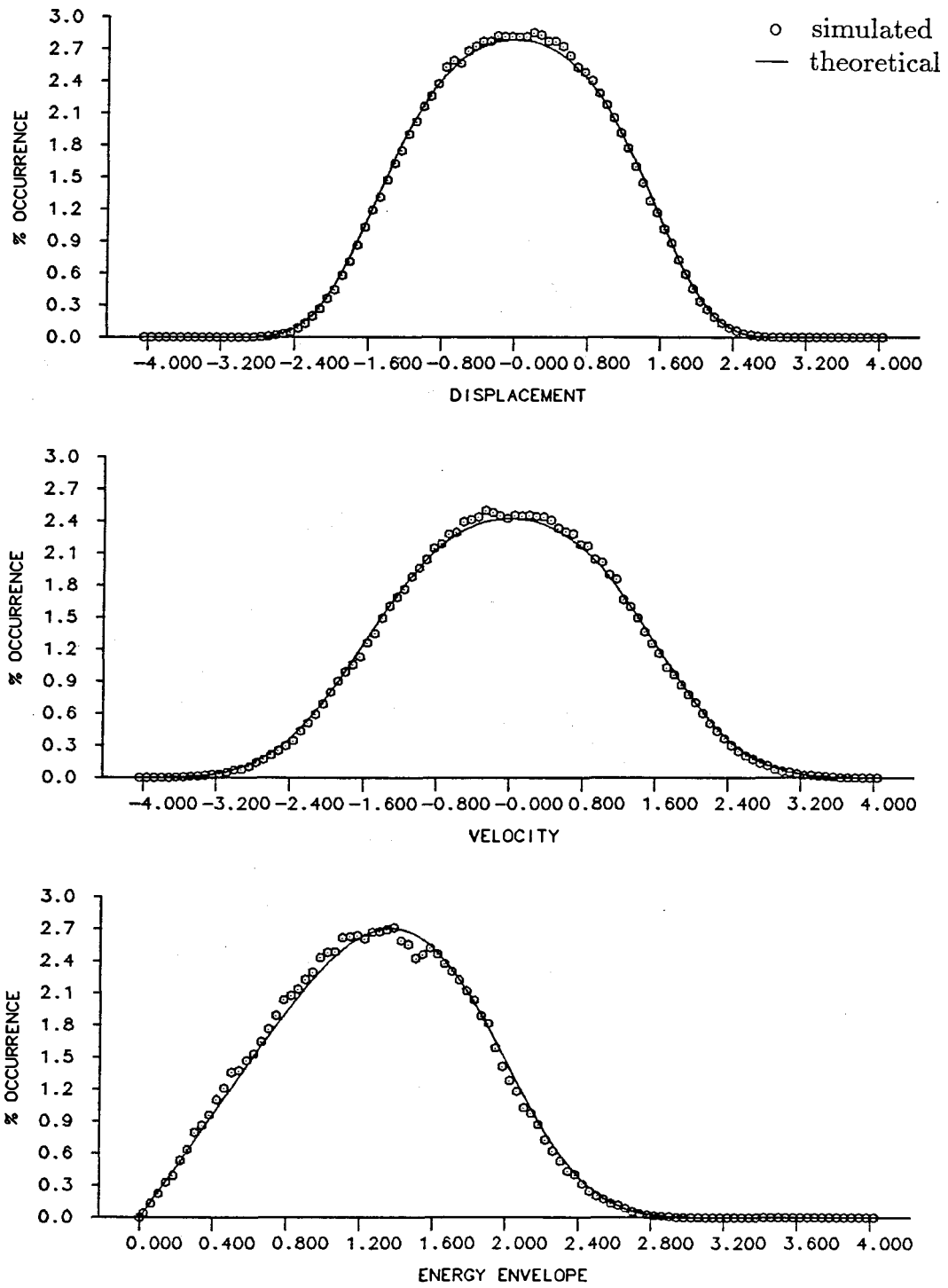
Figure 5.77

$(Velocity)^2$-Damping/Duffing Stiffness

$b_{02} = 0.02,\ e_0 = 1.00,\ e_1 = 0.20,\ D = 0.05$
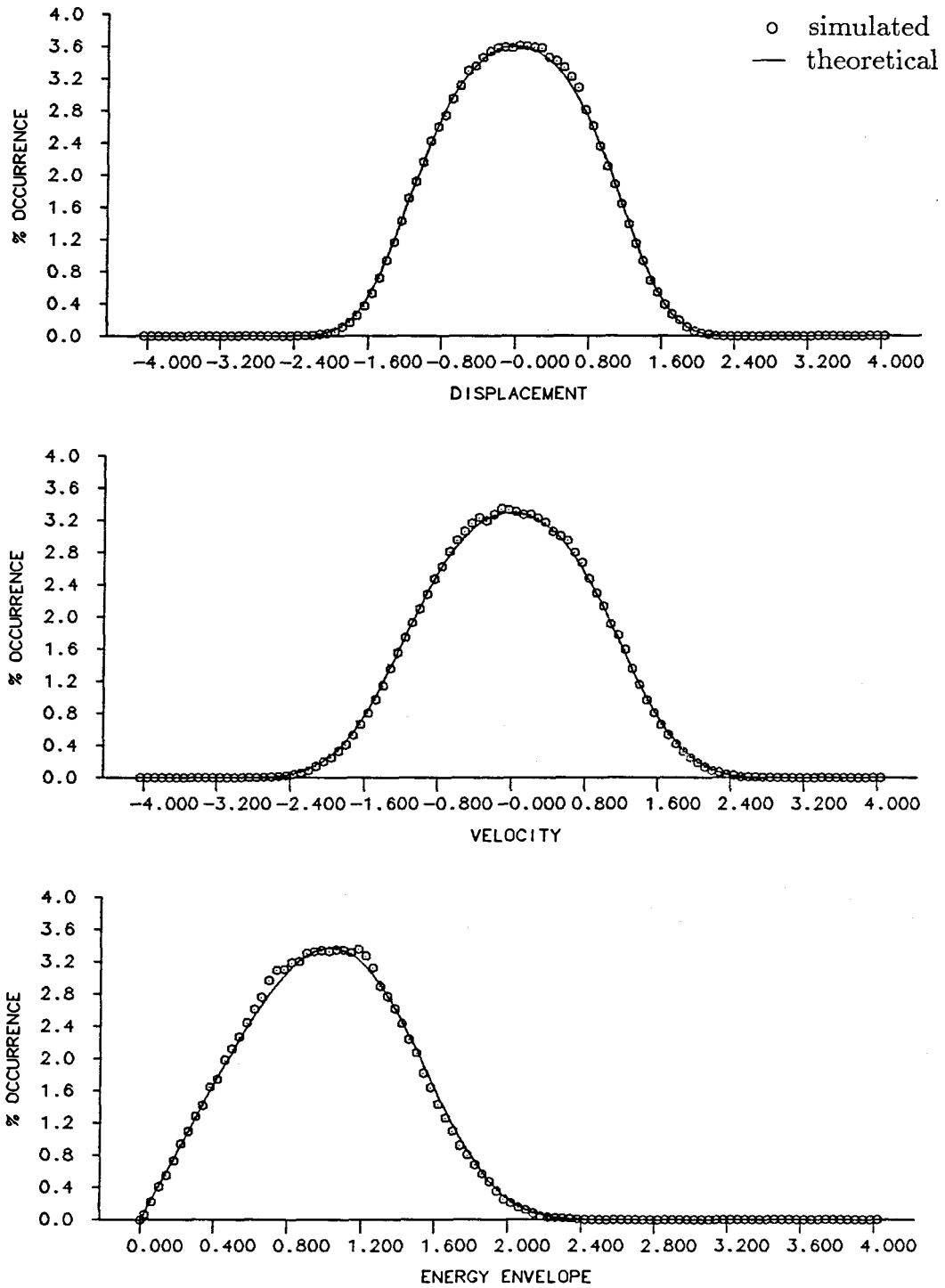
Figure 5.78

$(Velocity)^2$-Damping/Duffing Stiffness

$b_{02} = 0.05$, $e_0 = 1.00$, $e_1 = 0.20$, $D = 0.05$
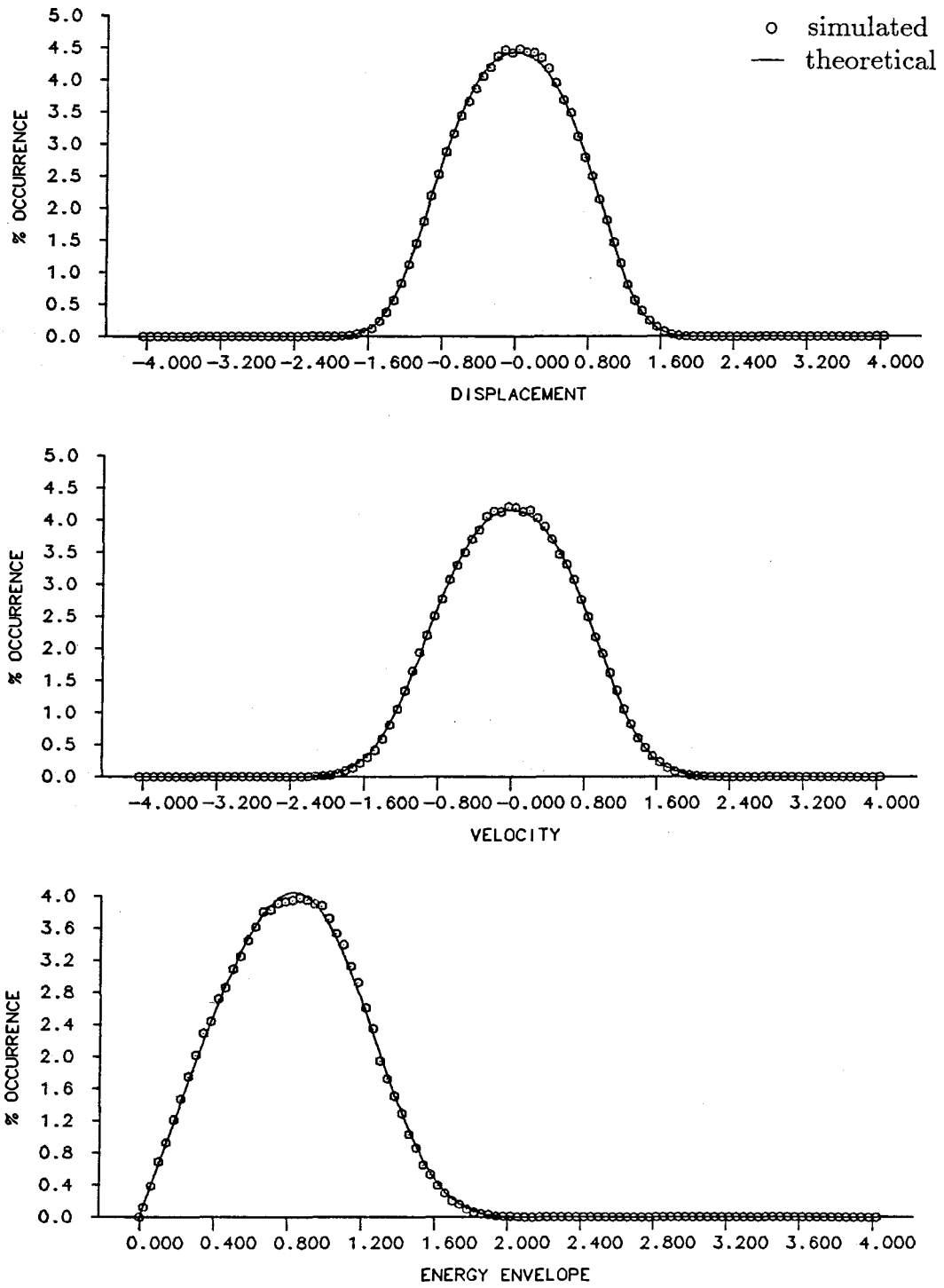
Figure 5.79

$(Velocity)^2$-Damping/Duffing Stiffness

$b_{02} = 0.10, \quad e_0 = 1.00, \quad e_1 = 0.20, \quad D = 0.05$
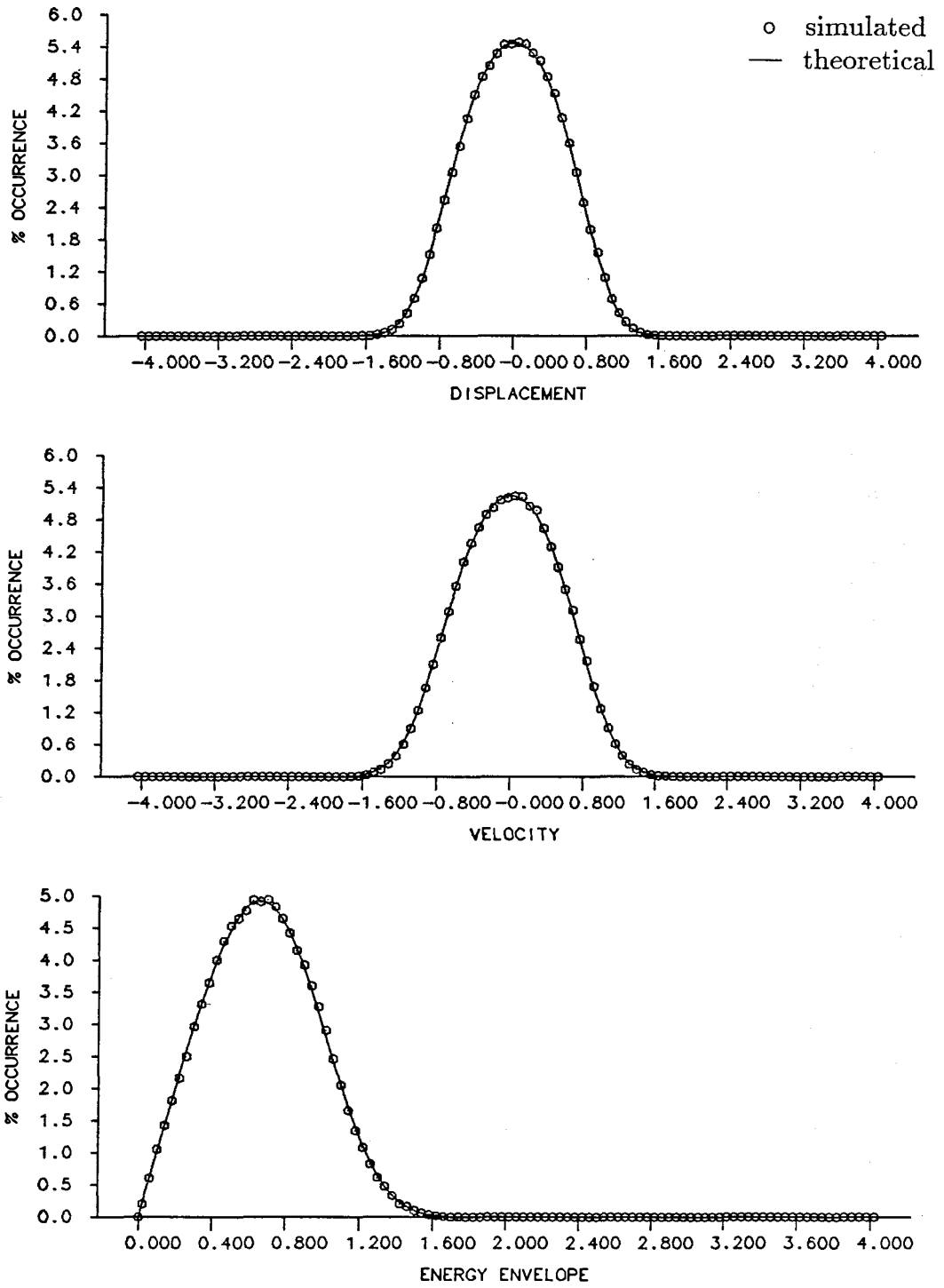
Figure 5.80

$(Velocity)^2$-Damping/Duffing Stiffness

$b_{02} = 0.20$, $e_0 = 1.00$, $e_1 = 0.20$, $D = 0.05$
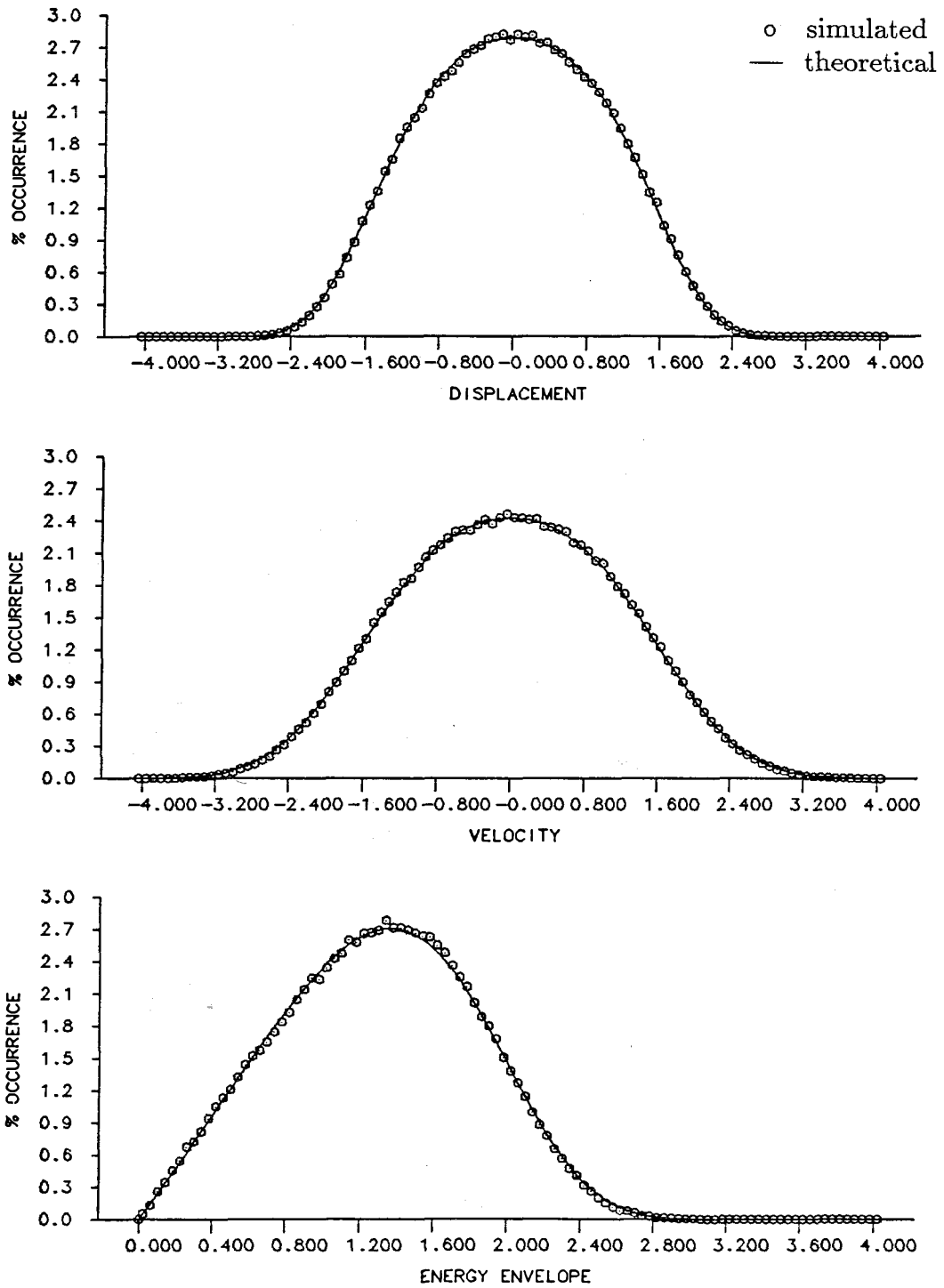
Figure 5.81

$(Velocity)^2$-Damping/Duffing Stiffness

$b_{02} = 0.10$, $e_0 = 1.00$, $e_1 = 0.20$, $D = 0.25$
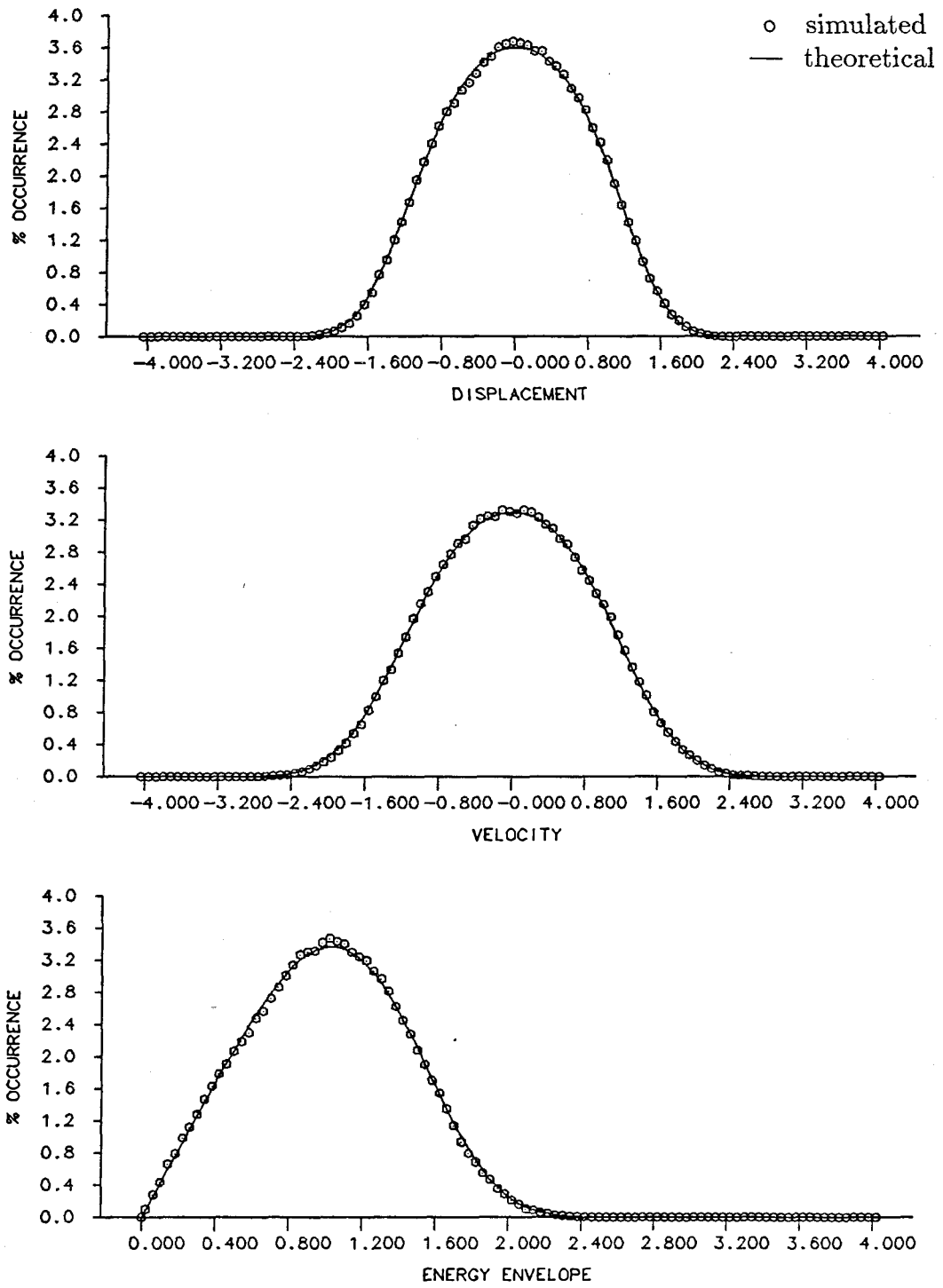
Figure 5.82

$(Velocity)^2$-Damping/Duffing Stiffness

$b_{02} = 0.10$, $e_0 = 1.00$, $e_1 = 0.20$, $D = 0.10$
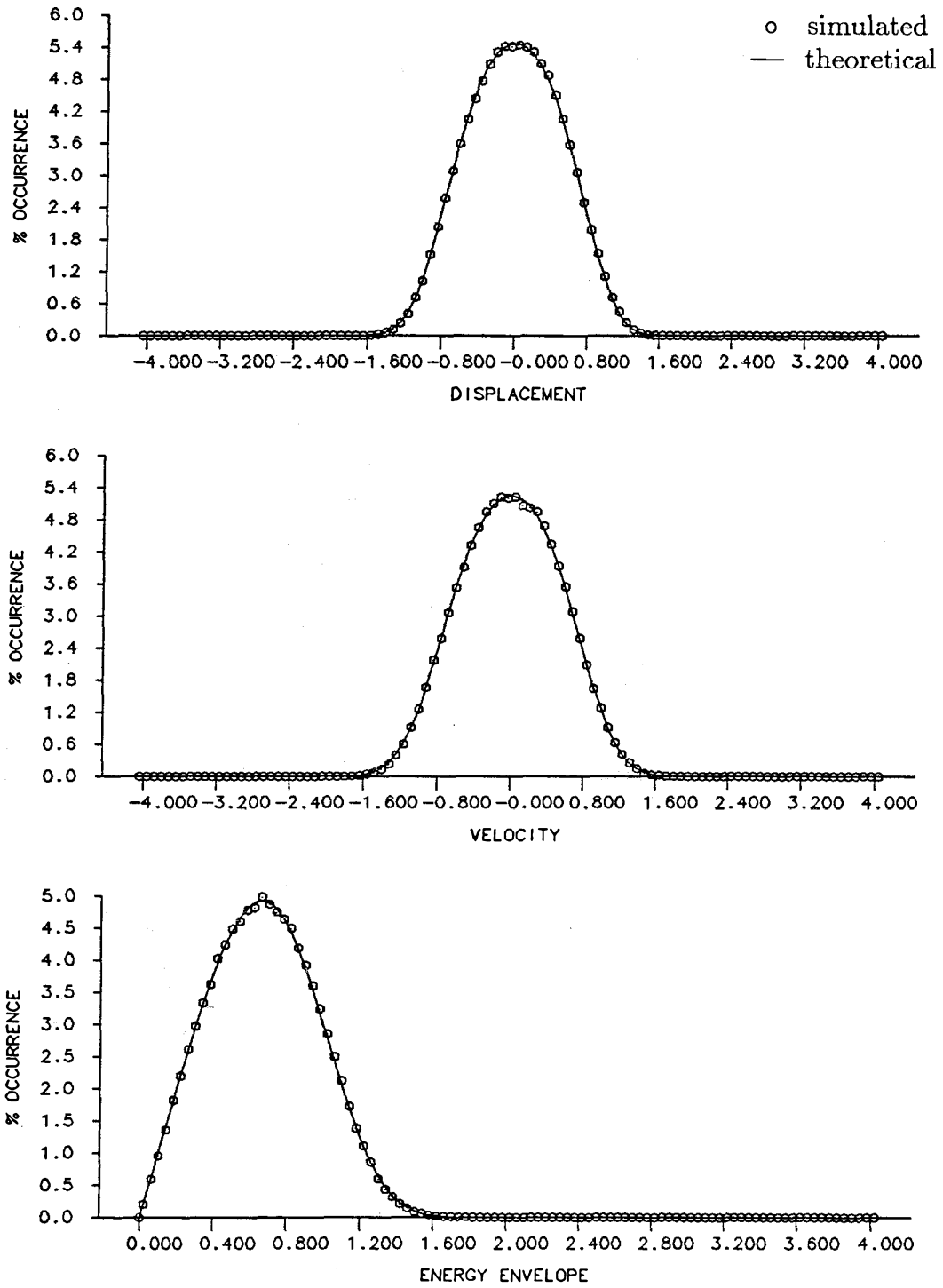
Figure 5.83

$(Velocity)^2$-Damping/Duffing Stiffness
$b_{02} = 0.10$, $e_0 = 1.00$, $e_1 = 0.20$, $D = 0.025$
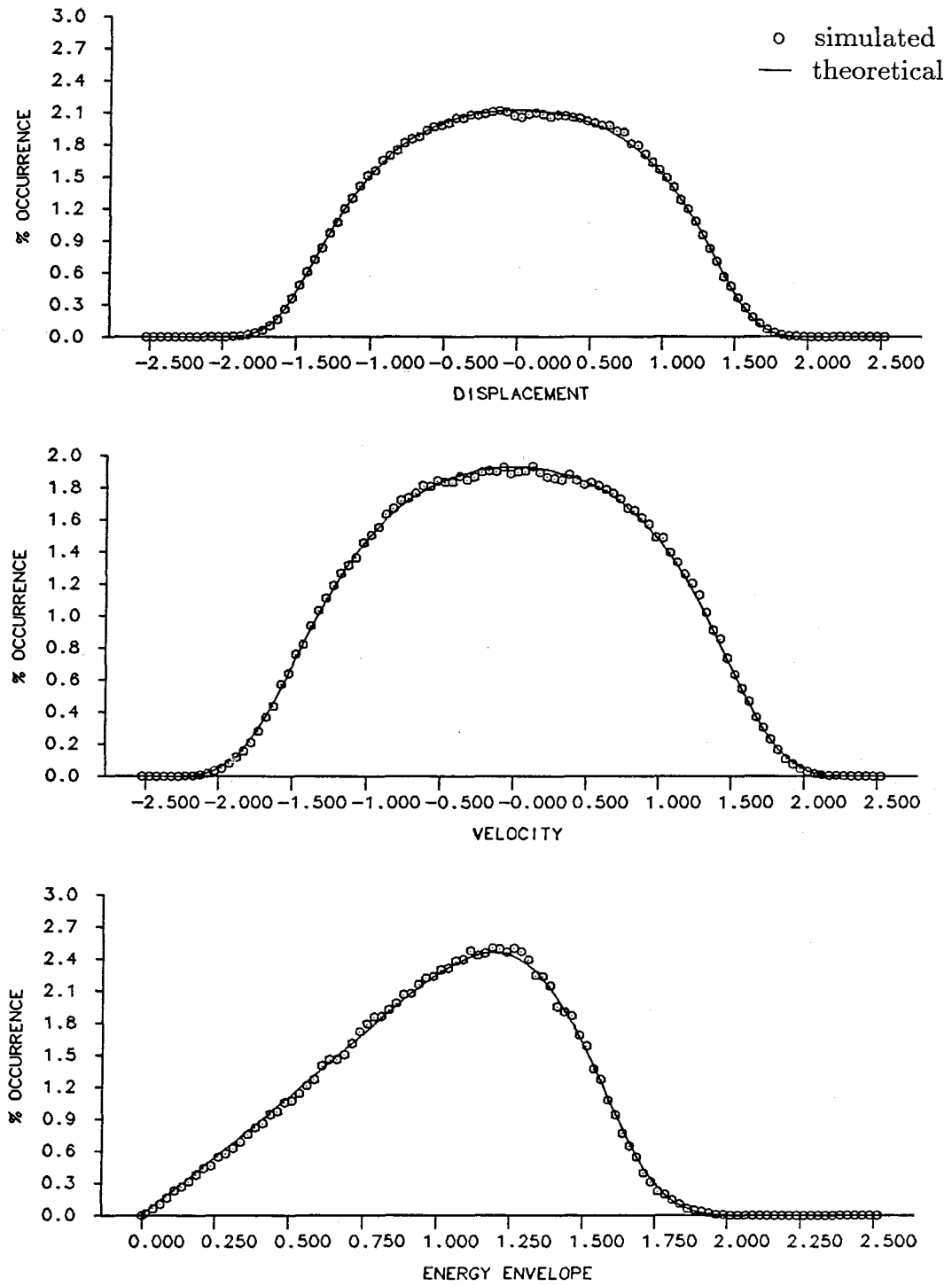
Figure 5.84

$(Velocity)^5$-Damping/Duffing Stiffness

$b_{05} = 0.02, \quad e_0 = 1.00, \quad e_1 = 0.20, \quad D = 0.05$
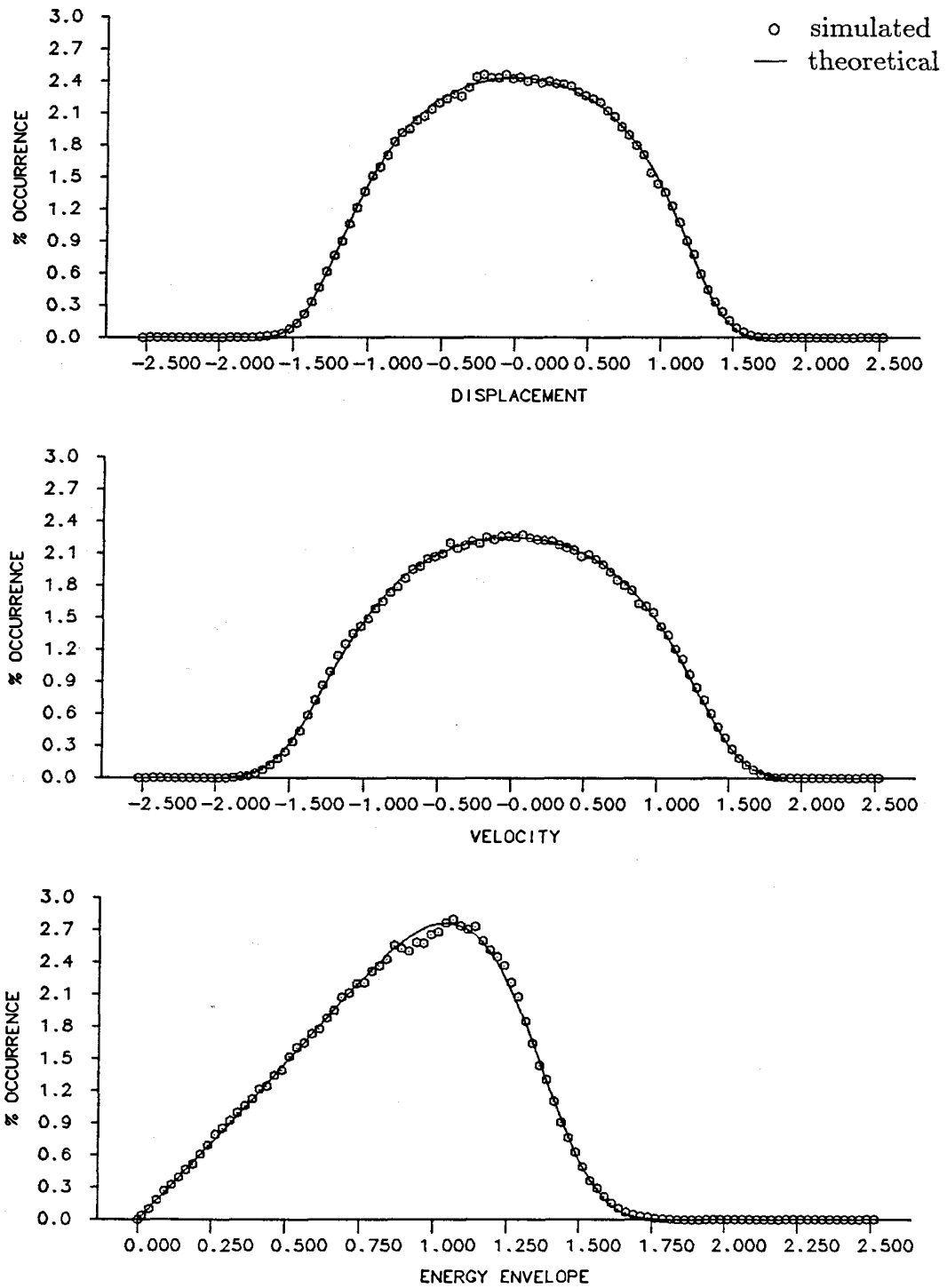
Figure 5.85

$(Velocity)^5$-Damping/Duffing Stiffness

$b_{05} = 0.05, \quad e_0 = 1.00, \quad e_1 = 0.20, \quad D = 0.05$
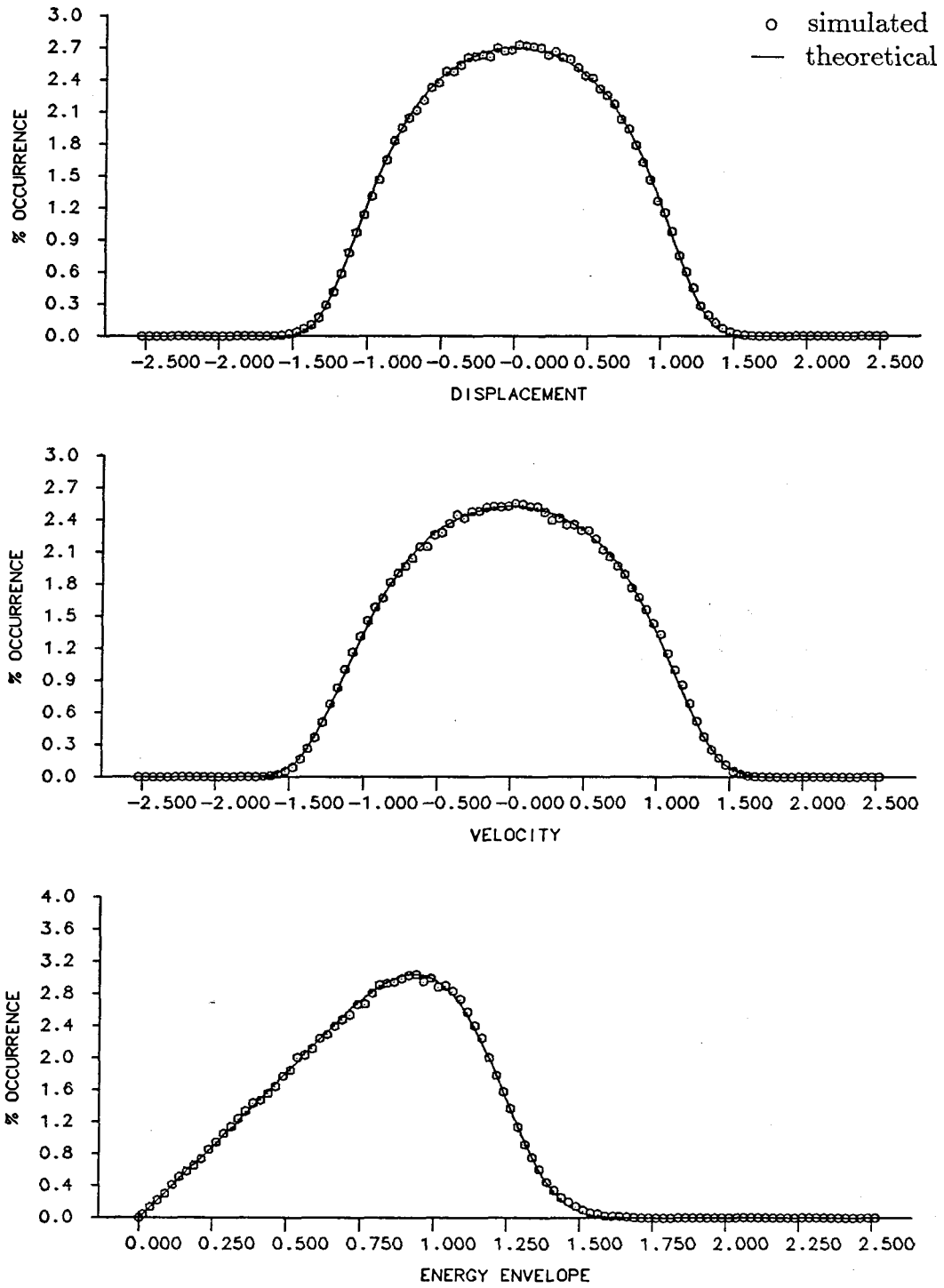
Figure 5.86

$(Velocity)^5$-Damping/Duffing Stiffness

$b_{05} = 0.10$, $e_0 = 1.00$, $e_1 = 0.20$, $D = 0.05$
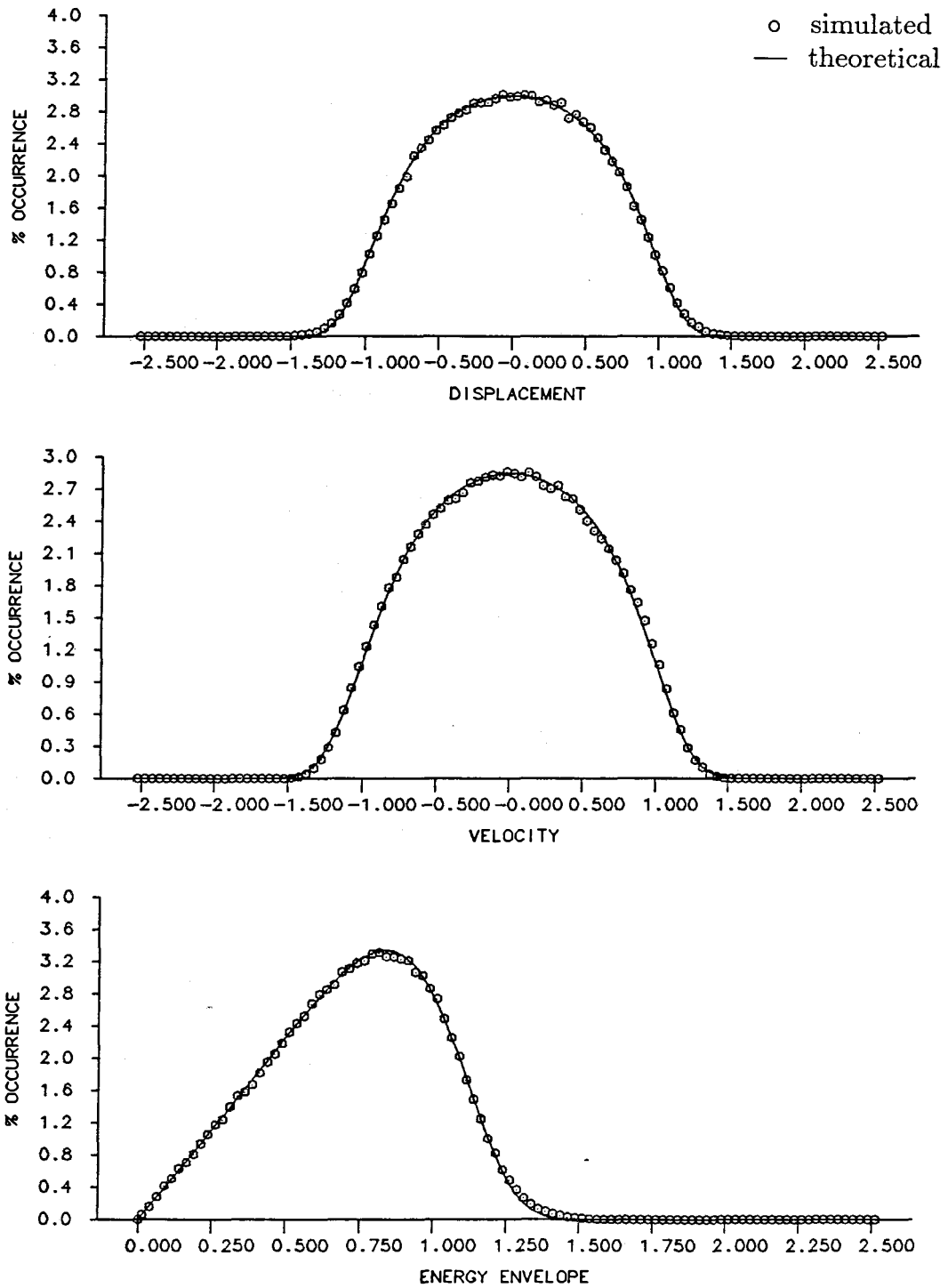
Figure 5.87

$(Velocity)^5$-Damping/Duffing Stiffness

$b_{05} = 0.20, \quad e_0 = 1.00, \quad e_1 = 0.20, \quad D = 0.05$
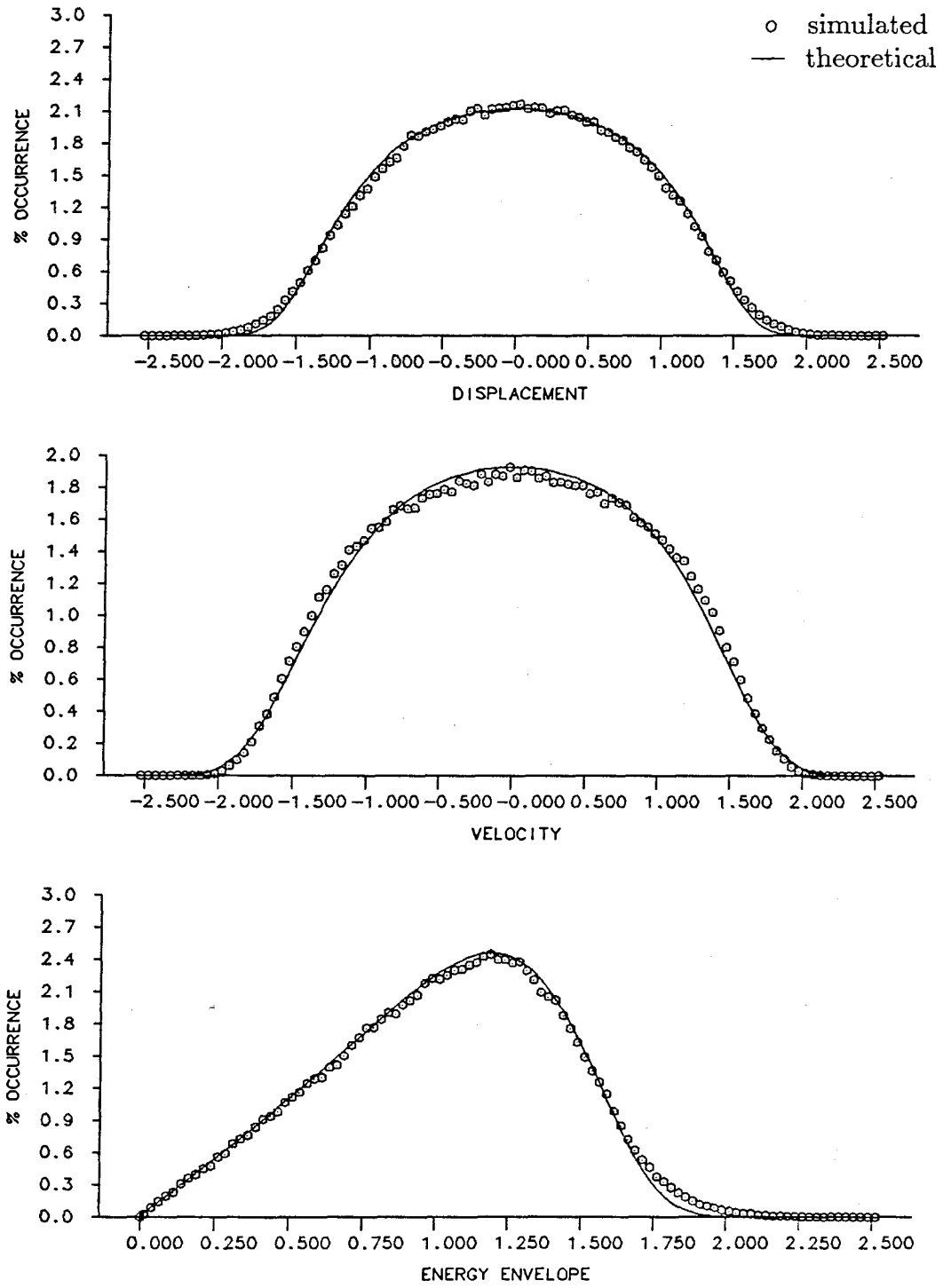
Figure 5.88

$(Velocity)^5$-Damping/Duffing Stiffness

$b_{05} = 0.10, \quad e_0 = 1.00, \quad e_1 = 0.20, \quad D = 0.25$
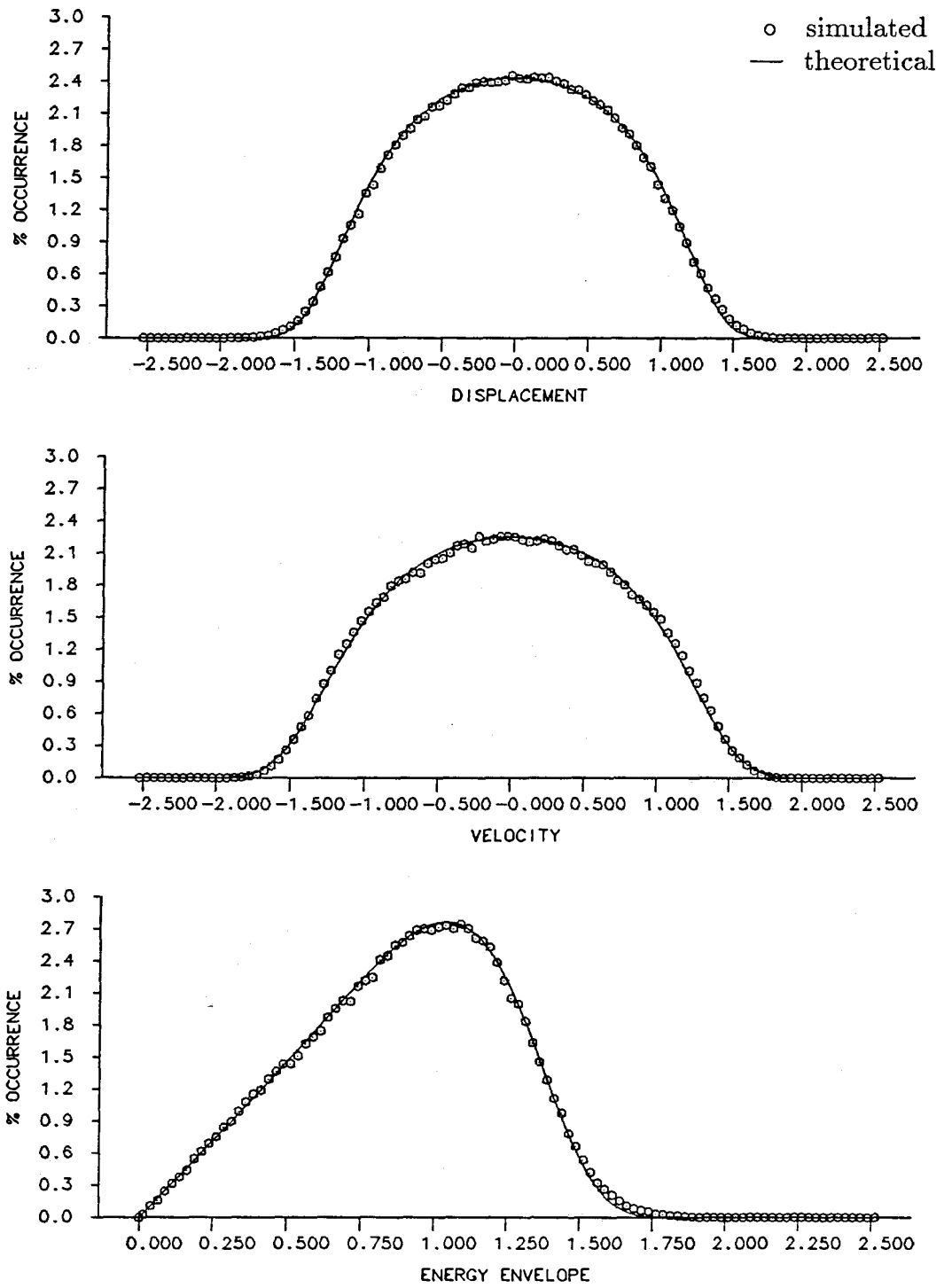
Figure 5.89

$(Velocity)^5$-Damping/Duffing Stiffness

$b_{05} = 0.10$, $e_0 = 1.00$, $e_1 = 0.20$, $D = 0.10$
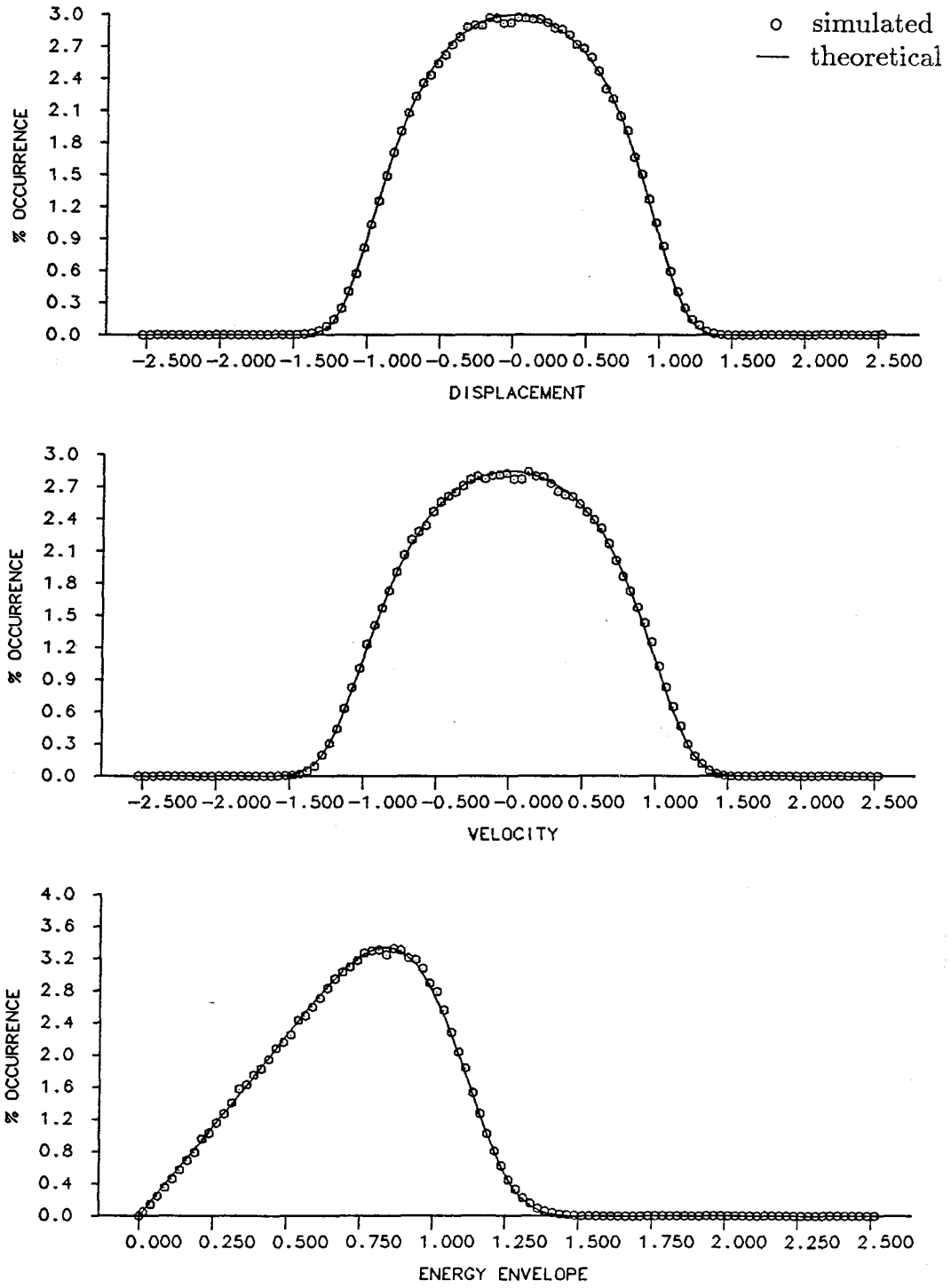
Figure 5.90

$(Velocity)^5$-Damping/Duffing Stiffness

$b_{05} = 0.10, \quad e_0 = 1.00, \quad e_1 = 0.20, \quad D = 0.025$

CHAPTER VI

SUMMARY AND CONCLUSIONS

The Method of Equivalent Nonlinearization, for obtaining approximate steady-state probability density function of response of nonlinear systems subjected to white-noise Gaussian excitation, has been evaluated based on extensive numerical simulations. The evaluation was performed for a class of oscillators with nonlinear damping for which there are no exact solutions. To the author's knowledge, it was the first time that such evaluation was performed to this extent.

In Chapter II, the theoretical background on the response of nonlinear oscillators to white-noise Gaussian random excitation was briefly reviewed. Even though the problem can be formulated, leading to the Fokker-Planck-Kolmogorov equation governing the transition probability density function of the response, solutions for this equation are very limited. The Method of Equivalent Linearization for obtaining approximate solutions for the steady-state probability density function of the response was also reviewed and applied to an oscillator with nonlinear damping to illustrate that the solutions obtained from the application of this method may not always be satisfactory.

In Chapter III, the Method of Equivalent Nonlinearization, a natural extension of the Method of Equivalent Linearization, was reviewed and systematically

applied to the class of oscillators with nonlinear damping mentioned above. Because existence of solutions for nonlinear oscillators is fundamental in the application of this method, the solution of the Fokker-Planck-Kolmogorov equation for the steady-state probability density function of the response for a wide class of nonlinear oscillators was also reviewed.

When the oscillator had nonlinear damping and linear stiffness, the application of the Method of Equivalent Nonlinearization generated a set of nonlinear algebraic equations that was solved analytically, yielding families of steady-state joint probabilty density function of displacement and velocity, functions of the oscillator and excitation parameters. When, on the other hand, the oscillator has nonlinear damping and nonlinear stiffness, the set of nonlinear algebraic equation can be solved only numerically. The numerical effort involved in this solution, however, is minimum compared to the effort involved in the numerical simulation of the exact solution. In either of these cases, the probability density functions generated are nonseparable in the displacement and velocity variables.

In Chapter IV, the background for the numerical simulation of the response of this class of oscillators was reviewed, and all the necessary algorithms were generated. Of relevance is the fact that the rather long lengths of simulated response required to generate adequate statistics, coupled with the varied computational resources used, necessitated the special tailoring of a time-domain integration scheme. The scheme developed was over an order of magnitude faster than an alternate scheme readily available at Caltech.

Finally, in Chapter V, the approximate solutions obtained in Chapter III were compared with the solutions based on the simulated response obtained with the numerical integration scheme developed in Chapter IV. In this chapter, results from nine different oscillators with nonlinear damping and linear and nonlinear stiffness were obtained and compared. The comparisons were conducted for a range of damping values and a range of excitation values that seemed to be adequate for practical structural dynamic problems. With only minor reservations, it can be stated that the agreement between approximate and numerically obtained exact solutions is excellent at the level of mean-square values, and what is even more important, at the level of density functions. An interesting result from these comparisons is that even though the exact solutions are functions of the damping level and excitation level, for the range of values used, this dependence is not very strong and can be modeled by the approximate solutions that are functions of the ratio of these two parameters.

The excellent agreement obtained certainly warrants further work in the area, and in this regard there are a number of extensions that can be researched. An evaluation study similar to this outside the range of the parameters used herein would certainly be useful. It is pointed out that it is not expected that the method will produce good approximations for the Van der Pol oscillator with damping levels greater than those used. Of particular interest is the extension of the method to nonlinear oscillators with hysteresis. In that respect the work by Lutes [28] should serve as the starting point. The extension of method to multidegree-of-freedom systems seems worth pursuing in view of the existence of nonlinear solutions for this class of systems [9,10]. And in general, the fact that the Method of Equivalent Nonlinearization is a natural extension of the Method of Equivalent Linearization

opens up all the areas in which the latter was used in the past thirty years, both theoretical and practical.

REFERENCES

[1] Bathe, K. J., and Wilson, E. L., **Numerical Methods in Finite Element Analysis**, Prentice-Hall, Inc., Englewood Cliffs, New Jersey, 1976.

[2] Booton, Jr., R. C., "The Analysis of Nonlinear Control Systems with Random Inputs," *Proceedings of the Symposium on Nonlinear Circuit Analysis*, Polytechnic Institute of Brooklyn, New York, 2, 369-391, 1953.

[3] Caughey, T. K., "Random Excitation of a System With Bilinear Hysteresis," *Journal of Applied Mechanics*, 649-652, December 1960.

[4] Caughey, T. K., "Equivalent Linearization Techniques," *The Journal of the Acoustical Society of America*, 35, no. 11, 1706-1711, November 1963.

[5] Caughey, T. K., "Derivation and Application of the Fokker-Plank Equation to Discrete Nonlinear Dynamic Systems Subjected to White Random Excitation," *The Journal of the Acoustical Society of America*, 35, no. 11, 1683-1692, November 1963.

[6] Caughey, T. K., and Payne, H. J., "On the Response of a Class of Self-Excited Oscillators to Stochastic Excitation," *International Journal of Non-Linear Mechanics*, 2, 125-151, 1967.

[7] Caughey, T. K., "Nonlinear Theory of Random Vibrations ," **Advances in Applied Mechanics**, C. Yih, editor, 11, Academic Press, New York, 1971, pp. 209-253.

[8] Caughey, T. K., and Ma, F., "The Exact Steady-State Solution of a Class of Non-Linear Stochastic Systems," *International Journal of Non-Linear Mechanics*, 17, no. 3, 137-142, 1982.

[9] Caughey, T. K., and Ma, F., "The Steady-State Response of a Class of Dynamical Systems to Stochastic Excitation," *Journal of Applied Mechanics*, 49, 629-632, September 1982.

[10] Caughey, T. K., "On the response of Non-linear Oscillators to Stochastic Excitation," **Random Vibrations**, T. C. Huang and P. D. Spanos, editors, AMD, 65, ASME, New York, 1984. pp. 9-14.

[11] Crandall, S. H., "Random Vibration of a Nonlinear System with a Set-up Spring," *Journal of Applied Mechanics*, 477-482, September 1962.

[12] Crandall, S. H., "Zero Crossings, Peaks, and Other Statistical Measures of Random Responses," *The Journal of the Acoustical Society of America*, 35, no. 11, 1693-1699, November 1963.

[13] Crandall, S. H., "Perturbation Techniques for Random Vibration of Nonlinear Systems," *The Journal of the Acoustical Society of America*, **35**, no. 11, 1700-1705, November 1963.

[14] Crandall, S. H., Khabbaz G. R., and Manning, J. E., "Random Vibration of an Oscillator with Nonlinear Damping," *The Journal of the Acoustical Society of America*, **36**, no. 7, 1330-1334, July 1964.

[15] Crandall, S. H., and Mark, W. D., **Random Vibration in Mechanical Systems**, Academic Press, New York, 1973.

[16] Crandall, S. H., "Non-Gaussian Closure for Random Vibration of Non-linear Oscillators," *International Journal of Non-Linear Mechanics*, **15**, 303-313, 1980.

[17] Crandall, S. H., and Zhu, W. Q., "Random Vibration: A Survey of Recent Developments," *Journal of Applied Mechanics*, **50**, 953-962, December 1983.

[18] Crandall, S. H., "Non-Gaussian Closure Techniques for Stationary Random Vibration," *International Journal of Non-Linear Mechanics*, **20**, no. 1, 1-8, 1985.

[19] Gentle, J. E., "Portability Considerations for Random Number Generators," IMSL Technical Report Series no. 8101, February 1981.

[20] Hogg, R. V., and Craig, A. T., **Introduction to Mathematical Statistics**, Macmillan Publishing Co.,Inc., New York, 1978.

[21] Iwan, W. D., and Spanos, P. T., "Response Envelope Statistics for Nonlinear Oscillators with Random Excitation," *Journal of Applied Mechanics*, **45**, 170-174, March 1978.

[22] Johnson, J. P., and Scott, R. A., "Extension of Eigenfunction- Expansion of a Fokker-Planck Equation-I. First Order System," *International Journal of Non-Linear Mechanics*, **14**, 315-324, 1980.

[23] Johnson, J. P., and Scott, R. A., "Extension of Eigenfunction- Expansion of a Fokker-Planck Equation-II. Second Order System," *International Journal of Non-Linear Mechanics*, **15**, 41-56, 1980.

[24] Kirk, C. L., "Application of the Fokker-Plank Equation to Random Vibration of Nonlinear Systems," Cranfield Report Aero no. 20, Cranfield Institute of Technology, Cranfield (England), April 1974.

[25] Knuth, D. E., **The art of Computer Programing: Seminumerical Algorithms**, Addison-Wesley Publishing Company, Reading, Massachusetts, 1981.

[26] Lewis, T. G., **Distribution Sampling for Computer Simulation**, Lexington Books, D. C. Heath and Company, Lexington, Massachusetts, 1975.

[27] Lin, Y. K., **Probabilistic Theory of Structural Dynamics**, Robert E. Krieger Publishing Company, Huntington, New York, 1976.

[28] Lutes, L. D., "Stationary Random Response of Bilinear Hysteretic Systems," Ph.D. Thesis, California Institute of Technology, 1967.

[29] Meirovitch, L., **Analytical Methods in Vibrations**, The Macmillan Company, New York, 1979.

[30] Minorsky, N., **Nonlinear Oscillations**, D. Van Nostrand Company, Inc., New Jersey, 1962.

[31] Modianos, D. T., Scott R. C., and Cornwell, L. W., "Testing Intrinsic Random Number Generators," *Byte Magazine*, January 1987.

[32] Noori, M. N., Saffar, A. and Davoodi, H., "A Comparison Between Non-Gaussian Closure and Statistical Linearization Techniques for Random Vibration of a Nonlinear Oscillator," *International Journal of Non-Linear Mechanics*, **26**, no. 6, 925-931, 1986.

[33] Payne, H. J., "The Response of Nonlinear Systems to Stochastic Excitation," Ph.D. Thesis, California Institute of Technology, 1967.

[34] Press W. H., Flannery B. P., Teukolski, S. A. and Vetterling, W. T., **Numerical Recipes, The Art of Scientific Computing**, Cambridge University Press, 1986.

[35] Roberts J. B., and Spanos P. D., "Stochastic Averaging: An Approximate Method of Solving Random Vibration Problems," *International Journal of Non-Linear Mechanics*, **21**, no. 2, 111-134, 1986.

[36] Spanos, P. D., "Stochastic Linearization in Structural Dynamics," *Applied Mechanics Reviews*, **34**, no. 1, 1-8, 1981.

[37] Vanmarcke, E. H., "Some Recent Developments in Random Vibration," *Applied Mechanics Reviews*, **32**, no. 10, 1197-1202, 1979.

[38] Whitney, C. A., "Generating and Testing Pseudorandom Numbers," *Byte Magazine*, October 1984.

[39] Wichmann, B. A., and Hill, I. D., "An efficient and Portable Pseudo-Random Number Generator," **Applied Statistics Algorithms**, Griffiths, P., Hill I. D., editors, Ellis Horwood Limited, 1986, pp. 238-242.

[40] Yang, I-M., "Stationary Random Response of Multi-Degree-of-Freedom- Systems," Ph.D. Thesis, California Institute of Technology, 1970.

APPENDIX A

COMPUTER PROGRAM

```
C
C.....THIS PROGRAM DIRECTLY INTEGRATES A NONLINEAR SECOND
C      ORDER DIFFERENTIAL EQUATION USING A COMBINATION OF
C      NEWMARK AND NEWTON-RAPHSON PROCEDURES.
C
C
C
C.....EXPLANATION OF INPUT:
C
C         NPTS ....... TOTAL NUMBER OF POINTS IN THE
C                      TIME HISTORY.
C         NSKIP ...... NUMBER OF POINTS TO BE SKIPPED
C                      AT THE BEGINNING OF THE
C                      TIME HISTORY.
C         DELT ....... TIME STEP INCREMENT.
C         TOLVEL ..... VELOCITY TOLERANCE.
C         TOLDIS ..... DISPLACEMENT TOLERANCE.
C         VO ......... INITIAL VELOCITY.
C         DO ......... INITIAL DISPLACEMENT.
C         B(IJ) ...... PARAMETERS IN THE DIFFERENTIAL EQUATION.
C         B,D ........ PARAMETERS IN THE THEORETICAL
C                      PROBABILITY DENSITY FUNCTIONS.
C         IND ........ INITIAL BIN BOUNDARY FOR THE HISTOGRAM
C                      OF DISPLACEMENTS.
C         INV ........ INITIAL BIN BOUNDARY FOR THE HISTOGRAM
C                      OF VELOCITIES.
C         INF ........ INITIAL BIN BOUNDARY FOR THE HISTOGRAM
C                      OF FORCES.
C         INE ........ INITIAL BIN BOUNDARY FOR THE HISTOGRAM
C                      OF ENVELOPE.
C         DELTAD ..... BIN WIDTH FOR THE HISTOGRAM OF
C                      DISPLACEMENTS.
C         DELTAV ..... BIN WIDTH FOR THE HISTOGRAM OF
C                      VELOCITIES.
C         DELTAF ..... BIN WIDTH FOR THE HISTOGRAM OF
C                      FORCES.
C         DELTAE ..... BIN WIDTH FOR THE HISTOGRAM OF
C                      ENVELOPE.
C         NDBND ...... NUMBER OF BIN BOUNDARIES FOR THE
C                      HISTOGRAM OF DISPLACEMENTS.
C         NVBND ...... NUMBER OF BIN BOUNDARIES FOR THE
C                      HISTOGRAM OF VELOCITIES.
C         NFBND ...... NUMBER OF BIN BOUNDARIES FOR THE
C                      HISTOGRAM OF FORCES.
C         NEBND ...... NUMBER OF BIN BOUNDARIES FOR THE
C                      HISTOGRAM OF ENVELOPE.
C
C.....EXPLANATION OF MAIN VARIABLES.
C
C         IX1 ........ RANDOM NUMBER INPUT SEED.
C         IX2 ........ RANDOM NUMBER INPUT SEED.
C         IX3 ........ RANDOM NUMBER INPUT SEED.
```

```
C                                 DENSITY OF FORCING FUNCTION.
C              AI/AF....... ACCELERATIONS.
C              VI/VF....... VELOCITIES.
C              DI/DF....... DISPLACEMENTS.
C              NI/NF....... FORCING FUNCTION.
C              EI/EF....... ENVELOPE.
C
C.....EXPLANATION OF MAIN ARRAYS.
C
C              DISBND...... BIN BOUNDARIES FOR THE HISTOGRAM OF
C                           NUMERICAL DISPLACEMENTS.
C              VELBND...... BIN BOUNDARIES FOR THE HISTOGRAM OF
C                           NUMERICAL VELOCITIES.
C              FORBND...... BIN BOUNDARIES FOR THE HISTOGRAM OF
C                           NUMERICAL FORCES.
C              ENVBND...... BIN BOUNDARIES FOR THE HISTOGRAM OF
C                           NUMERICAL ENVELOPE.
C              YDHIST...... NUMERICAL DISPLACEMENT HISTOGRAM.
C              YVHIST...... NUMERICAL VELOCITY HISTOGRAM.
C              YFHIST...... NUMERICAL FORCE HISTOGRAM.
C              YEHIST...... NUMERICAL ENVELOPE HISTOGRAM.
C
C              DTHE ....... BIN BOUNDARIES FOR THE HISTOGRAM OF
C                           THEORETICAL DISPLACEMENTS.
C              VTHE ....... BIN BOUNDARIES FOR THE HISTOGRAM OF
C                           THEORETICAL VELOCITIES.
C              FTHE ....... BIN BOUNDARIES FOR THE HISTOGRAM OF
C                           THEORETICAL FORCES.
C              ETHE ....... BIN BOUNDARIES FOR THE HISTOGRAM OF
C                           NUMERICAL ENVELOPE.
C              TYDHIST..... THEORETICAL DISPLACEMENT HISTOGRAM.
C              TYVHIST..... THEORETICAL VELOCITY HISTOGRAM.
C              TYFHIST..... THEORETICAL FORCE HISTOGRAM.
C              TYEHIST..... THEORETICAL ENVELOPE HISTOGRAM.
C              KNT ........ FREQUENCY OF OCCURRENCE COUNTER.
C              PERCNT ..... NUMERICAL PERCENT OF OCCURRENCE.
C              TPERCNT .... THEORETICAL PERCENT OF OCCURRENCE.
C
C
C
         IMPLICIT REAL*8(A-H,O-Z)
         INTEGER*4 IX
         REAL*8 N1,N2,NI,NF
         REAL*8 IND,INV,INF,INE
         CHARACTER*2 TO
         DIMENSION DISBND(102),VELBND(102),FORBND(102),
        1          ENVBND(102)
         DIMENSION YDHIST(102),YVHIST(102),YNHIST(102),
        1          YEHIST(102)
         DIMENSION DTHE(102),VTHE(102),FTHE(102),ETHE(102)
         DIMENSION TYDHIST(102),TYVHIST(102),TYNHIST(102),
        1          TYEHIST(102)
```

```
      DIMENSION KNT(102,102),PERCNT(103,103)
      DIMENSION TPERCNT(103,103)
      DIMENSION DIS(500),VEL(500),ACC(500),FOR(500),ENV(500),
     1          TIM(500)
      DATA DISBND,VELBND,FORBND,ENVBND/408*0.0/
      DATA YDHIST,YVHIST,YNHIST,YEHIST/408*0.0/
      DATA DTHE,VTHE,FTHE,ETHE/408*0.0/
      DATA TYDHIST,TYVHIST,TYNHIST,TYEHIST/408*0.0/
      DATA KNT/10404*0/
      DATA PERCNT/10609*0.0/
      DATA TPERCNT/10609*0.0/
      DATA TO/'TO'/
      DATA PI/3.14159265/
      DATA G13/2.6789385347/
      DATA G23/1.3541179394/
      DATA A1,A2,A3,A4,A5,A6/0.0705230784,  0.0422820123,
     1                       0.0092705272,  0.0001520143,
     1                       0.0002765672,  0.0000430638/
C
C.....FUNC1 IS F(X,X') SO THAT X"-F(X,X')=N(T)
C.....FUNC2 IS DF(X,X')/DX'
C.....FUNC3 IS DF(X,X')/DX
C
C
C.....EXAMPLE 1
C
C     FUNC1(X,XDOT,B00,B01,B02,B03,B10,B11,B12,B13,B20,B21,
C    1B22,B23,B30,B31,B32,B33)=
C    1     -(B00*4.0/PI*1.0/DSQRT(X**2+XDOT**2)*XDOT+X)
C
C
C.....EXAMPLE 2
C
C     FUNC1(X,XDOT,B00,B01,B02,B03,B10,B11,B12,B13,B20,B21,
C    1B22,B23,B30,B31,B32,B33)=
C    1     -(B00*8.0/(3.0*PI)*DSQRT(X**2+XDOT**2)*XDOT+X)
C
C
C.....EXAMPLES 3 THROUGH 9
C
      FUNC1(X,XDOT,B00,B01,B02,B03,B10,B11,B12,B13,B20,B21,
     1B22,B23,B30,B31,B32,B33,B05,B41)=
     1     -(B00*DSIGN(1.0,XDOT)+
     2       B01*XDOT+
     3       B02*XDOT**2*DSIGN(1.0,XDOT)+
     4       B03*XDOT**3+
     5       B10*DSIGN(1.0,XDOT)*DABS(X)+
     6       B11*XDOT*DABS(X)+
     7       B12*XDOT**2*DSIGN(1.0,XDOT)*DABS(X)+
     8       B13*XDOT**3*DABS(X)+
     9       B20*DSIGN(1.0,XDOT)*X**2+
     .       B21*XDOT*X**2+
```

```
     1          B22*XDOT**2*DSIGN(1.0,XDOT)*X**2+
     2          B23*XDOT**3*X**2+
     3          B30*DSIGN(1.0,XDOT)*DABS(X**3)+
     4          B31*XDOT*DABS(X**3)+
     5          B32*XDOT**2*DSIGN(1.0,XDOT)*DABS(X**3)+
     6          B33*XDOT**3*DABS(X**3)+B05*XDOT**5+
     7          B41*XDOT*X**4+X)
C
C
C
C.....EXAMPLE 1
C
C     FUNC2(X,XDOT,B00,B01,B02,B03,B10,B11,B12,B13,B20,B21,
C    1B22,B23,B30,B31,B32,B33)=
C    1     -(B00*4.0/PI*(-XDOT**2/(DSQRT(X**2+XDOT**2)**3)+
C    1       1.0/DSQRT(X**2+XDOT**2)))
C
C
C.....EXAMPLE 2
C
C     FUNC2(X,XDOT,B00,B01,B02,B03,B10,B11,B12,B13,B20,B21,
C    1B22,B23,B30,B31,B32,B33)=
C    1     -(B00*8.0/(3.0*PI)*(-XDOT**2/(DSQRT(X**2+XDOT**2))+
C    1       DSQRT(X**2+XDOT**2)))
C
C
C.....EXAMPLES 3 THROUGH 9
C
      FUNC2(X,XDOT,B00,B01,B02,B03,B10,B11,B12,B13,B20,B21,
     1B22,B23,B30,B31,B32,B33,B05,B41)=
     1     -(B00*0.0+
     2       B01*1.0+
     3       B02*2.0*DABS(XDOT)+
     4       B03*3.0*XDOT**2+
     5       B10*0.0+
     6       B11*DABS(X)+
     7       B12*2.0*DABS(XDOT)*DABS(X)+
     8       B13*3.0*XDOT**2*DABS(X)+
     9       B20*0.0+
     .       B21*X**2+
     1       B22*2.0*DABS(XDOT)*X**2+
     2       B23*3.0*XDOT**2*X**2+
     3       B30*0.0+
     4       B31*DABS(X**3)+
     5       B32*2.0*DABS(XDOT)*DABS(X**3)+
     6       B33*3.0*XDOT**2*DABS(X**3)+B05*5.0*XDOT**4+
     7       B41*X**4+0.0)
C
C
C.....EXAMPLE 1
C
C     FUNC3(X,XDOT,B00,B01,B02,B03,B10,B11,B12,B13,B20,B21,
```

```
C     1B22,B23,B30,B31,B32,B33)=
C     1     -(-B00*4.0/PI*XDOT*X/(DSQRT(X**2+XDOT**2)**3)+1.0)
C
C
C.....EXAMPLE 2
C
C     FUNC3(X,XDOT,B00,B01,B02,B03,B10,B11,B12,B13,B20,B21,
C     1B22,B23,B30,B31,B32,B33)=
C     1     -(-B00*8.0/(3.0*PI)*XDOT*X/(DSQRT(X**2+XDOT**2))
C     1        +1.0)
C
C
C.....EXAMPLES 3 THROUGH 9
C
      FUNC3(X,XDOT,B00,B01,B02,B03,B10,B11,B12,B13,B20,B21,
     1B22,B23,B30,B31,B32,B33,B05,B41)=
     1     -(B00*0.0+
     2        B01*0.0+
     3        B02*0.0+
     4        B03*0.0+
     5        B10*DSIGN(1.0,XDOT)*DSIGN(1.0,X)+
     6        B11*XDOT*DSIGN(1.0,X)+
     7        B12*XDOT**2*DSIGN(1.0,XDOT)*DSIGN(1.0,X)+
     8        B13*XDOT**3*DSIGN(1.0,X)+
     9        B20*DSIGN(1.0,XDOT)*2.0*X+
     .        B21*XDOT*2.0*X+
     1        B22*XDOT**2*DSIGN(1.0,XDOT)*2.0*X+
     2        B23*XDOT**3*2.0*X+
     3        B30*DSIGN(1.0,XDOT)*3.0*X**2*DSIGN(1.0,X)+
     4        B31*XDOT*3.0*X**2*DSIGN(1.0,X)+
     5        B32*XDOT**2*DSIGN(1.0,XDOT)*
     5        3.0*X**2*DSIGN(1.0,X)+
     6        B33*XDOT**3*3.0*X**2*DSIGN(1.0,X)+B05*0.0+
     7        B41*XDOT*4.0*X**3+1.0)
C
C.....COMPLEMENTARY ERROR FUNCTION ERFC(X) FOR X.LE.0.0
C
      ERFC(X)=2.0-
     1 1.0/((1.0-A1*X+A2*X**2-A3*X**3+A4*X**4-A5*X**5+A6*X**6)
     2 **16)
C
C.....EXAMPLE 1 (COULOMB DAMPING)
C
C.....DEFINE THE JOINT PROBABILITY DENSITY FUNCTION PDFJ AND
C     THE ENVELOPE DISTRIBUTION PDFE FOR EXAMPLE 1.
C
C
C     PDFJ(X,XDOT,B,D)=(1.0/(2.0*PI))*(4.0*B/(PI*D))**2*
C     1              DEXP(-(4.0*B/(PI*D)*DSQRT(X**2+XDOT**2)))
C
C
C     PDFE(A,B,D)=(4.0*B/(PI*D))**2*
```

```
C     1                 A*DEXP(-(4.0*B/(PI*D)*A))
C
C
C.....EXAMPLE 2 (VELOCITY SQUARE DAMPING)
C
C.....DEFINE THE JOINT PROBABILITY DENSITY FUNCTION PDFJ AND
C     THE ENVELOPE DISTRIBUTION PDFE FOR EXAMPLE 2.
C
C
C     PDFJ(X,XDOT,B,D)=(1.0/(2.0*PI))*(3.0/G23)*
C     1           (8.0*B/(9.0*PI*D))**0.6667*
C     2           DEXP(-(8.0*B/(9.0*PI*D)*(X**2+XDOT**2)**1.5))
C
C
C     PDFE(A,B,D)=(3.0/G23)*
C     1           (8.0*B/(9.0*PI*D))**0.6667*
C     2           A*DEXP(-(8.0*B/(9.0*PI*D)*A**3))
C
C
C     PDFJ(X,XDOT,B,D)=(1.0/(2.0*PI))*(3.0/G23)*
C     1           (8.2164*B/(9.0*PI*D))**0.6667*
C     2           DEXP(-(8.2164*B/(9.0*PI*D)*(X**2+XDOT**2)**1.5))
C
C
C     PDFE(A,B,D)=(3.0/G23)*
C     1           (8.2164*B/(9.0*PI*D))**0.6667*
C     2           A*DEXP(-(8.2164*B/(9.0*PI*D)*A**3))
C
C.....EXAMPLE 3 (VAN DER POL EQUATION)
C
C.....DEFINE THE JOINT PROBABILITY DENSITY FUNCTION PDFJ AND
C     THE ENVELOPE DISTRIBUTION PDFE FOR EXAMPLE 3.
C
C
C     PDFJ(X,XDOT,B,D)=(1.0/(2.0*PI))*(1.0/DSQRT(PI*D/B))*
C     1           (1.0/ERFC(-DSQRT(B/D)))*
C     2           DEXP(-(B/D*((1.0-(X**2+XDOT**2)/4.0)**2)))
C
C
C     PDFE(A,B,D)=(1.0/DSQRT(PI*D/B))*
C     1           (1.0/ERFC(-DSQRT(B/D)))*
C     2           A*DEXP(-(B/D*(1.0-A**2/4.0)**2))
C
C.....EXAMPLE 4 (VAN DER RAYLEIGH EQUATION)
C
C.....DEFINE THE JOINT PROBABILITY DENSITY FUNCTION PDFJ AND
C     THE ENVELOPE DISTRIBUTION PDFE FOR EXAMPLE 4.
C
C
C     PDFJ(X,XDOT,B,D)=(1.0/(2.0*PI))*
C     1           (1.0/DSQRT(PI*D/(4.0*B)))*
C     2           (1.0/ERFC(-DSQRT(B/(4.0*D))))*
```

```
C     3                 DEXP(-(B/(4.0*D)*((1.0-(X**2+XDOT**2))**2)))
C
C
C         PDFE(A,B,D)=(1.0/DSQRT(PI*D/(4.0*B)))*
C     1               (1.0/ERFC(-DSQRT(B/(4.0*D))))*
C     2               A*DEXP(-(B/(4.0*D)*(1.0-A**2)**2))
C
C.....EXAMPLE 5 (VELOCITY CUBED DAMPING)
C
C.....DEFINE THE JOINT PROBABILITY DENSITY FUNCTION PDFJ AND
C     THE ENVELOPE DISTRIBUTION PDFE FOR EXAMPLE 5.
C
C
C         PDFJ(X,XDOT,B,D)=(1.0/(2.0*PI))*
C     1               (1.0/DSQRT(PI*D/(3.0*B)))*
C     2               DEXP(-(3.0*B/(16.0*D)*(X**2+XDOT**2)**2))
C
C
C         PDFE(A,B,D)=(1.0/DSQRT(PI*D/(3.0*B)))*
C     1               A*DEXP(-(3.0*B/(16.0*D)*A**4))
C
C.....EXAMPLE 6 (VELOCITY FIFTH DAMPING)
C
C.....DEFINE THE JOINT PROBABILITY DENSITY FUNCTION PDFJ AND
C     THE ENVELOPE DISTRIBUTION PDFE FOR EXAMPLE 6.
C
C
C         PDFJ(X,XDOT,B,D)=(1.0/(2.0*PI))*
C     1               (3.0*(5.0*B/(6.0*D))**0.3333)/G13*
C     2               DEXP(-(5.0*B/(48.0*D)*(X**2+XDOT**2)**3))
C
C
C         PDFE(A,B,D)=(3.0*(5.0*B/(6.0*D))**0.3333)/G13*
C     1               A*DEXP(-(5.0*B/(48.0*D)*A**6))
C
C
C.....EXAMPLE 7 (LINEAR SYSTEM)
C
C.....DEFINE THE JOINT PROBABILITY DENSITY FUNCTION PDFJ AND
C     THE ENVELOPE DISTRIBUTION PDFE FOR EXAMPLE 7.
C
          PDFJ(X,XDOT,B,D)=(1.0/(2.0*PI))*(B/D)*
     1               DEXP(-(B/(2.0*D)*(X**2+XDOT**2)))
C
C
          PDFE(A,B,D)=B/D*
     1               A*DEXP(-(B/(2.0*D)*A**2))
C
C
C.....EXAMPLE 8 (CASE 1 OF HYBRID DAMPING (B*X**2*XDOT))
C
C.....DEFINE THE JOINT PROBABILITY DENSITY FUNCTION PDFJ AND
```

```
C       THE ENVELOPE DISTRIBUTION PDFE FOR EXAMPLE 8.
C
C
C       PDFJ(X,XDOT,B,D)=(1.0/(2.0*PI))*(4.0/DSQRT(PI))*
C     1                 (DSQRT(B/(16.0*D)))*
C     2                 DEXP(-(B/(16.0*D)*(X**2+XDOT**2)**2))
C
C
C       PDFE(A,B,D)=(4.0/DSQRT(PI))*
C     1             (DSQRT(B/(16.0*D)))*
C     2             A*DEXP(-(B/(16.0*D)*A**4))
C
C
C.....EXAMPLE 9 (CASE 2 OF HYBRID DAMPING
C               (A*X**2+B*XDOT**2)SGN(XDOT))
C
C.....DEFINE THE JOINT PROBABILITY DENSITY FUNCTION PDFJ AND
C     THE ENVELOPE DISTRIBUTION PDFE FOR EXAMPLE 9.
C
C
C       PDFJ(X,XDOT,B,D)=(1.0/(2.0*PI))*(3.0/G23)*
C     1             ((8.0/(9.0*PI*D))*(B02+B20/2.0))**0.6667*
C     2             DEXP(-(8.0/(9.0*PI*D)*(B02+B20/2.0)*
C     3                               (X**2+XDOT**2)**1.5))
C
C
C       PDFE(A,B,D)=(3.0/G23)*
C     1             ((8.0/(9.0*PI*D))*(B02+B20/2.0))**0.6667*
C     2             A*DEXP(-(8.0/(9.0*PI*D)*(B02+B20/2.0)*
C     3                                     A**3))
C
C
C.....NORMAL DISTRIBUTION N(0,S)
C
        PDFN(W,S)=(1.0/(S*DSQRT(2.0*PI)))*DEXP(-W**2/(2.0*S**2))
C
C.....READ INPUT CONTROL
C
        READ(5,*) NPTS, NSKIP, DELT, TOLVEL, TOLDIS, V0, D0
C
C.....NOTE THAT THE FIRST POINT CORRESPONDING TO TIME = 0.0
C     IS ALWAYS SKIPPED FROM HISTOGRAM CALCULATIONS BECAUSE
C     IT IS RELATED TO THE INITIAL CONDITIONS AND IS COMPUTED
C     OUTSIDE THE MAIN LOOP
C
        IF (NSKIP .EQ. 0) NSKIP = 1
C
        READ(5,*) B00,B10,B20,B30
        READ(5,*) B01,B11,B21,B31
        READ(5,*) B02,B12,B22,B32
        READ(5,*) B03,B13,B23,B33
        READ(5,*) B05,B41
```

```
      READ(5,*) B,D
      READ(5,*) IND,INV,INF,INE
      READ(5,*) DELTAD,DELTAV,DELTAF,DELTAE
      READ(5,*) NDBND,NVBND,NFBND,NEBND
      WRITE(6,600) NPTS, NSKIP, DELT, TOLVEL, TOLDIS, V0, D0
  600 FORMAT(1H1/2X,'NONLINEAR 2ND ORDER DIFFERENTIAL
     1EQUATION SOLVER'//
     1              5X,'NPTS  = ',I9/
     1              5X,'NSKIP = ',I9/
     1              5X,'DELT  = ',F9.4/
     1              5X,'TOLVEL= ',F9.4/
     1              5X,'TOLDIS= ',F9.4/
     1              5X,'V0    = ',F9.4/
     1              5X,'D0    = ',F9.4//)
      WRITE(6,601) B00,B10,B20,B30,B01,B11,B21,B31,B02,B12,
     1B22,B32,B03,B13,B23,B33,B05,B41
  601 FORMAT(2X,'PARAMETERS OF THE DIFFERENTIAL EQUATION'//
     1 5X,'B00  = ',F9.4,5X,'B10  = ',F9.4,5X,'B20  = ',F9.4,
     1 5X,'B30  =',F9.4/
     1 5X,'B01  = ',F9.4,5X,'B11  = ',F9.4,5X,'B21  = ',F9.4,
     1 5X,'B31  =',F9.4/
     1 5X,'B02  = ',F9.4,5X,'B12  = ',F9.4,5X,'B22  = ',F9.4,
     1 5X,'B32  =',F9.4/
     1 5X,'B03  = ',F9.4,5X,'B13  = ',F9.4,5X,'B23  = ',F9.4,
     1 5X,'B33  =',F9.4/
     1 5X,'B05  = ',F9.4,5X,'B41  = ',F9.4//)
C     1 5X,'B33  =',F9.4//)
      WRITE(6,6601) B,D
 6601 FORMAT(2X,'PARAMETERS OF THE THEORETICAL PDF S'//
     1              5X,'B  = ',F9.4/
     1              5X,'D  = ',F9.4//)
      WRITE(6,602) IND,INV,INF,INE
  602 FORMAT(2X,'INITIAL VALUES FOR HISTOGRAMS'//
     1              5X,'IND  = ',F9.4/
     1              5X,'INV  = ',F9.4/
     1              5X,'INF  = ',F9.4/
     1              5X,'INE  = ',F9.4//)
      WRITE(6,603) DELTAD,DELTAV,DELTAF,DELTAE
  603 FORMAT(2X,'RESOLUTION (WIDTH OF BINS) FOR HISTOGRAMS'//
     1              5X,'DELTAD  = ',F9.4/
     1              5X,'DELTAV  = ',F9.4/
     1              5X,'DELTAF  = ',F9.4/
     1              5X,'DELTAE  = ',F9.4//)
      WRITE(6,604) NDBND,NVBND,NFBND,NEBND
  604 FORMAT(2X,'NUMBER OF BIN BOUNDARIES FOR HISTOGRAMS'//
     1              5X,'NDBND  = ',I5/
     1              5X,'NVBND  = ',I5/
     1              5X,'NFBND  = ',I5/
     1              5X,'NEBND  = ',I5//)
C
C....INITIALIZING PARAMETERS
C
```

```
      BIG  = 1.0E+64
      SML  = -BIG
      BIGA = 0.0
      BIGV = 0.0
      BIGD = 0.0
      BIGN = 0.0
      BIGE = 0.0
      DBAR = 0.0
      D2BAR = 0.0
      VBAR = 0.0
      V2BAR = 0.0
      ABAR = 0.0
      A2BAR = 0.0
      FBAR = 0.0
      F2BAR = 0.0
      EBAR = 0.0
      E2BAR = 0.0
      TDSUM = 0.0
      TVSUM = 0.0
      TFSUM = 0.0
      TESUM = 0.0
      DCHISQ = 0.0
      VCHISQ = 0.0
      FCHISQ = 0.0
      ECHISQ = 0.0
C
C.....COMPUTE STANDARD DEVIATION OF THE FORCING FUNCTION BASED
C.....ON D AND DELT
C
      S = DSQRT(2.0*D/DELT)
C
C.....CREATING THE DISPLACEMENT BIN BOUNDARIES
C
      DISBND(1) = IND
      DO 11 I=2,NDBND
      DISBND(I) = DISBND(I-1)+DELTAD
   11 CONTINUE
C
C.....CREATING THE VELOCITY BIN BOUNDARIES
C
      VELBND(1) = INV
      DO 12 I=2,NVBND
      VELBND(I) = VELBND(I-1)+DELTAV
   12 CONTINUE
C
C.....CREATING THE FORCE BIN BOUNDARIES
C
      FORBND(1) = INF
      DO 13 I=2,NFBND
      FORBND(I) = FORBND(I-1)+DELTAF
   13 CONTINUE
C
```

```
C.....CREATING THE ENVELOPE BIN BOUNDARIES
C
      ENVBND(1) = INE
      DO 14 I=2,NEBND
      ENVBND(I) = ENVBND(I-1)+DELTAE
   14 CONTINUE
C
C ... START SOLVING DIFFERENTIAL EQUATION BY FINDING INITIAL
C     ACCELERATION.
C
      WRITE(6,614)
  614 FORMAT(1H1/24X,'TIME',10X,'DISPL',8X,'VELOC',8X,'ACCEL',
     18X,'FORCE',7X,'ENVEL')
C
C.....IF INITIAL CONDITIONS ARE BOTH ZERO, MAKE ONE OF THEM
C     SMALL ENOUGH BUT NOT ZERO.
C
      IF(D0.EQ.0.0.AND.V0.EQ.0.0)D0=0.001
C
C
C.....CREATING THE FORCING FUNCTION N(T) ZERO MEAN, GAUSSIAN
C     RANDOM NOISE
C
C.....INITIAL SEEDS FOR GENERATION OF N(T)
C
      IX1 = 14368
      IX2 = 13115
      IX3 =   365

      CALL RANDZ(IX1,IX2,IX3,NI)
C
C.....APPLY STANDARD DEVIATION TO THE FORCING FUNCTION N(0,1)
C
      NI = NI * S
C
C.....NOTE THAT FIRST POINT IS ALWAYS SKIPPED FROM HISTOGRAMS
C
      DI = D0
      VI = V0
      AI = FUNC1(D0,V0,B00,B01,B02,B03,B10,B11,B12,B13,
     1           B20,B21,B22,B23,B30,B31,B32,B33,B05,B41) + NI
      EI = DSQRT(DI**2+VI**2)
      TIME = 0.0
C     WRITE(6,6610) TIME, DI, VI, AI, NI, EI
C6610 FORMAT(20X,F13.3,5E13.5)
      IF (BIGD .LT. DABS(DI)) BIGD = DABS(DI)
      IF (BIGV .LT. DABS(VI)) BIGV = DABS(VI)
      IF (BIGA .LT. DABS(AI)) BIGA = DABS(AI)
      IF (BIGN .LT. DABS(NI)) BIGN = DABS(NI)
      IF (BIGE .LT. DABS(EI)) BIGE = DABS(EI)
C
C.....START THE FIRST STEP AFTER INITIAL CONDITIONS
```

```
C
      NPM1 = NPTS - 1
      NSAVE = NPTS - 100
      DO 50 I = 1, NPM1
      KOUNT = 0
C
C.....NEWTON RAPHSON ITERATION
C
      CALL RANDZ(IX1,IX2,IX3,NF)
C
C.....APPLY STANDARD DEVIATION TO THE FORCING FUNCTION N(0,1)
C
      NF = NF * S
      F1 = DI + DELT*VI + (DELT/2.0)**2 * (AI+NF)
      F2 = VI + (DELT/2.0)*(AI+NF)
   45 CONTINUE
      KOUNT= KOUNT + 1
      F     = FUNC1(DI,VI,B00,B01,B02,B03,B10,B11,B12,B13,
     1             B20,B21,B22,B23,B30,B31,B32,B33,B05,B41)
      DFDV = FUNC2(DI,VI,B00,B01,B02,B03,B10,B11,B12,B13,
     1             B20,B21,B22,B23,B30,B31,B32,B33,B05,B41)
      DFDD = FUNC3(DI,VI,B00,B01,B02,B03,B10,B11,B12,B13,
     1             B20,B21,B22,B23,B30,B31,B32,B33,B05,B41)
      DN1DD= 1.0 - (DELT/2.0)**2 * DFDD
      DN2DD= -(DELT/2.0) * DFDD
      DN1DV= -(DELT/2.0)**2 * DFDV
      DN2DV= 1.0 - (DELT/2.0)* DFDV
      N1   = DI - (DELT/2.0)**2 * F
      N2   = VI - (DELT/2.0) * F
      DELTA= DN1DD*DN2DV - DN1DV*DN2DD
      DF    = DI + ((F1-N1)*DN2DV - (F2-N2)*DN2DD) / DELTA
      VF    = VI +(-(F1-N1)*DN1DV + (F2-N2)*DN1DD) / DELTA
      IF ((DABS(DF-DI).LE.TOLDIS) .AND.
     1(DABS(VF-VI).LE.TOLVEL))GOTO 60
      IF (KOUNT .GT.1000) GO TO 91
      DI = DF
      VI = VF
      GO TO 45
   60 CONTINUE
      AF = FUNC1(DF,VF,B00,B01,B02,B03,B10,B11,B12,B13,
     1             B20,B21,B22,B23,B30,B31,B32,B33,B05,B41) + NF
      EF = DSQRT(DF**2+VF**2)
      TIME = I*DELT
C     WRITE(6,610) KOUNT, I+1, TIME, DF, VF, AF, NF, EF
C 610 FORMAT(2I10,F13.3,5E13.5)
      IF (BIGD .LT. DABS(DF)) BIGD = DABS(DF)
      IF (BIGV .LT. DABS(VF)) BIGV = DABS(VF)
      IF (BIGA .LT. DABS(AF)) BIGA = DABS(AF)
      IF (BIGN .LT. DABS(NF)) BIGN = DABS(NF)
      IF (BIGE .LT. DABS(EF)) BIGE = DABS(EF)
C
C.....COMPUTING JOINT DISTRIBUTION OF DISPLACEMENT AND
```

```
C      VELOCITY, DISTRIBUTION OF FORCING FUNCTION AND
C      DISTRIBUTION OF ENERGY ENVELOPE.
C
C.....SKIP THE FIRST NSKIP POINTS TO MAKE SURE THAT ONLY
C      STEADY STATE IS CONSIDERED.
C
C.....NOTE THAT THE .LT. IS USED BECAUSE THE FIRST POINT
C      CORRESPONDING TO TIME = 0.0 IS ALWAYS SKIPPED FROM
C      HISTOGRAM CALCULATIONS.
C
       IF (I .LT. NSKIP) GO TO 51
       DO 71 ID=1, NDBND
       IF (DF .LT. DISBND(ID)) GO TO 72
    71 CONTINUE
    72 CONTINUE
       DO 73 IV=1, NVBND
       IF (VF .LT. VELBND(IV)) GO TO 74
    73 CONTINUE
    74 CONTINUE
       KNT(ID,IV) = KNT(ID,IV) + 1
       DO 75 IN=1, NFBND
       IF (NF .LT. FORBND(IN)) GO TO 76
    75 CONTINUE
    76 CONTINUE
       YNHIST(IN) = YNHIST(IN) + 1
       DO 77 IE=1, NEBND
       IF (EF .LT. ENVBND(IE)) GO TO 78
    77 CONTINUE
    78 CONTINUE
       YEHIST(IE) = YEHIST(IE) + 1
C
C.....CALCULATING STATISTICS FOR ALL QUANTITIES
C
       DBAR  = DBAR + DF
       D2BAR = D2BAR + DF**2
       VBAR  = VBAR + VF
       V2BAR = V2BAR + VF**2
       ABAR  = ABAR + AF
       A2BAR = A2BAR + AF**2
       FBAR  = FBAR + NF
       F2BAR = F2BAR + NF**2
       EBAR  = EBAR + EF
       E2BAR = E2BAR +EF**2
C
C.....SAVE TIME HISTORIES STARTING FROM NSAVE
C
       IF (I .LT. NSAVE) GO TO 51
       J = I + 1 - NSAVE
       DIS(J) = DF
       VEL(J) = VF
       ACC(J) = AF
       FOR(J) = NF
```

```
         ENV(J) = EF
         TIM(J) = TIME
         WRITE(6,610) I+1,J,TIM(J),DIS(J),VEL(J),ACC(J),FOR(J),
       1ENV(J)
   610 FORMAT(2I10,F13.3,5E13.5)
    51 CONTINUE
C
C.....SETTING INITIAL CONDITIONS FOR NEXT INTEGRATION STEP
C
         DI = DF
         VI = VF
         AI = AF
    50 CONTINUE
C
C.....COMPUTE REAL NUMBER OF POINTS USED
C
         RNPTS = NPTS - NSKIP
C
C.....FINISH STATISTICS COMPUTATIONS
C
         DBAR = DBAR/RNPTS
         DVAR = D2BAR/RNPTS - DBAR**2
         DSTD = DSQRT(DVAR)
         VBAR = VBAR/RNPTS
         VVAR = V2BAR/RNPTS - VBAR**2
         VSTD = DSQRT(VVAR)
         ABAR = ABAR/RNPTS
         AVAR = A2BAR/RNPTS - ABAR**2
         ASTD = DSQRT(AVAR)
         FBAR = FBAR/RNPTS
         FVAR = F2BAR/RNPTS - FBAR**2
         FSTD = DSQRT(FVAR)
         EBAR = EBAR/RNPTS
         EVAR = E2BAR/RNPTS - EBAR**2
         ESTD = DSQRT(EVAR)
C
C.....WRITE OUT MAXIMA AND STATISTICS
C
         WRITE(6,605) BIGD, BIGV, BIGA, BIGN, BIGE
   605 FORMAT(1H1/2X,'MAXIMUM OF THE ABSOLUTE VALUES FOR'//
       1          5X,'DISPL  = ',F9.4/
       1          5X,'VELOC  = ',F9.4/
       1          5X,'ACCEL  = ',F9.4/
       1          5X,'FORCE  = ',F9.4/
       1          5X,'ENVEL  = ',F9.4//)
         WRITE(6,606) DBAR, DVAR, DSTD
   606 FORMAT(2X,'STATISTICS FOR DISPLACEMENTS'//
       1          5X,'MEAN   = ',F9.4/
       1          5X,'VAR    = ',F9.4/
       1          5X,'STDDEV = ',F9.4//)
         WRITE(6,607) VBAR, VVAR, VSTD
   607 FORMAT(2X,'STATISTICS FOR VELOCITIES'//
```

```
     1              5X,'MEAN   = ',F9.4/
     1              5X,'VAR    = ',F9.4/
     1              5X,'STDDEV = ',F9.4//)
        WRITE(6,608) ABAR, AVAR, ASTD
 608 FORMAT(2X,'STATISTICS FOR ACCELERATIONS'//
     1              5X,'MEAN   = ',F9.4/
     1              5X,'VAR    = ',F9.4/
     1              5X,'STDDEV = ',F9.4//)
        WRITE(6,609) FBAR, FVAR, FSTD
 609 FORMAT(2X,'STATISTICS FOR FORCES'//
     1              5X,'MEAN   = ',F9.4/
     1              5X,'VAR    = ',F9.4/
     1              5X,'STDDEV = ',F9.4//)
        WRITE(6,611) EBAR, EVAR, ESTD
 611 FORMAT(2X,'STATISTICS FOR THE ENVELOPE'//
     1              5X,'MEAN   = ',F9.4/
     1              5X,'VAR    = ',F9.4/
     1              5X,'STDDEV = ',F9.4//)
C
        NFP1 = NFBND + 1
        DO 80 IN=1, NFP1
        YNHIST(IN) = 100.0 * YNHIST(IN) / RNPTS
  80 CONTINUE
        NEP1 = NEBND + 1
        DO 81 IE=1, NEP1
        YEHIST(IE) = 100.0 * YEHIST(IE) / RNPTS
  81 CONTINUE
        NDP1 = NDBND + 1
        NVP1 = NVBND + 1
        DO 85 ID=1, NDP1
        DO 85 IV=1, NVP1
        PERCNT(ID,IV) = 100.0 * KNT(ID,IV) / RNPTS
        YDHIST(ID) = YDHIST(ID) + PERCNT(ID,IV)
        YVHIST(IV) = YVHIST(IV) + PERCNT(ID,IV)
  85 CONTINUE
C
C.....CALCULATING THEORETICAL HISTOGRAMS
C
C.....CREATING THE ARRAYS WITH CENTER OF BIN VALUES
C
        DTHE(1)=IND-DELTAD/2.0
        DO 100 ID=2, NDP1
 100 DTHE(ID)=DISBND(ID-1)+DELTAD/2.0
C    DO 2000 I=1,NDP1
C    WRITE(6,2001)I,DTHE(I)
C2001 FORMAT(I10,F10.5)
C2000 CONTINUE
C
        VTHE(1)=INV-DELTAV/2.0
        DO 101 IV=2, NVP1
 101 VTHE(IV)=VELBND(IV-1)+DELTAV/2.0
C    DO 2002 I=1,NVP1
```

```
C     WRITE(6,2001)I,VTHE(I)
C2002 CONTINUE
C
      FTHE(1)=INF-DELTAF/2.0
      DO 102 IF=2, NFP1
  102 FTHE(IF)=FORBND(IF-1)+DELTAF/2.0
C     DO 2003 I=1,NFP1
C     WRITE(6,2001)I,FTHE(I)
C2003 CONTINUE
C
      ETHE(1)=0.0
      DO 103 IE=2, NEP1
  103 ETHE(IE)=ENVBND(IE-1)+DELTAE/2.0
C     DO 2004 I=1,NEP1
C     WRITE(6,2001)I,ETHE(I)
C2004 CONTINUE
C
      DO 104 ID=1,NDP1
      DO 104 IV=1,NVP1
      TPERCNT(ID,IV)=100.0*PDFJ(DTHE(ID),VTHE(IV),B,D)*DELTAD*
     1DELTAV
C     WRITE(6,2005)B,D,ID,IV,DTHE(ID),VTHE(IV),TPERCNT(ID,IV)
C2005 FORMAT(2F10.5,2I10,3F15.7)
      TYDHIST(ID) = TYDHIST(ID) + TPERCNT(ID,IV)
  104 TYVHIST(IV) = TYVHIST(IV) + TPERCNT(ID,IV)
      DO 105 IF=1,NFP1
C     WRITE(6,2006)IF,FTHE(IF),PDFN(FTHE(IF),S)
  105 TYNHIST(IF) = 100.0*PDFN(FTHE(IF),S)*DELTAF
C2006 FORMAT(I10,2F15.7)
      DO 106 IE=1,NEP1
C     WRITE(6,2006)IE,ETHE(IE),PDFE(ETHE(IE),B,D)
  106 TYEHIST(IE) = 100.0*PDFE(ETHE(IE),B,D)*DELTAE
C
C.....CHECKING THE NORMALIZATION OF THE THEORETICAL
C     DISTRIBUTIONS.
C
      DO 300 ID = 1,NDP1
  300 TDSUM = TDSUM + TYDHIST(ID)/100.0
      DO 301 IV = 1,NVP1
  301 TVSUM = TVSUM + TYVHIST(IV)/100.0
      DO 302 IF = 1,NFP1
  302 TFSUM = TFSUM + TYNHIST(IF)/100.0
      DO 303 IE = 1,NEP1
  303 TESUM = TESUM + TYEHIST(IE)/100.0
      WRITE(6,612) TDSUM,TVSUM,TFSUM,TESUM
  612 FORMAT(1H1/2X,'AREA UNDER DISTRIBUTION FOR'//
     1              5X,'DISPL  = ',F9.4/
     1              5X,'VELOC  = ',F9.4/
     1              5X,'FORCE  = ',F9.4/
     1              5X,'ENVEL  = ',F9.4//)
C
C.....CALCULATE CHI-SQUARE STATISTICS FOR EACH OF THE
```

```
C       DISTRIBUTIONS.
C
        DO 304 ID = 1,NDP1
        DCHISQ = DCHISQ + ((YDHIST(ID)-TYDHIST(ID))*
     1RNPTS/100.0)**2/(TYDHIST(ID)*RNPTS/100.0)
  304 CONTINUE
        DO 305 IV = 1,NVP1
        VCHISQ = VCHISQ + ((YVHIST(IV)-TYVHIST(IV))*
     1RNPTS/100.0)**2/(TYVHIST(ID)*RNPTS/100.0)
  305 CONTINUE
        DO 306 IF = 1,NFP1
        FCHISQ = FCHISQ + ((YNHIST(IF)-TYNHIST(IF))*
     1RNPTS/100.0)**2/(TYNHIST(ID)*RNPTS/100.0)
  306 CONTINUE
        DO 307 IE = 2,NEP1
        ECHISQ = ECHISQ + ((YEHIST(IE)-TYEHIST(IE))*
     1RNPTS/100.0)**2/(TYEHIST(ID)*RNPTS/100.0)
  307 CONTINUE
        WRITE(6,613) DCHISQ,VCHISQ,FCHISQ,ECHISQ
  613 FORMAT(1H1/2X,'CHI-SQUARE STATISTICS FOR'//
     1          5X,'DISPL  = ',F11.4/
     1          5X,'VELOC  = ',F11.4/
     1          5X,'FORCE  = ',F11.4/
     1          5X,'ENVEL  = ',F11.4//)
C
C
C.....PRINT TABLE OF:
C         THE JOINT DISTRIBUTION OF DISPLACEMENT & VELOCITY
C         THE DISTRIBUTION OF DISPLACEMENT
C         THE DISTRIBUTION OF VELOCITY
C
C.....ROUNDING OFF NUMBER OF PAGES
C
        NVP2 = NVBND + 2
        DISBND(NDP1) = BIG
        NPAGE = (NVP2+12) / 13
C
C.....START TO PRINT
C
C.....PRINT TABLE WITH NUMERICAL VALUES
C
C
        DO 90 IPAGE = 1, NPAGE
        I1 = (IPAGE-1)*13 + 1
        I2 = I1 + 12
        IF (I2 .GT. NVP2) I2 = NVP2-1
        I3 = I2 -  1
        IF(IPAGE.EQ.1)WRITE(6,621)SML,(VELBND(IV),IV=I1,I3)
        I11 = I1 - 1
        IF(IPAGE.NE.1)WRITE(6,631)(VELBND(IV),IV=I11,I3)
        WRITE(6,622) (TO,IV=I1,I2)
        IF(IPAGE.EQ.NPAGE)WRITE(6,633)(VELBND(IV),IV=I1,I3),BIG
```

```fortran
      IF(IPAGE.NE.NPAGE)WRITE(6,623)(VELBND(IV),IV=I1,I2)
      WRITE(6,624)
      DISBND(NDP1) = BIG
      IF (IPAGE .EQ. NPAGE) I2 = I2 + 1
C
C.....PLACING THE TOTAL SUM OF DISPLACEMENT INTO PERCNT TABLE
C
      DO 95 ID=1, NDBND
      PERCNT(ID,NVP2) = YDHIST(ID)
      IF (ID .EQ. 1)
      IF(ID.EQ.1)WRITE(6,625)SML,DISBND(ID),
     1(PERCNT(ID,IV),IV=I1,I2)
      IF (ID.NE.1) WRITE(6,626)DISBND(ID-1),DISBND(ID),
     1(PERCNT(ID,IV),IV=I1,I2)
   95 CONTINUE
      PERCNT(NDP1,NVP2) = YDHIST(NDP1)
      WRITE(6,6626)DISBND(NDBND),BIG,
     1(PERCNT(NDP1,IV),IV=I1,I2)
      IF (IPAGE .EQ. NPAGE) I2 = I2 -1
      WRITE(6,627) (YVHIST(IV),IV=I1,I2)
   90 CONTINUE
C
C.....START TO PRINT
C
C.....PRINT TABLE WITH THEORETICAL VALUES
C
C
      DO 990 IPAGE = 1, NPAGE
      I1 = (IPAGE-1)*13 + 1
      I2 = I1 + 12
      IF (I2 .GT. NVP2) I2 = NVP2-1
      I3 = I2 - 1
      IF(IPAGE.EQ.1)WRITE(6,6621) SML,(VELBND(IV),IV=I1,I3)
      I11 = I1 - 1
      IF(IPAGE.NE.1)WRITE(6,6631)(VELBND(IV),IV=I11,I3)
      WRITE(6,622) (TO,IV=I1,I2)
      IF(IPAGE.EQ.NPAGE)WRITE(6,633)(VELBND(IV),IV=I1,I3),BIG
      IF(IPAGE.NE.NPAGE)WRITE(6,623)(VELBND(IV),IV=I1,I2)
      WRITE(6,624)
      DISBND(NDP1) = BIG
      IF (IPAGE .EQ. NPAGE) I2 = I2 + 1
C
C.....PLACING THE TOTAL SUM OF DISPLACEMENT INTO TPERCNT TABLE
C
      DO 995 ID=1, NDBND
      TPERCNT(ID,NVP2) = TYDHIST(ID)
      IF(ID.EQ.1)WRITE(6,625)SML,DISBND(ID),
     1(TPERCNT(ID,IV),IV=I1,I2)
      IF(ID.NE.1)WRITE(6,626)DISBND(ID-1),DISBND(ID),
     1(TPERCNT(ID,IV),IV=I1,I2)
  995 CONTINUE
      TPERCNT(NDP1,NVP2) = TYDHIST(NDP1)
```

```
       WRITE(6,6626) DISBND(NDBND),BIG,
      1(TPERCNT(NDP1,IV),IV=I1,I2)
       IF (IPAGE .EQ. NPAGE) I2 = I2 -1
       WRITE(6,627) (TYVHIST(IV),IV=I1,I2)
   990 CONTINUE
C
C.....FORCING FUNCTION NUMERICAL AND THEORETICAL
C
       WRITE(6,628) SML,TO,FORBND(1),YNHIST(1),TYNHIST(1)
       DO 96 IN=2,NFBND
       INM1 = IN - 1
       WRITE(6,629) FORBND(INM1), TO, FORBND(IN), YNHIST(IN),
      1TYNHIST(IN)
    96 CONTINUE
       WRITE(6,630) FORBND(NFBND), TO, BIG, YNHIST(NFP1),
      1TYNHIST(NFP1)
C
C.....ENERGY ENVELOPE NUMERICAL AND THEORETICAL
C
       WRITE(6,6628) SML,TO,ENVBND(1),YEHIST(1),TYEHIST(1)
       DO 97 IE=2,NEBND
       IEM1=IE-1
       WRITE(6,629) ENVBND(IEM1), TO, ENVBND(IE), YEHIST(IE),
      1TYEHIST(IE)
    97 CONTINUE
       WRITE(6,630) ENVBND(NEBND), TO, BIG, YEHIST(NEP1),
      1TYEHIST(NEP1)
   621 FORMAT(1H1///40X,' SIMULATED PERCENT OF OCCURRENCE
      1TABLE'//
      2 50X,'   VELOCITY          '/
      3 20X,E7.1,13F7.3)
  6621 FORMAT(1H1///39X,' THEORETICAL PERCENT OF OCCURRENCE
      1TABLE'//
      2 50X,'   VELOCITY          '/
      3 20X,E7.1,13F7.3)
   622 FORMAT(19X,13(5X,A2))
   623 FORMAT(4X,'DISPLACEMENT',4X,14F7.3)
   624 FORMAT(2X,'          ')
   625 FORMAT(1X,E7.1,' TO',F7.3,2X,13F7.3)
   626 FORMAT(1X,F7.3,' TO',F7.3,2X,13F7.3)
  6626 FORMAT(1X,F7.3,' TO',E8.1,1X,13F7.3)
   627 FORMAT(/2X,'VELOCITY TOTALS   ',13F7.3)
   628 FORMAT(1H1//10X,'FORCING FUNCTION RANGE',8X,'PERCENTAGE
      1OF OCCURRENCE'//42X,'SIMULATED',2X,'THEORETICAL'/
      2 /10X,E7.1,1X,A2,1X,F7.3,14X,F7.3,5X,F7.3)
  6628 FORMAT(1H1//10X,'ENERGY ENVELOPE RANGE',10X,'PERCENTAGE
      1OF OCCURRENCE'//42X,'SIMULATED',2X,'THEORETICAL'/
      2 /10X,E7.1,1X,A2,1X,F7.3,14X,F7.3,5X,F7.3)
   629 FORMAT(10X,F7.3,1X,A2,1X,F7.3,14X,F7.3,5X,F7.3)
   630 FORMAT(10X,F7.3,1X,A2,1X,E7.1,14X,F7.3,5X,F7.3)
   631 FORMAT(1H1///39X,' SIMULATED PERCENTAGE OF OCCURRENCE
      1TABLE'//
```

```
      2 50X,'    VELOCITY          '/
      3 20X,14F7.3)
 6631 FORMAT(1H1///38X,' THEORETICAL PERCENTAGE OF OCCURRENCE
     1TABLE'//
      2 50X,'    VELOCITY          '/
      3 20X,14F7.3)
C 633 FORMAT(4X,'DISPLACEMENT',4X,13(1X,F6.3))
  633 FORMAT(4X,'DISPLACEMENT',4X,13F7.3,E7.1)
      STOP
   91 CONTINUE
      WRITE(6,801) KOUNT, I
  801 FORMAT(/2X,'ERROR! NO CONVERGENCE AFTER',I5,' ITERATIONS
     1FOR', ' TIME STEP',I10)
      STOP
      END
C
C
C


      SUBROUTINE RANDZ(ISEED1,ISEED2,ISEED3,Z)
C
C
C
C
C
C ... THIS SUBROUTINE TRANSFORMS TWO UNIFORMLY DISTRIBUTED
C     RANDOM NUMBERS INTO TWO NORMALLY DISTRIBUTED RANDOM
C     NUMBERS WITH MEAN ZERO AND STANDARD DEVIATION ONE. UPON
C     LEAVING THE SUBROUTINE ONE NORMAL NUMBER IS RETURNED IN
C     Z. THE OTHER NORMAL NUMBER IS SAVED FOR THE SUBSEQUENT
C     CALL TO THE SUBROUTINE.
C
C


      IMPLICIT REAL*8(A-H,O-Z)
      DATA IFLAG/0/

      IF (IFLAG.EQ.0) THEN
   10 CALL RANDU(ISEED1,ISEED2,ISEED3,INT1,U1)
      CALL RANDU(ISEED1,ISEED2,ISEED3,INT2,U2)
      V1=2.*U1-1.
      V2=2.*U2-1.
      S=V1**2+V2**2
      IF(S.GE.1.)GO TO 10
      FAC=DSQRT(-2.*DLOG(S)/S)
      Z1=V1*FAC
      Z2=V2*FAC
      Z=Z1
      IFLAG=1

      ELSE
      Z=Z2
      IFLAG=0
```

```
      ENDIF

      RETURN
      END


C
C
C
      SUBROUTINE RANDU(ISEED1,ISEED2,ISEED3,INT,U)
C
C
C
C
C ... THIS SUBROUTINE GENERATES UNIFORM RANDOM NUMBERS IN
C     THE INTERVAL (0,1)
C
      IMPLICIT REAL*8(A-H,O-Z)

      ISEED1 = MOD(171*ISEED1,30269)
      ISEED2 = MOD(172*ISEED2,30307)
      ISEED3 = MOD(170*ISEED3,30323)

      U = DMOD((DBLE(ISEED1)/30269.0D0+DBLE(ISEED2)/30307.0D0+
     1          DBLE(ISEED3)/30323.0D0),1.0D0)

      INT = U*1000000000.

      RETURN
      END
```

APPENDIX B

MODDEQ WRITE-UP

IDENTIFICATION

MODDEQ/Differential Equation Solver - FORTRAN coded

Kiku Matsumoto
Program date (latest version) : September, 1976
Writeup date : September, 1976

PURPOSE

MODDEQ may be used to solve a system of first-order differential

equations with automatic control of truncation error.

RESTRICTIONS

The number of differential equations in the system to be solved

must not exceed 20.

METHOD

This routine has been programmed to allow the option of either

fixed interval size or variable interval size with automatic error

control (see USAGE). The method of Runge-Kutta-Gill is used to

start the integration process and is used to restart the integration

whenever the interval size has been changed. Let the system of

equations to be solved be given in the form:

$$(II.D.1) \quad \begin{cases} \dot{Y}_i & = f_i(t, Y_1, Y_2, \ldots, Y_n), \quad i = 1, 2, \ldots, n \\ \\ Y_i(t_o) & = Y_{io} \end{cases}$$

Let Y_{in} be the value of Y_i at $t = t_n$, f_{in} the derivative at $t = t_n$, and

Δt the interval size of the independent variable t.

The Runge-Kutta-Gill method uses the formulas:

$$(II.D.2) \quad \begin{cases} k_{io} = \Delta t f_i(t, Y_{in}) \\ Y_{in}^{(1)} = Y_{in} + \frac{1}{2} k_{io} \\ q_{i1} = k_{io} \end{cases}$$

$$(II.D.3) \quad \begin{cases} k_{i1} = \Delta t f_i(t + \frac{\Delta t}{2}, Y_{in}^{(1)}) \\ Y_{in}^{(2)} = Y_{in}^{(1)} + \frac{b_1}{2} (k_{i1} - q_{i1}) \\ q_{i2} = b_1 k_{i1} + c_1 q_{i1} \end{cases}$$

$$(II.D.4) \quad \begin{cases} k_{i2} = \Delta t f_i(t + \frac{\Delta t}{2}, Y_{in}^{(2)}) \\ Y_{in}^{(3)} = Y_{in}^{(2)} + \frac{b_2}{2} (k_{i2} - q_{i2}) \\ q_{i3} = b_2 k_{i2} + c_2 q_{i2} \end{cases}$$

$$(II.D.5) \quad \begin{cases} k_{i3} = \Delta t f_i(t + \Delta t, Y_{in}^{(3)}) \\ Y_{i, n+1} = Y_{in}^{(3)} + \frac{1}{6} k_{i3} - \frac{1}{3} q_{i3} \end{cases}$$

where

$$b_1 = 2 - \sqrt{2} \qquad c_1 = -2 + \frac{3\sqrt{2}}{2}$$

$$b_2 = 2 + \sqrt{2} \qquad c_2 = -2 - \frac{3\sqrt{2}}{2}$$

The Adams-Moulton predictor-corrector formulas are:

$$(II.D.6) \quad Y^{(p)}_{i,n+1} = Y_{i,n} + \frac{\Delta t}{24} (55f_{i,n} - 59f_{i,n-1} + 37f_{i,n-2} - 9f_{i,n-3})$$

$$(II.D.7) \quad Y^{(c)}_{i,n+1} = Y_{i,n} + \frac{\Delta t}{24} (9f_{i,n+1} + 19f_{i,n} - 5f_{i,n-1} + f_{i,n-2})$$

The corrector formula is applied only once so that only two derivative evaluations are needed for each Adams-Moulton integration step. The starting values are obtained using the Runge-Kutta-Gill method.

If the variable interval size mode is chosen, the interval size is determined as follows:

Let

$$(II.D.8) \quad \begin{cases} E_{n+1} = \text{Max} \dfrac{\left| Y^{(p)}_{i,n+1} - Y^{(c)}_{i,n+1} \right|}{14D_i} \\[20pt] D_i = \text{Max} \{ \left| Y^{(c)}_{i,n+1} \right| , .001 \} \end{cases}$$

An upper bound, $\overline{E}$, on the truncation error estimate, E_{n+1}, is input to the program. This is equivalent to specifying the number of significant figures which are to be preserved locally throughout the integration. A lower bound, $\underline{E}$, is computed by $\underline{E} = .02\overline{E}$.

If $\underline{E} < E_{n+1} \le \overline{E}$, the interval size, Δt, is unchanged. If $E_{n+1} \ge \overline{E}$, the program compares $\Delta t/4$ to Δt_{min}. If $\Delta t/4 < \Delta t_{min}$, an error return is made. If $\Delta t/4 \ge \Delta t_{min}$, Δt is replaced by $\Delta t/4$, the conditions at time

t_{n-1} are restored (i.e., $Y_{i,n-1}$, $f_{i,n-1}$), and three Runge-Kutta-Gill

integrations, and two Adams-Moulton integrations are performed.

It may be seen that the last Adams-Moulton integration step was an

integration from time t_n to time $t_n + \Delta t/4$. The truncation error

estimate, E_{n+1}, is computed at this point and the program continues

as above.

If $1/\Delta t \ [t_o + j\Delta t_{max} - t_{n+1}] \equiv 0$ mod 2, where j is a positive integer

and $t_o + (j - 1) \ \Delta t_{max} < t_{n+1} \leq t_o + j\Delta t_{max}$, the program compares

E_{n+1} to $\underline{E}$. If $E_{n+1} < \underline{E}$, the program performs integrations to times

t_{n+2} and t_{n+3} by the method of Adams-Moulton. If $E_{n+2} < \underline{E}$ and $E_{n+3} <$

$\underline{E}$ and $2\Delta t < \Delta t_{max}$, then Δt is replaced by $2\Delta t$.

While the truncation error test will guarantee that the local error does

not exceed $\overline{E}$, the cumulative error will usually exceed $\overline{E}$. Hence, $\overline{E}$

is chosen small enough to allow for an accumulation of truncation error.

There is no test in the truncation error in the initial interval.

Starting values for the Adams-Moulton method are always obtained using

the Runge-Kutta-Gill method whenever the interval size is changed, just

as at the beginning of the integration. An initial value for the interval

size is input to the program when using the variable mode. If at some

point in the integration the user wishes to change the maximum step size,

Δt, it is necessary to re-initialize by calling MODDEQ over again.

Both the Runge-Kutta-Gill method and the Adams-Moulton method incor-

porate round-off control features. This is accomplished by keeping the Y_{in}

in double precision and forming the sums $Y_{in} + \Delta Y_{in}$ in double precision.

C1069-314-370
MODDEQ

The derivative evaluations are all performed in single precision.
The procedure has been shown to be very effective in controlling the
growth of round-off error.

<u>USAGE</u>

To integrate from t_1 to $t_1 + \Delta t$

CALL MODDEQ(FUNCT,K,N,T,Y,YDOT,DT,EPS)

where

FUNCT is the name of the external subroutine subprogram
which computes the derivatives for any T. It must
be declared to be EXTERNAL in the calling program.
Description of arguments follows later.

K   must be an integer variable, initially set to 1 in
the calling program and must not be reset subse-
quently, since it is normally set to 2 by MODDEQ.
In the event that solution cannot be computed to the
precision specified by EPS, K will be set to (-1)
and an error message printed. <u>It is the user's</u>
<u>task to check K for (-1).</u>

N   is the number of first order equations to be solved.
If it exceeds 20, an error message will be printed.

T   is the independent variable which must be initialized.

Y   is the array containing the values of the dependent
variables at T.

YDOT is the array which upon returning from MODDEQ will
contain the derivatives of Y.

DT   is the maximum step size used in MODDEQ. This parameter must not be changed without initialization (i.e., reset K = 1)

EPS   is the maximum error permitted. EPS = 0.0 will cause computation to be in the fixed mode, with no attempt to check for precision, or to decrease the integration step. In normal computation with automatic error control, EPS should normally be $\geq 10^{-5}$, since single precision computation can fluctuate between 6 and 7 figures (for IBM 370/155)

The initial call to MODDEQ with K = 1 does nothing more than to save the input parameters and to evaluate the derivatives and update K to 2. MODDEQ in subsequent calls integrates from the current value of T to T + DT. Following the call to MODDEQ, the calling program should check whether an error return has occurred and whether integration has been completed.

The external subroutine must be of the following form:

SUBROUTINE FUNCT(N,T,Y,YDOT)

where all arguments are the same as described previously.

An example follows:

EXAMPLE

    Solve the following from x=0 to x=2π+1.0

$$\dot{Y} = 1 \text{ for } 0<X\leq 1 \quad \text{and } X>\pi+1$$

and $\dot{Y} = \sin^5 (X - 1) \sin [6(X - 1)] + 1 \text{ for } 1<X<\pi+1$

$$X = 0, \ Y(0) = 0, \ dx = .01 \text{ for } 0\leq x\leq\pi+1$$

$$dx = .02 \text{ for } \pi+1\leq x\leq 2\pi+1.0$$

This problem may be coded as follows:

```
          DATA PI/3.141593/

          EXTERNAL DERIV

          X    = 0.

          Y    = 0.

          XINC = 2.

          XMAX = PI+1.0

          DX   = 1.0E-2

    15    CONTINUE

          K    = 1

    20    CALL MODDEQ(DERIV,K,1,X,Y,YDOT,DX,1.E-4)

          IF(K .LT. 0)  GO  TO  100

          WRITE(6,510)  X,Y,YDOT

          IF(X .LT. XMAX)  GO  TO  20

 C        X GREATER OR EQUAL TO XMAX

          DX   = DX * XINC

          XMAX = XMAX + PI

          IF (DX .LE. .02)  GO  TO  15

          STOP

   510    FORMAT (1X3E20.7)

   100    CONTINUE

          WRITE(6,515)  X,Y,YDOT
```

```
515   FORMAT(/1X'ERROR'3E20.7)

      STOP

      END



      SUBROUTINE DERIV(N,X,Y,YDOT)

      IF(X .GT. 1.0)  GO  TO  20

10    YDOT  =  1.0

      RETURN        :

20    IF(X .GT. 4.14)  GO  TO  10

      YDOT  =  SIN(X-1.0)**5*SIN(6.0*(X-1.0))+1.0

      RETURN

      END
```

To use fixed mode, change the last argument in the call to MODDEQ to zero.

OPERATIONAL CHARACTERISTICS

Subprograms required and storage requirements
(compiled under FORTRAN H (OPT = 2))

MODDEQ	$(3048)_{10}$ bytes
MADAM	$(824)_{10}$
MGILL	$(1024)_{10}$
MREST,MSAVE	$(768)_{10}$
COMMON/SAVDEQ/	$(896)_{10}$
	6560

NOTES: Any modification to DIMENSION statements must also be made in the above programs and common.

These subprograms are available on the Time Sharing VAX FORTRAN library and the 370/3032 FORTRAN library. The accuracy on the Time Sharing VAX may not be identical to that on the IBM/3032.

C1079-314-370
MODDEQ